NASA
Technical
Paper
2508

August 1985

# Problems Experienced and Envisioned for Dynamical Physical Systems

Robert S. Ryan

NASA

**NASA Technical Paper 2508**

1985

# Problems Experienced and Envisioned for Dynamical Physical Systems

Robert S. Ryan

*George C. Marshall Space Flight Center*
*Marshall Space Flight Center, Alabama*

National Aeronautics and Space Administration

**Scientific and Technical Information Branch**

## TABLE OF CONTENTS

## LIST OF ILLUSTRATIONS

## LIST OF ILLUSTRATIONS (Continued)

## LIST OF ILLUSTRATIONS (Continued)

## LIST OF ILLUSTRATIONS (Continued)

## LIST OF ILLUSTRATIONS (Continued)

## LIST OF ILLUSTRATIONS (Concluded)

TECHNICAL PAPER

# PROBLEMS EXPERIENCED AND ENVISIONED FOR DYNAMICAL PHYSICAL SYSTEMS

## I. INTRODUCTION

The use of high performance systems, which is the trend of future space systems, naturally leads to lower margins and a higher sensitivity to parameter variations and, therefore, more problems of dynamic physical systems. To circumvent dynamic problems of these systems, appropriate design, verification analysis, and tests must be planned and conducted. The basic design goal is to define the problem before it occurs. The primary approach for meeting this goal is a good understanding and reviewing of the problems experienced in the past in terms of the system under design.

Dynamic problems have been a continual companion of space systems design. The nature of these problems has led to very dramatic situations including failures. In general, they have not been predicted, due to either a lack of understanding or simplistic analyses even when understanding existed, because of the large number of potential problems and limited resources. In addition, communication or the lack thereof between various engineering disciplines precludes dynamicists seeing or knowing about potential problem sources. Once the problem has occurred, dynamicists have a good batting average in reconstructing the cause. As stated previously, the basic design goal is to define the problem before it occurs and therefore preclude its occurrence by good design practices. This report reviews many of the dynamic problems experienced in space systems design and operation, categorizes them as to causes, and envisions future program implications, developing recommendations for analysis and test approaches.

## II. GENERAL

Dynamic problems take many forms and can be classified into several categories. These are determined by the basic phenomena or problem source that occur in each case. Misconceptions arise from the idea that dynamic problems are only associated with structures and are in a forced response mode. Dynamics are not only associated with structures. Dynamic oscillations are inherent in fluids, thermal, gas, and electrical systems, all with modal characteristics of comparable form to structure. These dynamical systems are amenable to analysis and test characterization. In space systems, most dynamic problems do not occur in one isolated discipline but are an interaction between several disciplines or subsystems required to meet mission objectives. Design analysis and test must simulate the interactions of all aspects of the phenomenon or problem areas, such as control, propulsion, structures, dynamics, natural environments, induced environments, and mechanical environments. Figure 1 illustrates to some degree the various interacting disciplines involved in stability and lifetime of a typical rocket engine. Obviously, each area should also be analyzed and understood separately as well as in system interaction. Essential in each area is a thorough understanding of the environments, physical model, and material characteristics as well as their interactions with the various design functions being supported by detailed engineering in each discipline area and the interactions in system analysis techniques. Figure 1 shows that after each discipline area is well defined, feedback or interaction changes occur in the discipline due to the multidiscipline interaction. First class space system design is a very intricate balancing act between these interactions where a breakdown in any part (discipline, tasks) unbalances and topples the system producing poor design with problem areas.

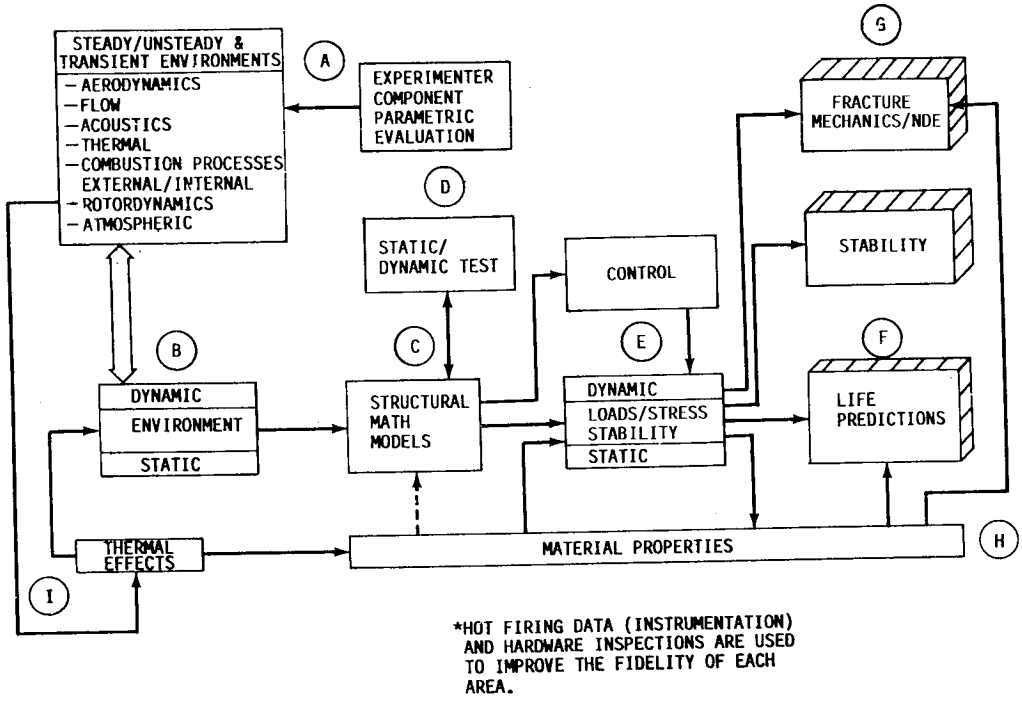


Figure 1. Classical design/analysis flow schematic.

Figure 2 is a schematic depicting this balancing act, showing all the components that support a design with acceptable dynamic characteristics. Properly balancing discipline and systems oriented tasks results in a quality, high performance product. A weakness in any leg causes problems and failures, which is the subject of this report.

The most dramatic of all dynamic phenomena occurs when two or more of these areas interact in a manner to create an instability (unbounded response). Instability, because of potential catastrophic consequences and lack of general understanding, is dicsussed in more detail in the next section. Following this discussion is a review of the various categories of dynamic problems to be discussed in this paper.

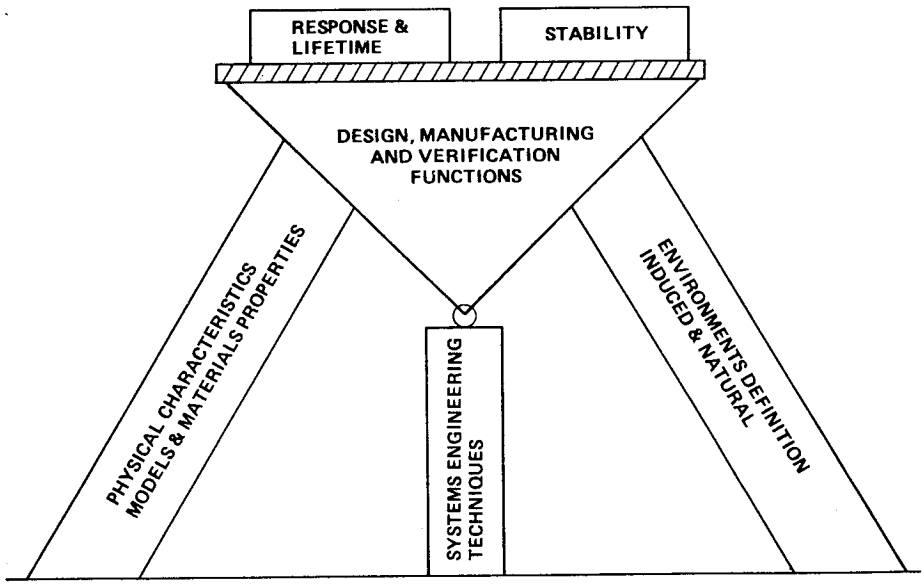


Figure 2. The balancing act of design and verification.

## A. Instability

Forced response of a structural system is a well understood and extensively documented area. Textbooks on the subject abound. The response is always limited by the level of structural damping, the forcing function, and the frequency ratio between force and response medium. The classical response of a damped, single degree-of-freedom system under sinusoidal excitation is shown on Figure 3, plotted with damping as a parameter. When the oscillatory force is removed, the amplitude always decays to static amplitude. Forced response problems usually occur as fatigue problems, although in some cases the force is large enough to cause nearly instantaneous failure.

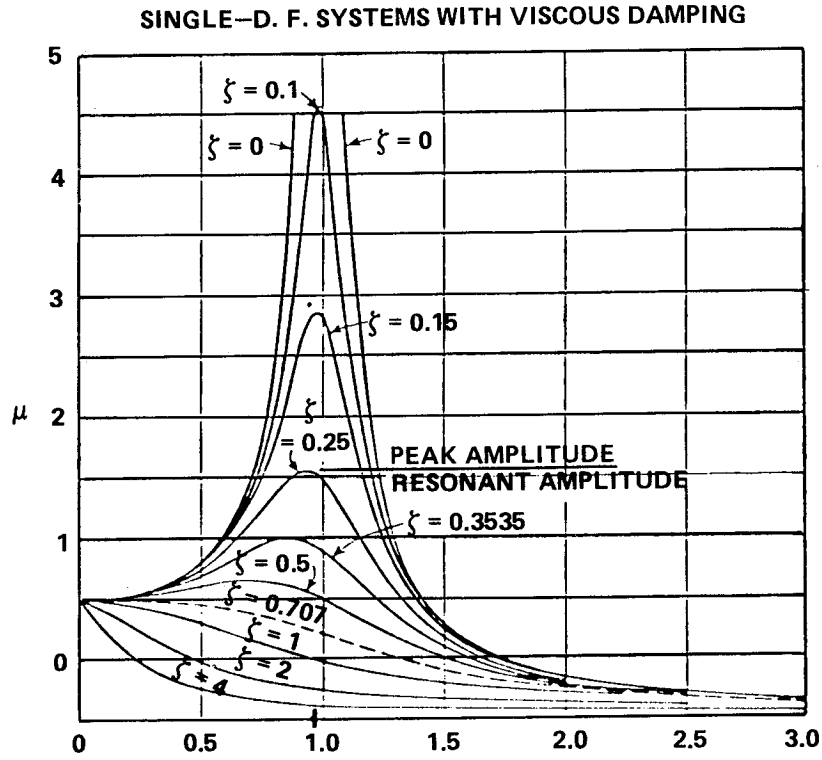


Figure 3. Forced response of single-degree-of-freedom system.

In an unstable or a marginally stable system, this is not the case. The response is caused by a motion in one part, such as structural element (example, aircraft wing) that creates a force (example, aerodynamic) which further increases the motion. The increased motion, therefore, creates larger forces. This closed loop continues until failure occurs or some limit is reached. Figure 4 shows the response of such an interaction as a function of the product of frequency and damping ($\sigma$) showing the response amplitude increasing as $-\sigma$ decreases in magnitude until zero is reached. At zero, the amplitude is unbounded and remains unbounded for positive values of $\sigma$. The only significance of very small negative values of $\sigma$ and the positive values of $\sigma$ is the rate at which a response value is obtained. Analysis of this response characterization leads to several generalizations.

1) Marginally stable systems are very sensitive to parameter variations and can easily move into unstable areas.

2) Systems near the instability point act like a limited forced response system, but can be easily driven into the instability range.

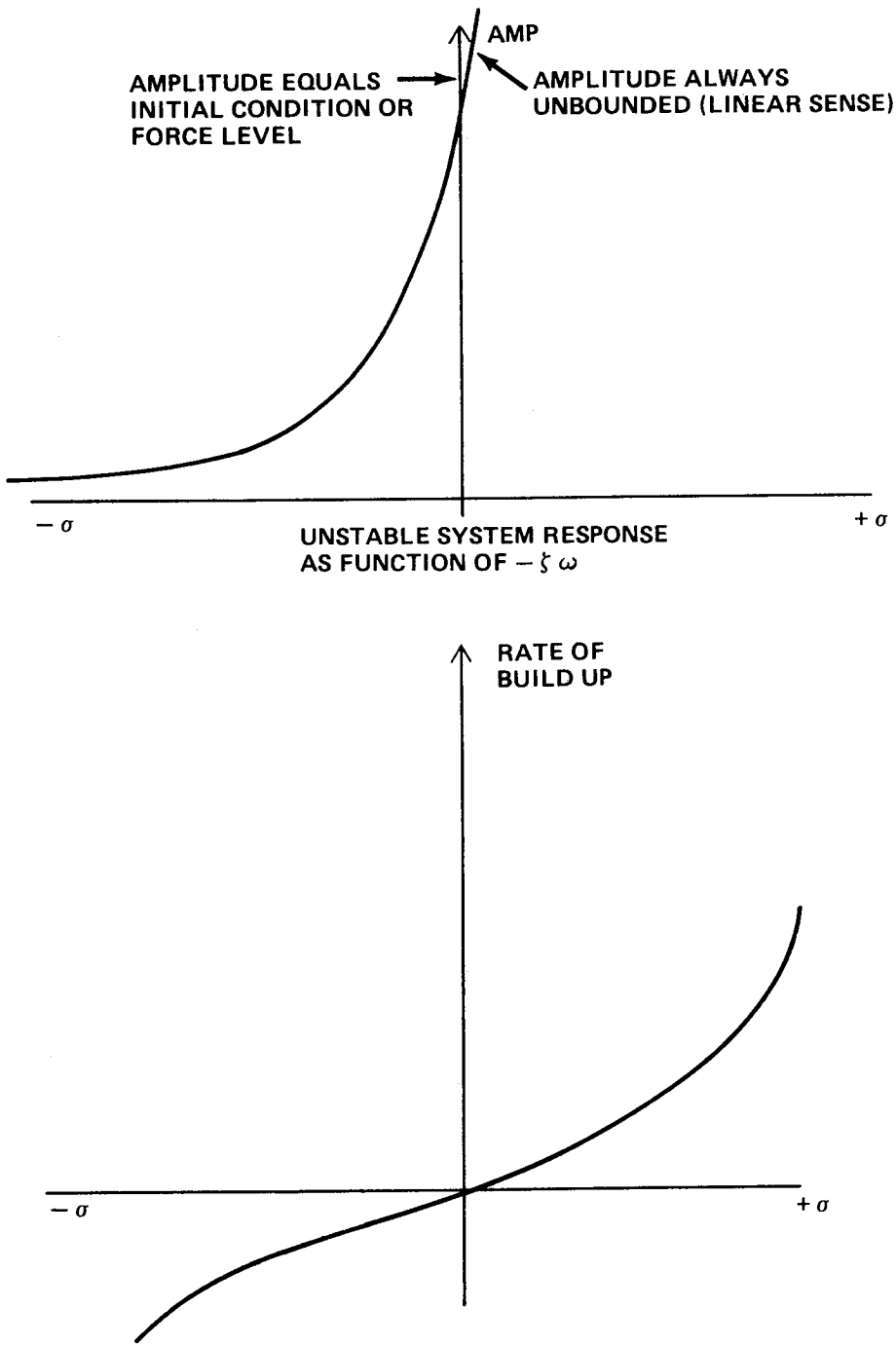


Figure 4. Marginally stable and unstable system response as function of real part of root $\sigma$.

3) Accurate definition of all forces, manufacturing, control, and the system models are required if the system must operate near the stability boundary, implying more stringent analyses, test, verification, and quality control.

The next section treats the categories, in addition to instabilities and forced response, used in this report as an outline for discussing dynamic problems.

## B. Additional Categories of Dynamic Problems

The other areas important to the discussion of dynamic problems experienced are environments, modeling, dynamic tuning, acoustical tuning, and manufacturing and quality.

Key to all dynamic problems is an understanding of environments. This involves the physics of the problem and the ability to characterize it within the defined limits. Natural and induced environments are included here. Typical environments are aerodynamics, propulsion, acoustics, atmosphere, solar, thermal, etc. The inability to accurately predict environments in both areas has been a key factor in many of the dynamic problems encountered and is selected as one category for problem discussion.

Dynamic modeling of the structure, fluid, etc., is fundamental and has been one source of mispredicting dynamic problems. The advent of finite element techniques in conjunction with high speed, large capacity computers is reducing these prediction problems; however, models are just that, models which are based on judgment and assumptions. In other words, you only model well what you understand well. System response can only predict what the model contains. Obviously, these same comments apply to the total model, environments, structures, fluids, etc., and are the key part of the response and stability analysis and becomes the next category for discussing problems.

Structural and fluid systems which are composed of more than one element of near equal size tune up dynamically, drastically changing overall characteristics of the system leading to very complex response characteristics. Because these system characteristics are very sensitive to small changes in the elements and result in dynamic tuning, this is a fundamental category for studying dynamic problems.

Acoustical tuning falls into this same dynamic tuning area but is split out separately for emphasis. Finally, the last category chosen for discussing problems is manufacturing and quality. This area is very critical for high performance systems since small errors in manufacturing or quality control produce large effects, including catastrophic failures in dynamic systems.

Fatigue and other areas are discussed in the response category as well as under modeling.

In summary, several categories have been selected for discussing dynamic problems.

1) Forced response

    a) Environment

    b) Response

2) Instabilities

3) Modeling

4) Acoustical tuning

5) Modal tuning

6) Manufacturing and quality

7) Dynamic testing (discussed under Modeling).

The choice is the author's and is certainly debatable. In some cases, a given problem will show up in more than one area, since more than one cause was present. For example, dynamic tuning could change the system, again leading to an instability. The problem will be discussed only under one category but listed in both areas.

Table 1 is a matrix of problems experienced listed by the above categories and is provided as a quick reference. All individual problems listed will be discussed to some extent. Certain projects do not show problems in all categories. This does not mean problems were not experienced, but that the author was not involved and did not have knowledge of the problems. The specific problems experienced will be discussed in the next section.

## III. DYNAMIC PROBLEMS EXPERIENCED

This section covers the problems by categories and by projects. Some areas contain more information than others, not necessarily because of importance but because of abundance or lack of documented data. As discussed previously, instabilities occur when some response generates a force which amplifies the response, thus increasing the forces continuing until failure or some limit occurs.

Instabilities are the most dramatic of all dynamic problems. Not only are they exciting to observe but are both challenging and exciting to analyze. Predicting and explaining instabilities requires the best of engineering, mathematics, and simulation. Instabilities of one type or another are part of the history of space exploration development. The following is a thumbnail sketch of these experiences, followed by a brief discussion of the experiences in the other categories.

### A. Instabilities

1. Redstone Potentiometer Feedback

The first dynamic problem experienced occurred early in the Redstone rocket program. A Redstone vehicle was in checkout and verification in a horizontal position in its transportation cradle. These early vehicles were manufactured at Redstone, checked out, then transported to Florida for launch. In this case, the control system was activated for checkout. The control sensors had a potentiometer pick up, due to some light shock, the wiper arm and moved it from one wire to another, which resulted in a control signal. As a result, the jet vanes moved, exciting a structural mode. The structural mode in turn caused the wiper arm to move back, creating a new signal. The result was a closed loop limit cycle instability between the sensor (pickup), jet vane (inertia), and structural mode, ringing out at the first mode frequency. The noise of this closed loop resonance was very loud, demonstrating vividly closed loop instabilities. The fix was simple in that a filter was incorporated in the loop which filtered out the frequencies associated with the modes and sensor pickup, breaking the loop and stabilizing the system. A later design also changed the pickup to a continuous magnetic type adding margin to the problem solution.

2. Jimspheres (Atmosphere Sounding Balloons Errativ Response)

Atmospheric environments are key to predicting space vehicle response during the ascent phase. Atmospheric winds are the key parameter to loads, flight mechanics, and control predictions. As a means of developing a statistical quantification of these winds, a balloon radar tracking system was developed by MSFC's atmospheric group under the leadership of Dr. William Vaughan. The goal was to

# TABLE 1. DYNAMIC PROBLEMS EXPERIENCED

X153

| PROGRAM | AEROELASTICITY & INSTABILITIES | FORCED RESPONSE | | MODELING | ACOUSTICAL TUNING | MODAL TUNING | MANUFACTURING/QUALITY |
|---|---|---|---|---|---|---|---|
| | | ENVIRONMENT | RESPONSE | | | | |
| APOLLO | 1. WIND SOUNDING BALLONS (JIMPSHERE)<br>2. S-IVB SHELL MODE CONTROL FEEDBACK<br>3. S-IVB PANEL FLUTTER<br>4. S-1C OSCILLATING PLUME<br>5. S 1C POGO SA-1<br>6. S-II POGO SA-2 → 8<br>7. GROUND WINDS VORTEX SHEDDING<br>8. S-II STAGE OSCILLATING SHOCK<br>9. ENGINE PROPELLANT LINE BELLOWS<br>10. S-IV PROP. UTIL. GUIDANCE & CONTROL COUPLING | S-IVB ZERO G SLOSHING | WIND GUST LOAD RELIEF | 1. INSTRUMENT UNIT (I. U.) LOCAL DEFLECTION<br>2. S-1C AND S-II PROPELLANT TANK HYDROELASTIC COUPLING<br>3. S-IVB SLOSH/INERTIA<br>4. S-IVB BAFFLE ORIENTATION<br>5. DYNAMIC TEST SUSPENSION SYSTEM COUPLING | | SATURN IB ELEMENT TUNING | |
| SKYLAB | 1. NON LINEAR APOLLO TELESCOPE MOUNT POINTING<br>2. 1/2 HZ. SYSTEM OSCILLATION | SOLAR WING LAUNCH FAIRING FAILURE | WIND GUST | | | | |
| VIKING | 1. VIKING SIMULATOR POGO<br>2. HELIOS POGO | | | | | VIKING SIMULATOR PAYLOAD/LONGITUDINAL MODE TUNING | |
| JUPITER | SLOSH CONTROL COUPLING | | | | | | |
| REDSTONE | 1. RATE GYRO POTENTIOMETER FEEDBACK<br>2. OSCILLATING SHOCK | | | | | | |
| SHUTTLE<br>a. SYSTEM | STOP SIGN FLUTTER (ON PAD FLUTTER) | 1. SRB IGNITION OVERPRESSURE<br>2. LIFTOFF ACOUSTICS<br>3. ORBITER WING DISTRIBUTION<br>4. SSME HYDROGEN LEAD POP (OVERPRESSURE) | 1. LIFT OFF LOADS SENSITIVITY<br>2. PAYLOAD LOADS SENSITIVITY<br>3. SRB HOLD DOWN BOLT LOAD<br>4. PERFORMANCE, LOADS, CONTROL COUPLING | 1. SRB RATE GYRO COLD PLATE LOCAL DEFLECTION<br>2. SRB/ET ROLL MODE<br>3. SRB CASE ELONGATION | | 1. LIFTOFF LOADS SENSITIVITY<br>2. PAYLOAD LOADS SENSITIVITY | |
| b. EXTERNAL TANK (ET) | | 1. PROPELLANT INLET DIFFUSER CRACKING<br>2. PROTUBERANCE LOADS (CROSS FLOW) | | | PROPELLANT INLET DIFFUSER CRACKING | 1. LOX TANK HYDROELASTIC DAMPING<br>2. UNSYMMETRICAL HYDROELASTIC COUPLING (LOX TANK) | |
| c. SOLID ROCKET BOOSTER (SRB) | AFT SKIRT THERMAL SHIELD FLUTTER | 1. PARACHUTE & SWITCH EARLY CLOSING<br>2. PARACHUTE HANGUP<br>3. WATER COLLAPSE LOADS<br>4. WATER IMPACT SKIRT/ NOZZLE LOADS REVERSAL<br>5. IEA ISOLATION<br>6. NOZZLE EROSION<br>7. SKIRT WATER IMPACT TRANSIENT LOADS | 1. PARACHUTE G-SWITCH EARLY CLOSING<br>2. PARACHUTE HANGUP<br>3. WATER IMPACT SKIRT/ NOZZLE LOADS REVERSAL<br>4. SKIRT WATER IMPACT TRANSIENT LOADS | 1. VISCOELASTIC MODES<br>2. PRESSURE STIFFENING<br>3. FILAMENT WOUND CASE COMPOSITE CHARACTERISTICS | 1. REENTRY ACOUSTICS (HIGH LEVELS)<br>2. INTERNAL MOTOR ACOUSTICAL TUNING | | NOZZLE EROSION |
| d. SPACE SHUTTLE MAIN ENGINE (SSME) | 1. HIGH PRESSURE LOX AND FUEL PUMP SUBSYNCHRONOUS WHIRL<br>2. BEARING LIFETIME (PUMPS)<br>3. PROPELLANT LINE CONVOLUTES (VORTEX SHEDDING)<br>4. BI STABLE PROPELLANT PUMPS | 1. STEERHORN FAILURE<br>2. LOX POST FATIGUE<br>3. MOV FATIGUE<br>4. LOX FLOWMETER CRACKS<br>5. ASI LINE FATIGUE<br>6. KAISER HAT/NUT FAILURE<br>7. CONTROLLER ISOLATION<br>8. TURBINE BLADE CRACKING<br>9. HEAT EXCHANGER COIL WEAR AND FAILURE | 1. ASI ORIFICE<br>2. CAPACITOR PROBE FATIGUE FAILURE<br>3. PUMP UNBALANCE<br>4. BEARING LIFETIME<br>5. PUMP SEALS ETC. RUBBING<br>6. MFV FATIGUE<br>7. IMPELLER FAILURE | | | 1. MOV SEAL FATIGUE FAILURE<br>2. ASI ORIFICE FAILURE | 1. WELD WIRE MIX UP<br>2. MOV SEAL FATIGUE FAILURE<br>3. PUMPS UNBALANCE<br>4. PUMPS SUBSYNCHRONOUS WHIRL<br>5. WELD OFFSET |
| SPACE TELESCOPE | 1. LINE OF SIGHT JITTER<br>2. THERMAL CREAK | | 1. LINE OF SIGHT JITTER<br>2. SCIENTIFIC INSTRUMENT VIBRATION FAILURE | LINE OF SIGHT JITTER | | | |
| GRAVITY PROBE A | INTERNAL DAMPING/ INERTIA COUPLING | | | | | | |
| HEAO | LAUNCH STAGE POGO | PAYLOAD THERMAL ISOLATOR | PAYLOAD THERMAL ISOLATOR | PAYLOAD THERMAL ISOLATOR | | | |
| IPS | | | PERFORMANCE LOSS | LATCHES | | | LATCHES |

not only measure large scale or mean environments but to get an accurate quantification of the wind gust down to 25 m wavelengths [1]. The attempt to measure these small gust effects met with frustration. The smooth skin balloons were unstable (type of flutter or vortex shedding). In a controlled, no disturbance environment, a rising sphere would oscillate (Fig. 5). A classical problem most would say. Dr. Jim Scoggins found the solution by observing the golf ball, then instead of small dimples, he added many conical spikes to the sphere's skin. The problem was solved. The sphere was stable (Fig. 6). The resulting data base used throughout NASA is evidence [2]. As a result, this modified sphere was named Jimsphere (after Jim Scoggins) as well as the data base (Fig. 7). Many have a small tie clasp with a miniature Jimsphere as a reminder of the agony one sometimes must go through the innovation required for solution to unexpected problems.

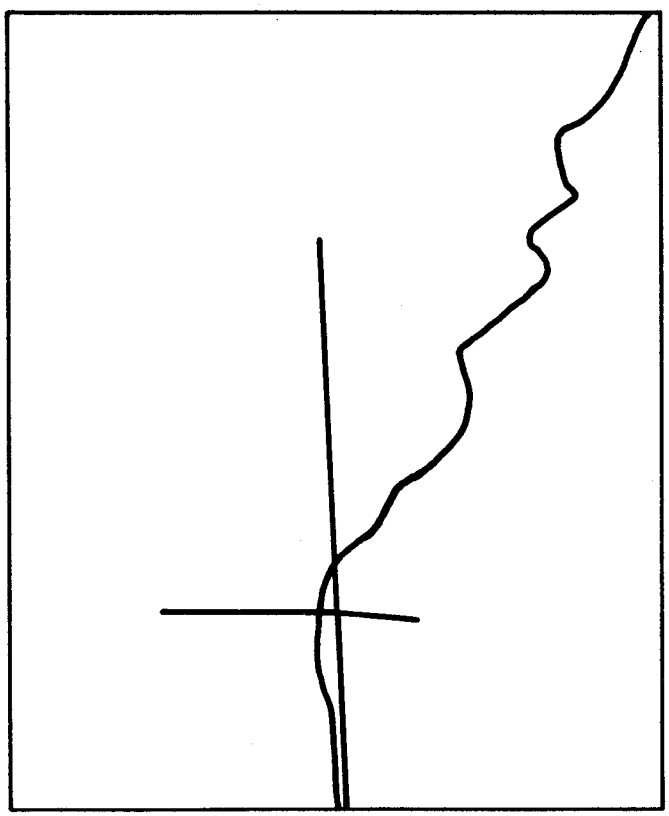

Figure 5. Time lapse trace of rose balloon released at 11:25 p.m., August 2, 1963, during stable atmospheric conditions and light winds.

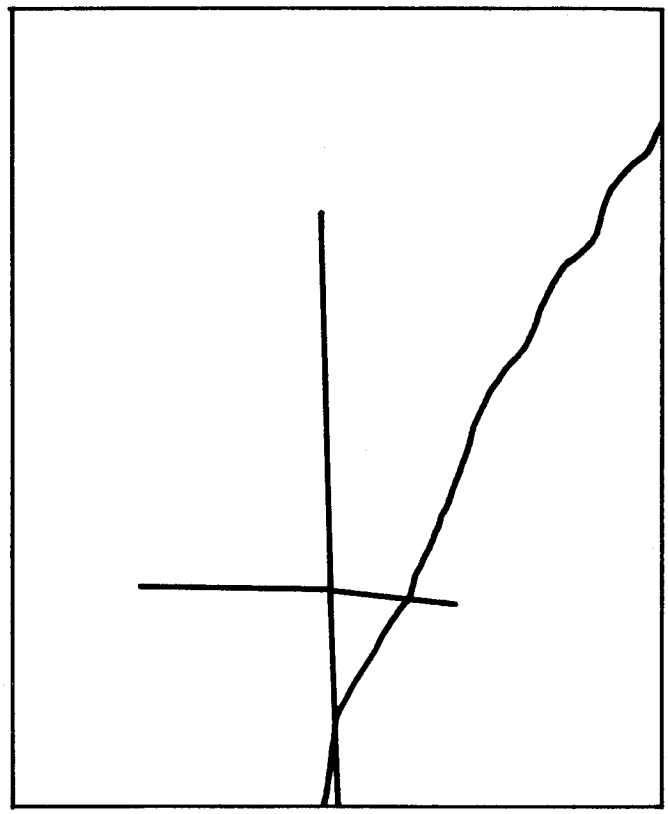

Figure 6. Time lapse trace of Jimsphere balloon released at 11:54 p.m., August 2, 1963, during stable atmospheric conditions and light winds.

## 3. Pogo

The most dramatic instabilities one experiences fall into the categories of aerodynamic flutter [3,4] and propulsion system structural coupling (pogo). Pogo occurs when a longitudinal structural oscillation is excited from some source such as combustion noise. This structural response sets up a pressure wave in the propellant system usually at the tank bulkhead. This pressure wave is amplified by propellant line modes including acoustics which are transferred through the engine system resulting in a fluctuating pressure in the propellant flow which results in a thrust oscillation. This thrust oscillation further amplifies the longitudinal structural mode creating the feedback or instability. The title "pogo" was coined from the children's pogo stick which bounces up and down on a spring and generally depicts

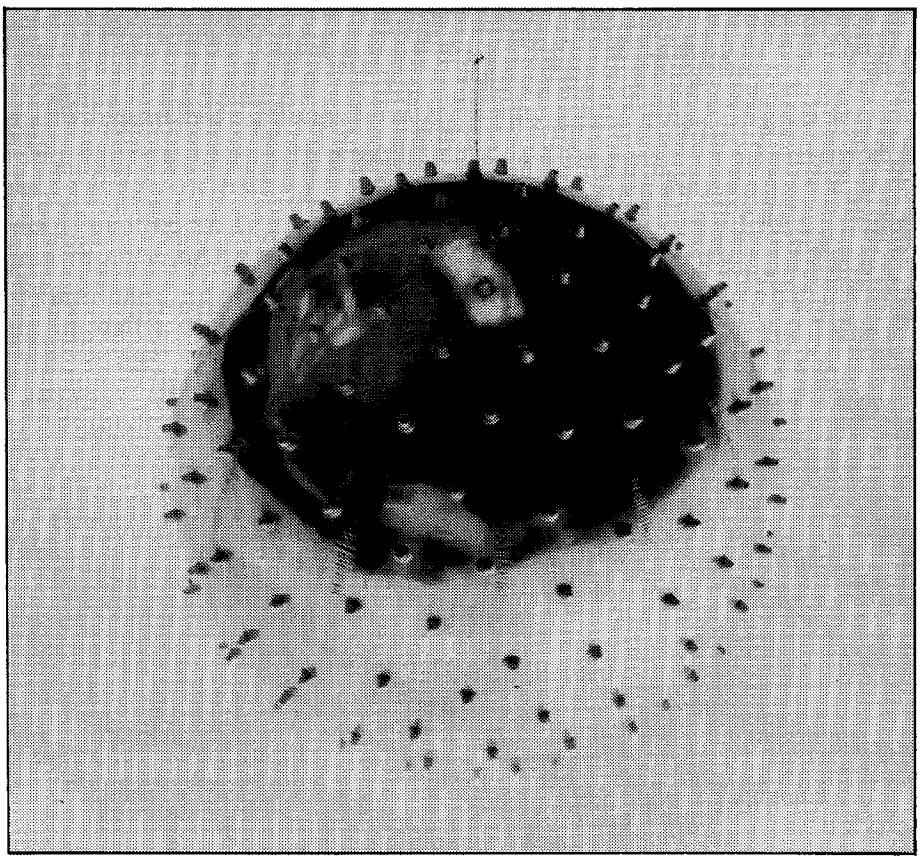

Figure 7. The Jimsphere balloon wind sensor.

what the space vehicle appears to do. Key parameters and models in predicting pogo are (1) structural dynamics model, (2) propellant line structural dynamic and acoustical model, (3) compliance of liquid at pumps, etc., (4) pump cavitation characteristics, (5) engine power head gains. Figure 8 shows these basic areas and the pogo loop. Space vehicles have been plagued with pogo problems. Four have been chosen for discussion. These are the ones experienced on MSFC developed launch vehicles or LeRC managed launch vehicles (Air Force developed) that MSFC has been involved in the solution approach. Other vehicles have had pogo but the author has no data associated with these.

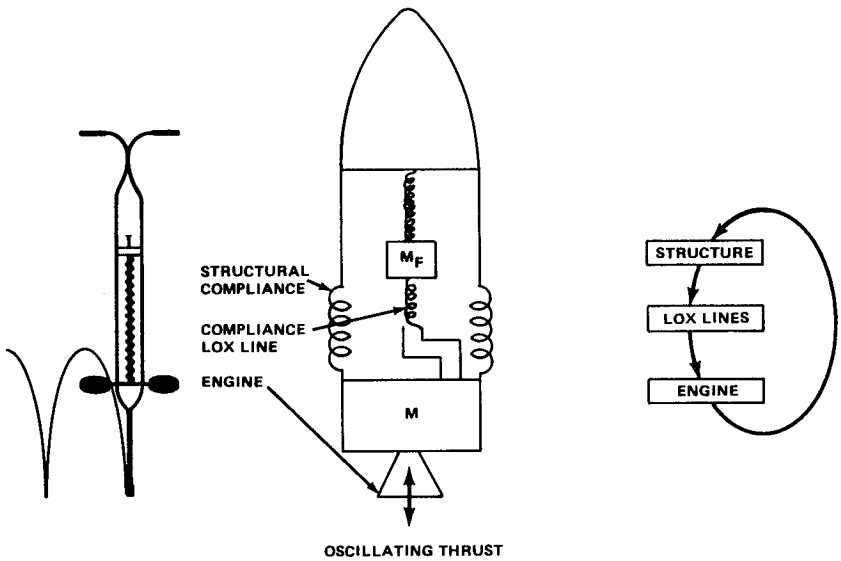


Figure 8. Schematic of pogo.

a. S-IC Pogo (AS-502 First Stage)

The Saturn V second launch experienced pogo during the first burn. The oscillation was near 5 Hz and produced both lateral and longitudinal accelerations of 0.3 g's and 0.5 g's, respectively, at the base of the LEM (Fig. 9). The primary structural mode was the first longitudinal free-free mode. The LEM was an unsymmetrical structure which also had a cross-coupled mode near 5 Hz. Thus, the reason for the lateral response [5,6]. The pogo instability acted as a forcing function driving the coupled LEM response. Conversely, the lateral LEM response was uncoupled from the pogo instability. An unrelated incident occurred during the pogo event. The SLA panel ruptured due to a flaw in the laminated honeycomb structure tearing apart from trapped sea level pressure (Fig. 10). This SLA failure caused some pain in that it focused investigation away from pogo, when in actuality, the two should have been pursued independently.

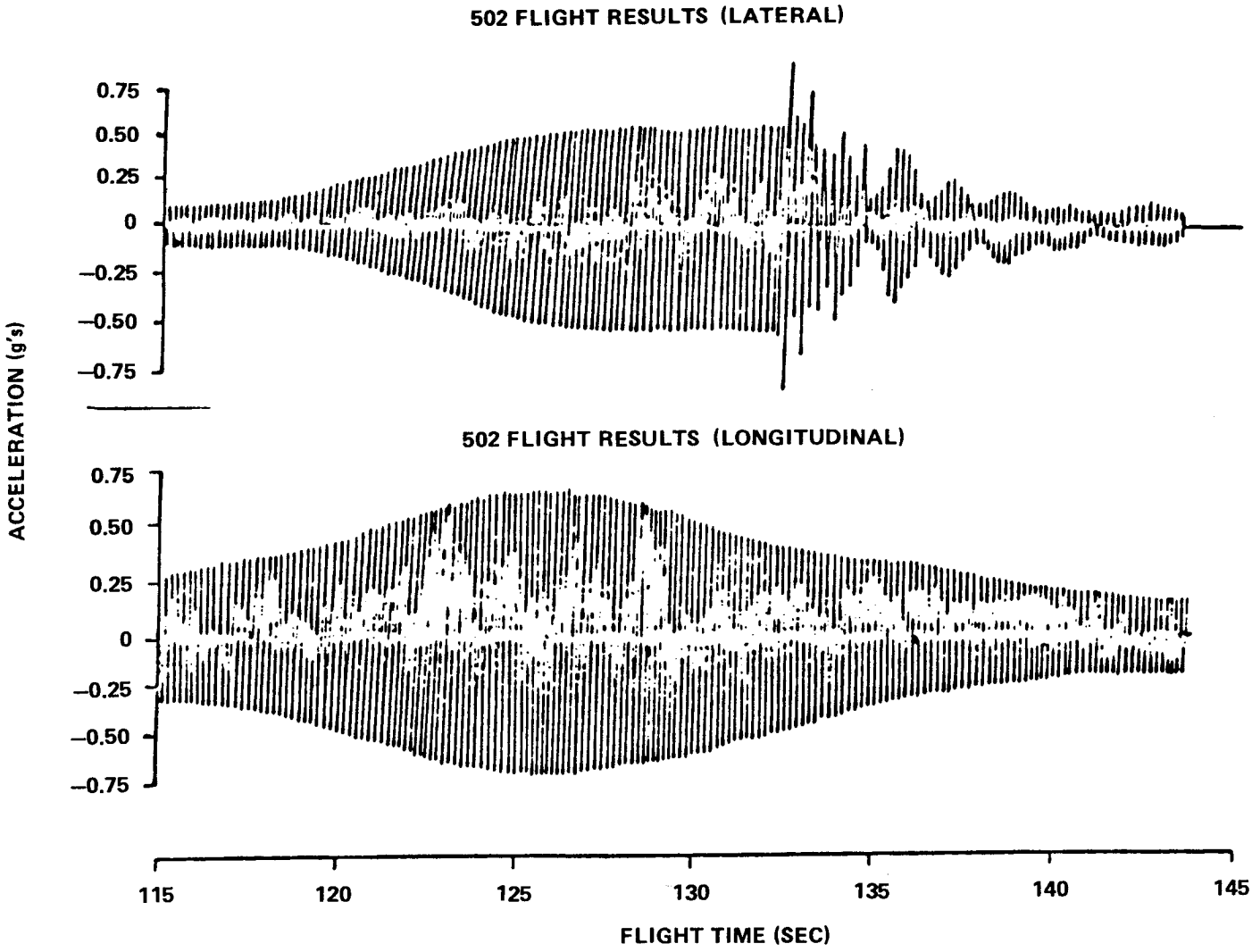


Figure 9. Flight results for the lateral and longitudinal acceleration of the LEM AS-502.

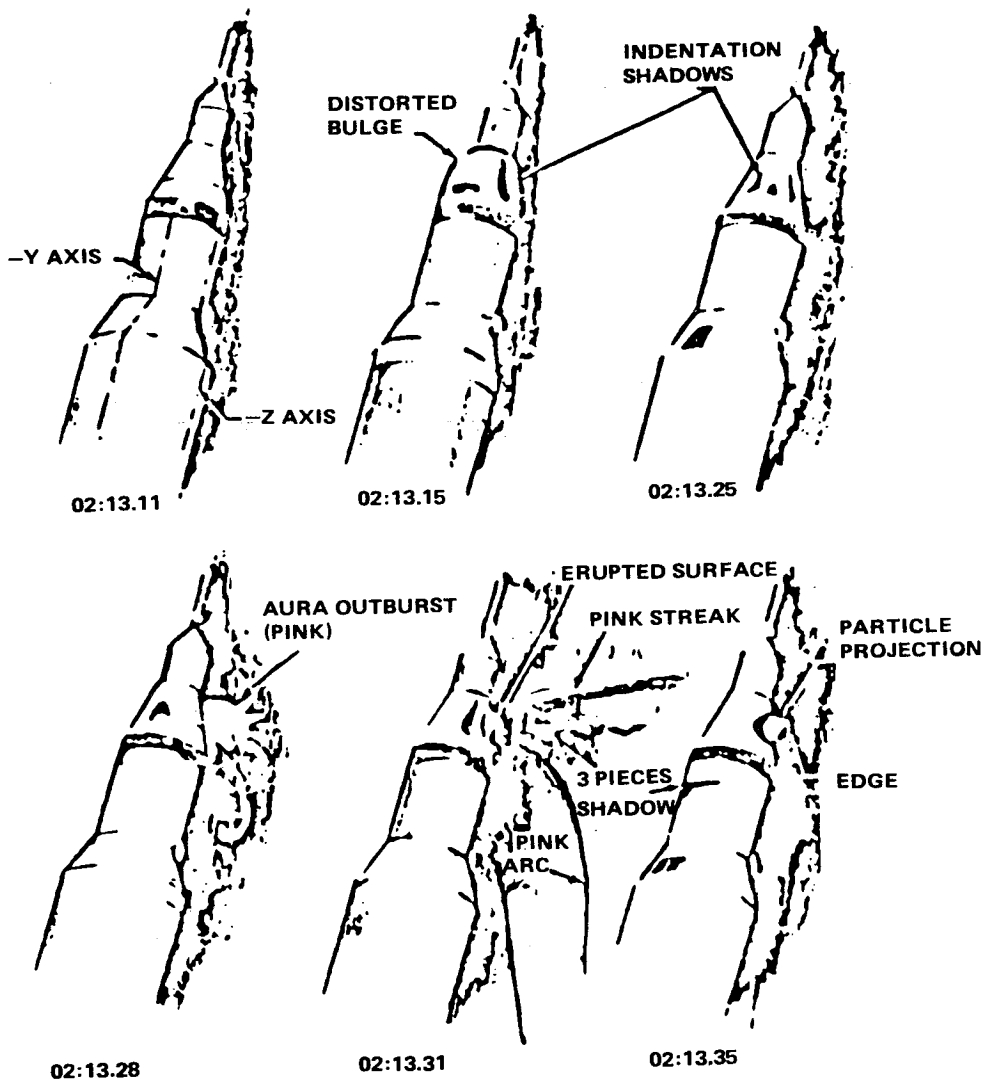


Figure 10. AS-502 SLA panel failure.

The response of the vehicle to pogo is shown on Figure 11, compared to an analytical model after the fact prediction of the response. Prediction of instability prior to flight was varied, most predicted a stable system while a few predicted slight instability. The early pogo models were, in fact, not accurate enough to handle the subtle changes that lead to problems. In fact, the first Saturn launch, AS-501, had no sign of pogo, while AS-502 had severe pogo. Why the difference? The only difference in the two vehicles was a 1,000-lb total weight change with a weight distribution change in the LEM area. Figure 11 shows the effect of this small weight change on the modal gain promiment in the pogo-coupled loop. This dramatically shows the effect of small changes creating large effects when a system is operating near a stability boundary and has a large energy source to feed the instability (engine thrust).

The problem was solved by incorporation of an accumulator in the fuel system (Fig. 12), detuning and desensitizing it. S-IC pogo did not reoccur during the Saturn program.

b. S-II Pogo (Second Stage AS-503-508)

The S-II stage of Saturn had a very intriguing and baffling series of pogo or so-called forced oscillation response culminating in the near disastrous AS-508 flight. The oscillation occurred early in

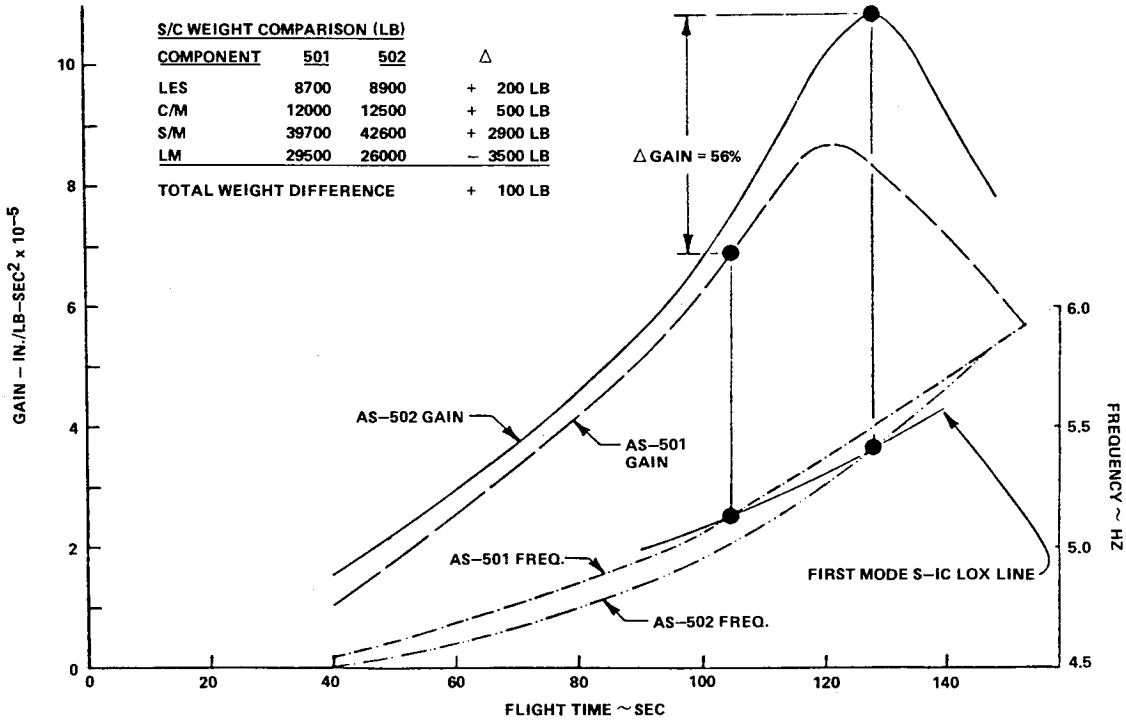


Figure 11. AS-501/AS-502 first mode longitudinal structural dynamic characteristics comparison.

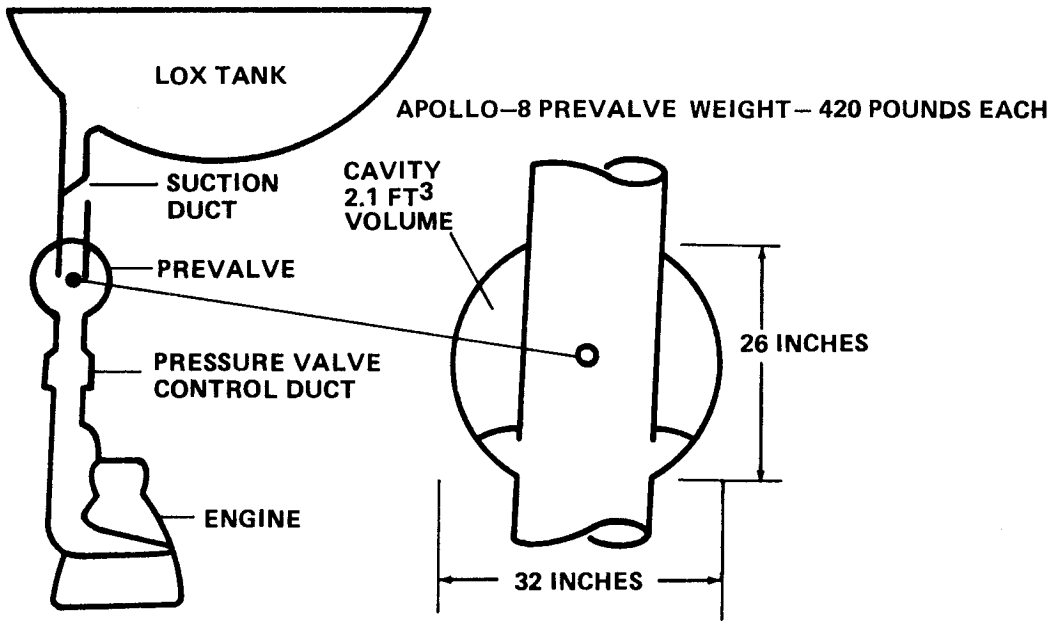


Figure 12. S-IC accumulator.

the S-II stage burn and reached large acceleration amplitudes (thrust frame cross beam) of 33 g's at 16 Hz, and the resulting large pressure oscillations shut the engine down at 160 sec of S-II burn. Figure 13 shows a short portion of the pressure in psig and the acceleration in g's. Notice the nonlinearity of the pressure and the linearity of the structural oscillations.

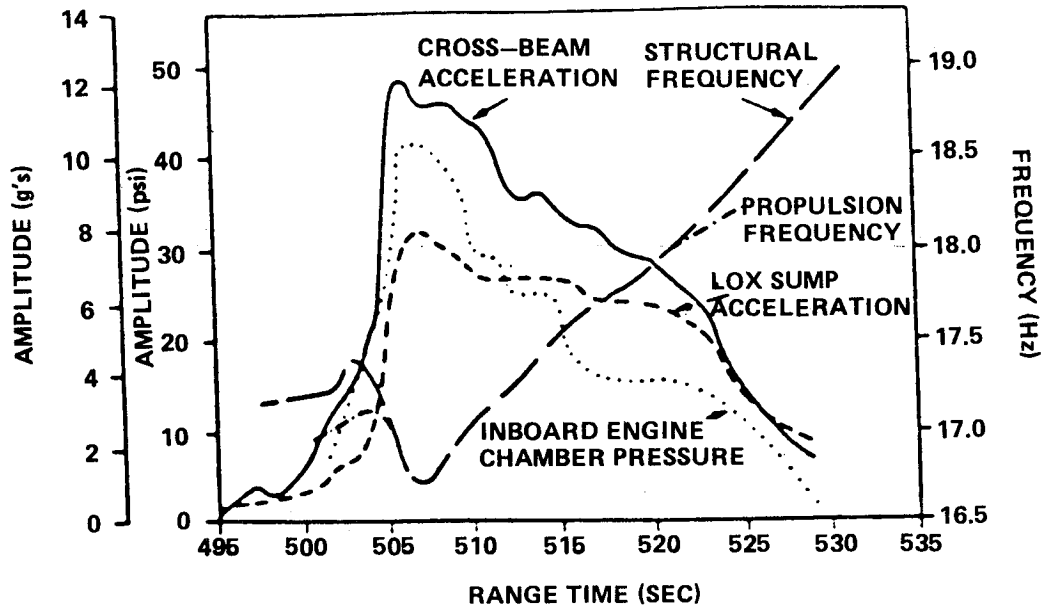


Figure 13. AS-504 flight data.

Looking into the details of each flight up to and including AS-508, one discovers quickly the intricacies and so-called anomalies of pogo. Pogo was not apparent for the S-II stage (probably because of poor instrumentation) until AS-503. AS-503 had a self-limiting, local pogo-type oscillation near 480 sec flight time. Concern was raised in the Pogo Working Group over this oscillation and potential vehicle problems. After much discussion and analysis, it was generally agreed that the next vehicle could be made pogo safe by increasing the ullage pressure which would raise the lox line frequency and decrease the pump gain [5,7].

AS-504 did not follow predictions. In fact, it did the opposite. Between 500 and 540 sec, a 17 Hz oscillation occurred locally in the thrust frame region and reached a peak amplitude of ±12 g's (Fig. 14). Again, the oscillation was self-limiting. A more detailed look at pump and engine test data revealed that indeed the increase in ullage pressure would bring into play nonlinearities which would increase the gain and thus the instability.

By now, it was becoming clear that many things were missing; more data must be acquired. Instrumentation of flight vehicles had to be improved in order to acquire better flight data. The ability to model the bulkhead hydroeleastic characteristics was very poor and limited to the first mode. Elimination of this shortcoming required updated analysis and a comprehensive hydroelastic test program for data and verification. Additional line and engine tests were required to better define these characteristics, particularly since no analytical approach was available. In the interim, in order to maintain launch schedules, it was decided to shut down the S-II center engine 60 sec early and avoid the pogo problem. This certainly appeared to be a winner, since no real performance loss was incurred. Several members of the Pogo Working Group, while agreeing with the approach, felt the problems were not licked. Others became complacent, attempting to reduce the effort being expended. The lack of real concern for the S-II pogo is exemplified by the coined identification of the S-II pogo characteristics as "mini pogo,"

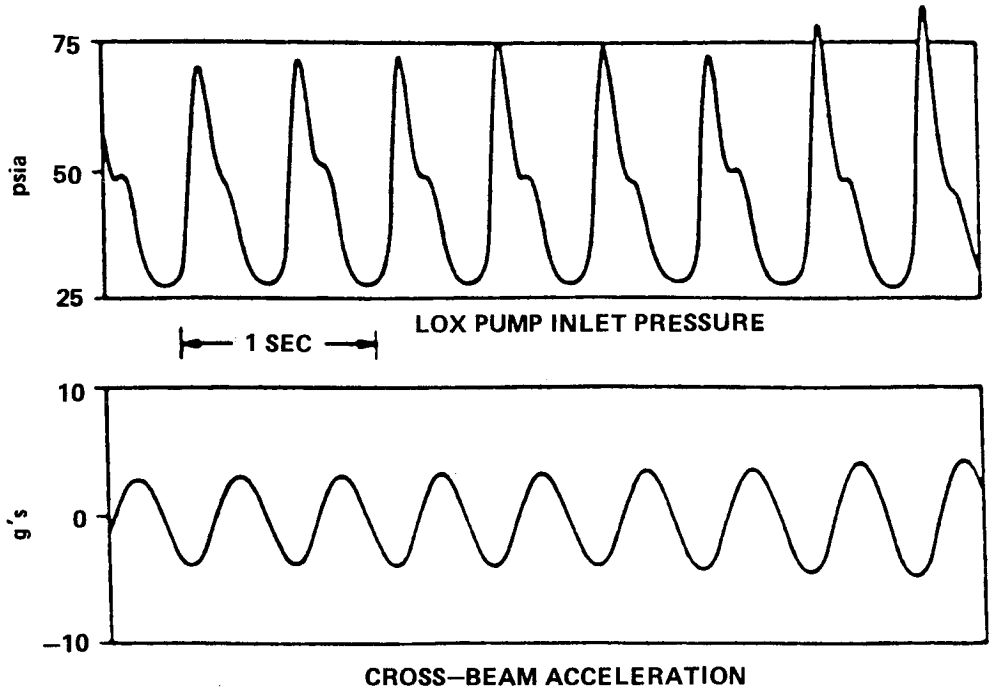


Figure 14. AS-508 flight response.

because of its localized and self-limiting characteristics. The AS-505 and AS-506 flights added to this attitude, since no pogo was observed using the center engine early cutoff. Improved instrumentation was still not on the flights and was planned for AS-507.

AS-507 was the next flight to experience significant pogo oscillations. Several bursts of pogo oscillations, termed "footballs," occurred in the vehicle response showing that the pogo loop was marginally stable at best. Figure 15 is an amplitude comparison of several S-II flights. The appearance of the footballs on the AS-507 flight caused much soul searching, analysis, etc. Nonlinear analysis was showing stable limit cycles. This led to the stable limit cycle theory. Many experts were disagreeing. Better line, engine, and hydroelastic data were becoming available, and the MSFC linear stability analysis was showing marginal to unstable conditions for AS-508. In spite of the variety of viewpoints, the stable limit cycle position was recommended to management and AS-508 was safe to fly.

AS-508 was the biggest surprise yet. Between 120 and 160 sec, oscillations started at 16 Hz producing an amplitude of 32 g's or greater. The poor prediction was due to inadequate nonlinear characterization of the system. After the fact, modal analyses were conducted using three flights and test-determined nonlinearities (Fig. 16), pump inlet compliance, nonlinear damping, and nonlinear pump gain, and showed that by using these nonlinearities, a reasonable duplication of all S-II pogo flights could be obtained without simulation adjustments other than known vehicle flight-to-flight differences. Figure 17 shows a comparison of the AS-508 delta PC trace and the simulation of the AS-508 delta PC using the nonlinear response analysis showing good agreement. This approach becomes important for verification of the fix since the accumulator had to be filled after S-II engine start.

The violent pogo oscillation occurs because the pump operating pressure head rise drops below the knee of the curve at Pcr, hence deep cavitation and large nonlinearities. Why did AS-508 go berserk and AS-507 did not? It is believed that small differences kept the oscillation below Pcr and, therefore, the nonlinear damping produced a stable limit cycle, while AS-508 reached an amplitude where the nonlinear damping was overridden by the nonlinear pump gain characteristics (Fig. 18).

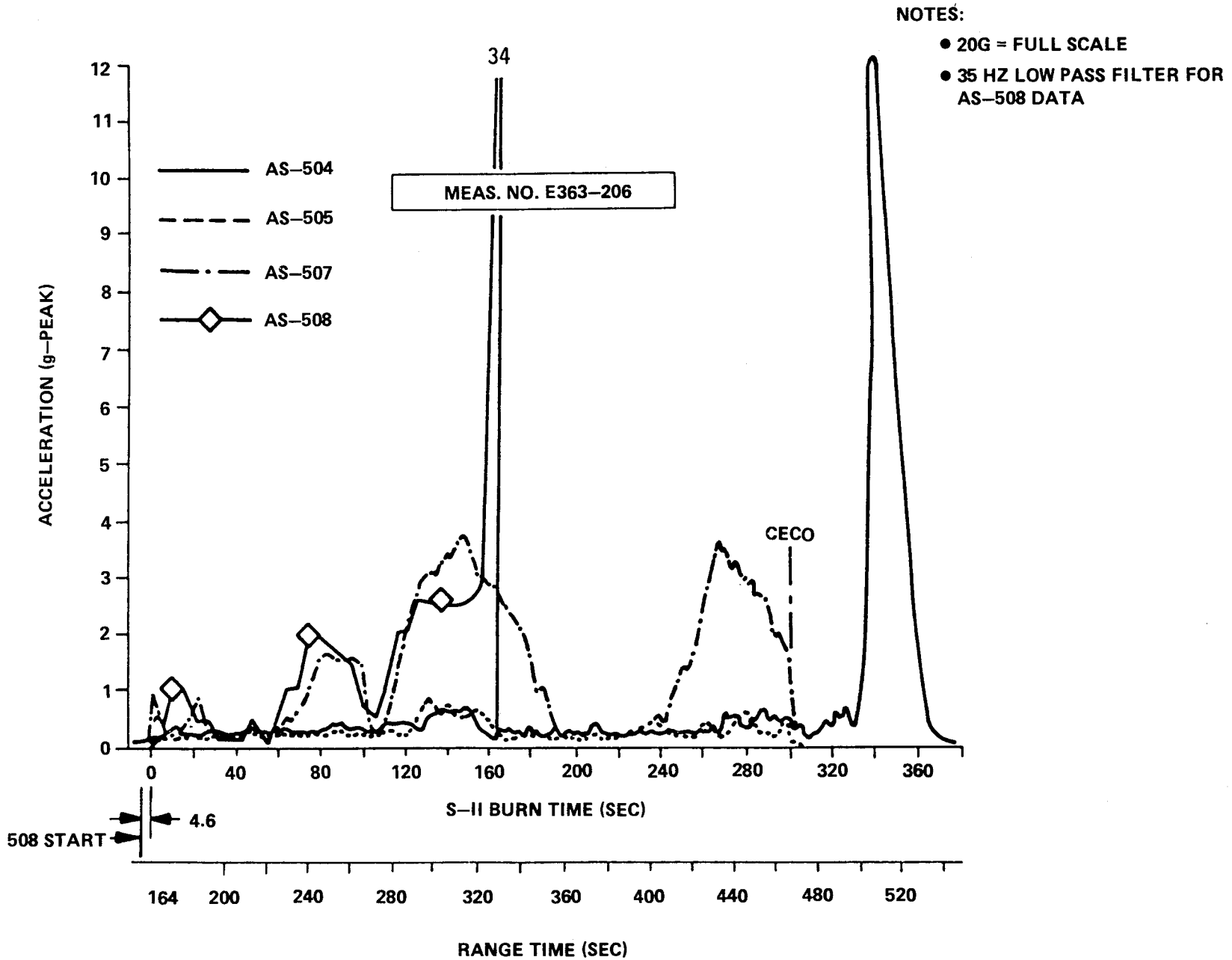


Figure 15. Comparison of telemetered center engine thrust pad acceleration envelopes.

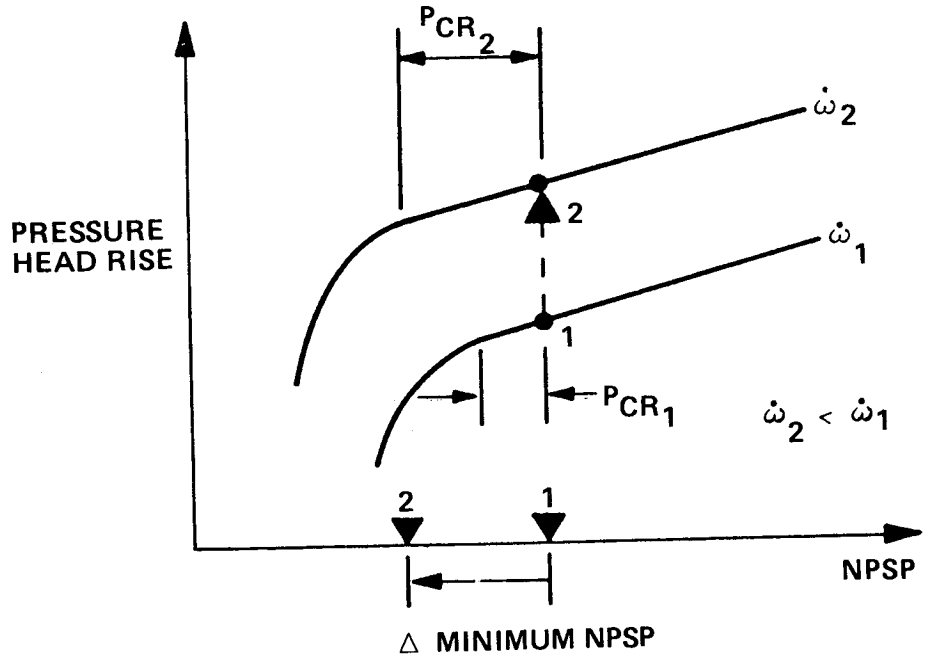


Figure 18. Effect of changing operating point on engine performance curves.

After AS-508, there were no doubters. The S-II pogo problem had to be fixed. This was not to be easily accomplished. Several different techniques were pursued as fixes. Helium injection into the propellant line would lower the lox line frequency and decouple the system. Because of potential system impacts, this was ruled out. The J-2 engines could not be started with helium being injected into the line. It was finally decided to put a wrap around accumulator on the line near the pump and fill it after starting the engine. This meant that the line frequency would sweep the bulkhead and cross beam modes/frequencies introducing momentary resonance and instabilities. It was feared that these oscillations might trigger nonlinearities and become catastrophic. Also, failure modes could cause partial filling of the accumulator and worse stability problems. Much analysis and detailed design considerations were required to eliminate problems and verify they would not occur. Future flights, pogo free, were icing on the cake.

c. Titan-Centaur/Viking

The Titan-Centaur was used as the launch vehicle for the Viking probes. Two very interesting and enlightening incidents occurred during this program. The first was a development launch using a Viking simulator. Two things occurred that led to a pogo oscillation (self-contained) that Viking could not sustain (structural loads limitations). (1) The Viking simulator dynamic mode (only mass simulate Viking, not dynamically) tuned with the overall vehicle mode greatly reducing damping and increasing the modal gain important to pogo. (2) The vehicle stood in a very cool wind changing the propulsion system gain. These two apparently minor changes show the sensitivity of systems that have a propensity of closed loop unstable oscillations with large energy sources.

The next launch using this vehicle was the German Helios spacecraft. A spacecraft somewhat comparable to the Viking in mass and dynamic characteristics. Since the Helios was not as load sensitive as the Viking, it was decided to take the pogo risks and launch without fixes. Again, surprises came.

This vehicle had a pogo oscillation larger than the Viking simulator launch and other previous Titan-Centaur launches. Again, two things were significant in the pogo oscillation. (1) The coupling of the payload with the launch vehicle (smallest factor). (2) The vehicle sat two days on the pad fueled. The propellant became effervescent (bubbles formed) changing the line/cavitation bubble frequency, thereby increasing the closed loop gain.

The message was clear: Titan must have pogo suppressors installed before Viking could fly. History shows that the fix was successful as was Viking. The message was don't flirt with pogo, design it out.

Other launch vehicles have had small pogo-type oscillations that were not damaging in nature. Examples are Atlas HEAO, Saturn S-IVB stage, and Titans.

This very brief discussion has shown the very interesting and potentially dangerous aspects of structural propulsion closed-loop coupling, clearly indicating the requirement to design out sensitivities of the system to this type coupling. Illustrated dramatically were the large effects of very small and apparently insignificant changes.

4. Ground Winds (Vortex Shedding), Panel Flutter, Separated and Oscillating Shocks, Control Feedback Flutter

Aeroelastic instabilities are classical in nature and are well documented. Reference 8 provides an excellent history and summary. Several excellent textbooks are also available. These type instabilities result from a structural oscillation setting up an aerodynamic (or flow) force phased such that the structural oscillation is reinforced. They take many forms, such as classical flutter, vortex shedding, divergence, buffet, stall, etc. Readers desiring more information should go to the numerous textbooks, articles, etc.

a. Ground Winds Vortex Shedding

The Saturn V Apollo was analyzed early for classical vortex shedding using both analytical and scale model testing. Being essentially a cylinder, the vehicle showed clear vortex shedding problems, particularly since it must spend up to 30 days on the pad exposed to ground winds. As a result, a system was designed which damped the vehicle against the test stand. In addition, a wind velocity criterion was used which required installation of the damper when above critical wind levels were being predicted. Also, dampers were used during any free standing time on the pad. Figure 19 is a picture of Saturn V with dampers installed. Figure 20 shows the maximum ground winds (speed) versus bending moment capability. Figure 21 translates these critical wind velocities by critical axis.

Space Shuttle was not a configuration susceptible to classical vortex shedding; however, it falls into the arena of the classical stop sign flutter, named from road signs fluttering at certain wind speeds. Scale model wind tunnel tests verified the stop sign flutter potential. The flutter limit was determined relative to the pad Shuttle interface stiffness. The final design showed no stop sign flutter problem due to the naturally large torsional stiffness arising from the vehicle configuration and the four holddown/supports on each SRB.

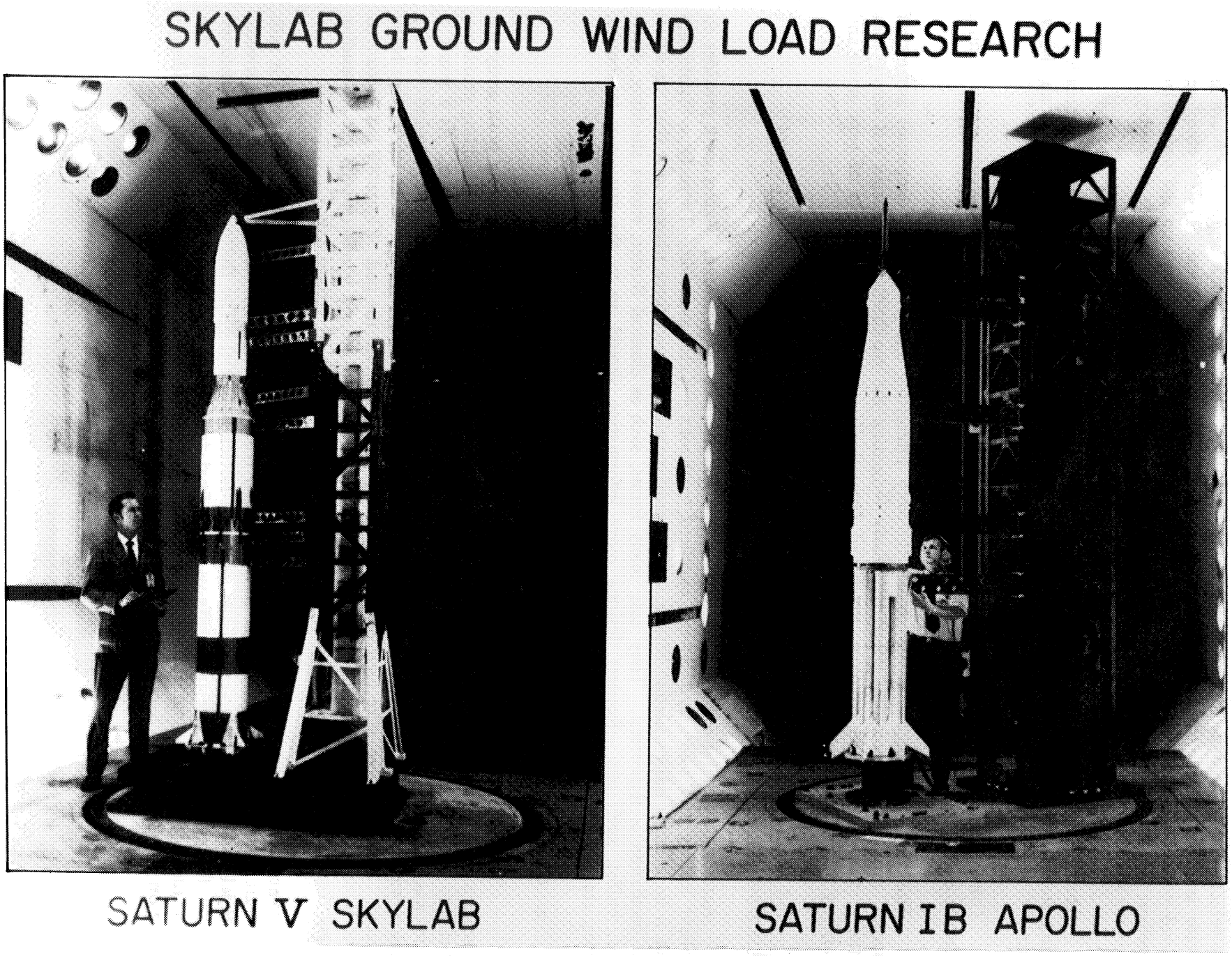


Figure 19. Saturn V with dampers installed.

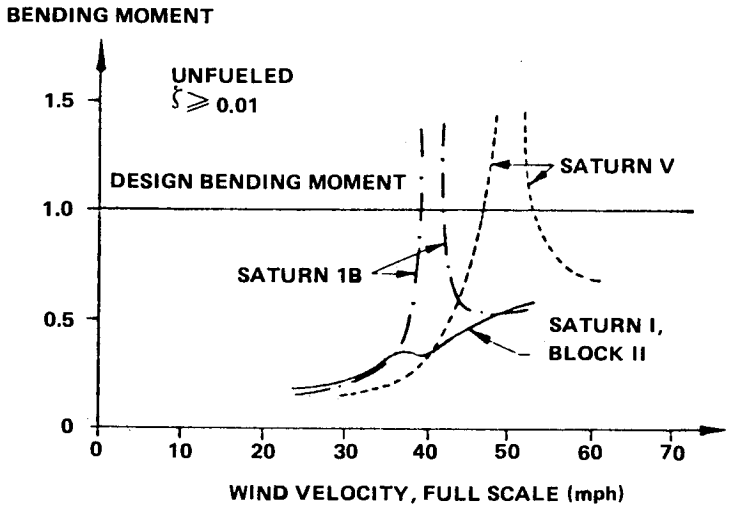


Figure 20. Saturn V ground wind speed and bending moment capabilities.

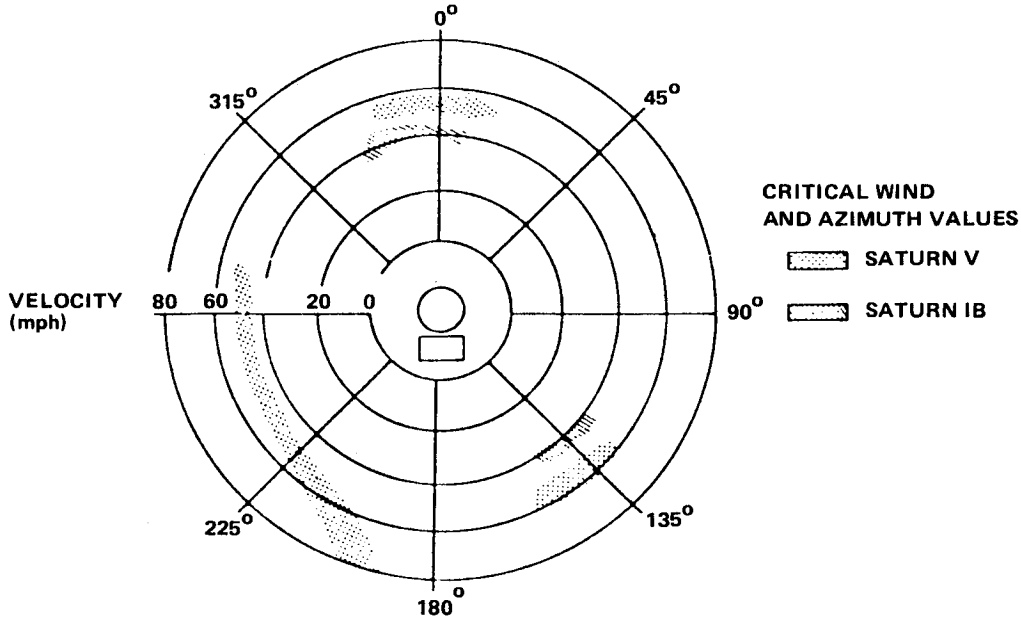


Figure 21. Saturn V critical wind velocities by axis.

b. Panel Flutter

Panel flutter has been a concern on all space vehicles. Most were analyzed, tested, and shown not to be a problem. The Saturn Apollo S-IVB Stage in early analysis and wind tunnel tests showed a potential panel flutter problem. Initially, a flutter suppression kit was installed and flown. After the flight using flight instrumentation, it was shown that the delta P, buckling, threshold durations, etc., was such that no flutter instability existed, and the kit was not flown on subsequent flights.

c. Oscillating Shocks Waves

Separated and oscillation shocks have been a major concern in design of space vehicles, in particular the cylindrical ones with various diameters with transition zones (cones) between stages. Experiences bear out the validity of these concerns. The S-IC Stage of the Saturn V Apollo had an

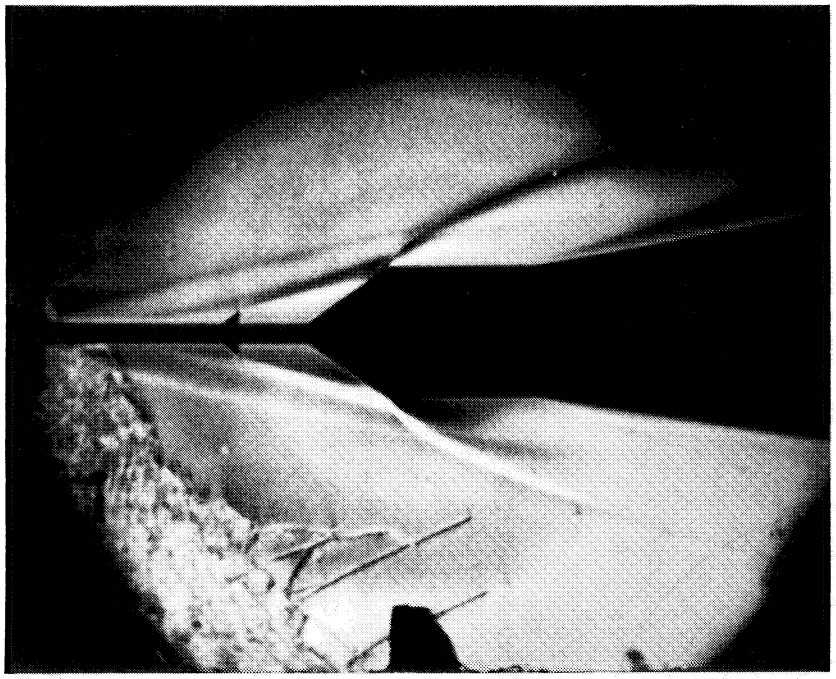

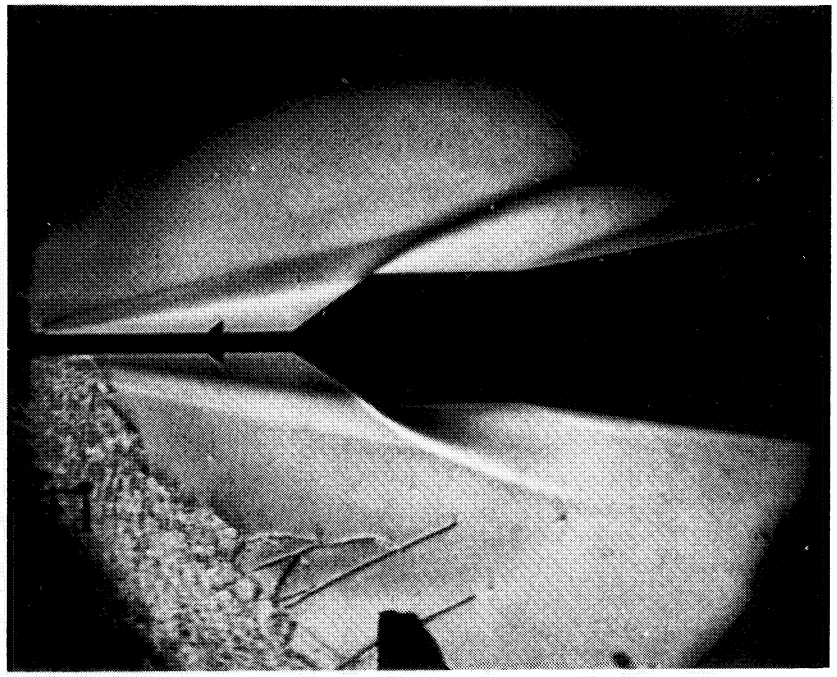

$T_W/T_T = 0.22$
$M_\infty = 6.00; \alpha = 0^o$

$T_W/T_T = 0.88$
$M_\infty = 6.00; \alpha = 0^o$

SCHLIERENS OF SATURN IB/APOLLO/2ND STAGE FLIGHT CONFIGURATION

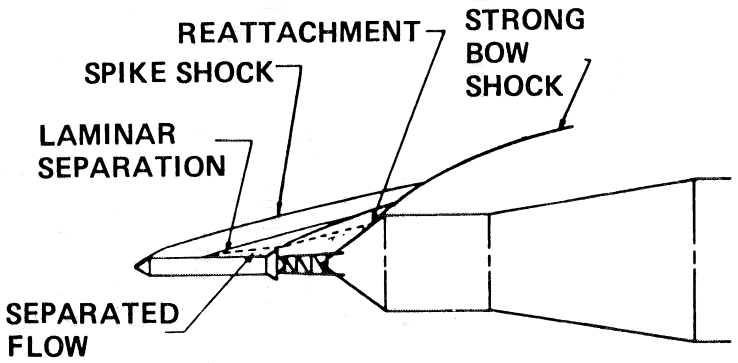


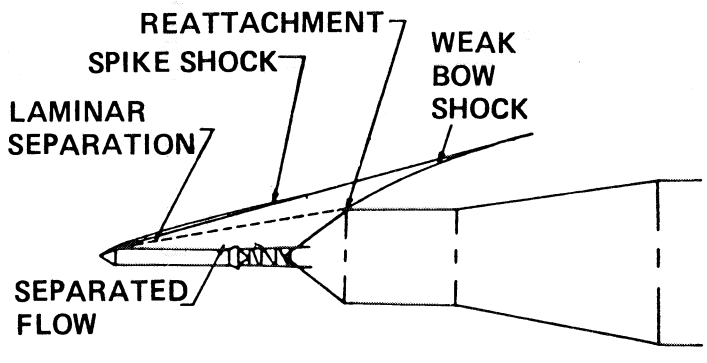


ENGINEERING INTERPRETATIONS OF SCHLIERENS

Figure 22. Typical shock wave.

oscillating, separate shock at the rear that coupled with the plume causing an overall oscillation of the shock and plume. Detailed movies of this area during ascent clearly showed the oscillation. This oscillation did not couple with or drive the structure; therefore, nothing was done to eliminate it. The S-II Stage did have an oscillating separation shock which drove the panel, creating loads problems. Longitudinal stringers were installed as stiffeners for stabilization, solving the problem. Figure 22 shows a typical shock obtained from wind tunnel (Apollo S-IVB fairings). The shortness of this discussion does not imply corresponding lack of concern or effort. The opposite was true. Much analysis and wind tunnel testing was used to clear the design.

d. Control Feedback Instabilities

1) Jupiter Sloshing Instabilities. A closed loop control instability occurred on the early Jupiter firings. The Jupiter was a liquid propelled military vehicle. Sloshing propellant coupled through the control system and became unstable. This instability saturated the control system, the vehicle went out of control during maximum dynamic pressure regime of launch, and broke up. The results were dynamic with beautiful fireworks high in the sky, but very costly to the program. The instability was aggravated by the trajectory tilt program. The tilt program was a series of discrete steps instead of a continuous functional change which started the oscillation and reinforced the amplitudes of the wave through a forced oscillation [9,10]. At this early phase in the rockets and space age, models did not exist for analyzing problems of this type. As a result, several things happened. Propellant sloshing data had to be obtained quickly. No analytical solutions were readily available. A test program was started that included both scale model and full scale testing. A slosh suppressor had to be found before the next launch. In order to meet this goal, a full size propellant tank filled with water was placed on a railroad car. The railroad car was bumped against the track end stop as an excitation source. The first test was without suppression devices. Water was used to simulate propellant to establish frequencies, etc. Various devices were tried next as suppressors. The one chosen was called beer cans, which consisted of long perforated cylinders with flotation spheres at the top. The entire surface of the propellant was covered with these devices (Fig. 23). The test showed more than adequate suppression was achieved, and the next launch was slosh free. In the meantime, other solutions were pursued including development of analytical characterization of the sloshing propellant. This resulted in the development of slosh baffles [rings inside the tank that became part of the structural stiffness (Fig. 24)], as the most effective analytical means of suppressing slosh, and parametric test data were acquired for oscillating propellants in both zero and high g fields. All space vehicles today are analyzed and designed with this phenomenon in focus as a potential problem. The lack of analytical and experimental data prior to launching as well as lack of experience in these type problems led to the failure of the Jupiter missile due to propellant sloshing control system coupling. The fix was fairly easy and did not impact flight schedules drastically. This is not always the case and repeats of this type instability should be avoided if possible. The innovative way special tests were conceived and conducted to meet launch schedules should be a lesson in this age of precise testing, etc. [10,11].

2) S-IVB/IU Shell Mode Coupling. Another example of control instability was the shell modes of the S-IVB/IU coupling with the control system (rate gyros and reaction jet control system). The amplitude was limited by the maximum pulse level of the jets. This was a classical structural control interaction instability. The occurrence did not cause any real problem to the flight; however, due to concerns of gyro saturation, etc., the problem was fixed by filtering the shell modes signals out of the control loop.

3) S-IV Guidance and Propellant Utilization System Coupling. A very interesting and unusual instability occurred on the S-IV stage of the Saturn I vehicle due to a coupling between the guidance system and the propulsion system. A propellant utilization system was used which measured the propellant levels in each tank changing the mixture ratio so that better efficiency could be obtained

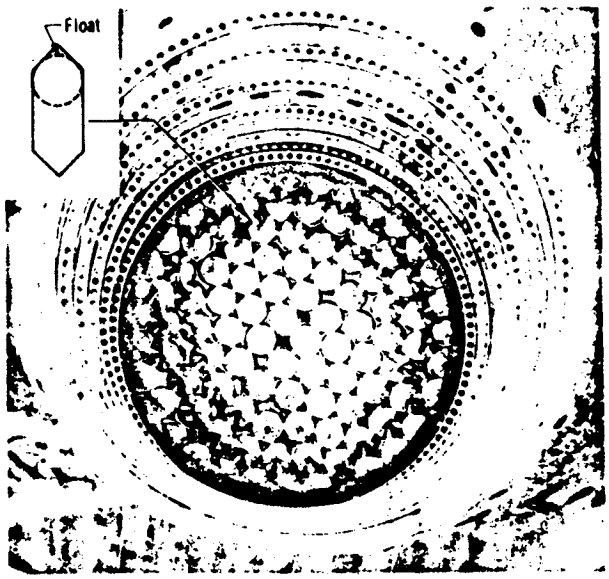


Figure 23. Floating can slosh suppression device.

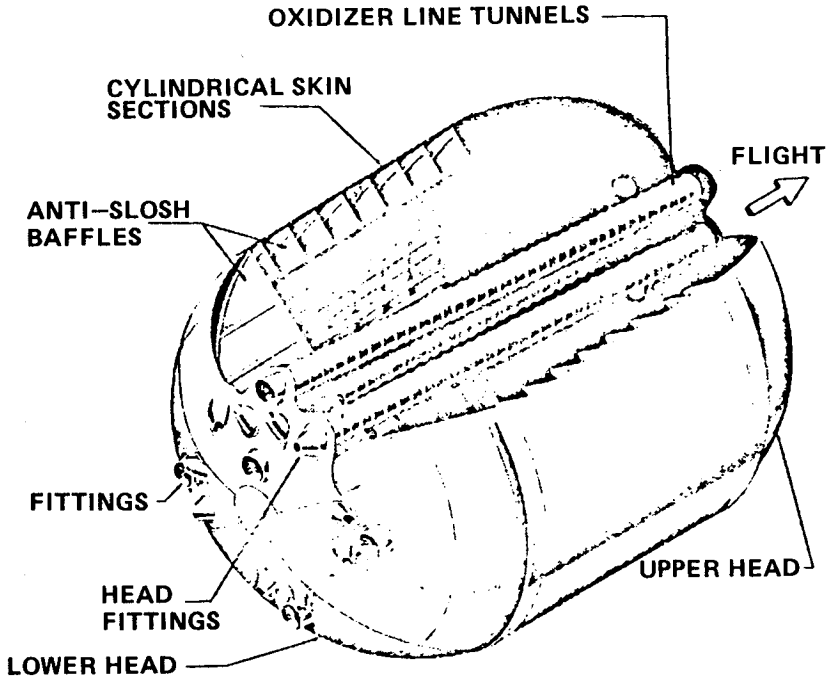


Figure 24. Typical ring baffles for sloshing.

through simultaneous propellant depletion. This information was fed into the guidance system. When a guidance command was given, the vehicle rotated causing propellant sloshing, which created changing propellant levels, hence more guidance commands. As the guidance gains increased towards the end of flight, the system became unstable. Simulations that had trajectory, control, guidance, propellant utilization system, and sloshing were required to understand the problem and design filters to solve the problem (Fig. 25). Digital and analog simulations were the main ones. Luckily, this problem was uncovered and solved just prior to the 201 flight circumventing an unstable situation and possible loss of mission [12].

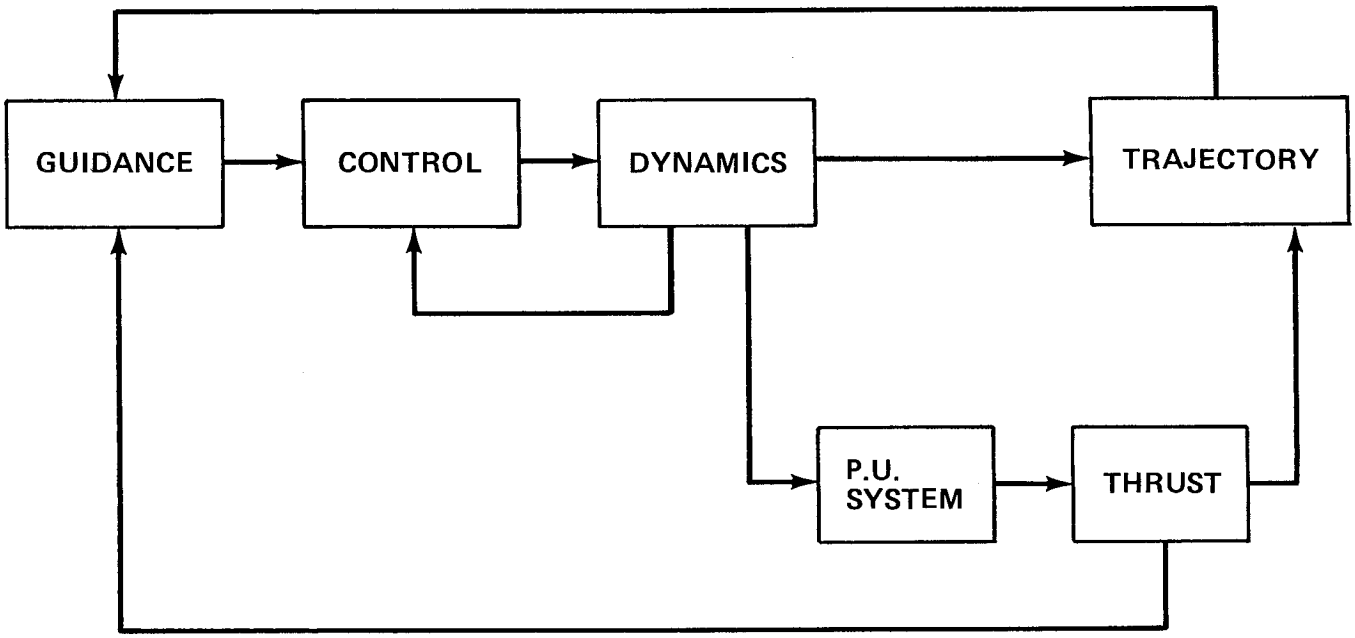


Figure 25. Systems integration schematic.

4) Clustered Engine Cross Talk. One control problem with clustered engines stands out. During static firing of the cluster and engine gimballing, the engines started cross talking due to the flexible thrust frame. Additional stiffness was added after simulations verified the fix. The problem illustrates clearly the need for hot firing control system checkout through gimballing, etc. Dynamic test did not uncover this problem.

e. Classical Flutter

An unusual flutter problem occurred on the Space Shuttle SRB aft thermal shield (heat shield) (Fig. 26). This heat shield was installed to protect the APU system during ascent flight and to augment protection during SRB reentry. During water impact, the shield had to rip out at fairly low load levels; otherwise, it would introduce substantial damage to aft skirt and nozzle hardware. This limited the stiffness that could be designed into the shield. During reentry, the SRB comes in nozzle first and at an angle of attack in the neighborhood of 100 deg creating cross flow on the shield. As a result of the q (reentry maximum dynamic pressure), the shield flutters and destroys itself. This phenomenon was observed during reentry acoustics environment wind tunnel testing. A major effort was expended trying to characterize this flutter and develop suppression devices (ones that would be very stiff during max q and then fail at water impact). It was decided to fly the first Shuttle flights without fixes and see what happened (not a manned flight safety issue). The shield did flutter and destruct; however, the thermal environments were not adverse. The end result has been to accept the flutter and lose the heat shield during reentry. In fact, a lighter shield has been designed based on eliminating reentry design requirements and which meets all ascent design requirements.

f. Flow Instabilities of Convoluted Bellows

The last area which falls into the flutter category is flow instabilities of convoluted bellows. The instability is one of vortex or turbulence being set up on the down side of the convolute reinforcing the natural modes of the line. High pressure lines on the Saturn engines failed due to this instability,

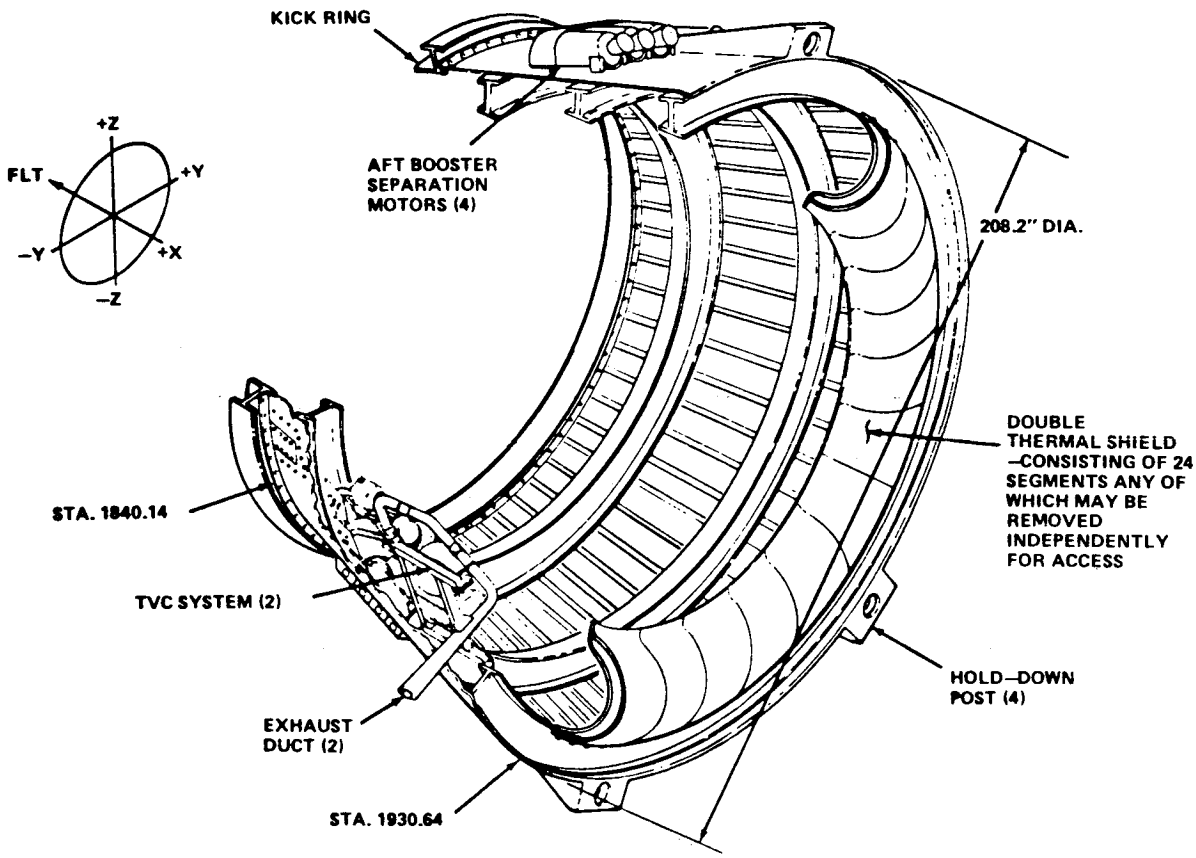


Figure 26. SRB heat shield.

creating many problems early in the program. After much work (analytical and test) at Southwest Research Institute, criteria and corresponding monograms for predicting problems were generated. In addition, it is the current practice to put smooth liners inside all bellows that have potential problems.

5. Rotary Dynamic Instabilities

Fluid elastic vibrations are characterized by a critical flow velocity, below which the vibration amplitudes are small, and above which the amplitudes increase very rapidly. The more familiar examples of fluid elastic vibration are seen in flutter and transmission line galloping, involving single bodies essentially isolated in a uniform flow field. The excitation mechanism is mainly due to the variations that occur in the lift force as the angle of attack changes. Since the change in angle of attack is a direct result of the vibrational motion, the oscillations are self excited. Under certain conditions, isolated circular cylinders can develop plunging oscillations (galloping), and this phenomenon is associated with changing angle of attack. Fluid elastic or motion interaction in turbomachinery fit to some extent these simple examples; however, the mechanism is much more complex.

Various types of instabilities have been experienced in the world of turbomachinery, all of which are classically treated in literature; however, specific problems and solutions associated with space vehicles have only recently appeared in publications. Due to the high performance of these systems and extremely high energy concentration, these problems are very complex and difficult to analyze.

a. Bistable Pumps

One classical problem which becomes more critical on high performance, throttleable engines is the bistable pump. This is a condition that exists on pumps optimized at the high output side and occurs at some point off optimum, say 65 percent power level. At this point, a hysteresis loop exists in the performance indicator, lift versus angle of attack (Fig. 27). This hysteresis loop at low angles of attack (low speeds) create the bistable oscillation.

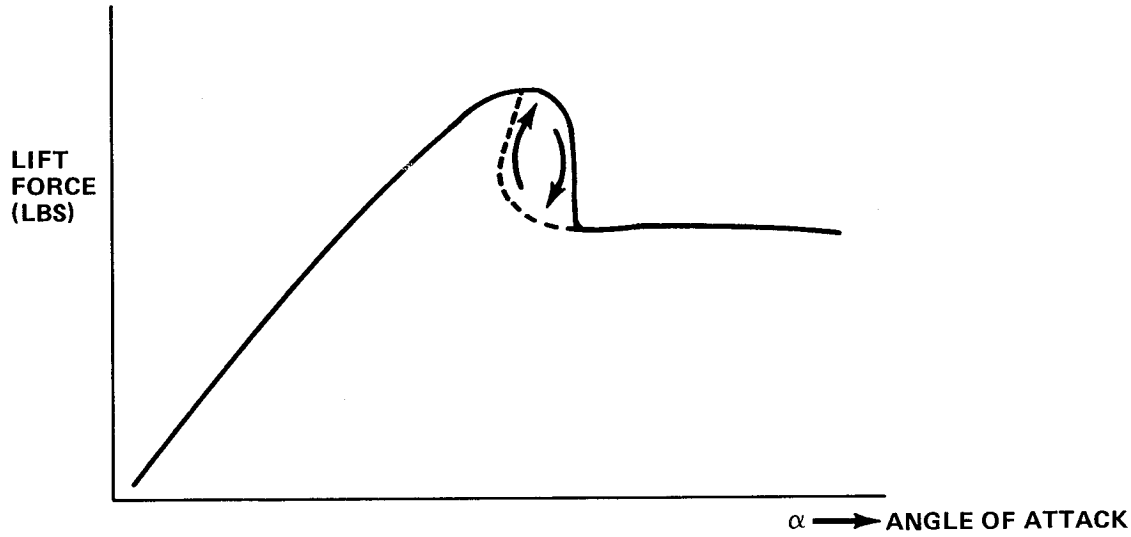


Figure 27. Bistable pump characteristics.

The pump starts a limit cycle oscillation producing fluctuating flow resulting in a fluctuating thrust. In general, no damage occurs on the pumps; however, the engine thrust can cause vehicle loads problems. For the Shuttle system, there is a potential loads problem if the bistable condition occurs. Due to the high performance requirements of the Space Shuttle Main Engines, some pump to pump fluctuation in the stability point occurs, due to small variations in geometry arising from manufacturing tolerances. As a result, some pumps are bistable while most are not. Since the engine must operate anywhere between 65 percent and 109 percent of rated power level and bistable induced thrust fluctuations create loads and pogo problems, all pumps must be verified to be free of the bistable condition before flying. Pumps are acceptance tested at 65 percent to show they are clear of instabilities.

b. Subsynchronous Whirl

Subsynchronous whirl, a problem plaguing rotary machinery, has been a major problem on the Space Shuttle Main Engine. This motion takes the form of whirling or whipping of the flexed rotor (i.e., lateral vibration) at one of the rotor's natural frequencies below the running speed. This subsynchronous vibration motion appears suddenly at some "speed or power-level of onset" with very large amplitudes and sustains or blooms at higher speeds so that either additional increases in running speed or power are impossible. This class of vibration is particularly destructive since the rotor is whirling at a speed different from that of its rotational speed. Instabilities impose a continuing restraint on the performance capabilities of turbomachinery and continue to cause difficulties in the design and operation of high-performance turbomachinery, particularly because the underlying causes are aggravated by design trends to higher loadings, lighter weight, higher speeds, and closer clearances between static and rotating parts. The difference between a stable and unstable machine may be very small in magnitude and subtle

in nature, so that the occurrence will vary from unit to unit of the same design and even from time to time on the same unit. Variations in assembly tolerances within specifications can be the difference. In self-excited vibration or rotating machinery, the excitation mechanism is a steady tangential force induced by some fluid or friction mechanism and is proportional to or increases with the shaft's deflection from its rotational centerline. This is referred to as the "cross coupled" stiffness coefficient, which is often a function of the rotational speed of the shaft or of other environmental variables that vary with shaft speed. At a rotor speed above a limiting value, the destabilizing tangential force exceeds the stabilizing external damping. The shaft will whirl at its critical speed, independent of the rotational speed. The destabilizing force for most whirling mechanisms is in the same direction as the shaft rotation, giving rise to forward whirl. Occasionally, the destabilizing force, and hence the whirling motion, are opposite to shaft rotation, producing backward whirl. Reference 13 is an excellent paper on the various aspects of whirl delineating all key parameters and the various characteristics of the responses. In summary, according to Childs and Ehrich, the following lesson can be drawn.

1) Rotors are destabilized by cross-coupled stiffness coefficients that yield tangential reaction forces that are normal to future radial displacement and in the direction of shaft rotation or, less frequently, opposite to shaft rotation. Rotors are stabilized by decreasing the cross-coupling coefficient or, more desirably, eliminating the mechanism altogether.

2) Rotors become more sensitive to instability problems as the ratio of running speed to critical speed (natural frequency) increases. Increasing a shaft's critical speed by increasing its stiffness or decreasing its mass enhances stability, as does reduction of operating speed.

3) Rotor stability is enhanced by increasing external damping, which tends to delay onset of instability to higher speed (ideally, above the operating range).

They summarized the two classes of vibration of rotating machinery in tabular form (Table 2).

The Shuttle Main Engine development program has been plagued with whirl problems. Early in the Shuttle development program, the fuel pump had a 50 percent subsynchronous whirl problem which was solved by a design change of the seals. The lox pump has had a 90 percent subsynchronous whirl, the solution being more illusive than the fuel pump. Figure 28 shows a lox pump external acceleration measurement (isoplot) for a 500-sec run at various power levels. Notice that whirl is only present during the 109 percent power portion. A special seal (Fig. 29) has been designed which provides this increased stiffness and damping and is now being tested for verification. Figure 30 is the whirl history of the full power level (FPL) SSME lox pump design. Notice that some pump builds do not whirl, while others grow into whirl. Also, notice how fast the response amplitude grows with the next firing once whirl is present. Obviously, the higher performance requirements of these pumps has resulted in a marginal whirl situation. Small differences in manufacturing (within specification) produce some pumps which whirl. Additional damping and other solutions are being pursued to solve this problem.

Whirl is a very interesting and complex phenomenon. It is very destructive to the bearings, limiting life and can lead to pump failures which could be catastrophic in nature. Although a classic problem and treated extensively in literature, most of this work has been on systems that are not of very high energy density and performance. The rotary dynamic elements of the Shuttle are the first of this new breed [13-16]. The high pressure fuel pump, for example, develops a maximum of 75,000 h.p. in a space volume of a 1-ft-diameter and 2-ft-length and weighs approximately 250 lb. As a result, sensitivities, accuracies, and analysis techniques are pushing the state-of-the-art. Future systems must extend these tools dramatically and are currently a very large technology effort.

TABLE 2. SUMMARY OF TWO CLASSES OF VIBRATION OF ROTATING MACHINERY

| | | |
|---|---|---|
| VIBRATION FREQUENCY/SPEED RELATIONSHIP | FREQUENCY IS EQUAL TO (i.e., SYNCHRONOUS WITH) RPM OR A WHOLE NUMBER OR RATIONAL FRACTION OF RPM. | FREQUENCY IS NEARLY CONSTANT AND ESSENTIALLY INDEPENDENT OF ROTOR ROTATIONAL SPEED, OR ANY EXTERNAL STIMULUS AND IS AT OR NEAR ONE OF THE SHAFT CRITICAL OR NATURAL FREQUENCIES. |
| VIBRATION AMPLITUDE/SPEED RELATIONSHIP | AMPLITUDE WILL PEAK IN A NARROW BAND OF RPM WHEREIN THE ROTOR'S CRITICAL FREQUENCY IS EQUAL TO THE ROTOR SPEED OR TO A WHOLE NUMBER MULTIPLE OR A RATIONAL FRACTION OF THE SPEED OR AN EXTERNAL STIMULUS. | AMPLITUDE WILL SUDDENLY INCREASE AT AN "ONSET" SPEED ON POWER LEVEL AND CONTINUE AT HIGH OR INCREASING LEVELS AS SPEED IS INCREASED. |
| WHIRL DIRECTION | WHIRLING IS ALWAYS FORWARD, i.e., IN DIRECTION OF SHAFT ROTATION | WHIRLING IS GENERALLY FORWARD, BUT MAY BE BACKWARD IN CERTAIN INSTANCES. |
| ROTOR FIBER STRESS | FOR SYNCHRONOUS VIBRATION THE ROTOR VIBRATES IN FROZEN, DE-FLECTED STATE, WITHOUT OSCILLA-TORY FIBER-STRESS. | ROTOR FIBERS ARE SUBJECT TO OSCILLATORY STRESS AT A FREQUENCY EQUAL TO THE DIFFERENCE BETWEEN ROTOR SPEED AND WHIRLING SPEED. |
| AVOIDANCE OR ELIMINATION | 1) INTRODUCE DAMPING TO LIMIT PEAK AMPLITUDES AT CRITICAL SPEEDS THAT MUST BE TRAVERSED.<br>2) TUNE THE SYSTEM'S CRITICAL FREQUENCIES TO BE OUT OF THE RPM OPERATING RANGE.<br>3) ELIMINATE ALL DEVIATIONS FROM AXIAL SYMMETRY IN THE SYSTEM AS BUILT OR AS INDUCED DURING OPERATION (e.g., BALANCING). | 1) INTRODUCE DAMPING TO RAISE THE INSTABILITY ONSET SPEED TO ABOVE THE OPERATING SPEED RANGE.<br>2) RAISE THE NATURAL FREQUENCY OF THE ROTOR AS HIGH AS FEASIBLE.<br>3) DEFEAT OR ELIMINATE THE INSTABILITY MECHANISM. |
| INFLUENCE OF DAMPING | ADDITION OF DAMPING MAY REDUCE PEAK AMPLITUDE, BUT NOT MATERI-ALLY AFFECT RPM AT WHICH PEAK AMPLITUDE OCCURS. | ADDITION OF DAMPING MAY DEFER ONSET TO A HIGHER SPEED, BUT NOT MATERIALLY AFFECT AMPLITUDE AFTER ONSET. |
| INFLUENCE OF SYSTEM GEOMETRY | EXCITATION LEVEL AND HENCE AMPLITUDE ARE DEPENDENT ON SOME LACK OF AXIAL SYMMETRY IN THE ROTOR MASS DISTRIBUTION OR GEOMETRY, OR EXTERNAL FORCES APPLIED TO THE ROTOR. AMPLITUDES MAY BE REDUCED BY REFINING THE SYSTEM TO MAKE IT MORE PERFECTLY AXI-SYMMETRIC, (e.g., BALANCING). | AMPLITUDES ARE INDEPENDENT OF SYSTEM AXIAL SYMMETRY. GIVEN AN INFINITESIMAL DEFLECTION TO AN OTHERWIDE AXI-SYMMETRIC SYSTEM, THE AMPLITUDE WILL SELF-PROPAGATE FOR WHIPPING SPEEDS ABOVE THE INSTABILITY ONSET SPEED. |

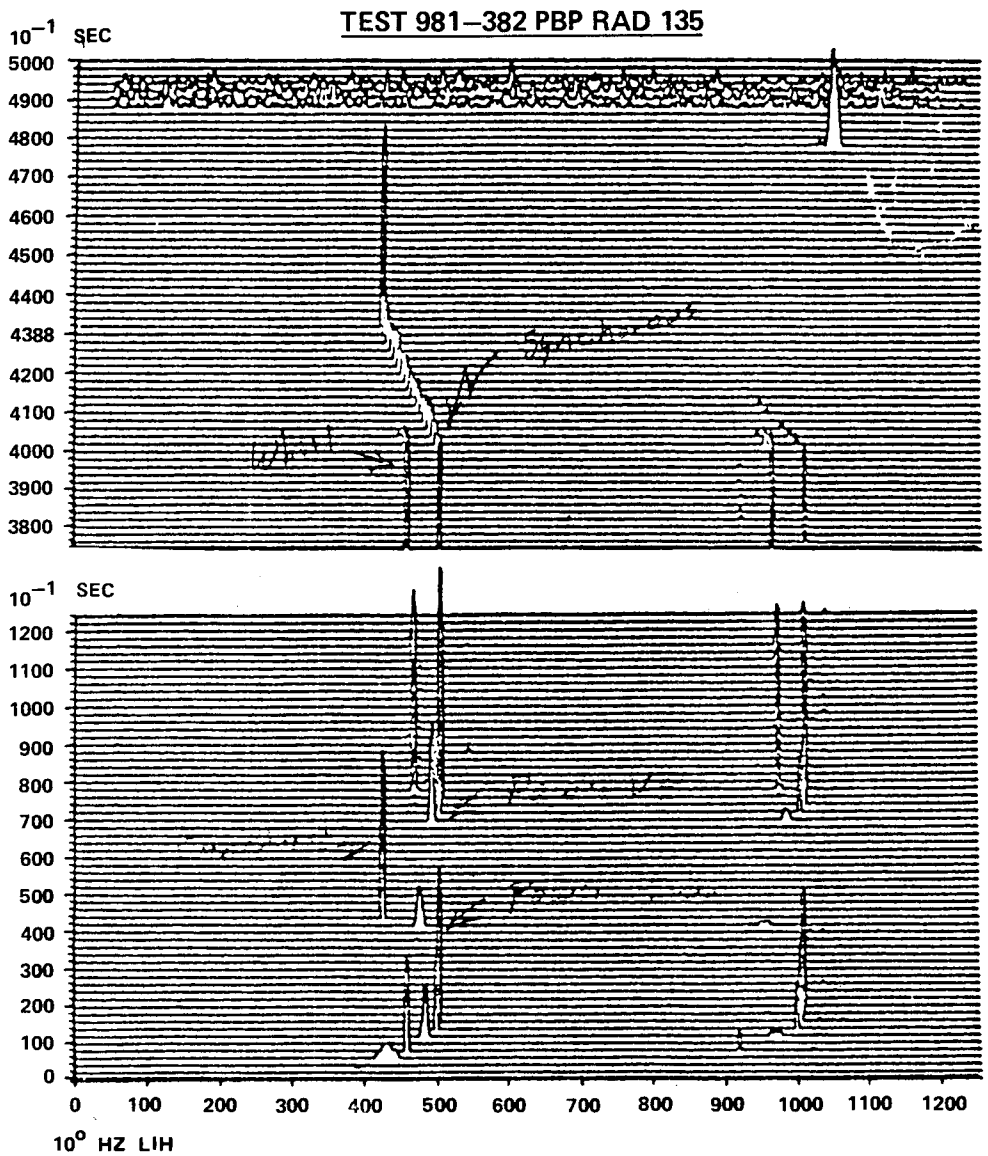


## WHIRL CHARACTERISTICS

- INTERNAL ROTOR DAMPING DESTABILIZES
- EXTERNAL (NON–ROTATING) DAMPING STABILIZES
- FLUID CROSS COUPLING FORCES DE–STABILIZE (ROTOR TRANSLATION GENERATES CIRCUMFERENTIAL FORCES IN DIRECTION OF ROTATION

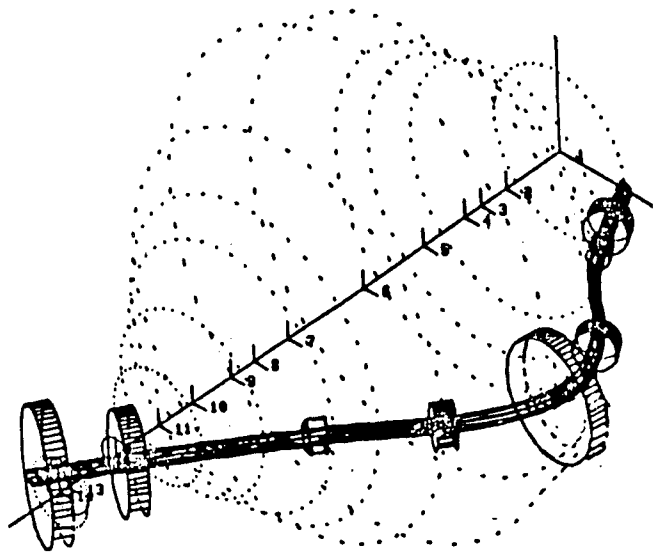

Figure 28. Whirl characteristics.

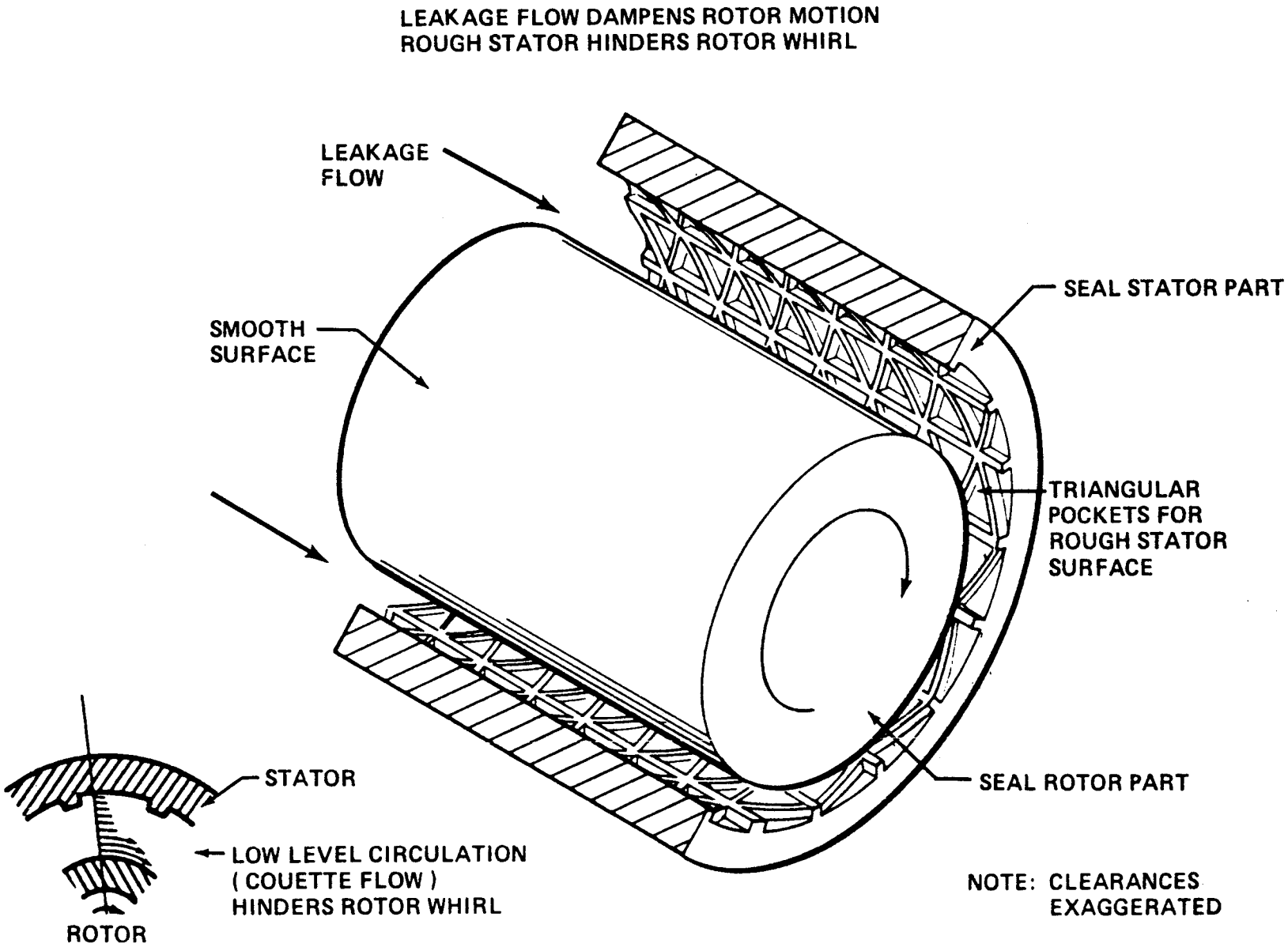


Figure 29. Damping seals.

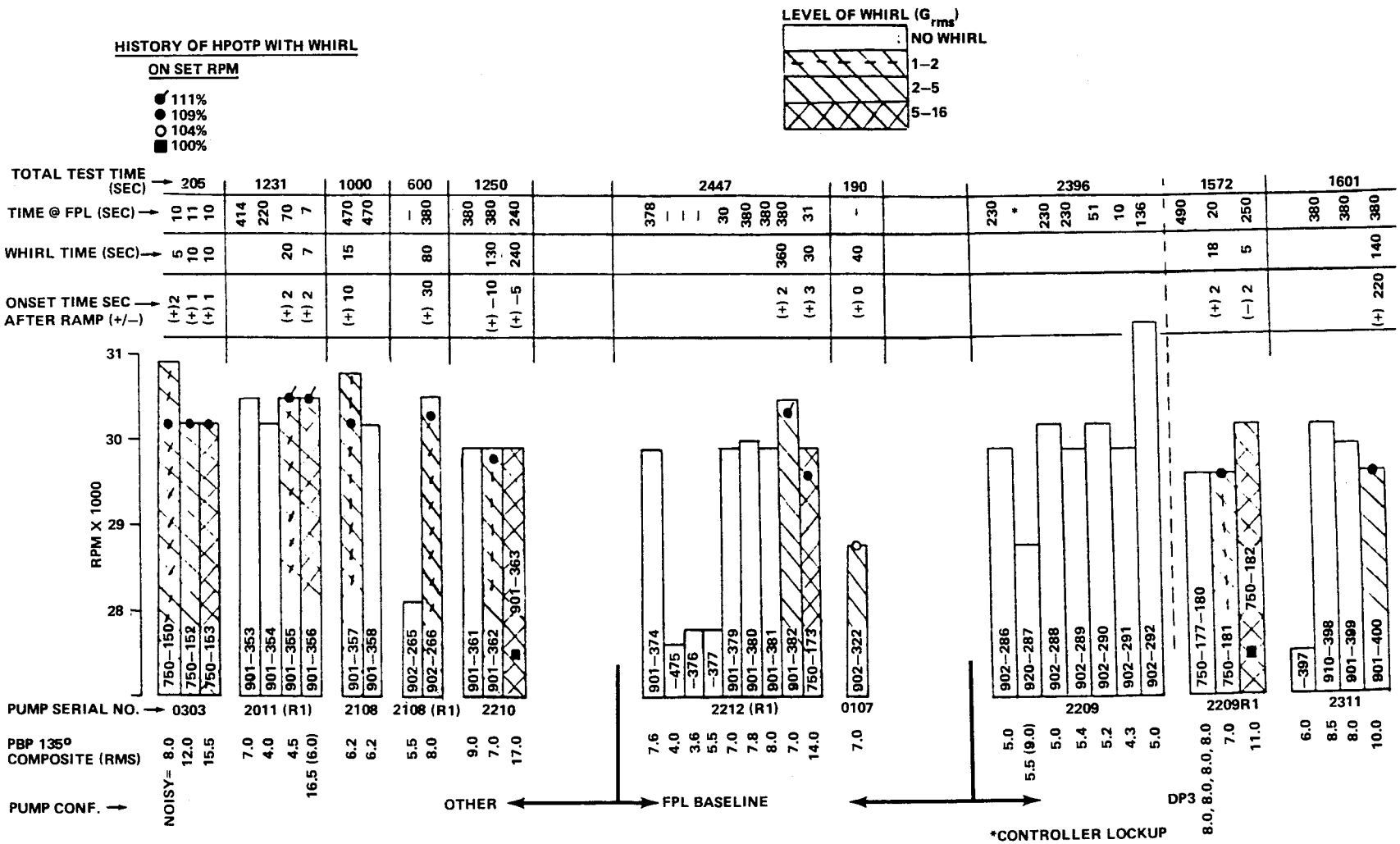


Figure 30. Lox pump whirl history.

## 6. Creak, Jitter, and Other Special Problems

High performance, orbiting space systems such as special satellites and Space Telescopes have considerations that are variations of the old classical problems in structures and dynamics. The Space Telescope has very stringent pointing accuracy requirements which drive many aspects of the design, analysis, and operations tasks. As a result, coupling between thermal environments, structural dynamics, and deflection results in dynamic disturbances to the line-of-sight accuracy when pointing at stars, etc. Although the problems are not necessarily instabilities, the basic problem can be put in this category. Figure 31 shows the Space Telescope with the various components. The line of sight for a radial SI is shown on Figure 32.

### a. Creak

One problem occurs when thermal expansion is retarded by some type of friction restricting the motion (normally at a joint) until the load increases enough to break friction setting up dynamic excitation disturbing the line of sight. Most of the work today has been analytical and is of some concern operationally for Space Telescope. This is obvious when one sees the thermal cycle per orbit. The basic phenomenon is shown on Figure 33. Typical responses are shown on Figures 34 and 35. Experimental results have shown that with the force levels experienced on ST no creak problem will result.

### b. Jitter

Jitter, a structural response caused when the momentum wheel speed passes through a structural mode frequency, in the Space Telescope clouds the images causing loss of goodness for the sighting. The main source of jitter is the momentum reaction wheels used for pointing control. Control actuation is accomplished by changing the speed of the various wheels. As the wheel speed sweeps through, high gain bending mode frequency structural response are excited causing jitter. Figures 36, 37, and 38 are typical responses in terms of light of sight for a particular experiment. The problem is compounded by the fact that modes through 100 Hz must be included for jitter analysis. This means a larger number of modes must be developed. High order modes are very difficult to predict. Key also is the value of the structural damping for each mode which again is not easily predicted or obtained. Assuming a minimum value for damping, the predicted jitter was excessive. This meant that some means of reaction wheel isolation should be developed as a backup fix.

Isolation was actively pursued going to all known vendors. Isolators were available; however, problems existed in characterizing their response at the low force levels expected in the Space Telescope applications. The force level to be isolated was around 500 millipounds. Insuring that an isolator would work at such low force amplitudes and determining the nonlinear response was a major problem. A small shaker was used on the isolator in conjunction with spectrum analyzers to determine the response characteristics. Figure 39 shows the responses for various input forces versus frequency. Notice the nonlinearity in frequency and in damping. Damping values are written for each force frequency spectrum. The great task was developing the test approach and data analysis system previously described to verify isolator.

This concludes the discussion of experiences associated with instabilities. It is believed that these should be representative, but not all encompassing, and will serve as a good guide in what to expect. As a general rule, every effort should be expended to anticipate and design out instabilities and not depend on response limiting.

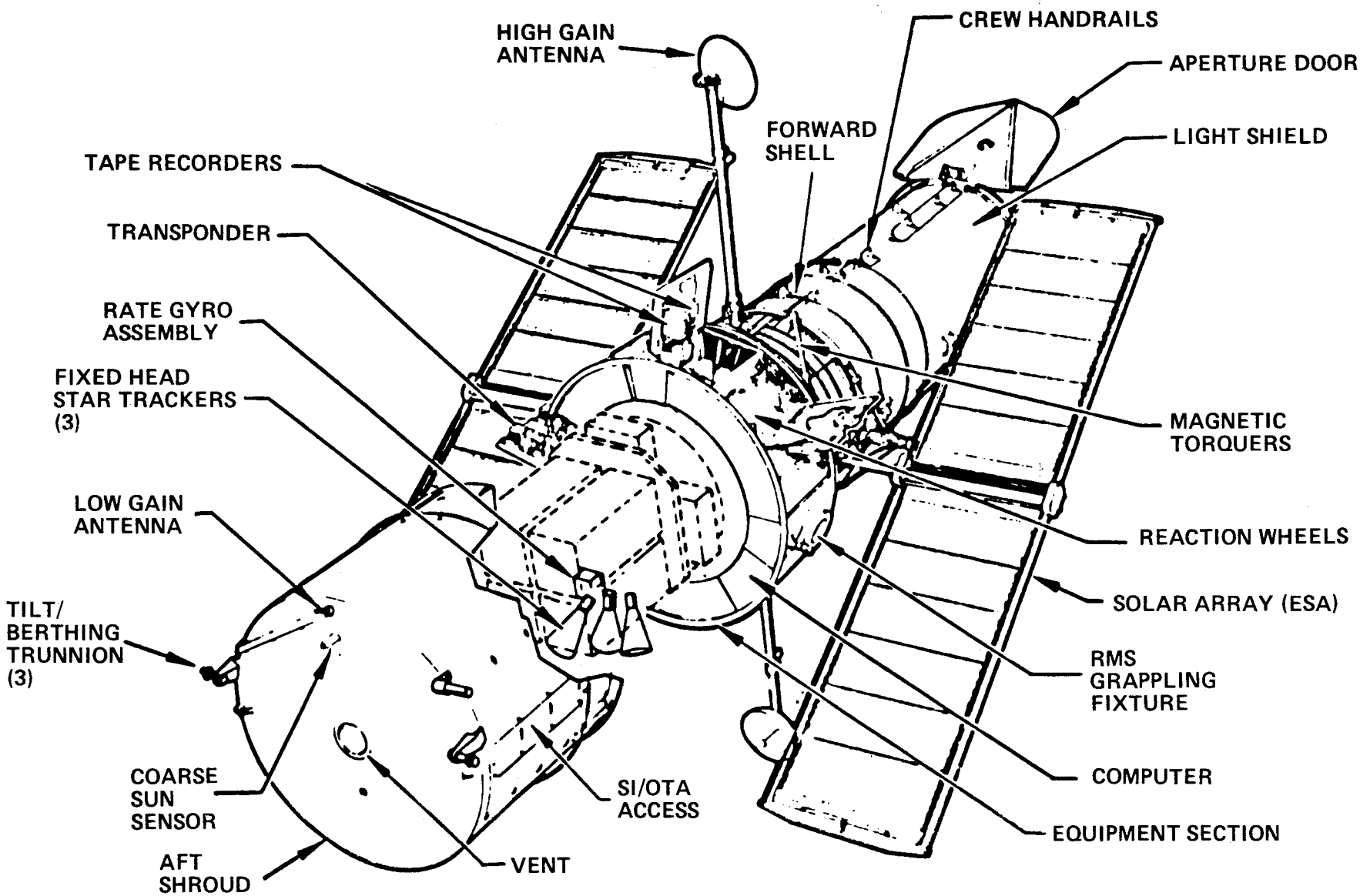


Figure 31. Space Telescope schematic.

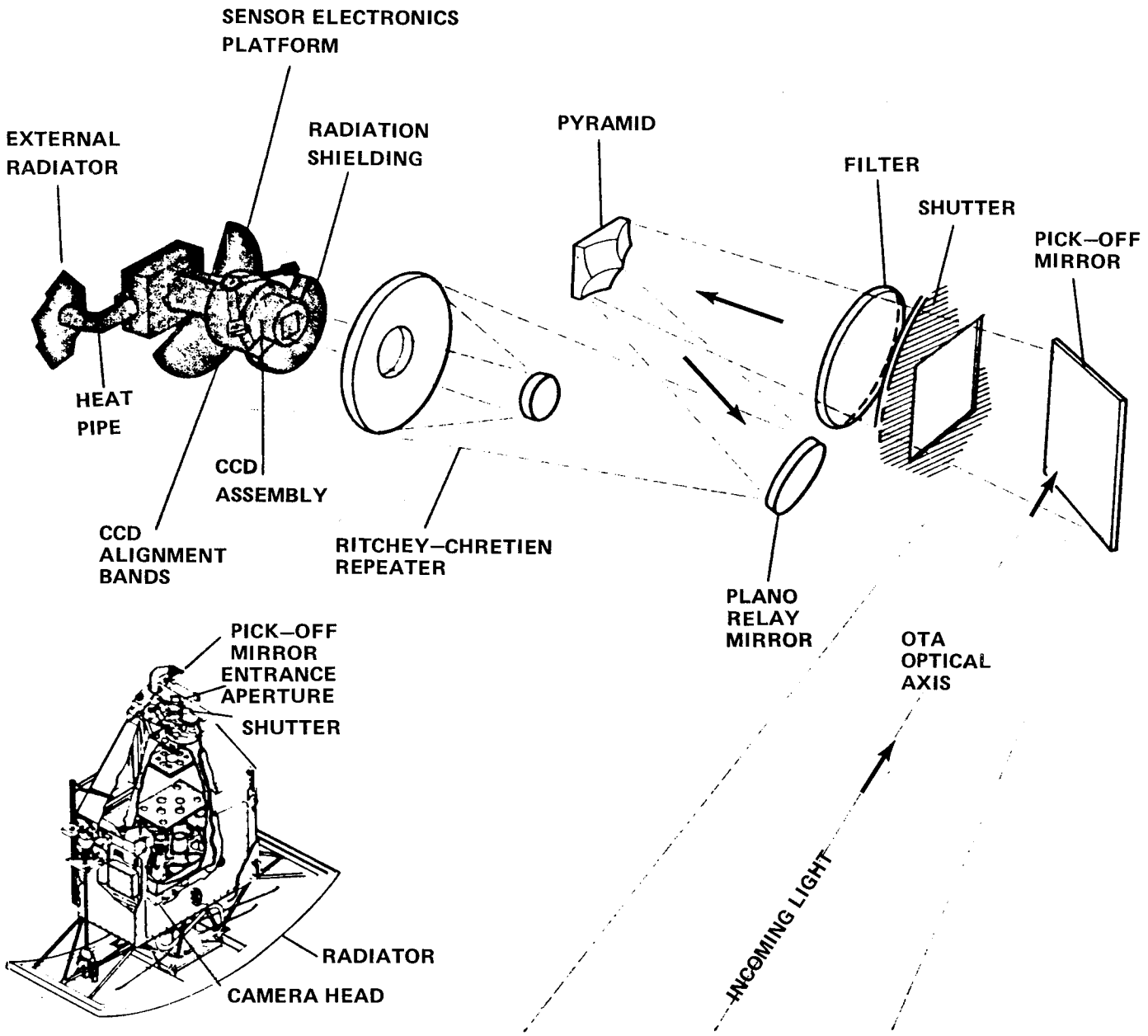


Figure 32. Line-of-sight for wide field planetary camera.

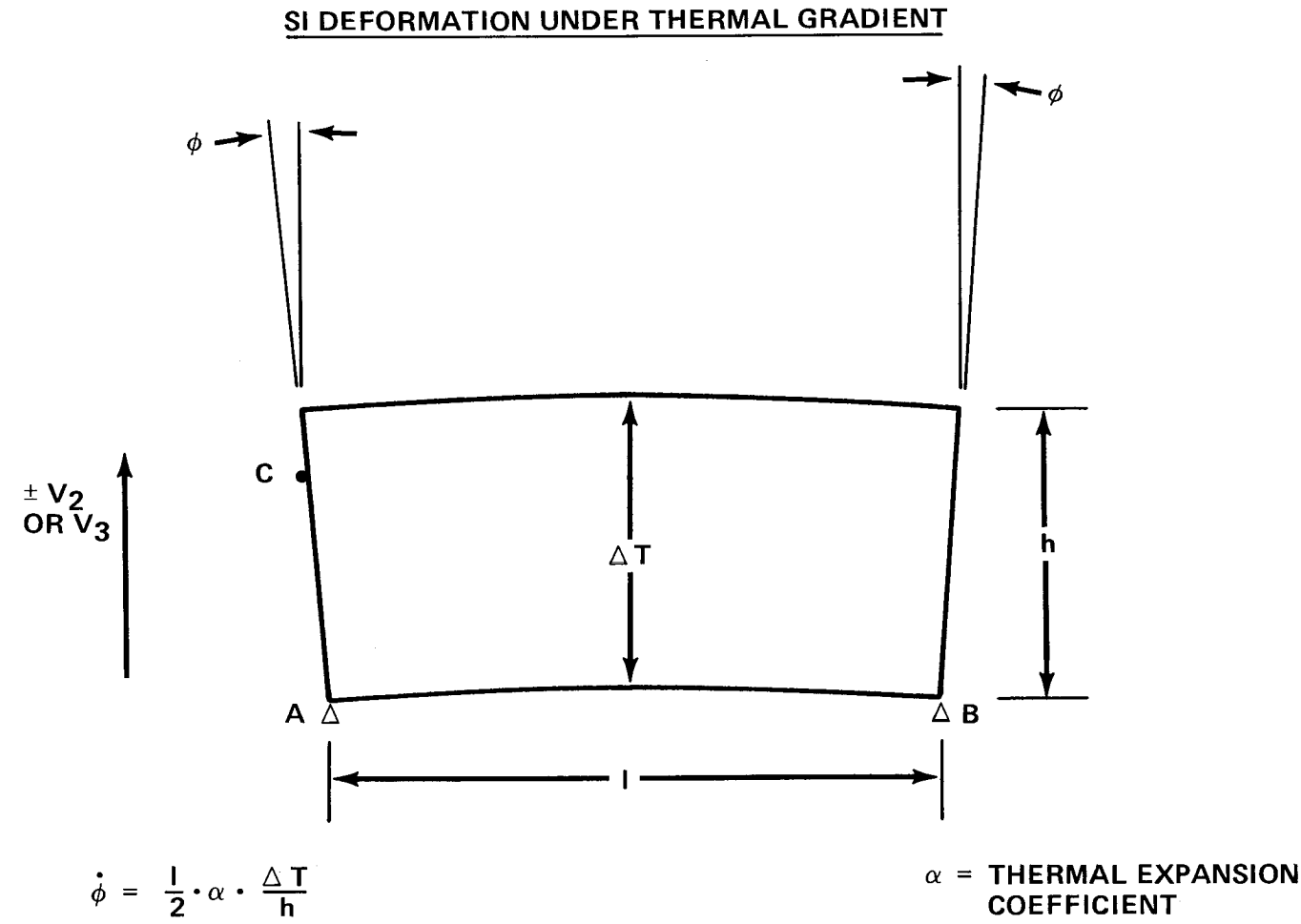


Figure 33. SI deformation under thermal gradient.

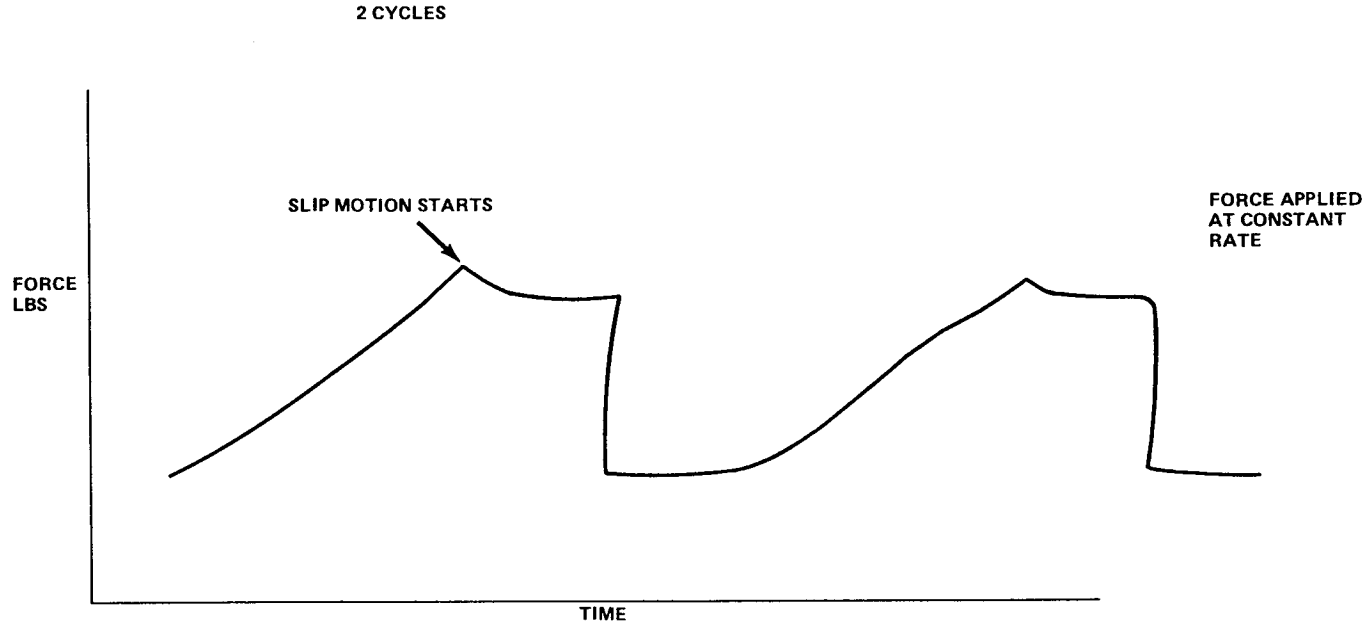


Figure 34. Typical creak response.

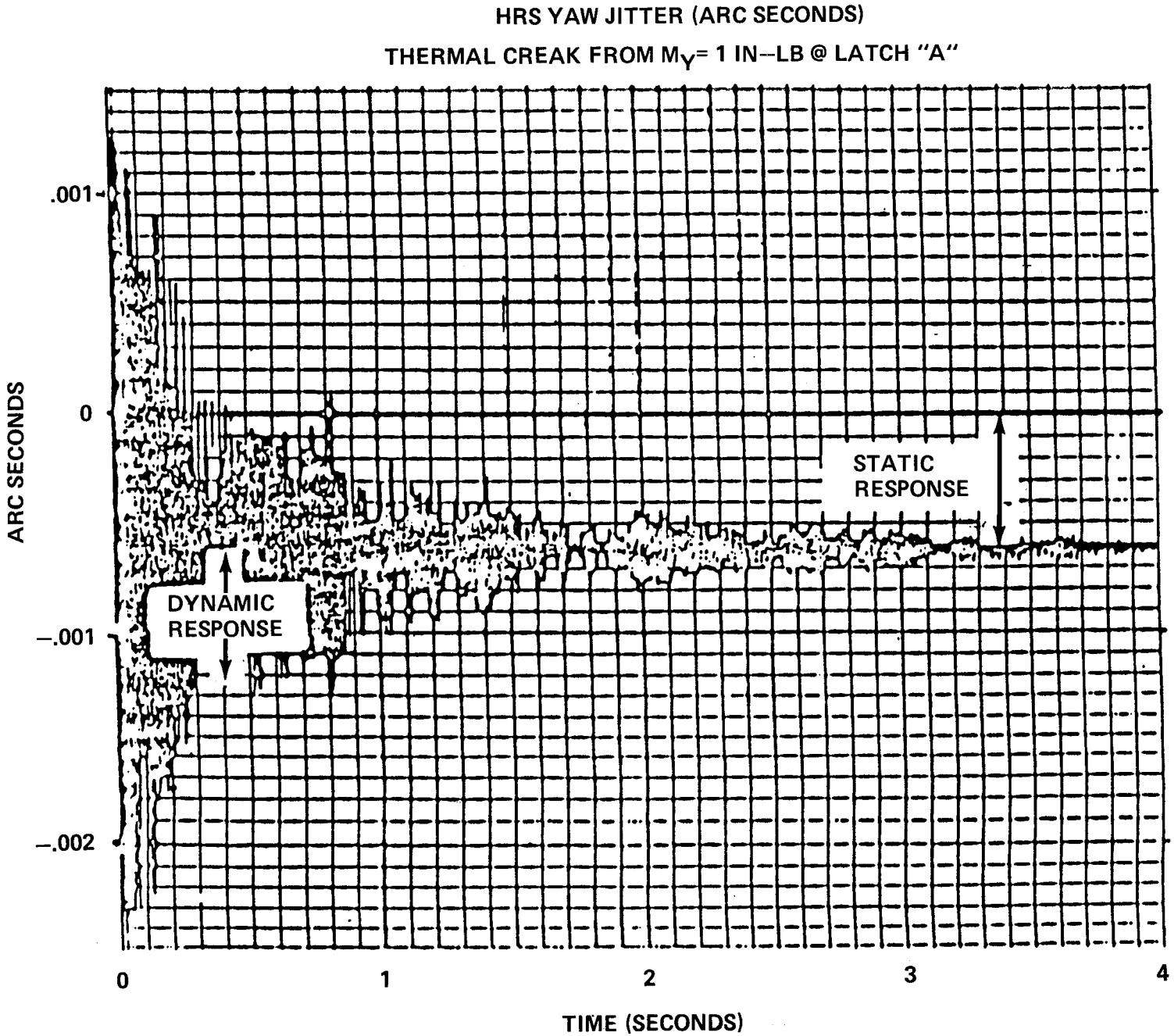


Figure 35. Overall creak response.

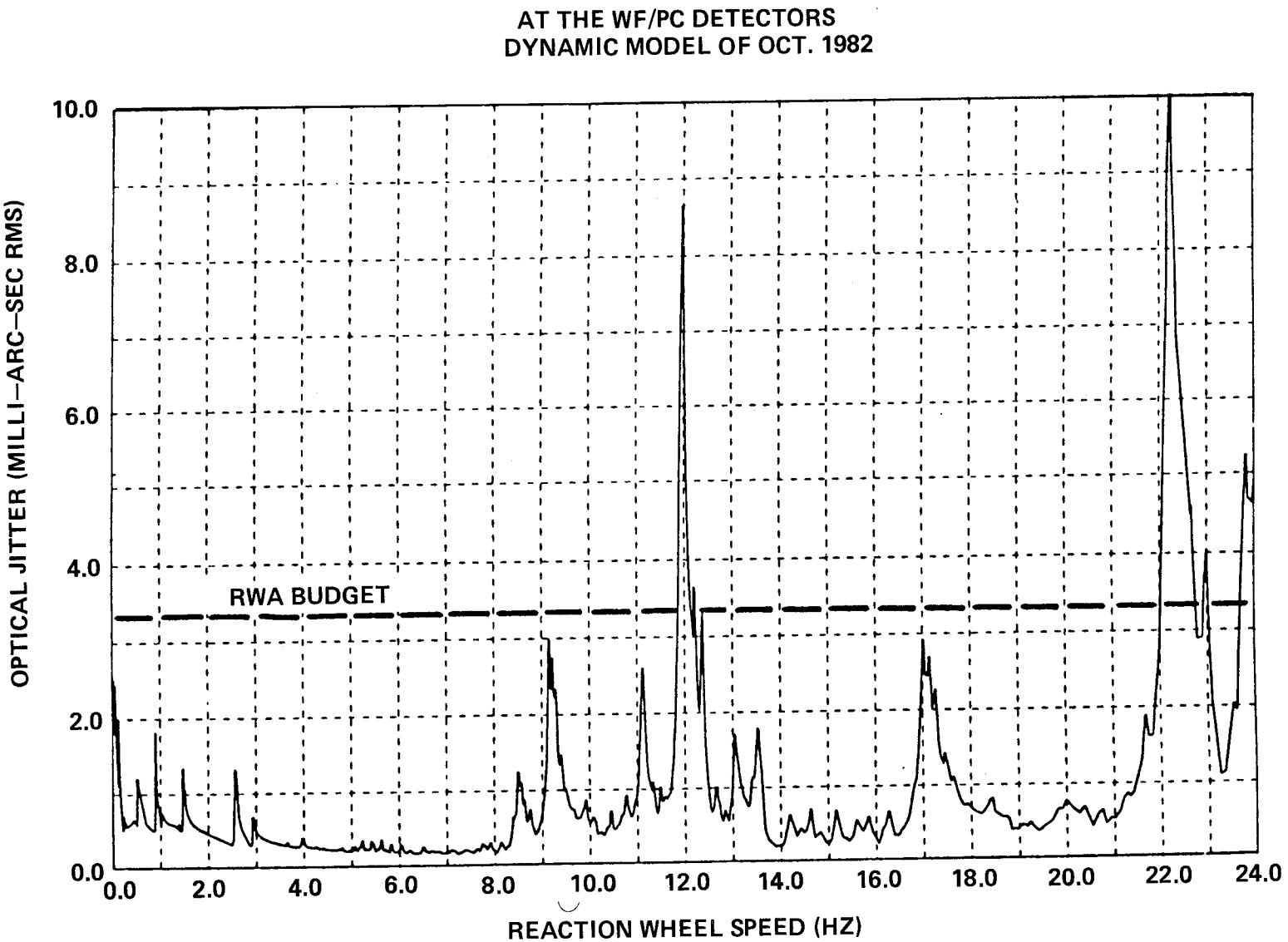


Figure 36. Typical line-of-sight jitter.

CHARACTERISTICS OF ST MATH MODEL AND RESPONSE PREDICTIONS

- 280 MODES BELOW 70 HZ. HIGHER FREQUENCY MODES MAY BE DRIVERS
- ASSUME 0.3% CRITICAL DAMPING (BASED ON ENGINEERING SIMULATOR TESTS) IN ALL MODES, EXCEPT 1% CRITICAL DAMPING ON THE AXIAL ROTOR MODE (BASED ON MEASUREMENT AT SPERRY)
- MAJOR HARMONIC COMPONENTS FORCE MODEL AS STEADY STATE SINE WAVE
- SPEEDS AND PHASE OF WHEELS NOT CORRELATED, HENCE TOTAL RESPONSE IN RSS OF WHEEL INDUCED JITTER

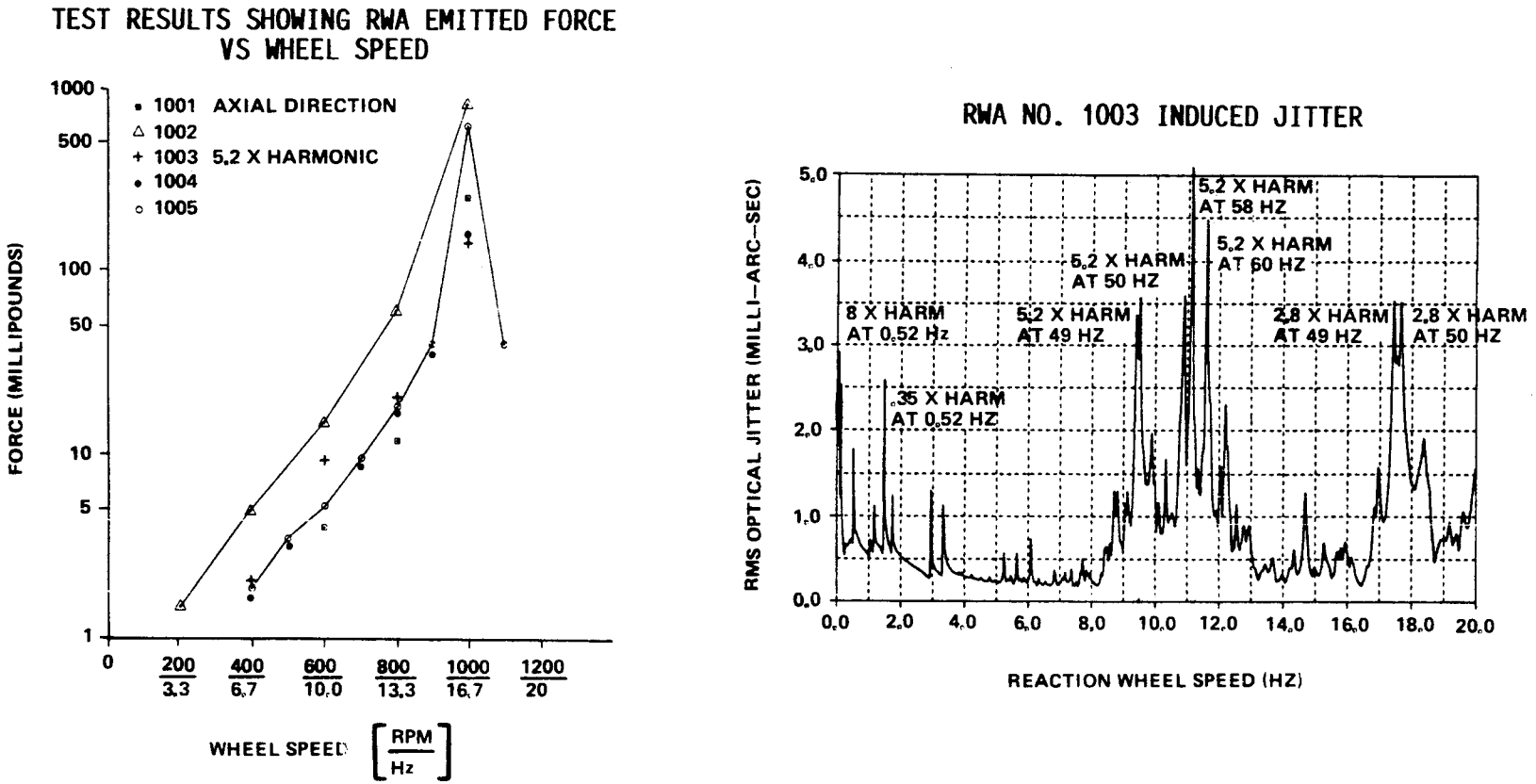


Figure 37. Reaction wheel assembly force and jitter.

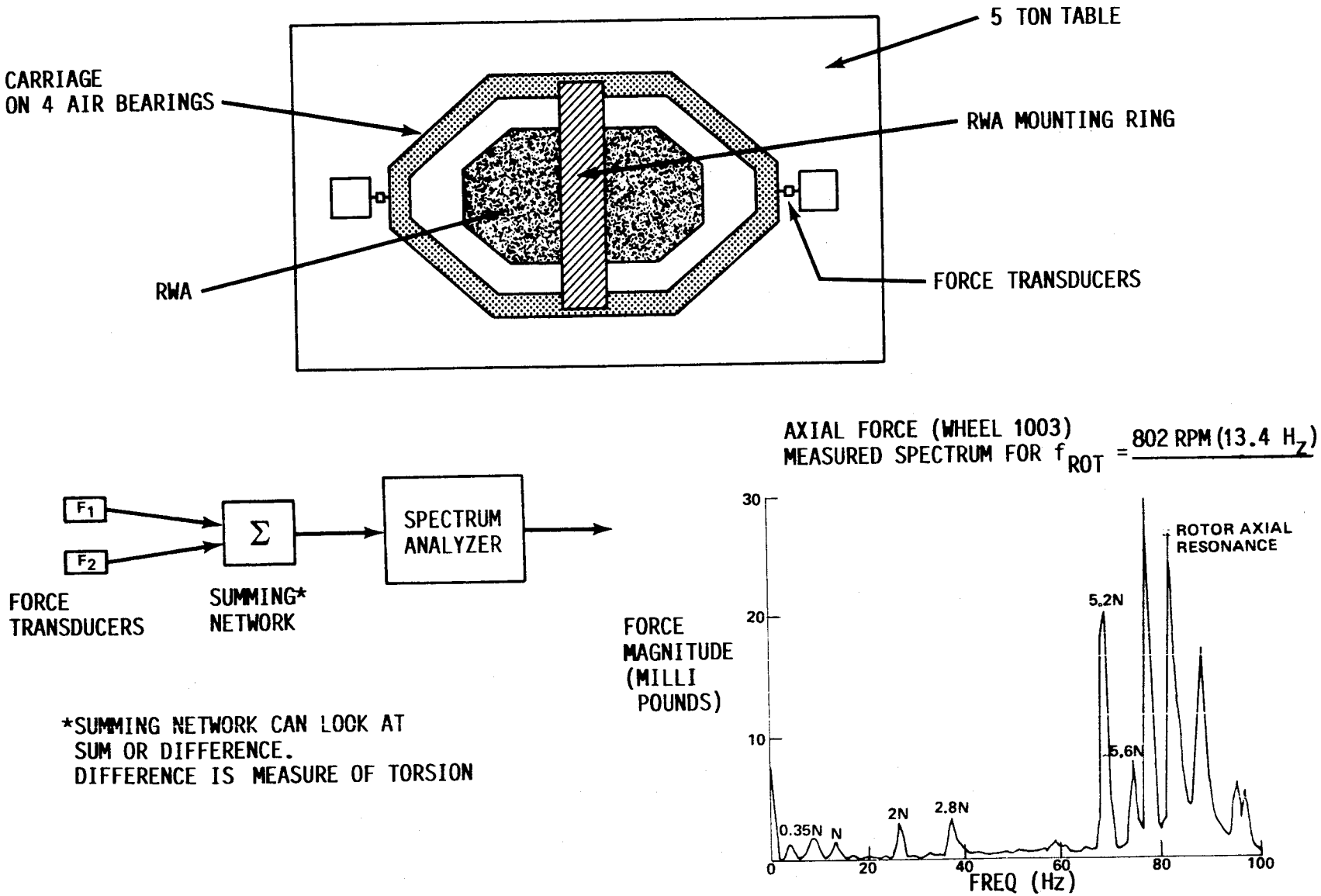


Figure 38. Reaction wheel assembly response measurements.

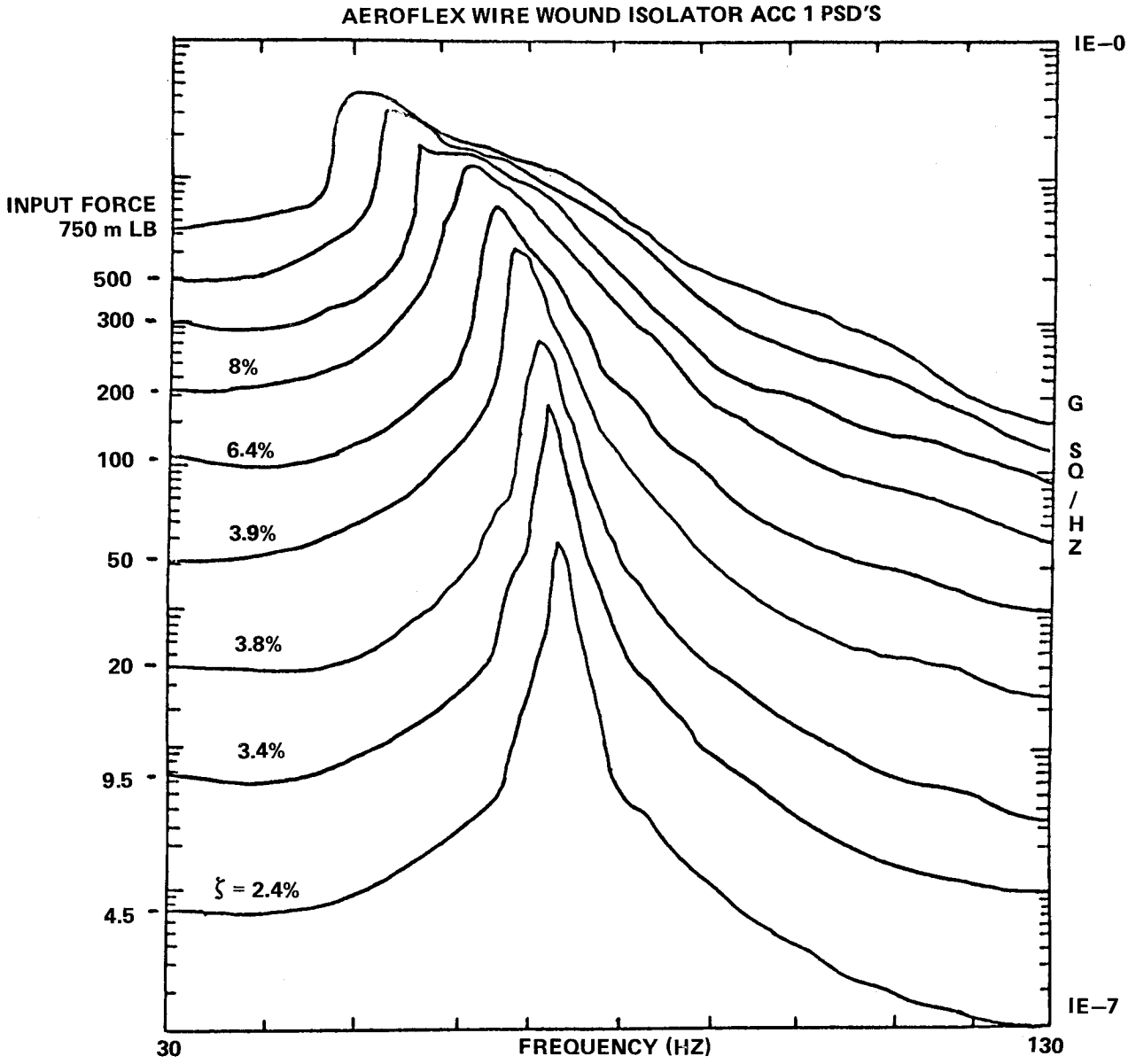


Figure 39. Nonlinear isolator response.

### B. Forced Response

The area of forced response is the one engineers are most familiar with, yet it is where a high percentage of problems have occurred. In general, the response area is separated in terms of environments and the system response to these environments. Accurate models with inadequate environments produce poor response results and vice versa. Therefore, the engineer must have both accurate environments and response models. For convenience, environment and response will be treated simultaneously under the general heading of forced response. Early space vehicles/missiles had very few forced response problems due to very conservative design approaches. As designs become more optimum (weight critical), response problems have occurred. The following are the major problems experienced in the forced response area.

1. Saturn IB Zero G Sloshing

The Saturn IB, since it was to go into orbit and restart as a forerunner verification test for Saturn/Apollo, had problems in describing and controlling propellant behavior in zero g. The problem existed in two distinct areas. The first occurred when the energy of any residual sloshing from high "q" at engine shutdown going into orbit was transferred into very large liquid motions in zero "g." In many cases, the motion could be very violent (uncontrolled). The propellant had to be controlled and seated for engine restart. The second occurs during the orbit coast period where control impulses can excite the propellant dynamically. The basic fluid phenomenon is one of capillary action, surface tension, etc., instead of strong inertia forces requiring new analysis and testing techniques. Very complex analytical models were derived to handle these different conditions. Testing was accomplished using free falling containers inside a free falling vacuum chamber in order to get zero-g simulations. Exotic excitation and data acquisition systems, including motion picture coverage of the internal test container, were required. As a result of detailed testing and analysis, a nylon net baffle was designed to be placed at the liquid system to contain the fluid and suppress the slosh. A very good characterization of fluid motion in zero g was experimentally determined for fluid motion amplitude as a function of initial conditions at orbit insertion and as a function of control impulses. Limited success was achieved analytically to describe the motion. The philosophy used was not to attempt to control the zero-g sloshing using control. Simulations were developed, both digital and analog as well as the drop test program, to verify that the philosophy had been met [17,18].

2. Saturn V Load Relief Wind Gust Response Coupling

Early in the Apollo design, it was decided to incorporate rigid body load relief (angle-of-attack reduction) using accelerometers in the control loop. Rigid body loads resulting from the average or mean wind was reduced significantly using this approach; however, the accelerometer loop increased the elastic body response to wind gust on the forward third of the vehicle. This increase was more than enough to offset the decrease on this section of the vehicle achieved with load relief. A real problem existed. Load relief reduced the rigid body quasi-steady state loads and, therefore, saved weight on the first stage; however, loads on the most weight sensitive portion of the vehicle was increased or stayed the same with the loads becoming transient elastic body loads instead of rigid body trim loads. Figures 40 and 41 show the effect of the load relief control system gain on bending moment for two vehicle stations, station 25 in the S-IC lox tank and station 90 in the command module. Clearly, the addition of load relief increases the transient dynamic response while decreasing the overall moment at the forward vehicle station (Sta. 90). Figure 42 is a schematic of Saturn V showing materials and what event designed each section of the vehicle. As a result of this sensitivity of the vehicle to wind gust, two distinct efforts were made in the design phases of the Saturn program: (1) Wind environments containing 25 m gusts lengths and greater were obtained and a data bank built. A sample of 150 wind profiles for each month of the year was compiled [19,20]. (2) A Monte Carlo simulation of vehicle response to these measured wind ensembles was developed using a high speed repetitive analog computer [19,21-29]. This allowed the simultaneous assessment of wind speed, wind shear, and wind gust in a true statistical sense. In the past, all analyses had used the synthetic wind profile approach which had an assumed phasing between shear and gust superimposed on the 95 percent wind speed.

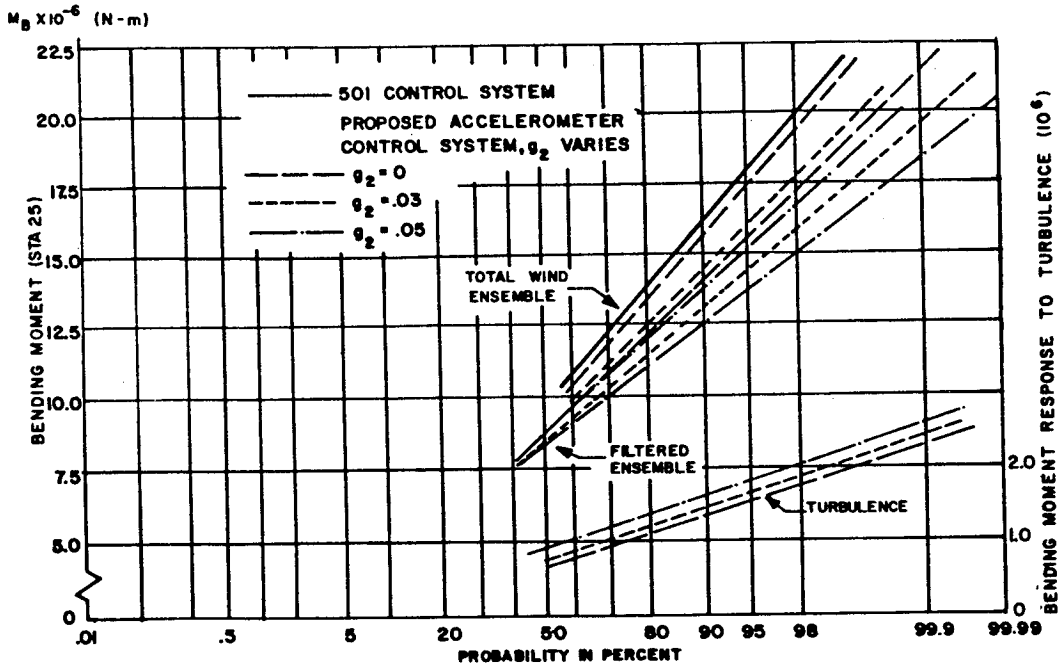


Figure 40. Bending moment at station 25 versus probability of not exceeding for total wind ensemble and filtered ensemble.

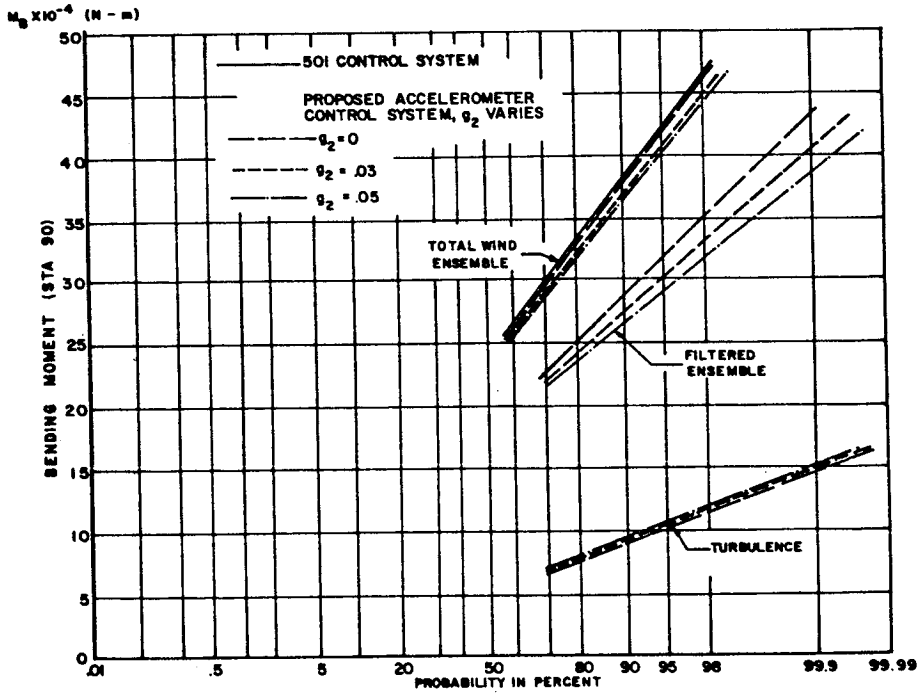


Figure 41. Bending moment at station 90 versus probability of not exceeding for total wind ensemble and filtered ensemble.

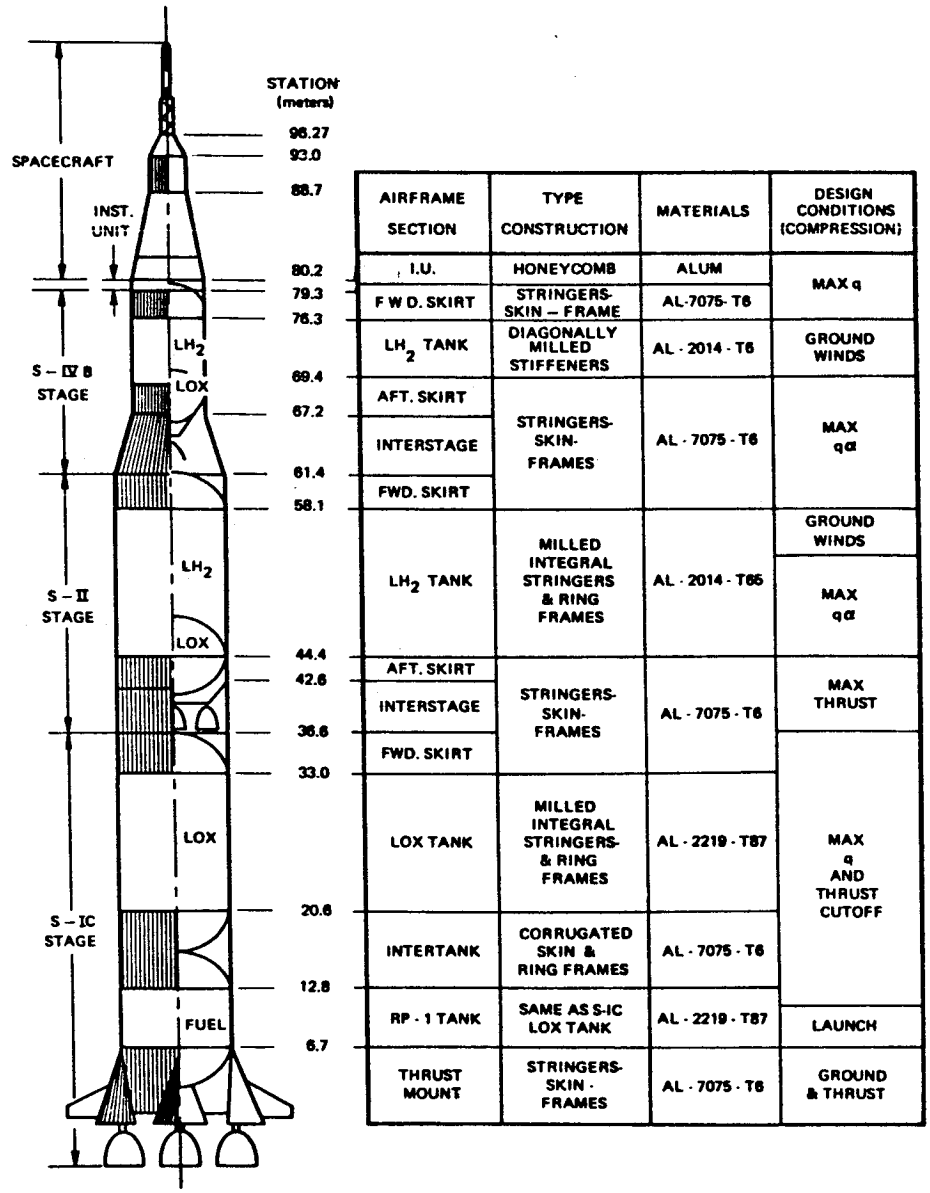


| AIRFRAME SECTION | TYPE CONSTRUCTION | MATERIALS | DESIGN CONDITIONS (COMPRESSION) |
|---|---|---|---|
| I.U. | HONEYCOMB | ALUM | MAX q |
| F W D. SKIRT | STRINGERS-SKIN – FRAME | AL-7075-T6 | |
| $LH_2$ TANK | DIAGONALLY MILLED STIFFENERS | AL - 2014 - T6 | GROUND WINDS |
| AFT. SKIRT | STRINGERS-SKIN-FRAMES | AL - 7075 - T6 | MAX $q\alpha$ |
| INTERSTAGE | | | |
| FWD. SKIRT | | | |
| $LH_2$ TANK | MILLED INTEGRAL STRINGERS & RING FRAMES | AL - 2014 - T65 | GROUND WINDS |
| | | | MAX $q\alpha$ |
| AFT. SKIRT | STRINGERS-SKIN-FRAMES | AL - 7075 - T6 | MAX THRUST |
| INTERSTAGE | | | |
| FWD. SKIRT | | | MAX q AND THRUST CUTOFF |
| LOX TANK | MILLED INTEGRAL STRINGERS & RING FRAMES | AL - 2219 - T87 | |
| INTERTANK | CORRUGATED SKIN & RING FRAMES | AL - 7075 - T6 | |
| RP - 1 TANK | SAME AS S-IC LOX TANK | AL - 2219 - T87 | LAUNCH |
| THRUST MOUNT | STRINGERS-SKIN - FRAMES | AL - 7075 - T6 | GROUND & THRUST |

Figure 42. Airframe structure of Saturn V launch vehicle.

In addition to the deletion of the planned load relief system due to the increased bending mode response, the control system added damping to both the first and second bending modes. This was done to further reduce modal response to these wind gusts, since there was tuning between gusts and the modes. Also, wind biasing was used in the operational phase to produce much needed load margins to meet ever increasing performance requirements. In addition, a very elaborate day of launch wind monitoring and launch constraint approach was developed which consisted of wind measurements periodically before launch (24, 12, 8, 4, 2, and 1 hr). These wind measurements were used as inputs to a control and loads simulation which was used to clear the vehicle for flight. In fact, if potential problems existed, the wind balloon could directly feed the simulation and control response program and loads generated up until a few minutes before launch. No constraints were ever imposed on Apollo launches. Shuttle is using the same basic approach with the addition of load indicators (strength capability as a function of trajectory parameters) for all critical vehicle stations.

There is no way this short paragraph can capture the effort in manpower, dollars, and mental anguish required to uncover and solve this problem. These efforts had to be focused and coordinated into a system approach. These were (1) obtaining proper wind environments (see discussion on Jimspheres), (2) appropriate vehicle models including elastic body effects, (3) simulation techniques (Monte Carlo trajectory with elastic body vehicle and measured winds).

Many other aeroelastic effects were studied in detail to insure that they did not compound this problem. Gust penetration and lift growth [30,31] were the two major efforts. As a result of all these activities, the vehicle flew without problems or major redesign effort.

3. Skylab Launch Probability

The Saturn V derivative used to launch the Skylab further exemplifies the wind gust elastic body response coupling problem. The Skylab was placed forward of the S-II stage with a nose cone on the front instead of the command module. This change in external configuration changed the aerodynamic distribution, thus the response to winds. Figures 43 and 44 compare the two. This apparently small configuration change had a substantial effect on the resulting loads.

The Saturn V without wind biasing had approximately a 95 percent launch probability and greater than 99 percent with wind biasing. Saturn V flew with wind biasing for added margin. This assessment was made using synthetic wind profiles. Using the Monte Carlo approach and the measured wind ensembles, the unbiased case was greater than 99 percent. Skylab had less than 50 percent launch probability without wind biasing and 80 percent with wind biasing using the synthetic profile. Verification and operational analysis for Skylab was accomplished using the Monte Carlo approach. The results

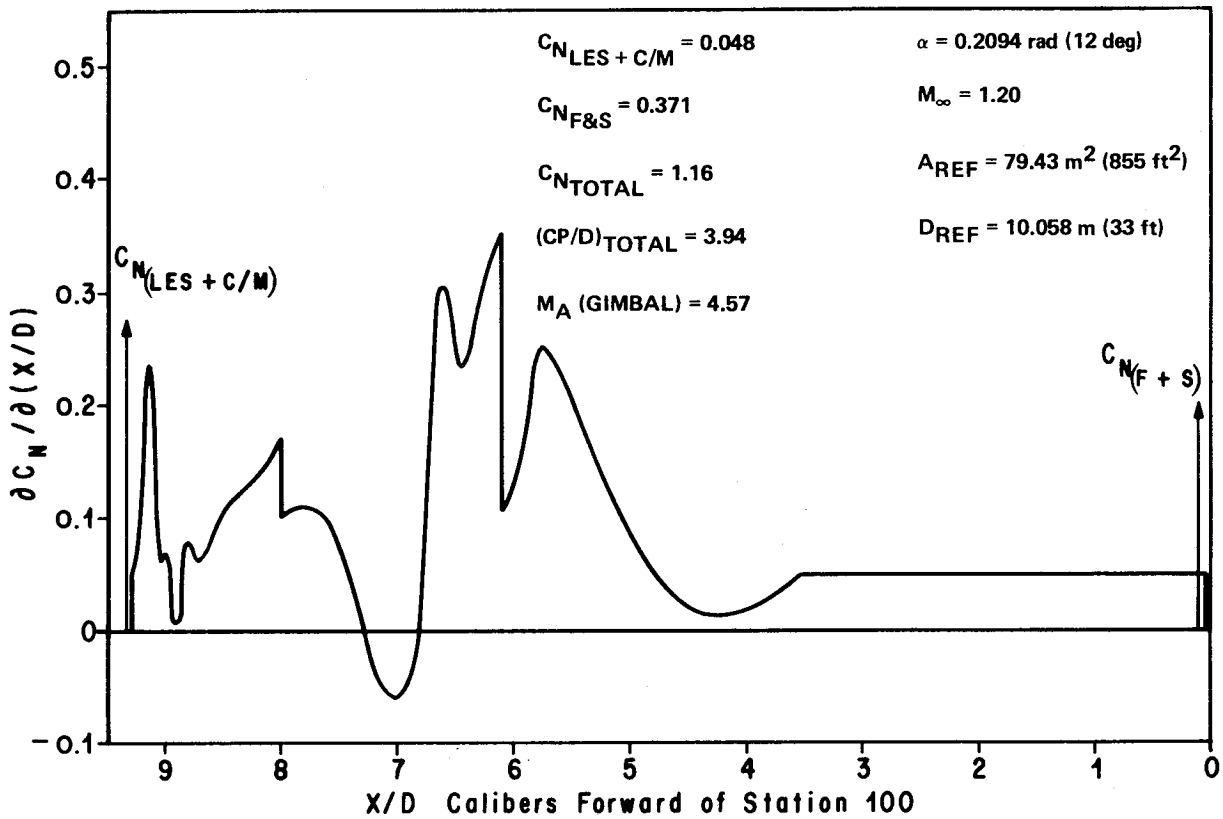


Figure 43. Normal flow distribution for Saturn V.

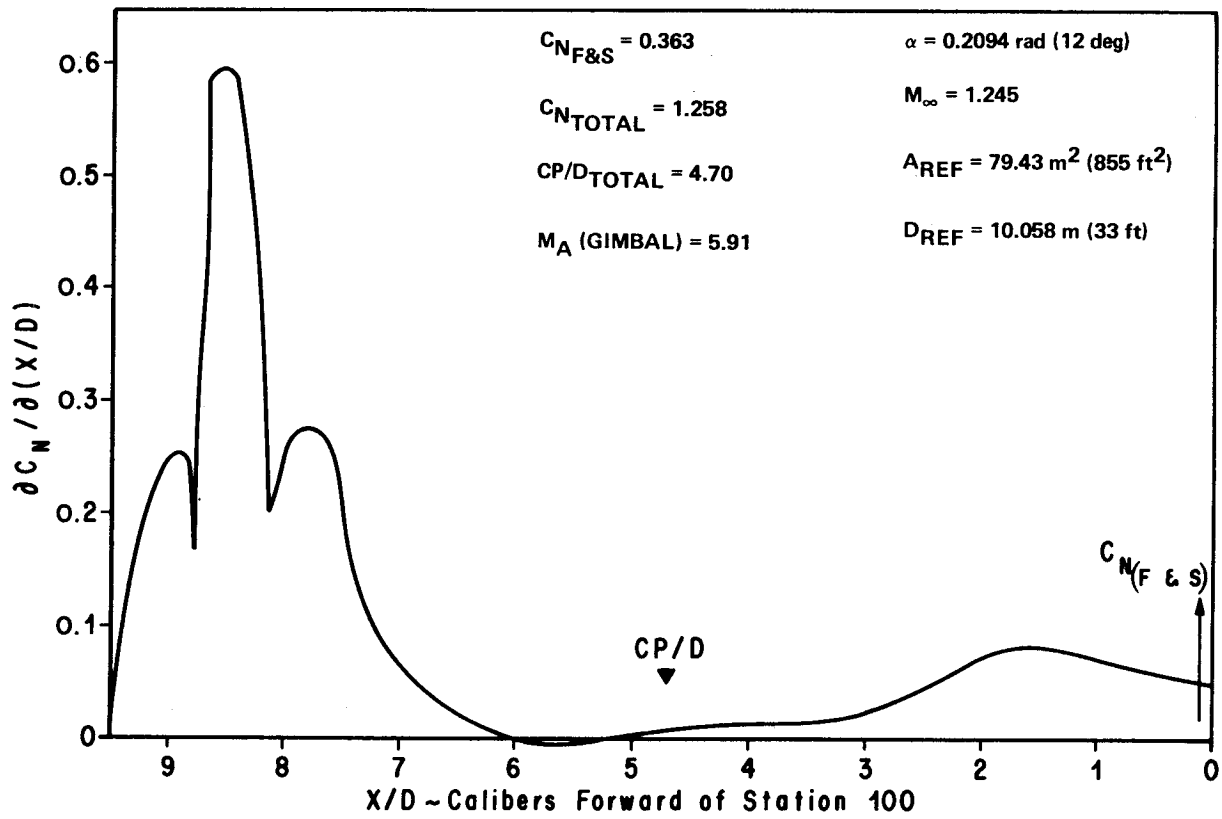


Figure 44. Normal force distribution for Saturn V Skylab.

are shown on Figure 45 for one flight time, both with and without wind biasing giving 65 percent and 98 percent probability, respectively. As a result, the problem was solved using wind biasing and verified using Monte Carlo response analysis. Figure 46 shows the structural limit and bending moment versus flight time. Probability levels with and without wind biasing are used as parameters [32]. Skylab flew with a very good launch probability as a result of the wind bias profile and the change to a more realistic verification analysis approach.

The lesson is clear, small changes can easily eat up large margins. Analysis must be refined to match the problem requirements.

4. Skylab Solar Wing

Skylab, the first orbiting space station, came close to being a total failure. Only through hard work, innovative engineering, and thorough management was the mission salvaged to become a great success. The problem occurred during the ascent phase of the flight when one solar wing was lost due to improper venting. The other wing stayed attached to Skylab, but was inoperable since it was held undeployed by a strap. In addition, insulation required for maintaining proper environments for man was lost. When the crew got to the Skylab, the first task was deployment of a thermal shield through an access door. This shield was overlayed later with a much bigger shield using the crew in an extra-vehicular mode. This second thermal shield was added by the crew on the second mission. Much analysis and testing were required to verify that the control system jet plumes would not force the thermal shields to oscillate and break. The other task facing the first crew was to unblock the solar wing. The crew was sent outside with a bolt cutter, cutting the strap and letting the wing deploy. Great success out of apparent failure was a result. Forced response takes many forms, many times in the least

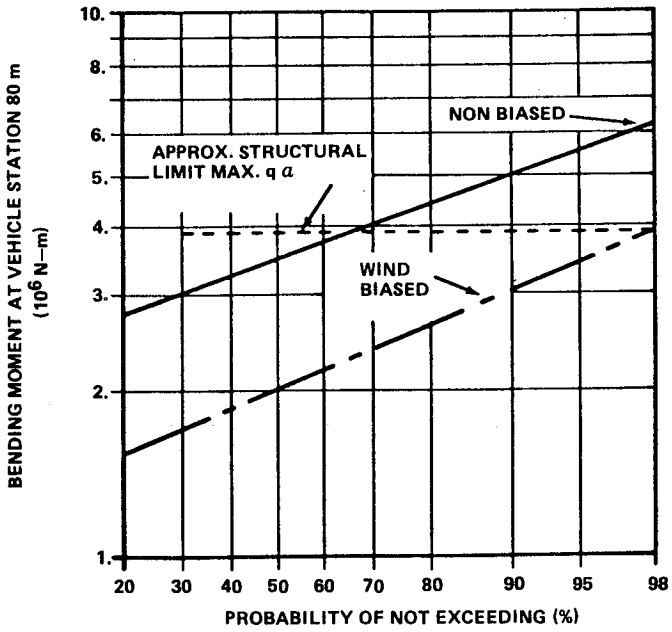


Figure 45. Maximum bending moment at vehicle station 80 m versus probability of not exceeding for March sample of Jimsphere winds.

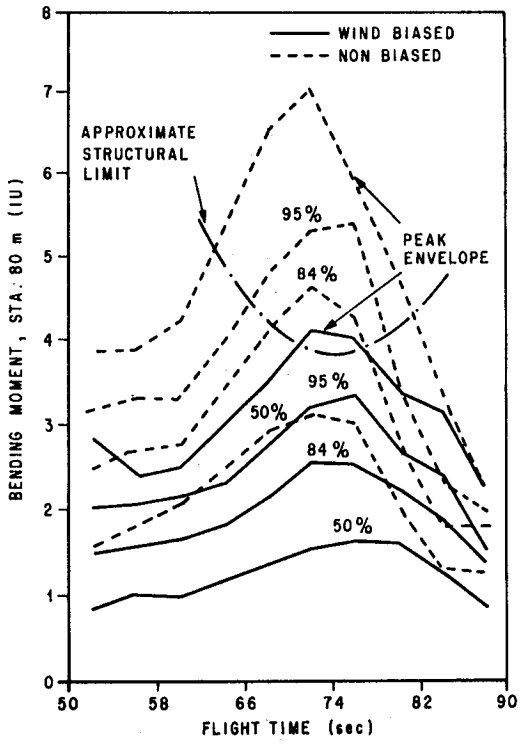


Figure 46. Skylab response to Jimsphere wind ensemble.

expected manner. Skylab's initial failure refocused engineering towards a systems' viewpoint with the warning to not neglect anything. Skylab's salvation was very costly, but demonstrates how teamwork and good systems engineering can solve problems. Many times one is not so fortunate and the mission is lost. Figure 47 shows the orbiting Skylab with only one solar wing and the man-deployed sun shield.

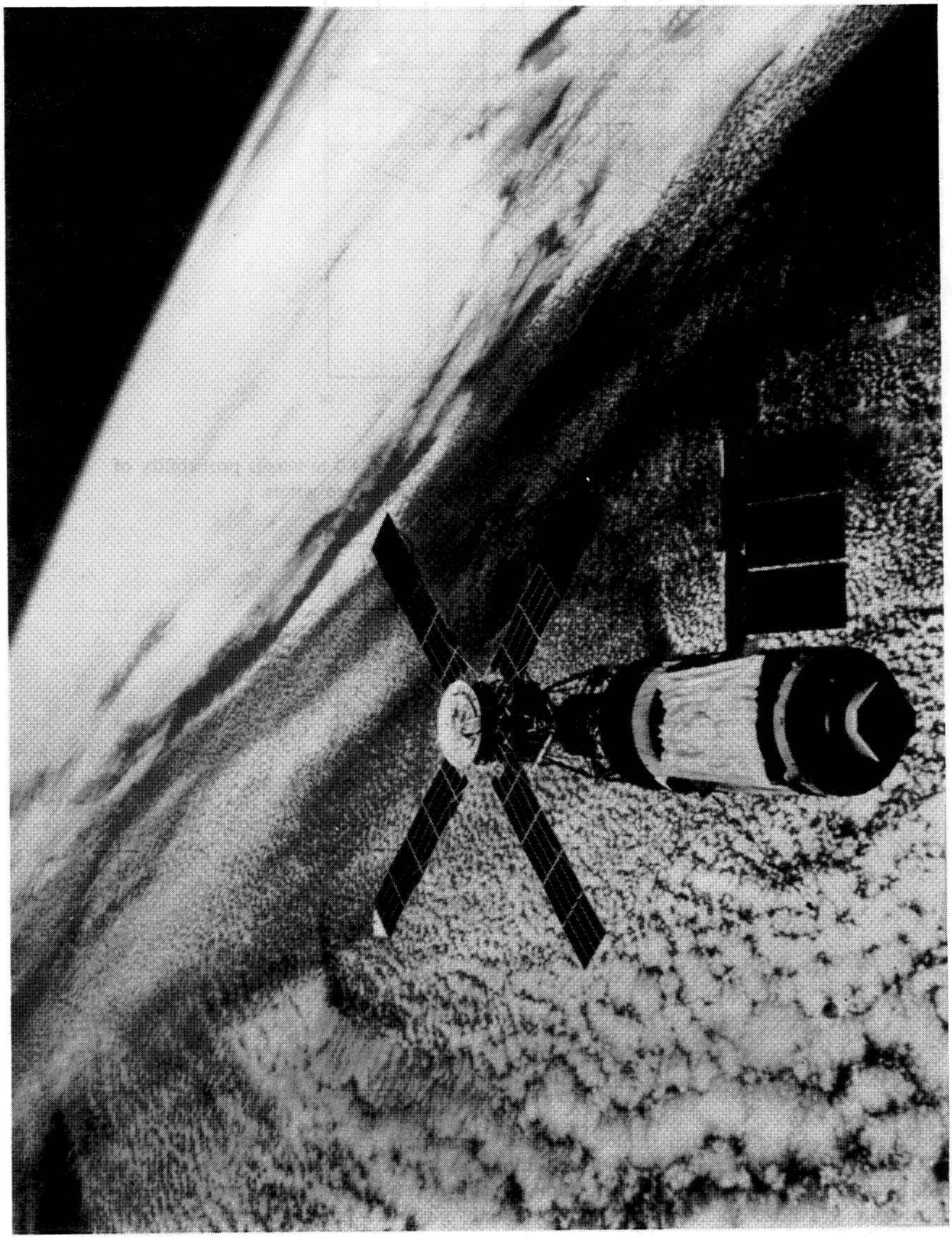

Figure 47. Skylab in orbit.

## 5. Shuttle Response Problems

The Space Shuttle had several forced response problems, none of which were disastrous; however, each required design or operational fixes. These are delineated by system and element, External Tank (ET), Main Engine (SSME), and Solid Rocket Booster (SRB). The discussion will not necessarily be in chronological order.

### a. Systems

1) Acoustics and Ignition Overpressure. Several problems occurred in the Shuttle systems. Early in the Shuttle Program, it was predicted that the acoustical environment would greatly exceed desired levels. The problem was aggravated by the close proximity of the payload to the energy source. Using a 6.4 percent propulsion model of the Shuttle and Shuttle launch pad (MLP), MSFC analyzed this problem (Fig. 48). Extensive testing was done to define the environments, then to design an acoustical suppressor. This was accomplished using a water injection and spray system. Figure 49 is a picture of this water system operating (scale model). Figures 50 and 51 show a comparison between no suppressor and final selected suppressor. Full scale operational data showed the levels to be lower than scale model predictions adding margins to solving the problem. The same approach has been taken for the Western Test Range (WTR) launch facility. Finding the problem early in the design phase allowed for an integrated design with small, if any, impacts.

The small 6.4 percent scale model was used to predict ignition overpressure waves. Although some predicted from these data that the levels would be high, most did not [33-35]. Scaling of overpressure was not totally understood, hence the differences in predictions. STS-1 was launched without any major concern for overpressure. Luck prevailed. The SRB ignition overpressure was there in full force creating large vehicle responses but no failures. Launch film analysis showed large elevon deflections and accelerometers showed big responses in the payload bay, some very near the design values. The overpressure wave is caused by the high momentum exhaust displacing the air within the flame bucket (Fig. 52). It is a function of thrust rise rate, thrust magnitude, thermal conditions, and density. Clearly, it was too risky to launch the next Shuttle without a fix. The MSFC 6.4 percent model was reactivated along with the other special tests. A special intercenter working group was formed to direct the activities. Two basic approaches, wave blockage and plume injection with water, were pursued. Specialists were called upon and testing started. Adding water directly to SRM plumes greatly reduced the overpressure, in fact, sufficiently to eliminate the response problem. Several people raised concerns over the ability to scale the data to full scale. These concerns resulted in the use of larger water troughs (in conjunction with the water injection) in each SRB primary and drift (secondary) exhaust hole, creating a shield or blockage. The troughs were quickly destroyed when the SRB thrust impinged on them after liftoff. Permanent steel blockage could not be effectively used. The plates would have to be in place during the time of the overpressure wave, then moved out of plume impingement. The water troughs met these requirements. Since Eastern Test Range (ETR) was using water for acoustic suppression, additional lines were run and the system finalized. Figure 53 shows the water system and water troughs in place for STS-2. STS-2 was launched on time. The overpressure suppression system worked better than predicted. Figure 54 shows the overpressure magnitude for STS-1 (before fix) and STS-2 (after fix) [27-29]. Nine more launches have further proven the success of this concept. Space Shuttle slipped through the overpressure problem; however, the message is clear. When a potential problem exists that can cause such large responses, analytical and testing work should totally ring out the details. This was not done on Shuttle and, in retrospect, we were lucky. When a dissenter exists, understand his point before proceeding. The high pressure of getting the Shuttle launched in conjunction with a low budget is probably the main reason the problem was missed.

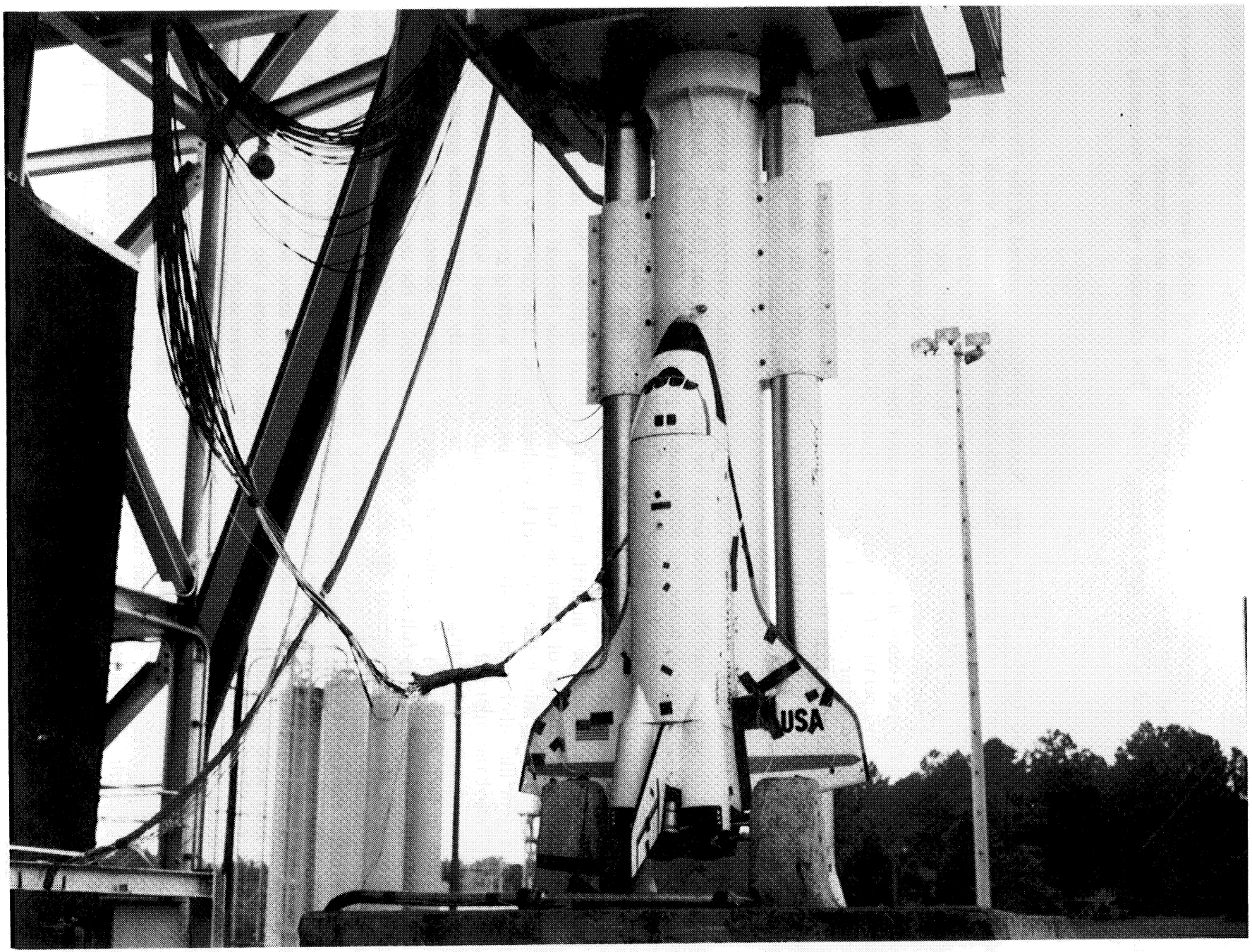


Figure 48. 6.4 percent Shuttle acoustics and overpressure model.

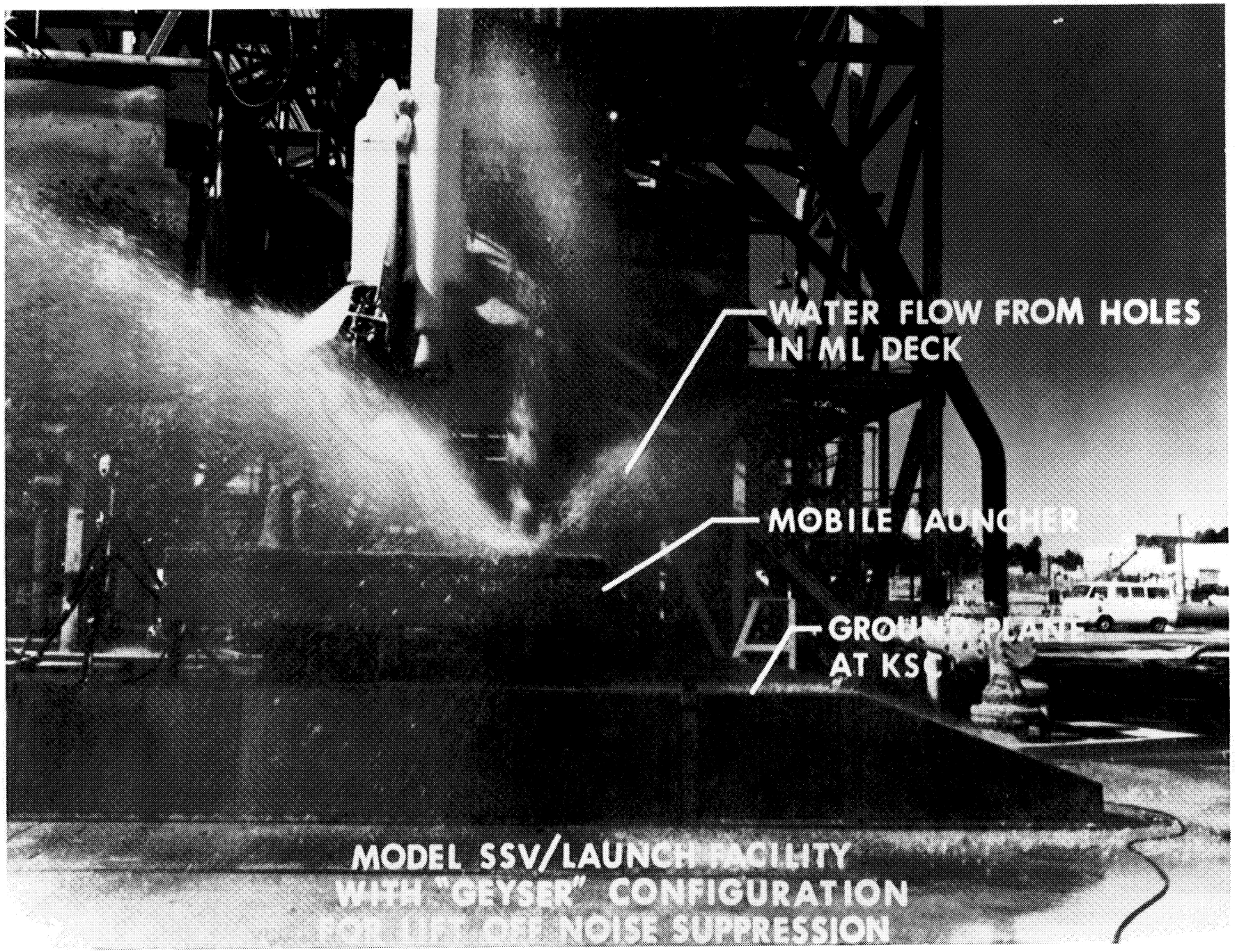


Figure 49. Acoustic suppression water spray system.

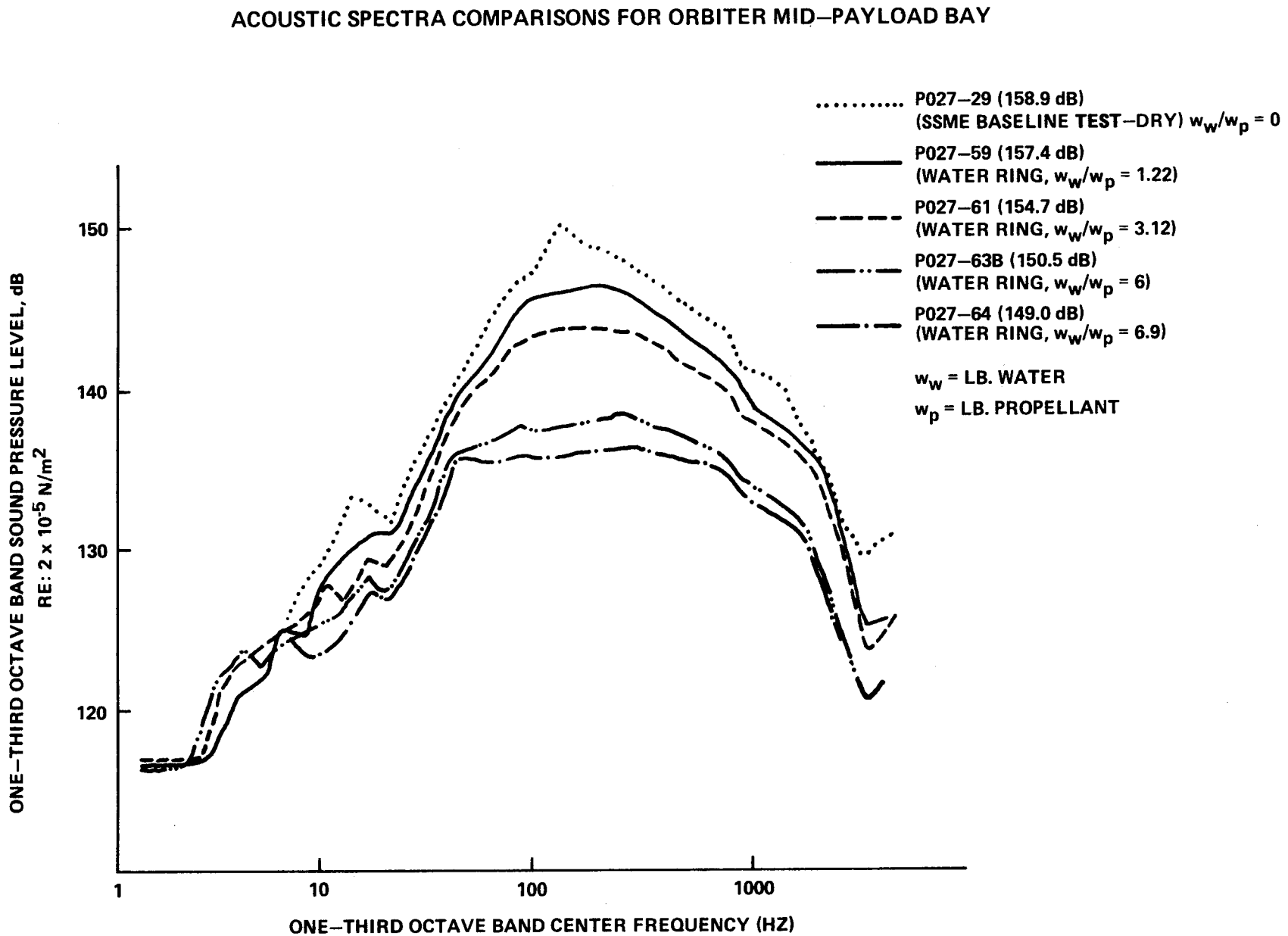


Figure 50. Acoustic levels with and without suppression.

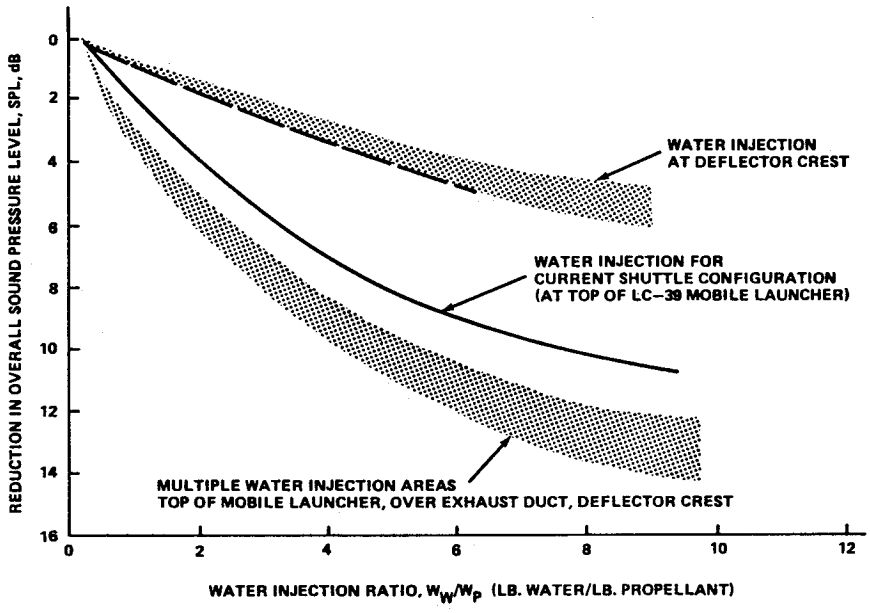


Figure 51. Acoustic levels with and without suppression.

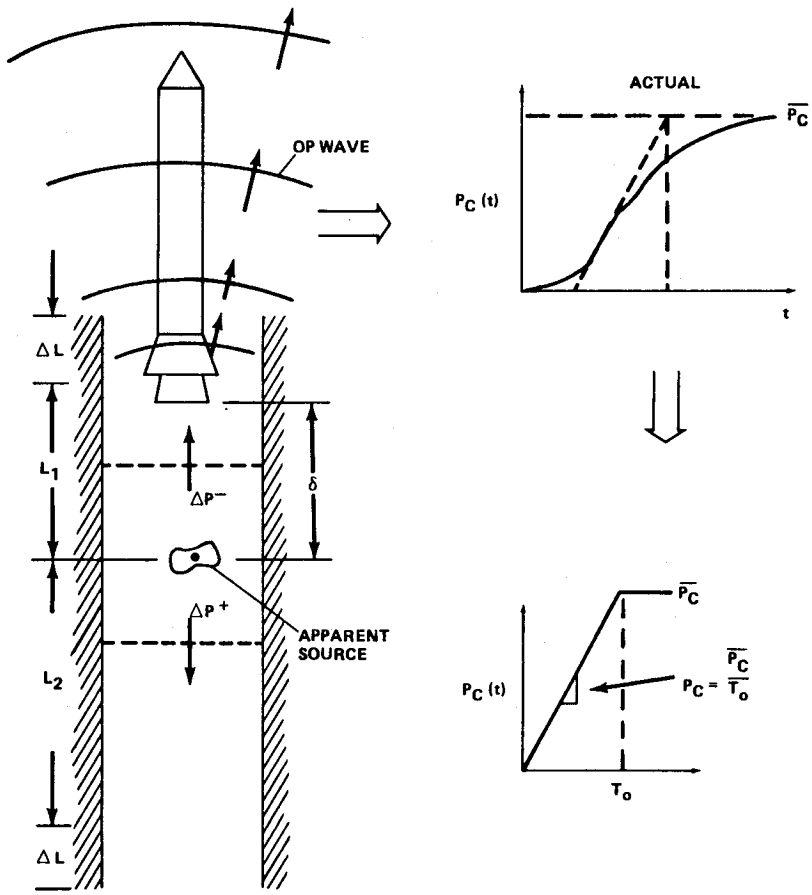


Figure 52. Overpressure model.

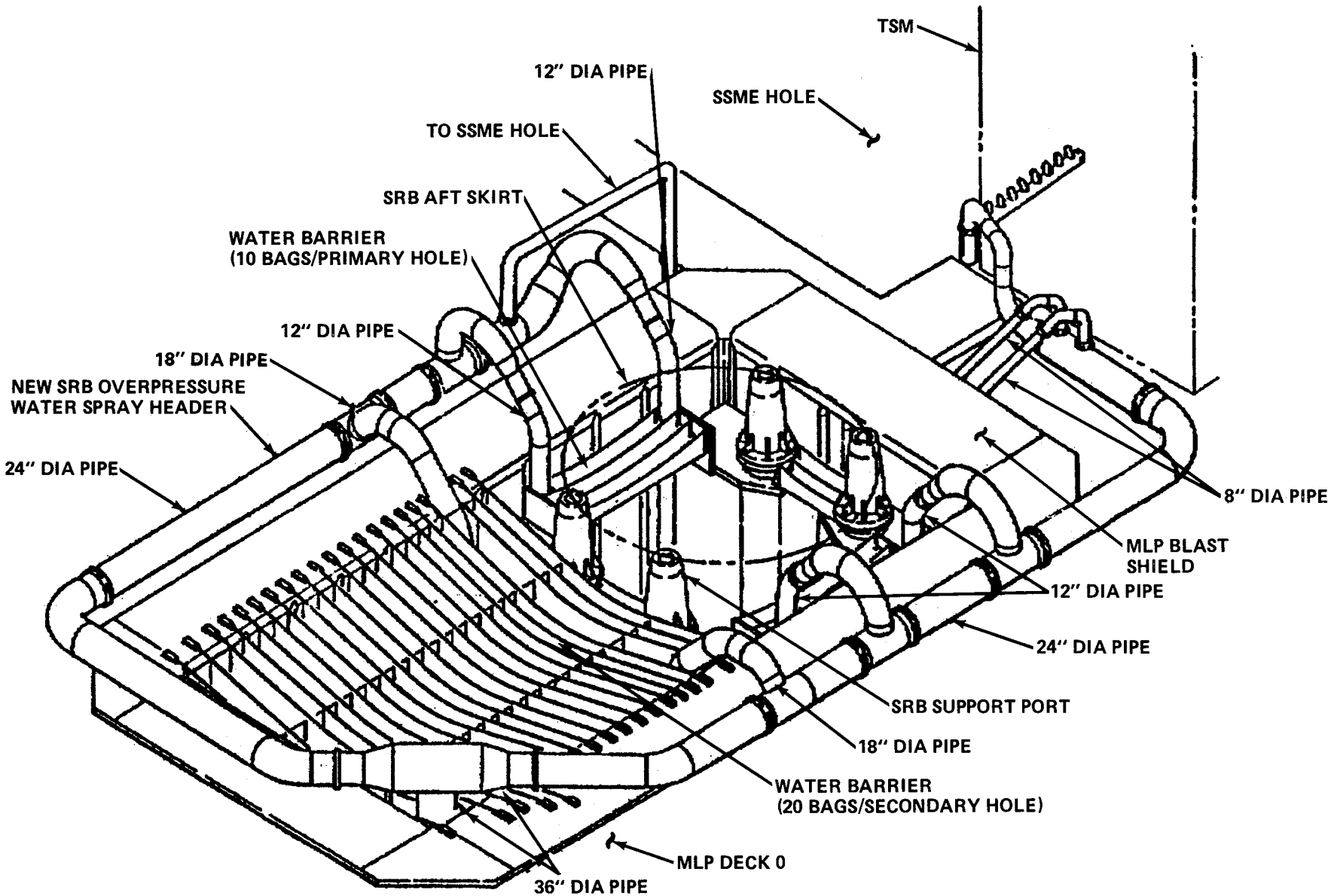


Figure 53. Overpressure mods STS-2 configuration.

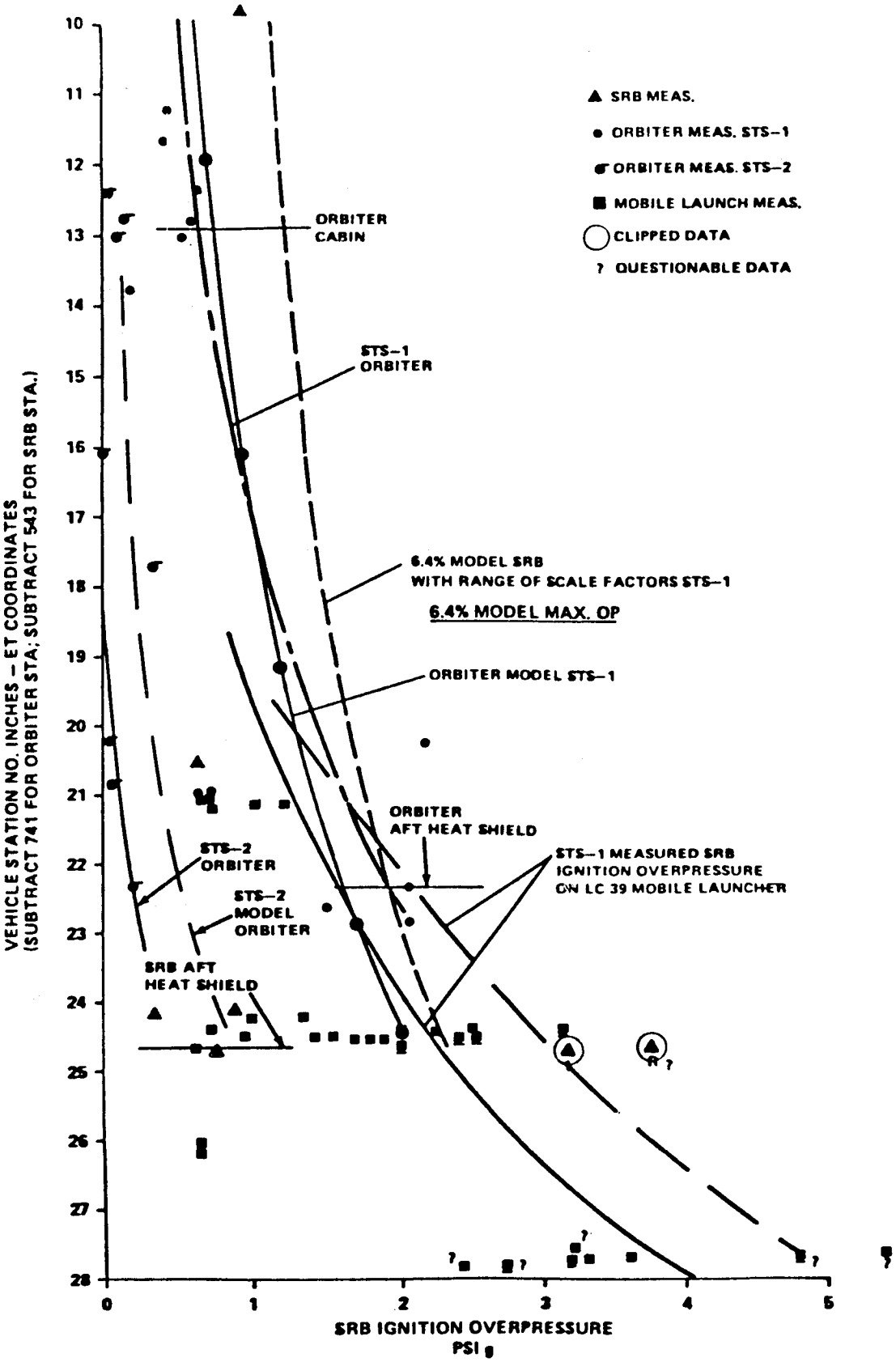


Figure 54. STS-1 measured SRB ignition overpressure versus vehicle station.

One additional problem occurred in the overpressure area. The SSME's start sequence has a hydrogen lead which allows free hydrogen to collect in pockets around the engine or launch stand. When the engine starts, this collected free hydrogen ignites (pops) creating overpressure waves in the neighborhood of 3.5 psi. This pressure wave level created load problems on the Orbiter heat shield and had to be eliminated. Several approaches, geared toward burning the free hydrogen as it collects, were tried. In general, they were some type of burner. Hydrogen flame jets were not effective due to the small area of the flames. The final solution was solid burning ROFI's which had a wide flame span including the spewing hot particles. This solved the problem, cutting the overpressure levels to around 0.5 psi. The system was verified on MPT (Main Propulsion Test). All Shuttle launches have used the system with no adverse problems. Figure 55 shows the launch configuration.

2) Liftoff Transient Loads. The Space Shuttle and its payload experience a very large transient load at liftoff due to a large asymmetrical coupling (static and dynamic). As the SSME's thrust comes up to full power, the vehicle is bent over and stretched storing energy elastically. At a predetermined time (timing to minimize twang loads) (Fig. 56), the SRB's light up with a very high thrust and internal pressure stretching the solids, adding more energy to the twang. SRB ignition time is very critical to the maximum load experienced. A time of 2.5 sec after SSME start gives minimum stored elastic energy and has been used on all Shuttle launches. Other factors or parameters that aggravate this response problem are thrust imbalance between solids, ground winds, thrust misalignment, and structural uncertainties. Since the Shuttle and its payloads are a multibody, unsymmetrical structural and structural dynamic configuration, the response is very sensitive to parameter changes. Analysis of this event has required the development of a very complex simulation program using up to 300 elastic body modes [36]. Without modern day computers, this problem could not be analyzed [2]. Figure 57 shows the results of a Shuttle launch response in the cargo bay indicating that the model has accurately predicted these low frequency responses. Table 3 shows the load changes from one ST configuration to another.

An example of the sensitivity and complexity of the liftoff twang response (loads) is the Space Telescope in the Shuttle cargo bay. Analyzing the ST loads during liftoff led to a very interesting conclusion. In an attempt to reduce the number of computer cases to run, the thrust differences between the two solids had a 15 millisecond lag put into the thrust trace to account for certain electronic lags in the control/computer system. ST loads with this SRB thrust lag was a factor of 5 higher than without it [32]. Sensitivities of this magnitude meant that the environments had to be very accurate or erroneous results would occur. Also, it meant that environmental changes had to be evaluated and reevaluated in order not to create a problem.

Another problem that occurred during liftoff was the SRB holddown bolt design loads. Each SRB is held to the pad by four holddown bolts through footpads (Fig. 58). These bolts are designed to take the load from the SSME buildup and then to be fractured (pyrotechnics) at SRM ignition. In addition, the bolts must be captured so that they do not become a debris source. Predicting and measuring this load was a major problem due to the complex load paths from the load origin to a load in the bolt. Early attempts to back the bolt load out of flight data showed loads slightly in excess of design (safety factor less than 1.4), not a desirable situation. Using laboratory tests and finally a strain gauged bolt, it was shown that bolt loads were within design and no problem existed. Holddown bolts also showed the potential of not extruding when the pyros fired. In fact, the flight films have shown three examples where bolts did not extrude. Nonextrusion is not a problem, since the vehicle liftoff motion would pull the footpads off the bolt with no adverse effects. It was found that timing differences between firing of the redundant charge on each bolt could cause bolt hangup by setting up coupled dynamic motion of the bolt which caused the bolt to hang up. Additional analysis showed that as long as the pyros fire (nut fractured), Shuttle would lift off successfully, pulling the bolts out as a result of liftoff.

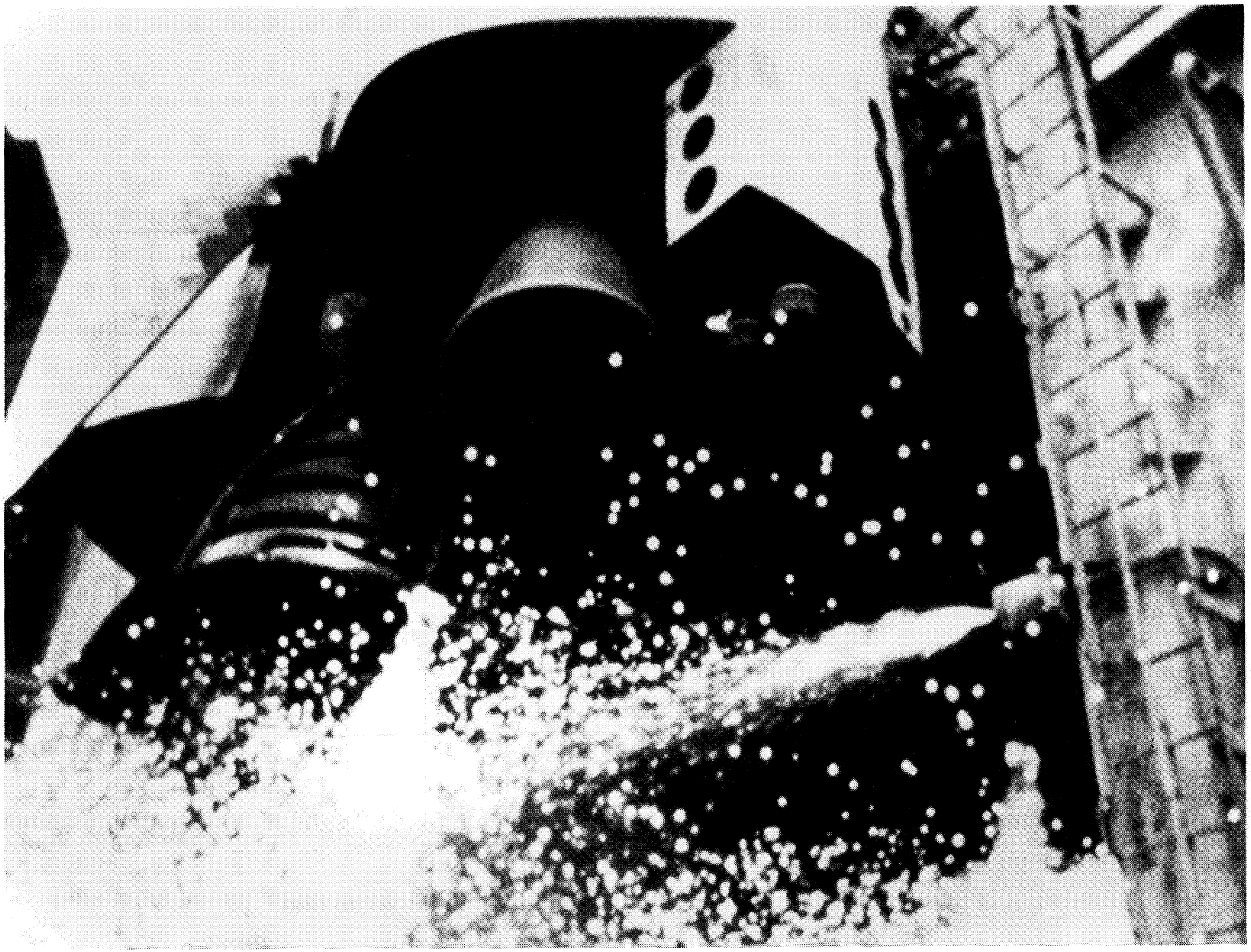

Figure 55. Radially outward firing initiator (ROFI) located on KSC's LC-39.

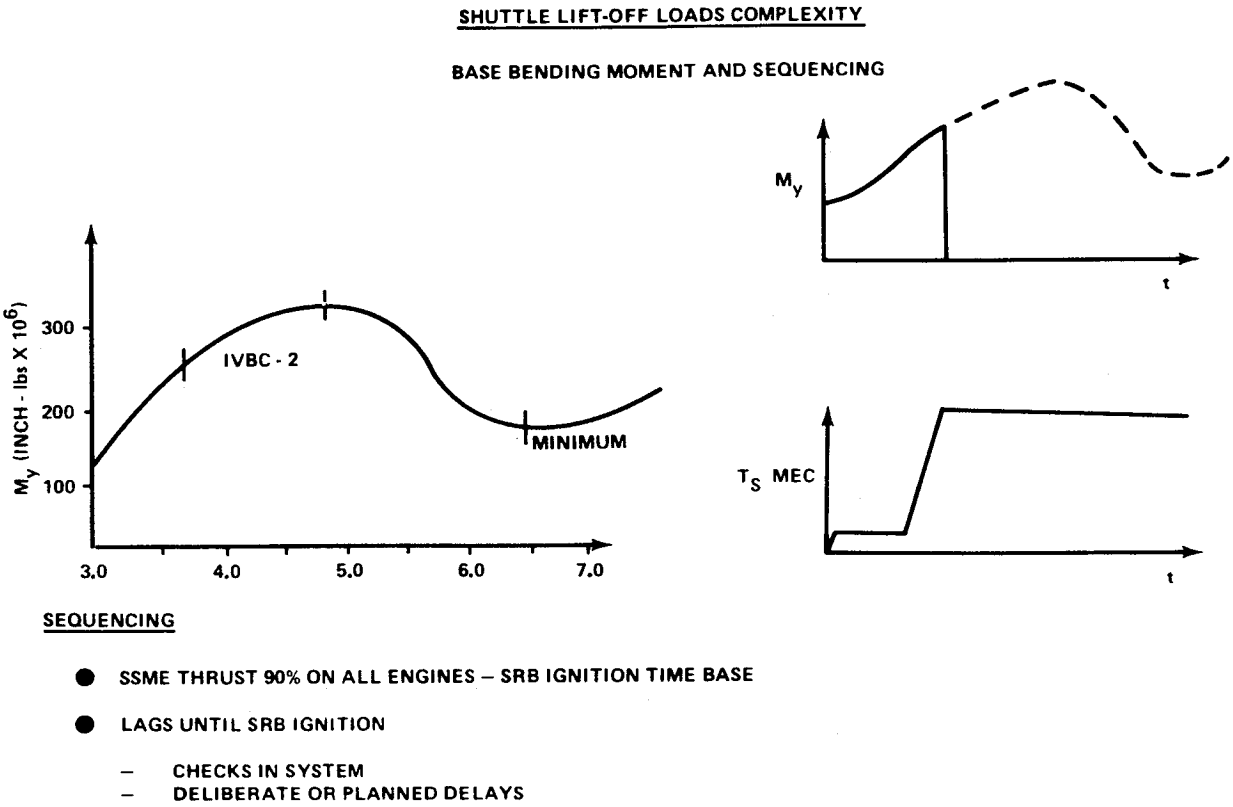


Figure 56. Shuttle liftoff sequence characteristics.

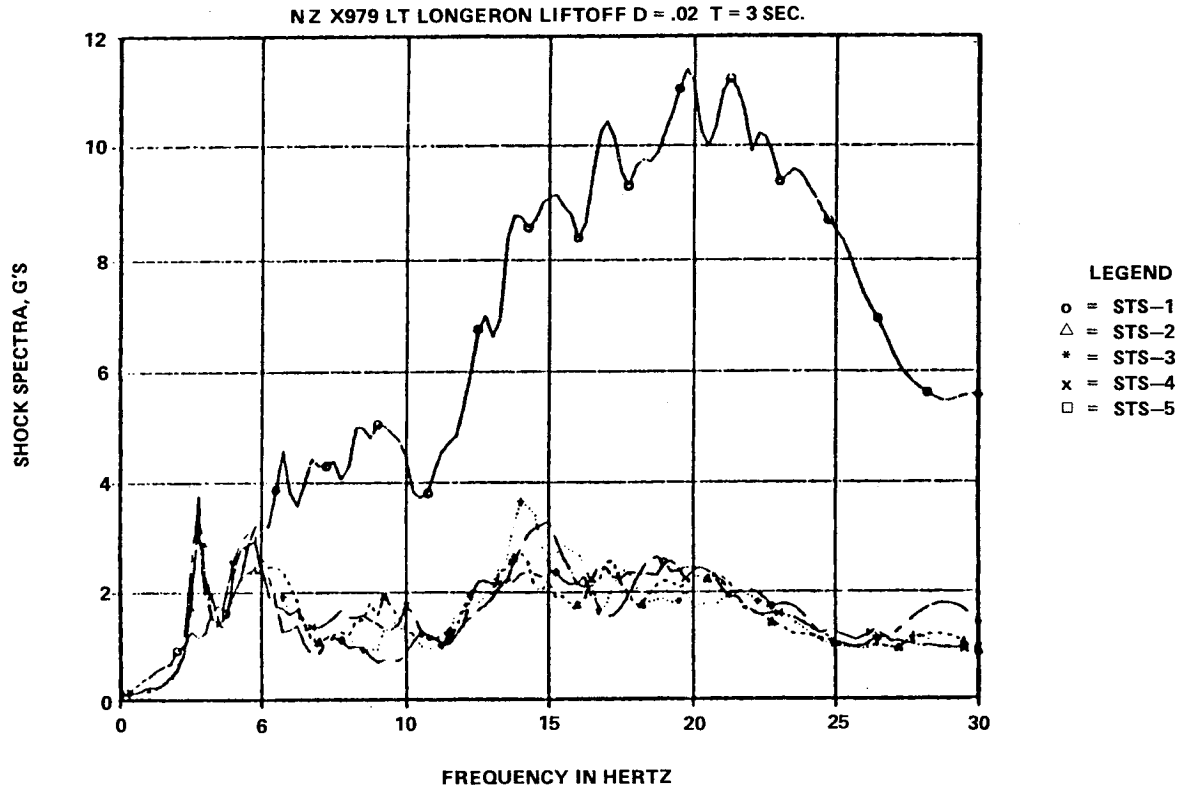


Figure 57. Shuttle flight loads (payloads) versus predicted.

TABLE 3. PAYLOAD LOAD CHANGES SENSITIVITIES

| COMPONENT | DIR. | MAXIMUM ACCELERATIONS (G'S) LIFTOFF LOADS | | | |
|---|---|---|---|---|---|
| | | DESIGN VALUE | P. L. C. | I. L. C. | C. D. R. |
| PRIMARY MIRROR | X | 3.7 | 3.1 | 3.5 | 4.5 |
| | Y | 2.4 | 1.1 | 1.2 | 0.9 |
| | Z | 3.7 | 2.6 | 2.0 | 3.2 |
| SECONDARY MIRROR | X | 3.8 | 3.1 | 3.4 | 4.5 |
| | Y | 3.5 | 2.3 | 2.6 | 2.3 |
| | Z | 6.7 | 5.0 | 3.3 | 12.9 |

P. L. C. = PRELIMINARY LOAD CYCLE, USED 5.4 SHUTTLE DATA
I. L. C. = INTERMEDIATE LOAD CYCLE, USED 5.7 SHUTTLE DATA
C. D. R. = CRITICAL DESIGN REVIEW LOAD CYCLE, USED 5.8 SHUTTLE DATA

One further example of the liftoff load sensitivity occurred when the WTR configuration was analyzed. The much stiffer pad/holddown post was the culprit changing dynamic tuning significantly. This led to designing softness on the holddown post at WTR to keep loads within the Shuttle design envelope.

3) High "g" (Maximum Dynamic Pressure) Inflight Loads. A very interesting problem occurred on the Orbiter wing during ascent flight. The inflight measured loads were very different and much higher for certain wing locations than prelaunch predictions. The major reason this occurred was a shift in the shock wave on the wing changing the aerodynamic distribution, probably due to the engine and SRB plumes. This change was not large; however, the integrated effect was significant. In fact, for a nominal trajectory, the predicted load was approximately 70 percent of the measured flight loads (wing root area). Figure 59 shows this effect in graphic form, showing the shift in loads. The chart makes the point that the vehicle is very strongly coupled between performance, loads, and launch probability, requiring that the trajectory be shaped to fly at an optimum balance between these three areas which occurred at an $\alpha$ of -2 deg for the original wind tunnel derived aero distribution. In addition, the shifting distribution changed the critical areas on the wing and also the leading edge becomes critical flying design type trajectories. There are several fixes to this problem: (1) beef up leading edge, wing root, etc., (2) fix leading edge and fly more negative $q\alpha$'s and take either performance or launch probability hit (balance them), (3) get an aerodynamic fix changing aerodynamic distribution to approximately the original prediction, and (4) fix leading edge, do minor fixes to wing span to fly moderately more negative $q\alpha$'s, increase q boundary (819 psf) and rebalance system between launch probability and performance. The key technical parameters in this total system trade are "q" (maximum dynamic pressure and $\alpha$ vehicle (vehicle angle of attack). Figure 60 shows how these parameters were traded during design and how the Shuttle Orbiting Flight Test (OFT) results changed in order to balance performance, loads, and launch probability. Figure 61 shows the change where the vehicle must fly to keep wing loads below design. This results in some performance hits. Beefing up the wing span and adding leading edge moment ties solves the problem. Final trade studies have shown that by allowing a maximum dispersed q of 819 psf, very little performance hit is taken at $q\alpha$ of -3000. This in conjunction with minor modifications to the Orbiter wing structure raised the launch probability to desirable levels. This was the solution chosen by NASA/JSC to the wing problem.

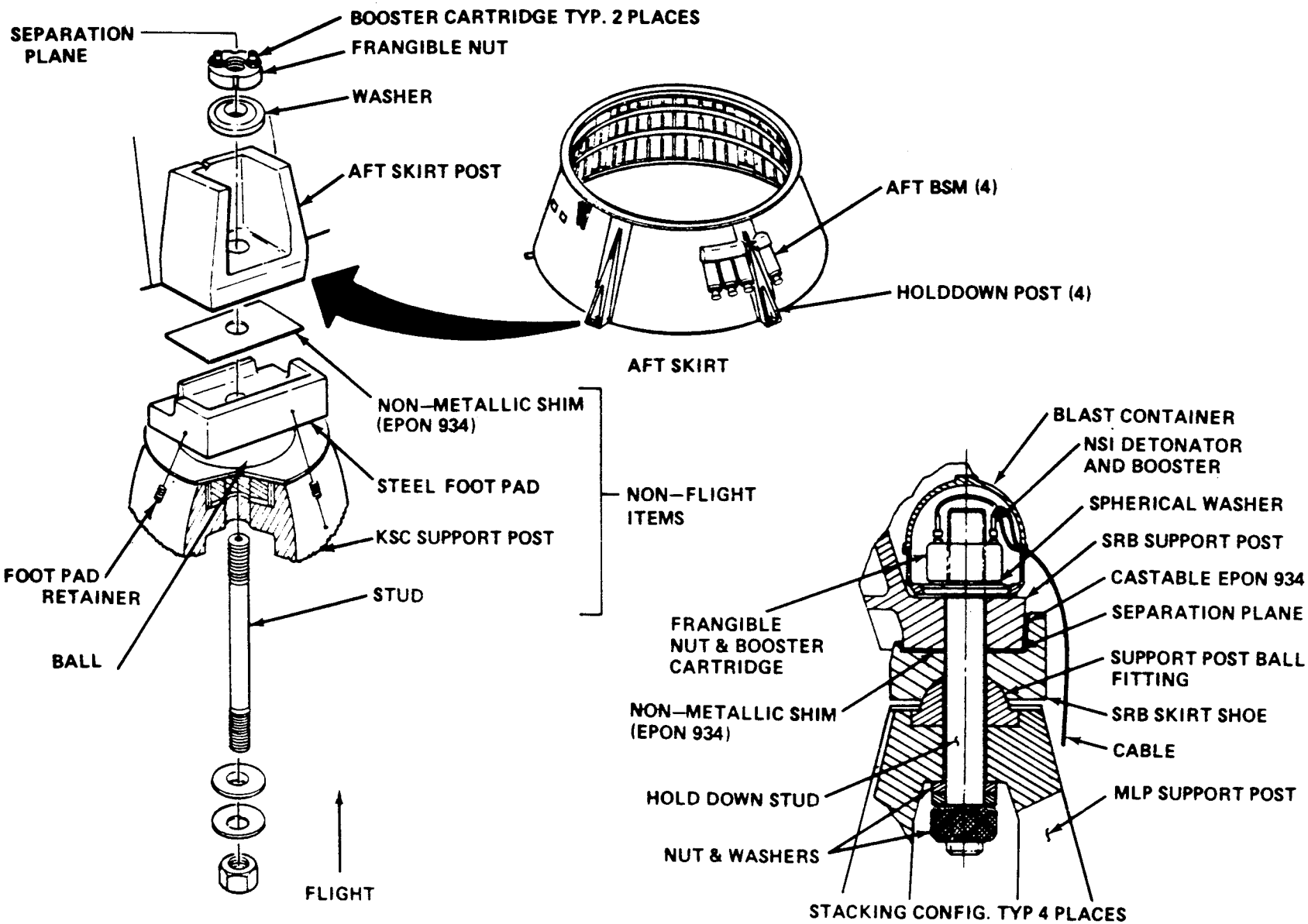


Figure 58. SRB holddown bolt and foot pad.

# LOAD & PERFORMANCE RELATIONSHIPS

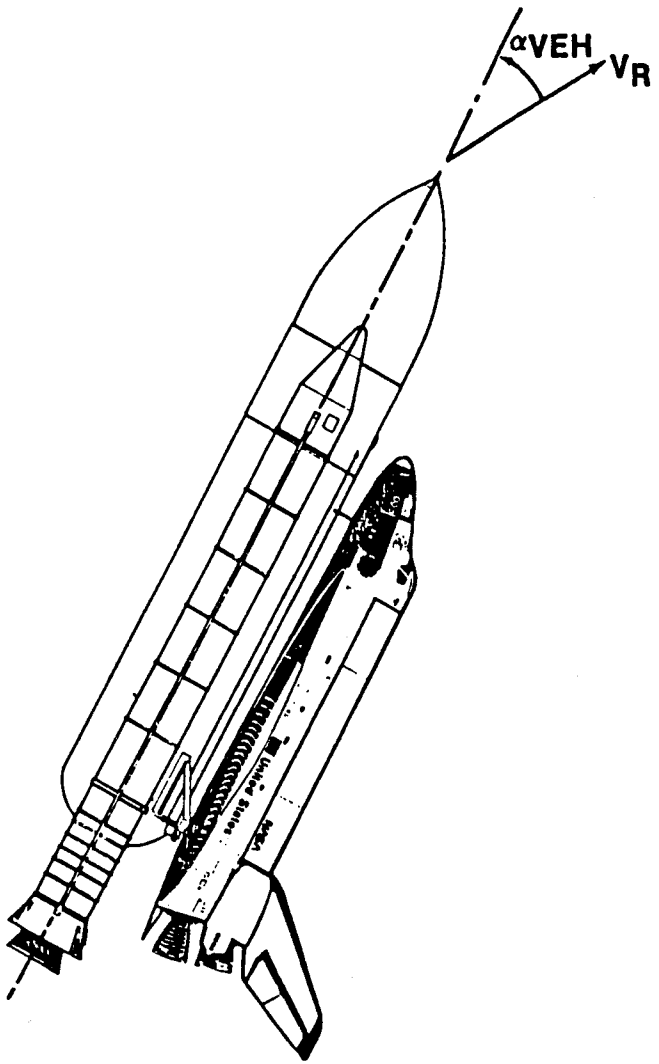


- ORIGINAL DESIGN ACHIEVED OPTIMUM BALANCE (PERFORMANCE, LOADS, LAUNCH PROBABILITY) AT $\alpha_{VEH} \approx -2°$
- GENERAL FEATURES OF WING LOAD ARE:

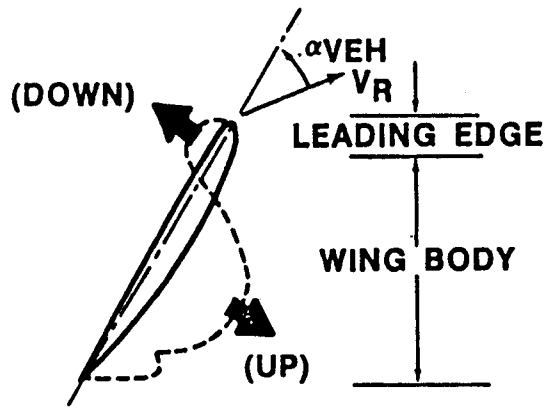


- IF $\alpha_{VEH}$ SHIFTS MORE NEGATIVE:
  - LEADING EDGE LOADS INCREASE
  - EXTERNAL TANK LOADS INCREASE (PROTUBERANCES)
  - WING BODY LOADS DECREASE
  - TRAJECTORY TENDS TO LOFT (PERFORMANCE LOSS)

Figure 59. Load and performance relationships.

# ASCENT PARAMETERS

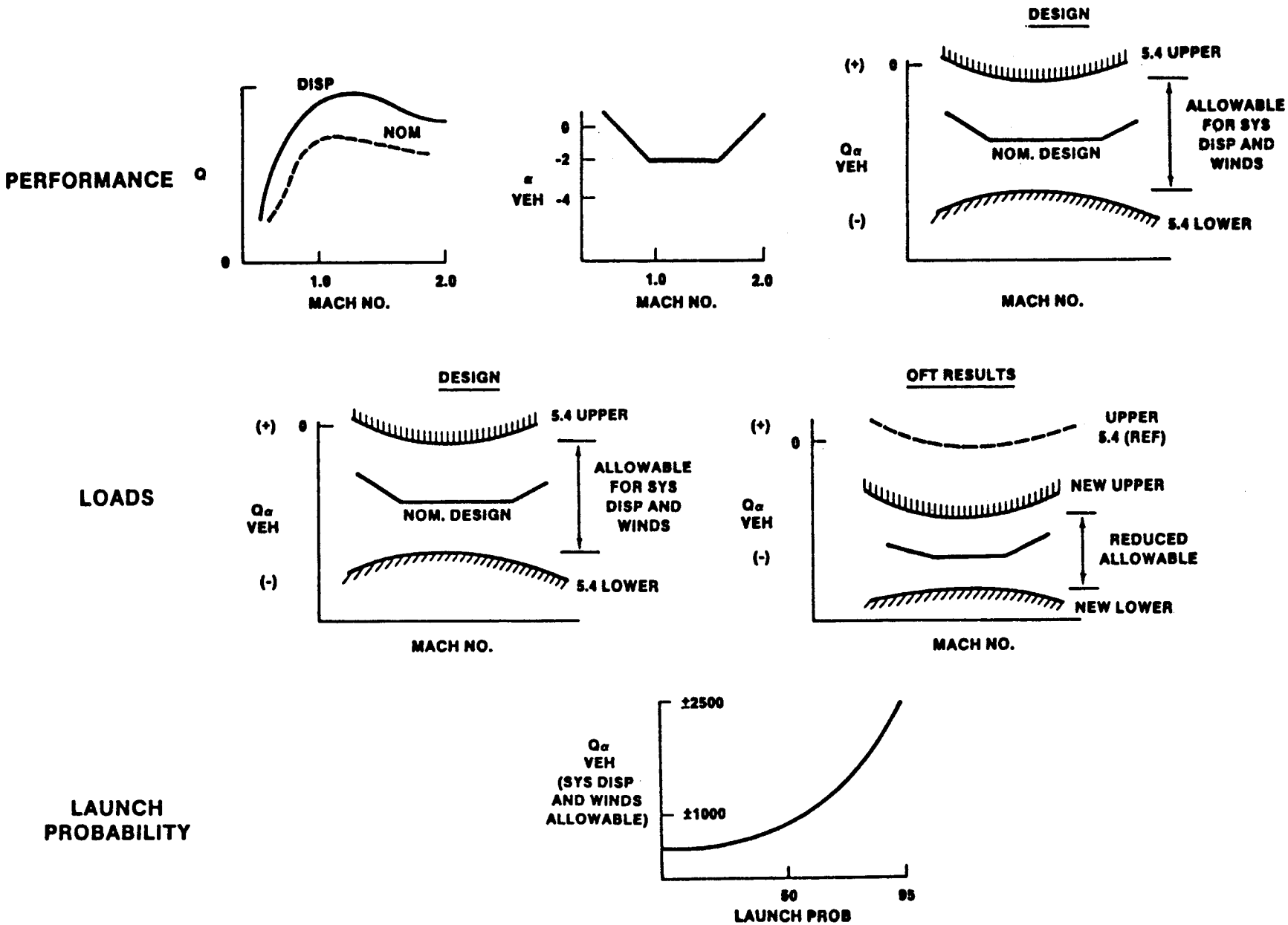


Figure 60. Ascent parameters.

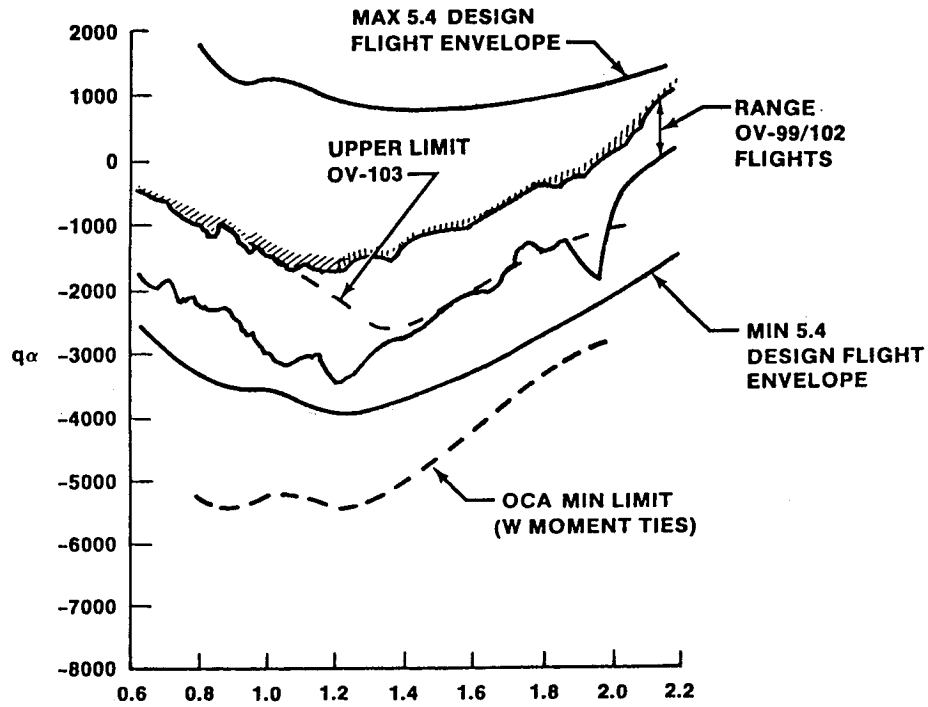


Figure 61. Ascent flight envelope limits.

This problem illustrates the system interactions and the problems encountered when the state-of-the-art is being extended as was the case of the Shuttle. Simulating plumes in scale model testing was the major hurdle that only flight data could resolve. This is also an example of flying developmental missions. This approach was chosen for Shuttle. The wing load problem illustrates the wisdom of the approach.

The Orbiter wing was not an MSFC responsibility (JSC responsibility); however, the systems impacts on MSFC elements meant heavy involvement by MSFC in all aspects of the problem through the Ascent Flight Systems Integration Group (AFSIG) and the various technical panels. Data presented were obtained working with JSC in these groups. Approximately two years effort was required to understand and solve the problem.

b. External Tank (ET)

Two different response problems occurred on the ET, one associated with internal flow and the other with external aerodynamic flow. The first was a failure of the diffuser. The second was the response of tank external protuberances. Although no failure was experienced with the protuberances, redesign and verification testing had to be accomplished to insure a safe flight.

1) Propellant Diffuser. The ET diffuser was a baffling problem in that during ground testing, including the systems main propulsion test, cracks occurred and pieces broke out (Fig. 62). Existing accelerometers on the external tank skin provides no clues. A series of mechanical vibration tests could not produce a failure. Neither could acoustical analysis. This led to the development of a series of flow tests that duplicated the inlet pipe geometry, flow rates, and gas density. This test was the clincher. When the system characteristics were duplicated, the diffuser failed. What was happening is clear in retrospect, the turbulence of the flow contained a large amount of energy at the natural frequency of the diffuser shell mode. The forced response of this shell mode, to turbulent flow, failed the diffuser shell. Redesigning the diffuser to detune it and have more strength resulted in an acceptable solution.

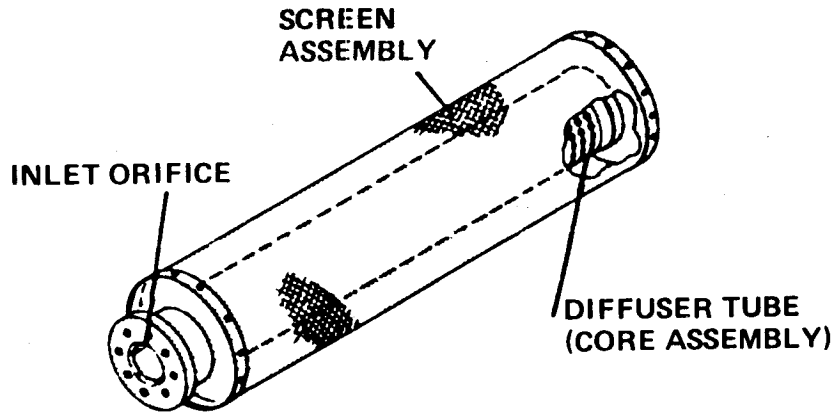


Figure 62. ET diffuser.

2) Protuberances, External Aerodynamic Loads. The protuberance problems arise from an inadequate environment definition early in the program. These early predictions basically assumed no cross flow around the tank and were based on smooth body flow. As wind tunnel testing proceeded, this assumption broke down, since substantial cross flow existed for the tank in the ascent configuration (Figs. 63, 64, and 65). Protuberance model testing showed original drag loads for smooth body flow to be in error. This led to loads which exceeded design specifications. The end result was some redesign and, in other cases, verification testing at a higher limit load. With these changes and additional verification testing, ET protuberances have shown no problems in Shuttle operations.

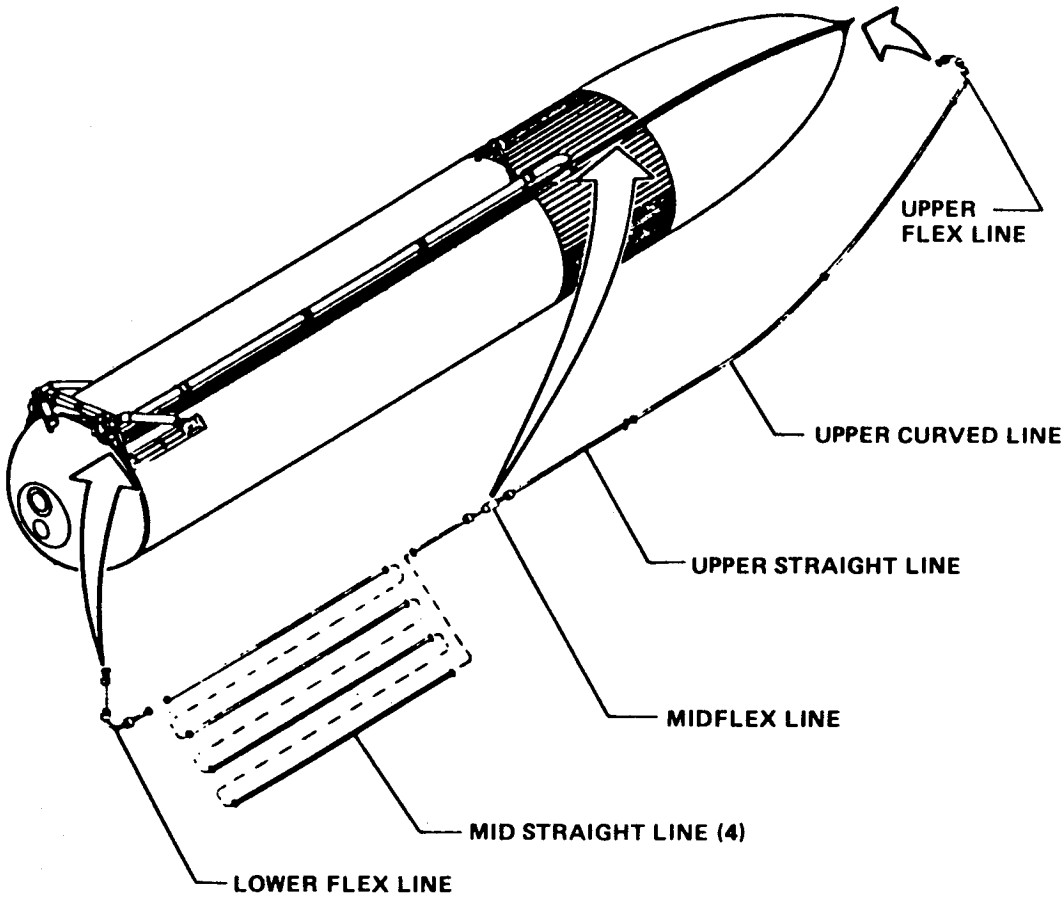


Figure 63. ET protuberance cross flow.

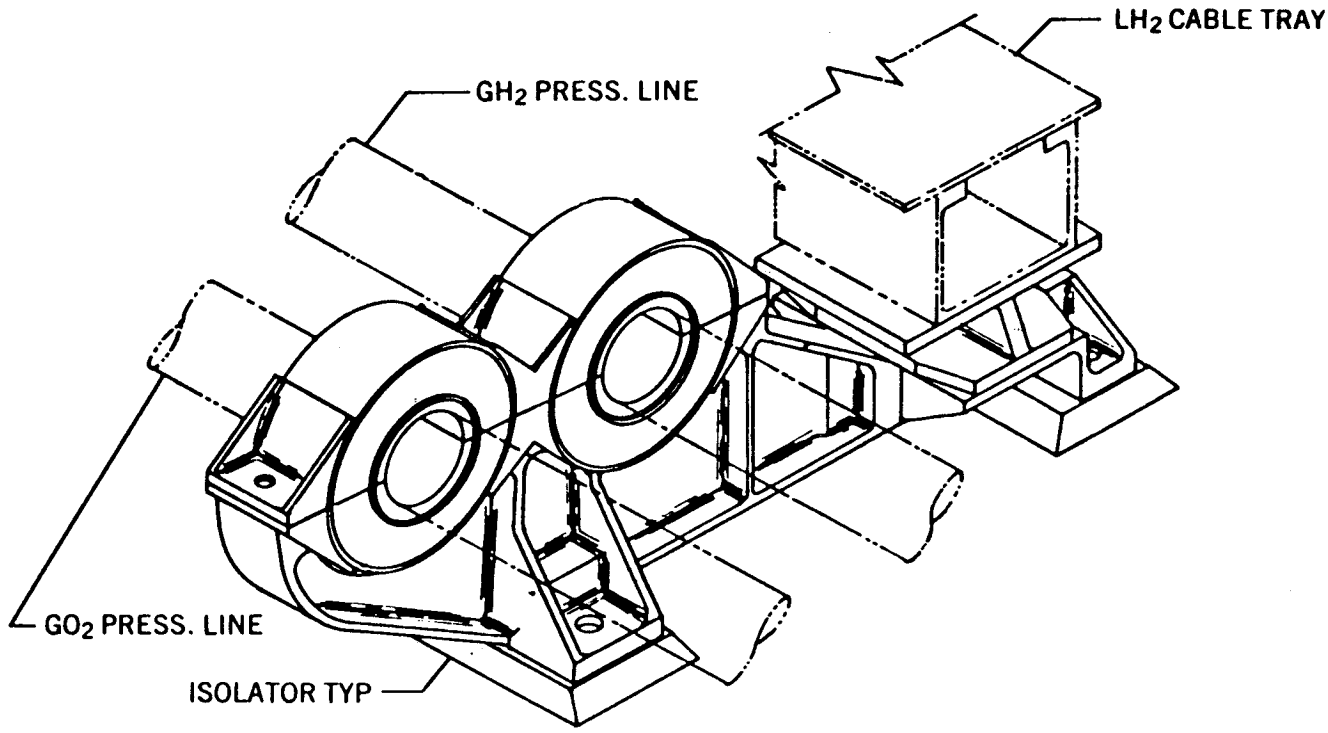


Figure 64. ET protuberance cross flow.

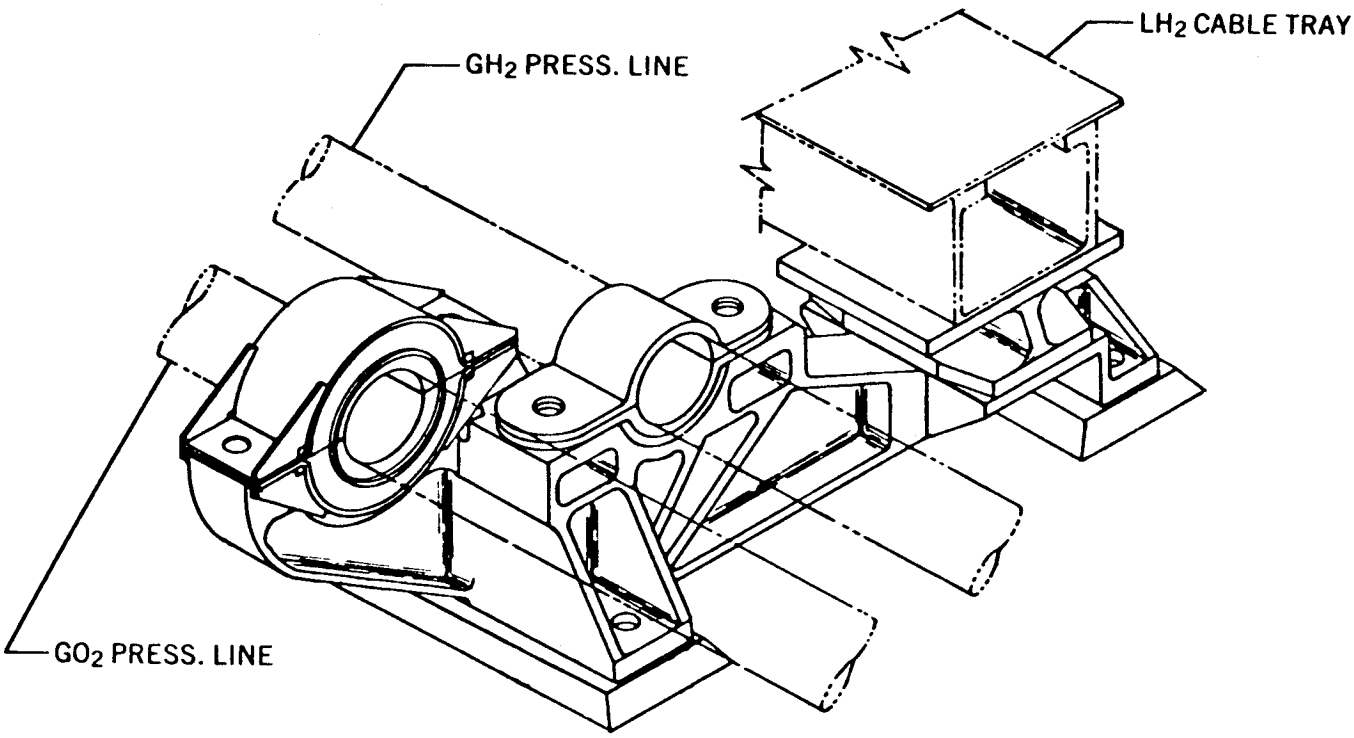


Figure 65. ET protuberance cross flow.

c. Solid Rocket Booster (SRB)

Several response problems have been observed in SRB during testing and during flight operations. In general, these problems occurred during recovery and water impact. The Integrated Electronics Assembly (IEA) was an exception where the vibroacoustics environment was higher than predicted, leading to the requirement for isolation and requalification. Key problems in other areas have been the most interesting.

1) Parachute Release G-Switch Failure. A very interesting problem occurred on STS-4. The parachute G-switch activated early on both SRB's, releasing the chute from the SRB resulting in a loss of both the SRB's. The G-switch was installed to release one of the two parachute risers at water impact enhancing SRB recovery. In this case, the switches were activated during the time of frustum severance before chute deployment during the atmospheric reentry phase. The severance is accomplished using a linear shaped charge. Figure 66 shows the frustum chute package and linear shaped charge. The G-switch was mounted to the SRB skirt after of the linear shaped charge on the IEA firewall which was mounted on the forward skirt reaction ring (Fig. 67). The problem occurred in this manner. The linear shaped charge caused a shock wave in the SRB skirt which excited the reaction ring in its first cantilevered mode of 85 HZ. This drove the IEA, hence the G-switch. The G-switch natural frequency was near 70 Hz and should have been critically damped. The G-switch response triggered the chute attach bolt, hence the loss of the chute performance and the SRB's. The first three Shuttle flights (six SRB's) had no problem; however, STS-4 had the same problem on each SRB. Why the difference? It turned out after much testing (pyro and G-switch response) that all flights were near a problem. These two SRB's exceeded limits because of two factors relating to G-switch damping. The temperature decreased the damping and the switches were fabricated on the low damping side but not outside the specs. This, combined with the expected variation in pyro shock response, led to the problem. The switch had been qualified to the shock load without the effect of the resonant mode of the support ring and, therefore, never showed a problem. In the qualification test, no switch came close to an inadvertent closing. The ring was stiffened substantially prior to the first flight to solve a local effect associated with the SRB rate gyros. This stiffness moved the ring frequency beyond the G-switch frequency spectrum and was not a contributor to the problem. No one thought that the G-switch of such a low frequency would respond to the shock based on above qualification test, hence the problem was missed. Many months of investigation time were required to find the culprit, although all pieces of the data existed prior to the failures. The problem was putting the pieces together in the proper manner.

2) Recovery System Loads Problems. The SRB is recoverable and reusable for twenty flights at a cost savings to Shuttle operations. Several problems have occurred in the recovery system and the water impact associated with recovery. These problem areas were (1) chute hangup and failure, (2) water collapse loads on SRB shell, (3) skirt and support rings transient response to impact, and (4) flow reversal during impact.

The recovery subsystem consists of a 11.5-ft-diameter pilot parachute assembly, a 54-ft-diameter drogue parachute assembly, and three 115-ft-diameter main parachute assemblies with retention components. The subsystem is located within the nose cap and frustum of the nose assemblies of each SRB and provides the required terminal velocity and attitude for water impact of the SRB and SRB nose assembly frustum.

An altitude sensing switch activates the recovery subsystem by initiating the ejection of the SRB nose cap. The jettisoned nose cap pulls away the pilot chute pack and deploys it. Full deployment of the pilot chute releases the drogue chute retention straps and rotates the drogue chute from its mounting on the deck of the frustum. The pilot chute then pulls the drogue chute and pack away from the SRB to deploy the chute into its first reefed position.

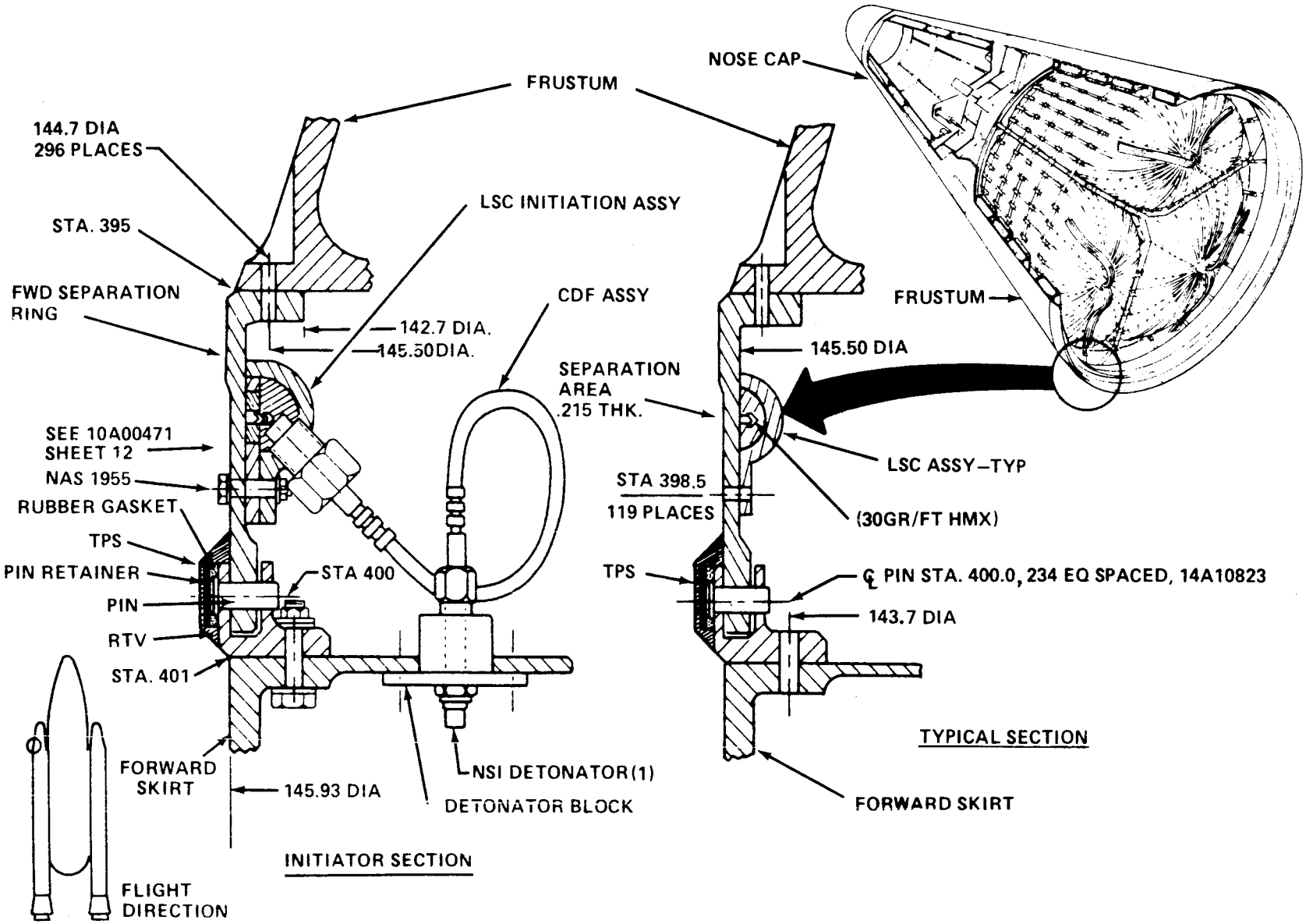


Figure 66. SRB forward frustum, packed chutes, and linear-shaped charge.

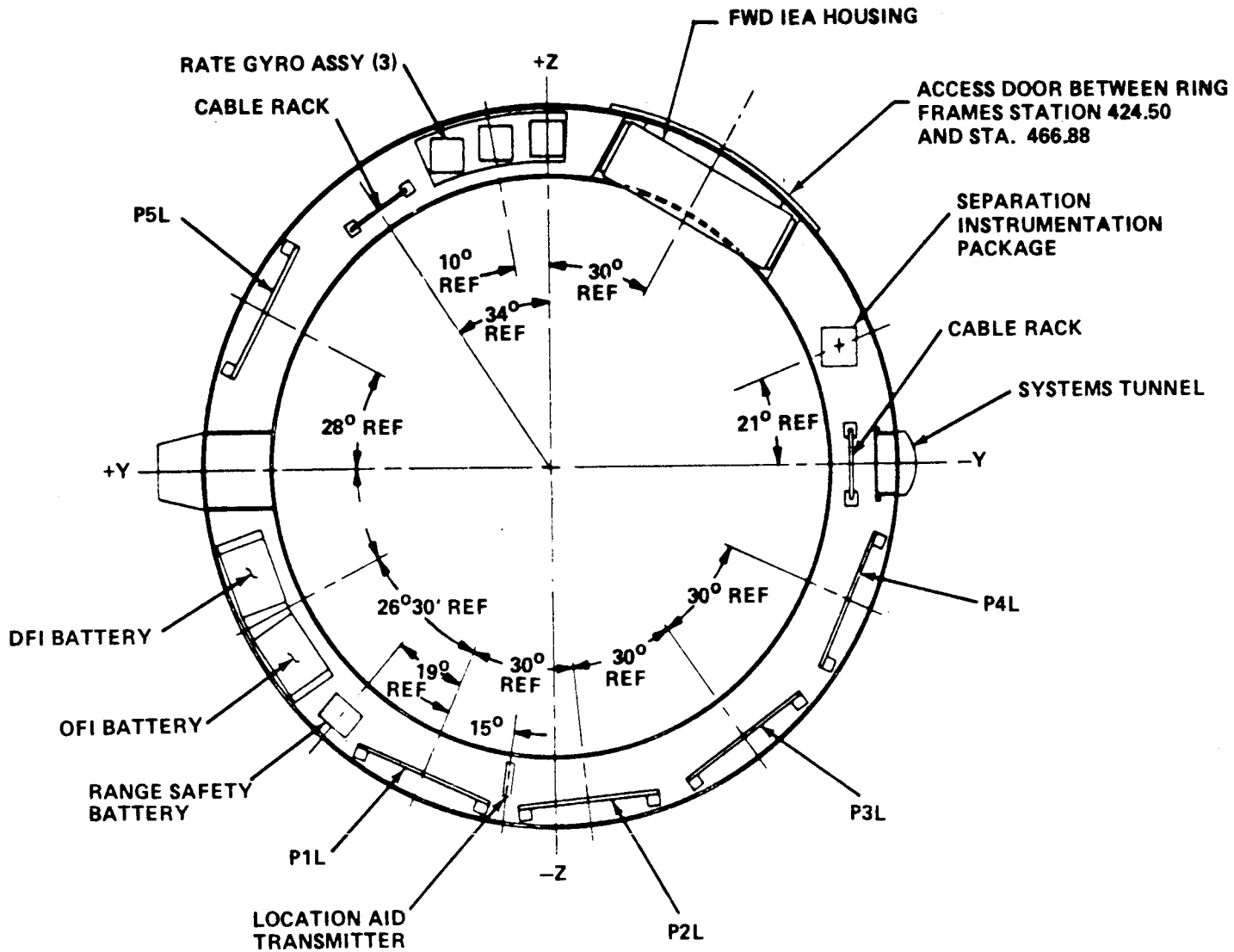


Figure 67. Forward skirt instrument mounting ring.

The reefed drogue chute starts the rotation of the SRB into an axial alignment with the relative airstream. Approximately seven seconds after drogue chute line stretch, reefing line cutters fire to allow the drogue chute to inflate to its second reefed condition. The final disreef to full open occurs 12 sec after line stretch.

At a nominal altitude of 6,600 ft, the frustum separates from the SRB. The drogue chute pulls the frustum away from the SRB. The main chute risers are pulled out from the main chute bags, and the chutes begin to deploy. At line stretch, the main chute reefing line cutters are initiated. The main chutes open to a first stage reefed position. The first stage reefing cutters fire about 10 sec after line stretch, allowing the chutes to expand to the second stage reefed position. About 17 sec after line stretch, the second stage cutters fire, allowing the chutes to achieve full diameter.

Figure 68 depicts the critical areas during chute deployment. The drogue chute goes through the second disreefing and fully opens. The critical area for this sequence is chute skirt loading. At this time, the frustum releases with separation loading and bag stripping the critical areas.

a) Parachute Tear Problem. The problem that has occurred concerns the main chute during frustum extraction. The chute is burned, ripped, and either does not have correct inflation or does not inflate at all. Two problems have been uncovered, one is associated with how the chute is packed allowing it to skip out and catch other parts, such as reefing cutters. The other has been associated with the high speed extraction burning the material reducing its strength or cutting inside the frustum. The first was solved by repacking. The second by removing all potential sources of contact with foreign objects. References 37 through 45 give the overall parachute design and verification program including sled testing and drop testing.

b) Excessive Water Impact Loads. Several events take place during water impact. It was found that some of these required pressure scaling to properly define the loads. Figure 69 gives the significant loading events and where pressure scaling was required. To satisfy the pressure scaling requirements, Navy Ordnance Laboratory and their pressure scale facility were used. Using these test data, water collapse load rings were installed for flight. On most of the Shuttle flights, the water collapse load rings have been damaged indicating the magnitude of these loads. Cavity collapse loads can occur with either the tail trailing or leading the vehicle. The tail trailing case has low pressures and loads while the tail leading has high pressure and loads. These are summarized in graphics form in Figures 70 and 71. In general, SRB impacts the water tail leading. Since the rings are a small refurbishment item and no other collapse load damage has occurred, no fix is intended. Large chutes under development for the skirt loads problem will help the water collapse problem.

As stated previously, the other problem area has been the water impact loads of the skirt. These SRB nozzle loads could not be determined directly in the scale model test due to scaling problems. The nozzle system is composed of actuators, the nozzle, a series of laminated rings to allow for gimballing the nozzle, and a snubber for response containment. Figure 72 is a schematic of this arrangement. Scaling these rigid body test loads up to a full scale elastic body response using detailed elastic body impulse response mispredicted the actual loads experienced in flight. Much damage has been incurred to skirt, actuators, etc., leading to much higher than predicted refurbishment. This has resulted in many test programs, both full scale (skirt only) and scale model, in order to better define these loads and arrive at fixes. Fixes have included clips on the rings, foam to change water flow, etc. Presently, minimum damage is occurring; however, large parachutes are scheduled for use that would eliminate the problem.

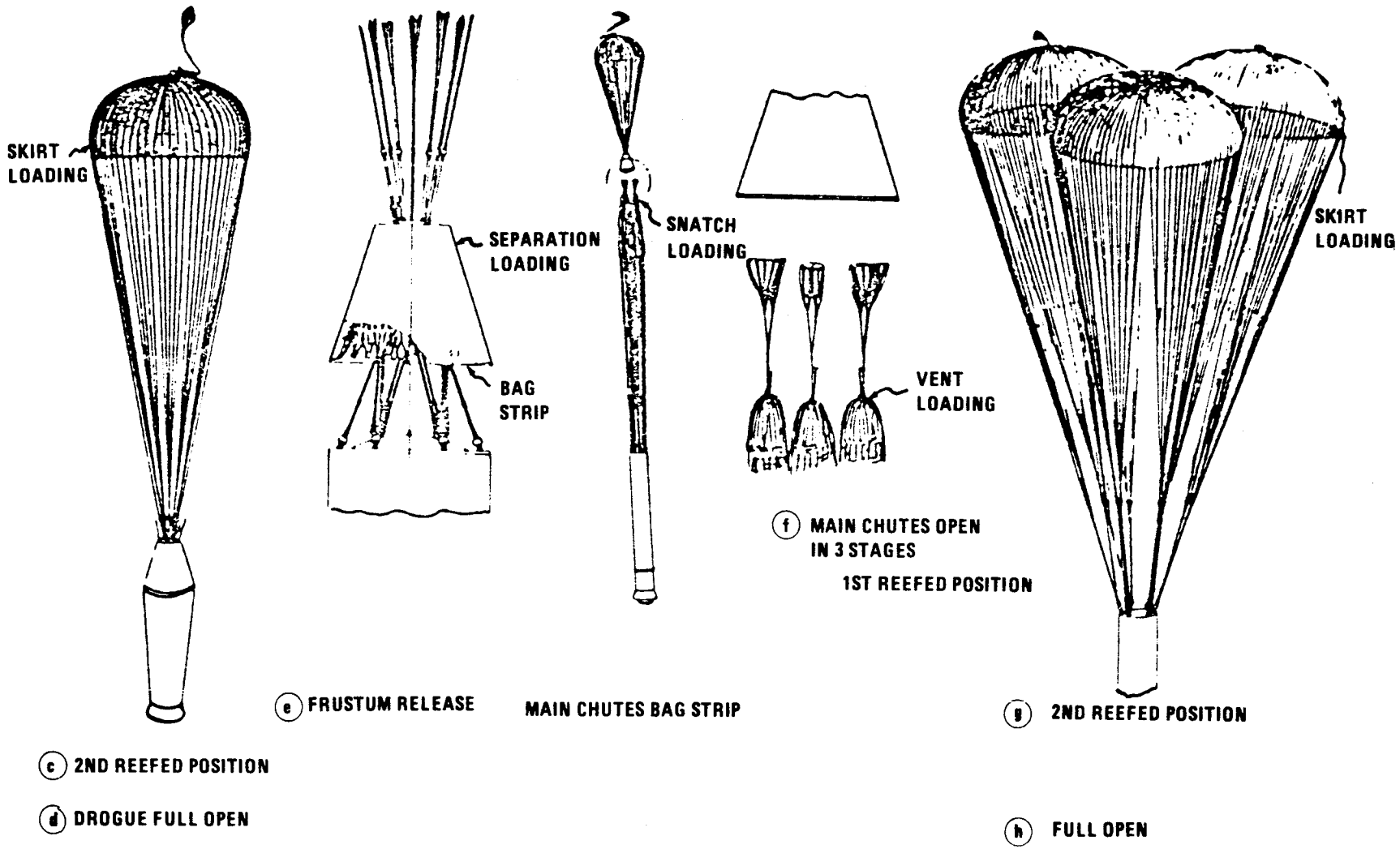


Figure 68. SRB parachute sequence of events.

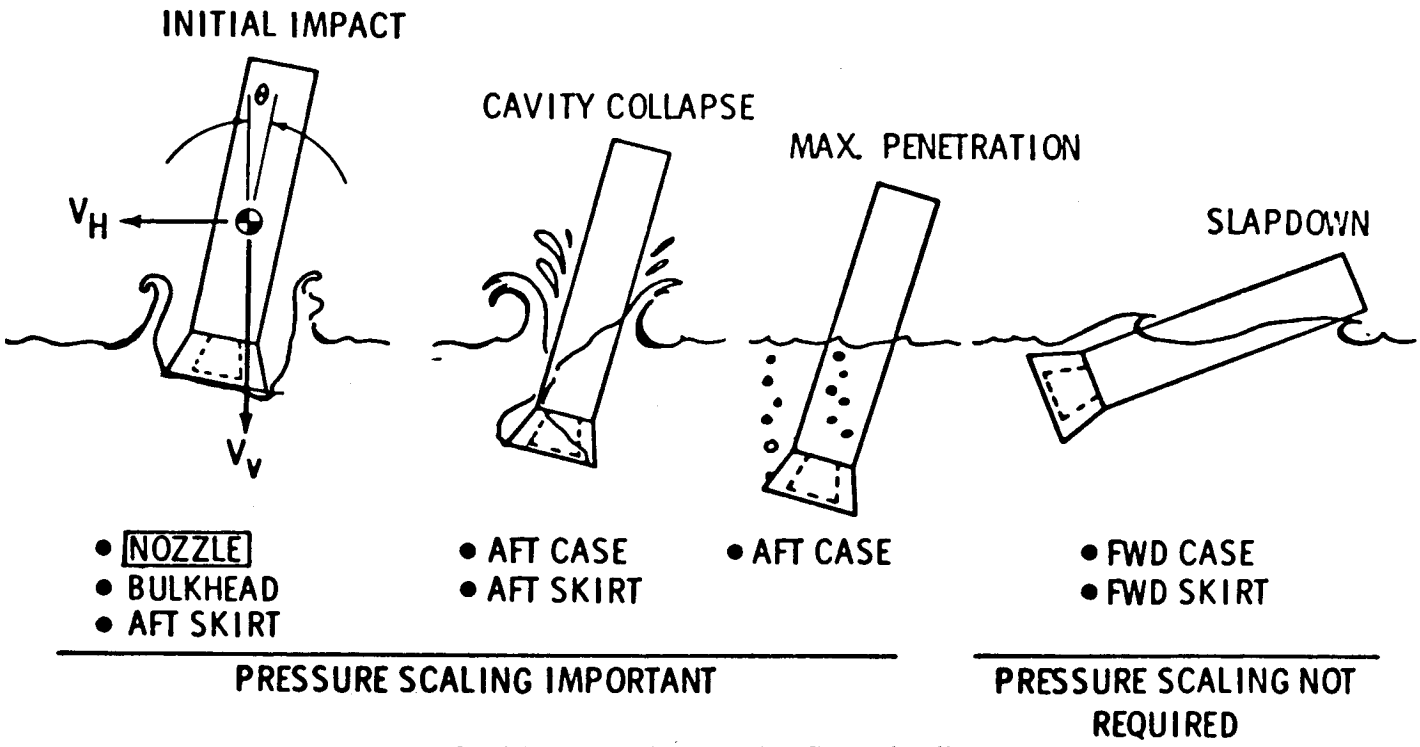


Figure 69. SRB water impact significant loading events.

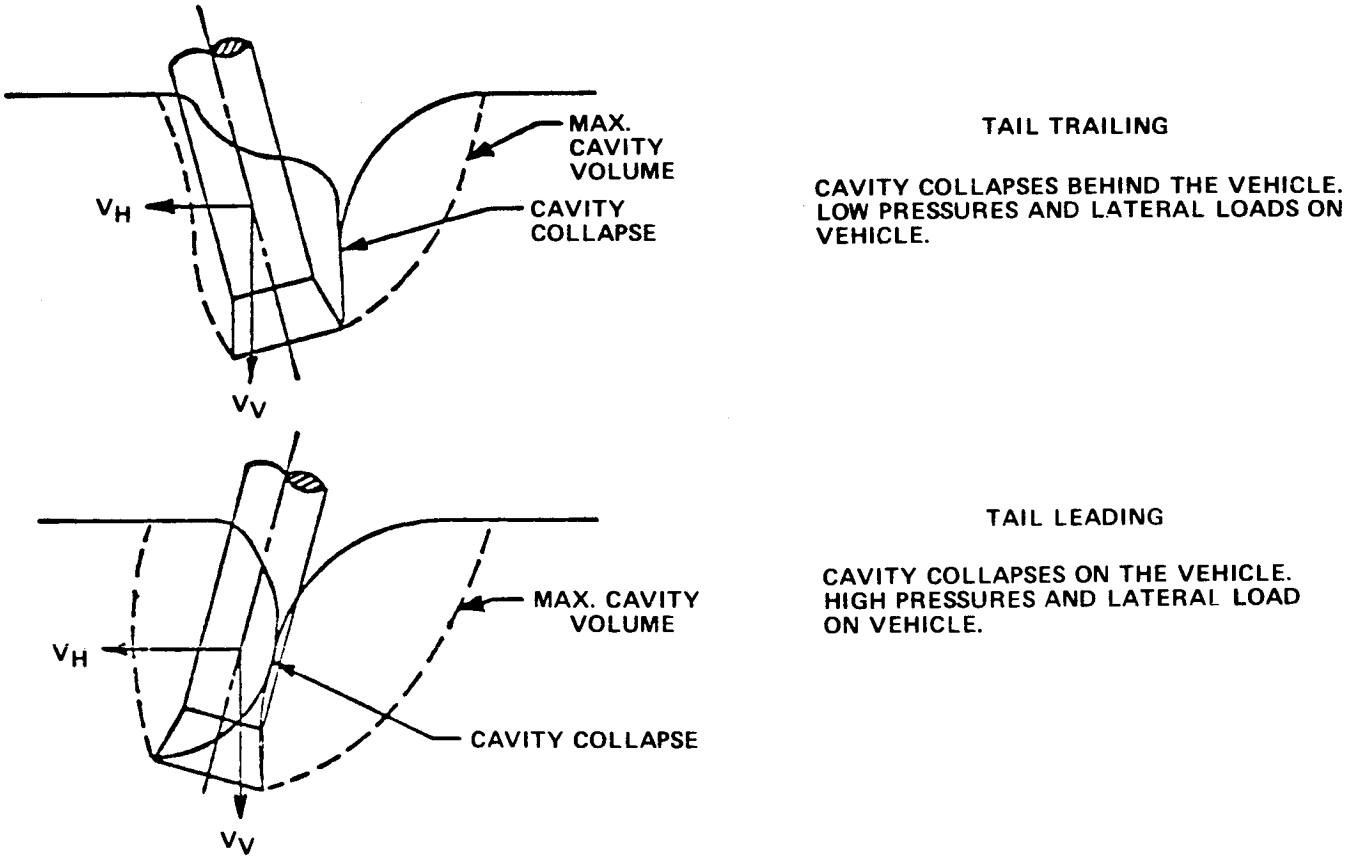


Figure 70. SRB cavity collapse loads.

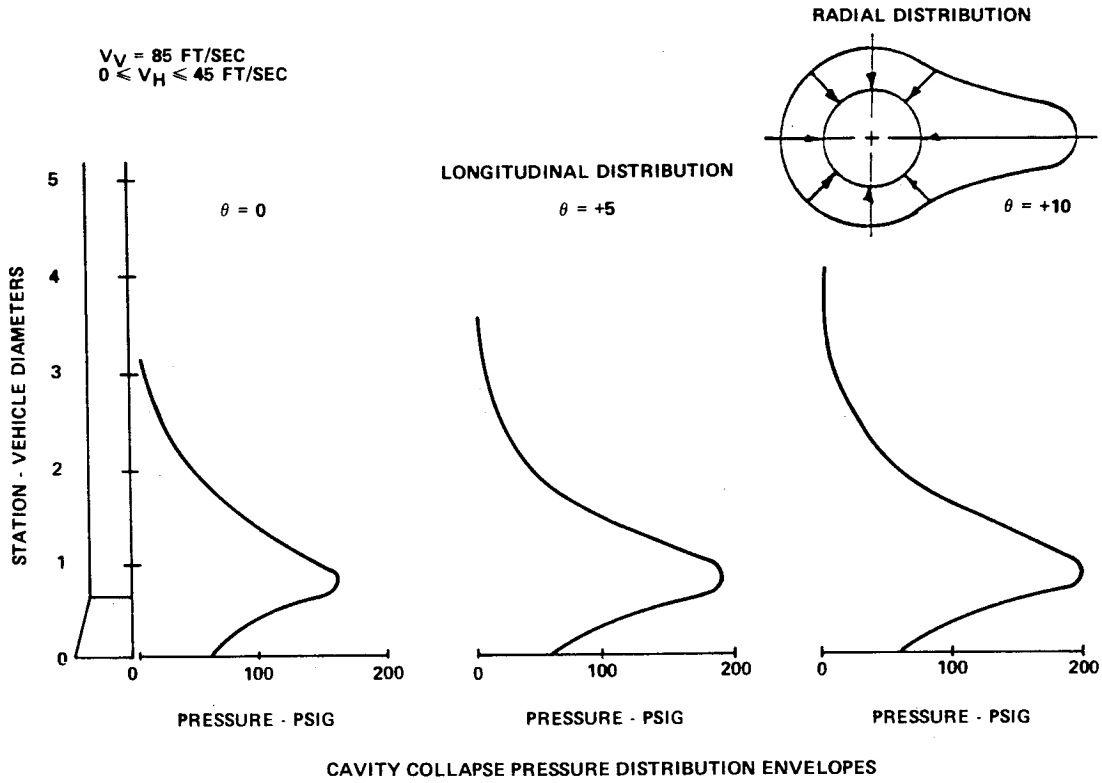


Figure 71. SRB aft skirt water impact loads.

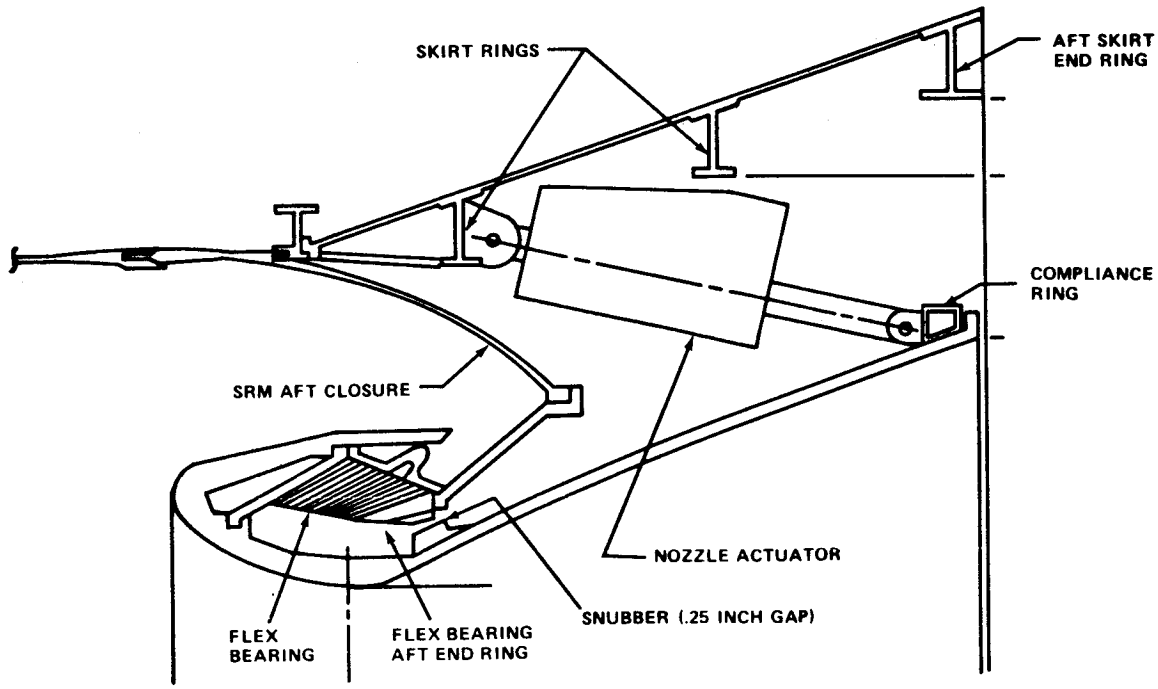


Figure 72. SRB nozzle configuration during water entry.

One interesting phenomenon occurred during initial impact in the nozzle area. The nozzle was first loaded in a positive direction as the nozzle attempted to move into the water. The water subsequently filled the aft skirt, then circulated, thereby creating a negative loading on the nozzle, the negative direction load being the peak load. Figure 73 shows this event and the loads for the nozzle, bulkhead pressure, internal skirt pressure, and internal and external nozzle pressure.

In summary, SRB water recovery loads have been full of surprises in spite of extensive testing and analysis during the development phase, indicating again the need for a better analysis and test tool.

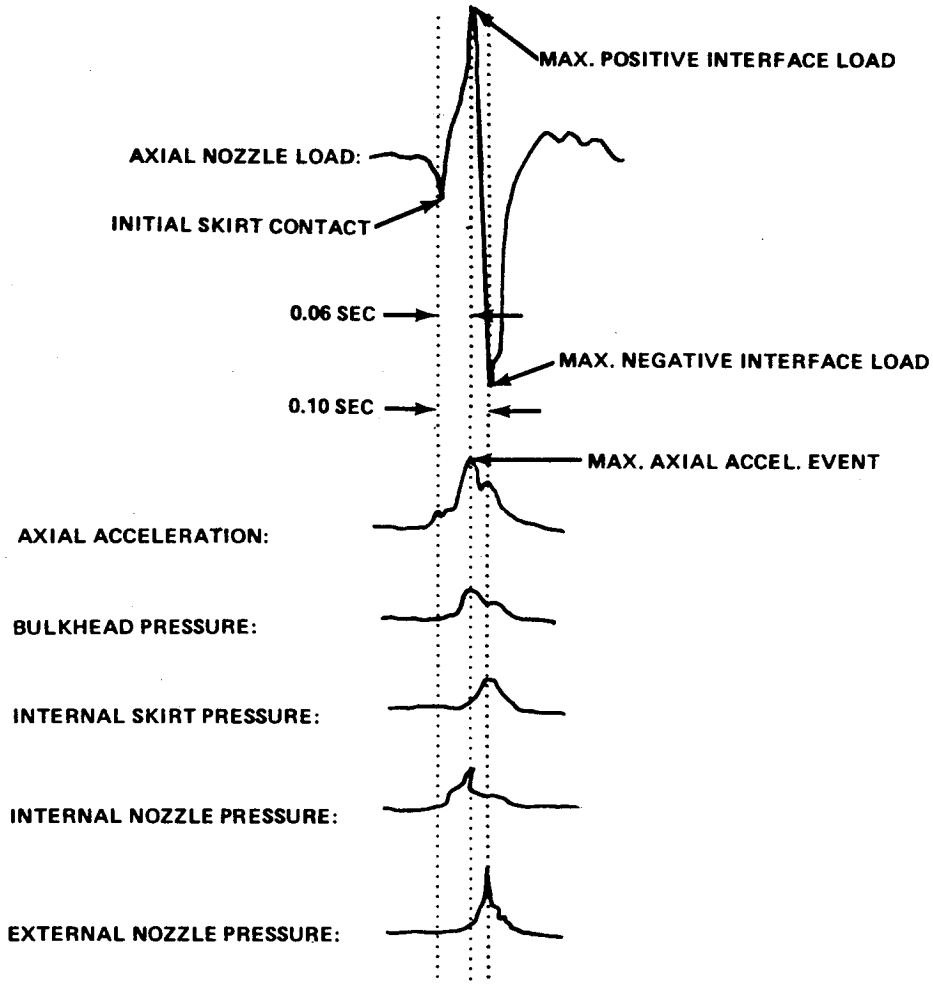


Figure 73. Typical initial impact dynamic events.

3) Excessive Nozzle Erosion. The SRB has experienced a problem associated with the thermal lining in the nozzle. In the throat area, erosion pockets have occurred on two flights, one of which was close to a burn through (Fig. 74). The thermal lining is a carbon epoxy composite laid up in layers with specific fiber orientation. During manufacturing if any contamination or process flow interruptions occur, then the material properties degrade, making the liner more susceptible to environments. The liners are several inches thick and are built up (fiber lay up) and machined in sections and fastened to the inside of the nozzle (Fig. 75). Because of manufacturing (lay up) problems, ring sections 403 and 404 have different fiber angles than the other ring sections (Fig. 76). Herein lies the problem. Manufacturing problems (quality) in conjunction with the flow and thermal environment induces tension in the surface which then turns loose, continuing until equilibrium or burn through occurs. Complete resolution of this problem has not been completed at this time. All aspects of thermal dynamics flow, etc., are being pursued to better understand the problem.

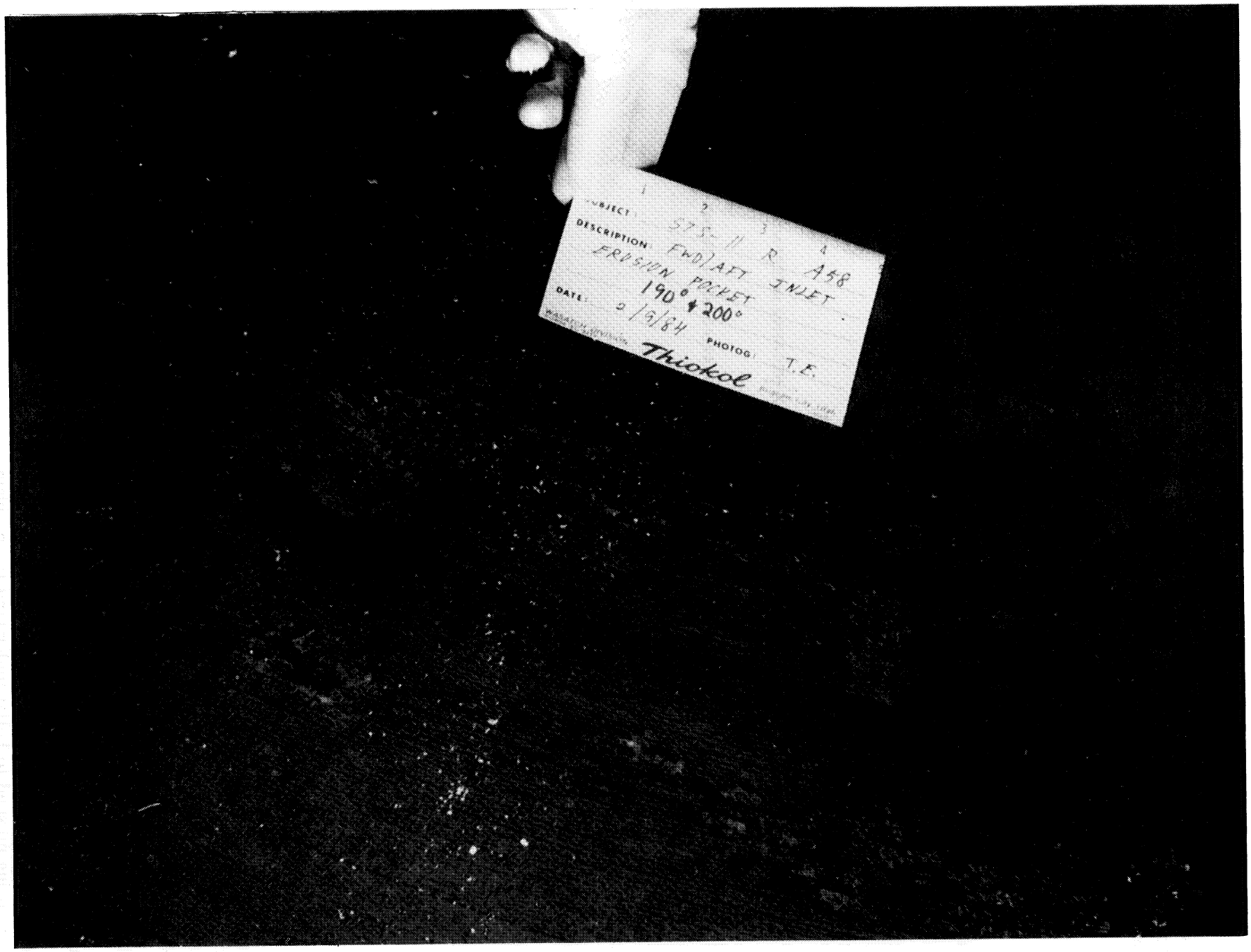


Figure 74. SRM nozzle liner erosion.

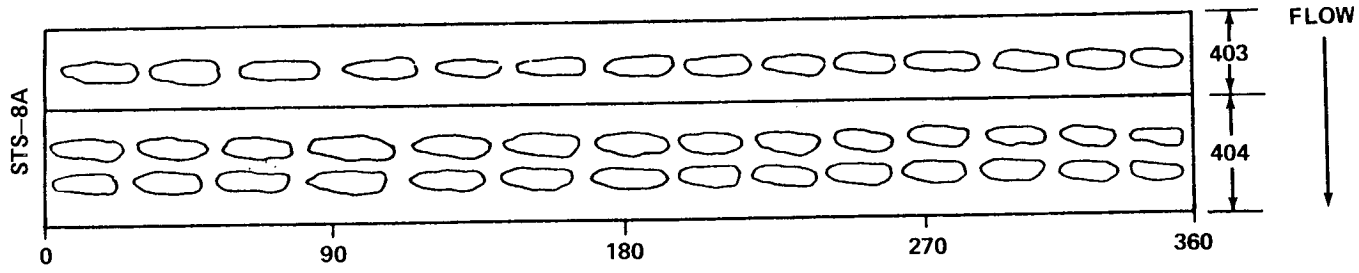


NOTE: INDIVIDUAL POCKET EROSION DATA NOT AVAILABLE. SEE SUBSEQUENT CHARTS FOR MAXIMUM CONDITIONS

Figure 75. STS-11 nozzle flight assessment.

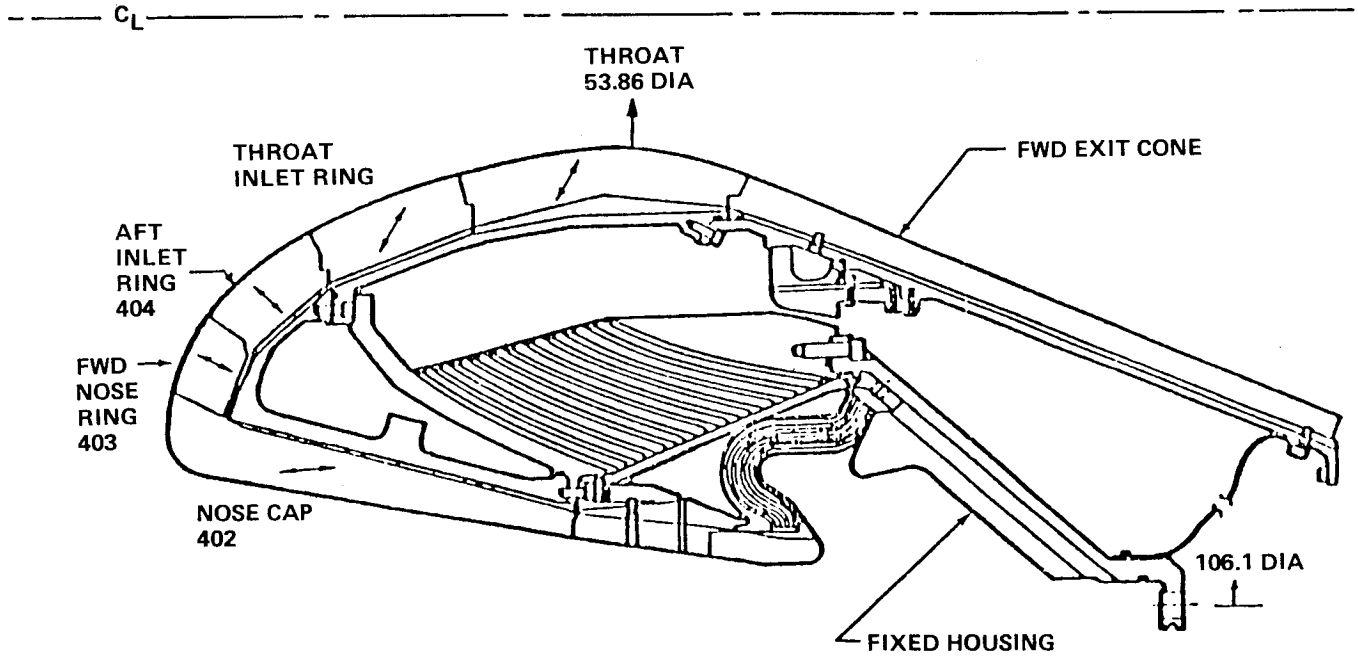


Figure 76. SRM nozzle liner assembly.

4) IEA Isolation. SRB had a typical problem associated with the IEA during development vibration testing. Several failures occurred; however, the box was qualified in the laboratory after many structural modifications and flown successfully on STS-1 through STS-5 flights, but vibration exceedances were noted during reentry. Therefore, a delta qualification program with isolators designed and incorporated were used to qualify for the new vibration criteria, which were based on the flight exceedances. Unfortunately, the new design experienced exceedances during ascent portions of the flight, attributed to the isolators. Therefore, another delta qualification program was conducted to requalify the IEA. This raises another problem of qualifying protoflight hardware. Extensive qualification testing reduces life of the flight hardware forcing vibration criteria formulation to be less conservative in order to avert costly flight hardware failures.

d. Space Shuttle Main Engine (SSME)

The planned missions for the Space Shuttle dictated a unique and technology-extending rocket engine. The high Isp (performance) requirements in conjunction with a 55-mission lifetime, plus volume and weight constraints, produced unique structural design, manufacturing, and verification

requirements. In order to achieve the high performance (Isp), a two-stage pump system is used in conjunction with preburners which burn the fuel rich gas, furnishing the power for the pumps. This extremely hot fuel rich gas feeds the main combustion chamber, efficiently developing the engine thrust. This system results in unprecedented operating regimes of temperatures, pressures, and rotating machinery speeds. The high rotary speeds and the combustion processes create mechanical, acoustical, and fluctuating pressure environments. The volumetric and weight constraints drive the design toward a high concentration of energy and minimum structure sizing (thickness, etc.). The energy concentration can be illustrated by observing the size of the high pressure fuel pump, which generates 70,000 h.p. within an envelope 18 in. in diameter by 30 in. long and rotates at speeds up to approximately 40,000 rpm [2,4,13,14-16,31,46-58].

These SSME operating conditions generate environments where many parts are operating at or beyond their endurance limits, producing a limited lifetime. The design point on the SN curve is very flat, making lifetime very sensitive to small changes in the static and alternating stresses (5 percent alternating stresses change lifetime up to an order of magnitude), manufacturing errors, and material deterioration (Fig. 77).

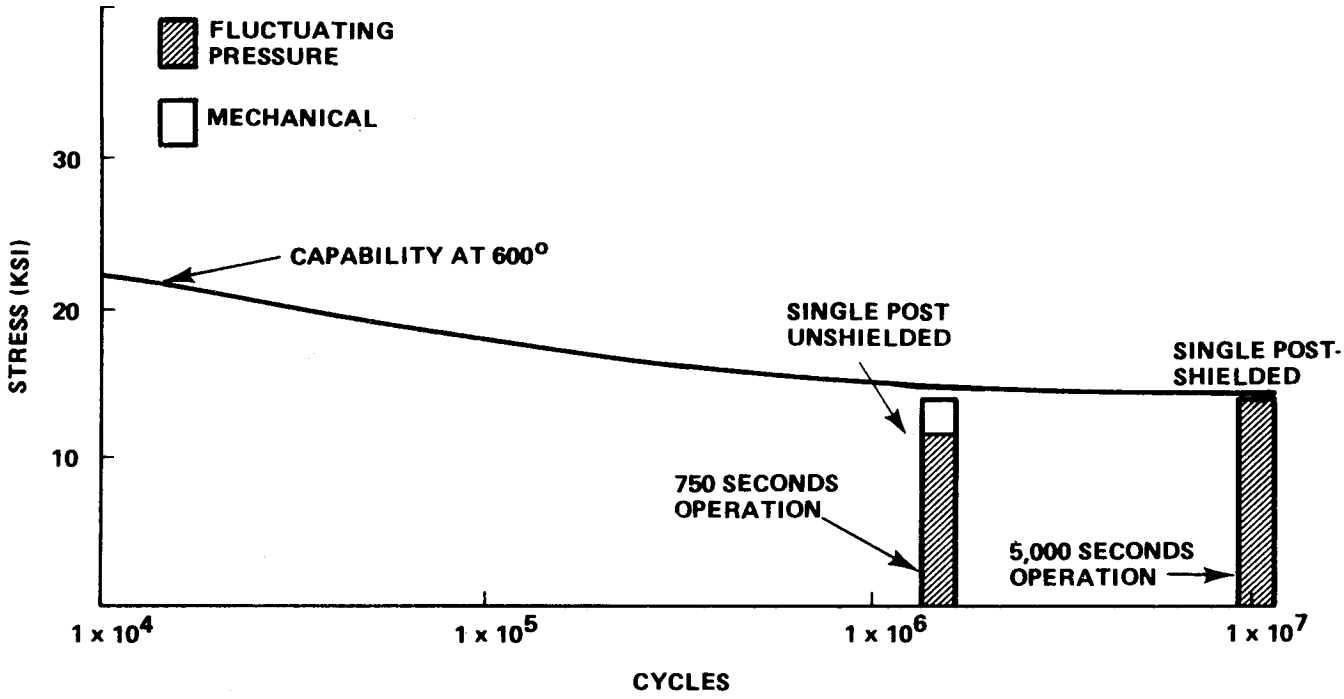


Figure 77. Alternating stress versus lifetime.

As a result of these design requirements, many problem areas have resulted in hot firing failures with large schedule slippage and hardware loss. Table 4 lists the major failures that have occurred in SSME hot fire testing. Not all have been related to dynamics and will not be discussed. These failures have occurred because the environment was not adequately defined, the response wrongly predicted, the phenomenon not predicted, or quality defects. The following paragraphs discuss most of the key problems experienced. The more dramatic one, Main Oxidizer Valve (MOV), will be discussed in the acoustical tuning section, and the weld wire mixup in the manufacturing and quality sections.

1) Lox Post. The main injector lox posts have been the source of three failures during hot firing. The main injector is part of the hot gas section, which is the heart of the SSME. It includes a hot gas manifold, primary and secondary face plates, a lox dome, and 600 lox posts or feed tubes

TABLE 4. SPACE SHUTTLE MAIN ENGINE, SUMMARY ENGINE FAILURES

| ENGINE | TEST NO. | DATE | FAILURE | CAUSE | REASON |
|---|---|---|---|---|---|
| 2002 | SF6–03 | 11–4–79 | NOZZLE FUEL FEED DUCT | ENVIRONMENT | IMPROPER WELD WIRE |
| 0006 | SF10–01 | 7–12–80 | FPB BODY BURNTHROUGH | LOCAL HIGH TEMPERATURE | CONTAMINATION |
| 2004 | 902–108 | 7–23–80 | MAIN INJECTOR – OXIDI–ZER POST CRACK | ENVIRONMENT | DESIGN EFFICIENCY |
| 0010 | 901–284 | 7–30–80 | HPOTP FIRE–OFF NOMINAL OPERATION – "Pc LEE JET" | IMPROPER INSTALLATION | DESIGN DEFICIENCY |
| 0009 | 901–307 | 1–29–81 | FPB INJECTOR OXIDIZER POST CRACK | ENVIRONMENT | DESIGN DEFICIENCY |
| 0204 | 902–244 | 7–14–81 | FPB INJECTOR OXIDIZER POST CRACK | ENVIRONMENT | DESIGN DEFICIENCY |
| 2108 | 901–331 | 7–15–81 | MAIN INJECTOR OXIDIZER POST CRACK | ENVIRONMENT | DESIGN DEFICIENCY |
| 0110 | 750–148 | 9–2–81 | MAIN INJECTOR OXIDIZER POST CRACK | ENVIRONMENT | DESIGN DEFICIENCY |
| 0204 | 902–249 | 9–21–83 | HPFTP TURBINE BLADE FAILURE | NON–UNIFORM – HOT GAS TEMPERATURE | ENGR MOD TO CORRECT PRIOR TEST PROBLEM |
| 0110F | 750–160 | 2–12–82 | HPFTP – OVER TEMPERA–TURE | WATER IN FUEL SYSTEM | PROCEDURE DEFICIENCY |
| 2013 | 901–364 | 4–7–82 | HPFTP – TURBINE BEARING FAILURE | HOT GAS ENTERING HPFTP COOLANT SYSTEM | DESIGN DEFICIENCY |
| 0107 | 750–168 | 5–15–82 | OPOV SEAL BURNING | HOT GAS BACKFLOW OPB | SEQUENCE DESIGN DEFIC. MORE SEVERE AT FPL |
| 2208 | 750–175 | 8–27–82 | HIGH PRESSURE OXIDIZER DUCT CRACK – SPECIAL INSTRUMENTATION | ENVIRONMENT | DESIGN DEFICIENCY (R&D DESIGN) |
| | | | KAIZER HAT NUT | ENVIRONMENT/DESIGN | BAD LEAK PATH DESIGN |
| | | | HIGH PRESSURE FUEL PUMP TURNAROUND DUCT COLLAPSE | ENVIRONMENT/DESIGN | SEAL LEAK |

between the lox dome and the primary injector plate. Figure 78 shows a top plane view of the lox post array with the three transfer tubes from the hydrogen preburner and the two transfer tubes from the lox preburner.

High velocity gas at a temperature of approximately 1800°F flows through the injector, then through the gap at the base of each post and around the tip of the injector plate, where it mixes with the liquid oxygen flowing down the center of the post. This flow environment, coupled with mechanical vibrations and variable dynamic characteristics, produces severe high cycle fatigue loading on the lox posts. This is worsened by high static stresses from the thermal and static pressure loads. Flow shields (Fig. 79) have been added to the outermost row, but the posts are still high cycle fatigue life limited, and there have since been two related engine failures during demonstration firings.

Metallurgical analysis determined that the failure mechanism was high cycle fatigue, initiating in the threads of the face plate retainer. Sources of alternating stress at that point are mechanical oscillations, vortex shedding, and fluctuating pressures (flow and acoustics). Static loads arising from thermal gradients and internal flow induced pressures are superimposed as a high mean stress to the alternating loads. Despite the presence of the flow shields, the highest fatigue loads and most frequent occurrence of fatigue cracks are in the outermost posts, row 13, and the next row, 12.

The approach used to rationalize the hypothesized failure mode was the approach shown on Figure 80. This is an alternate approach derived for attacking SSME lifetime problems in the absence of adequate flow data. A component failure is used as an empirical failure reference point, determining the stress level required for failure from the SN curve (minimum properties, maximum predicted temperature and pressures). The environments are "backed out" of these empirically derived data using the analytical dynamic model. The environments thus derived serve as a means of evaluating new designs and higher engine performance levels, as well as determining life limits.

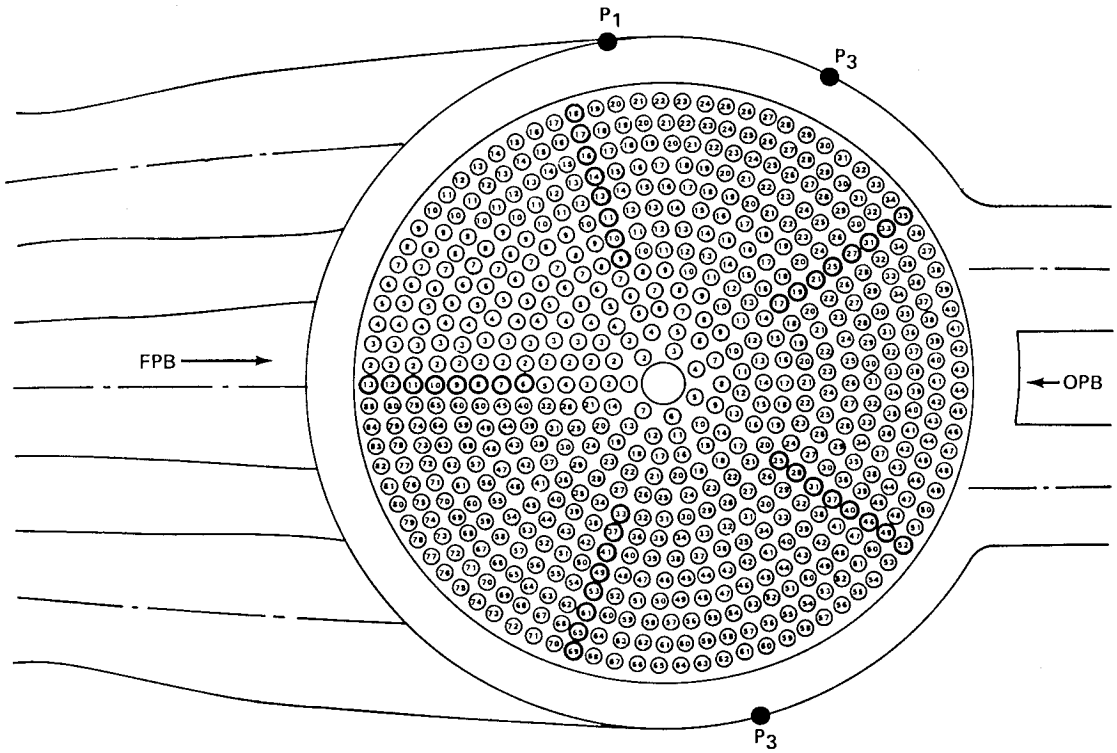


Figure 78. High-frequency pressure transducer locations in engine.

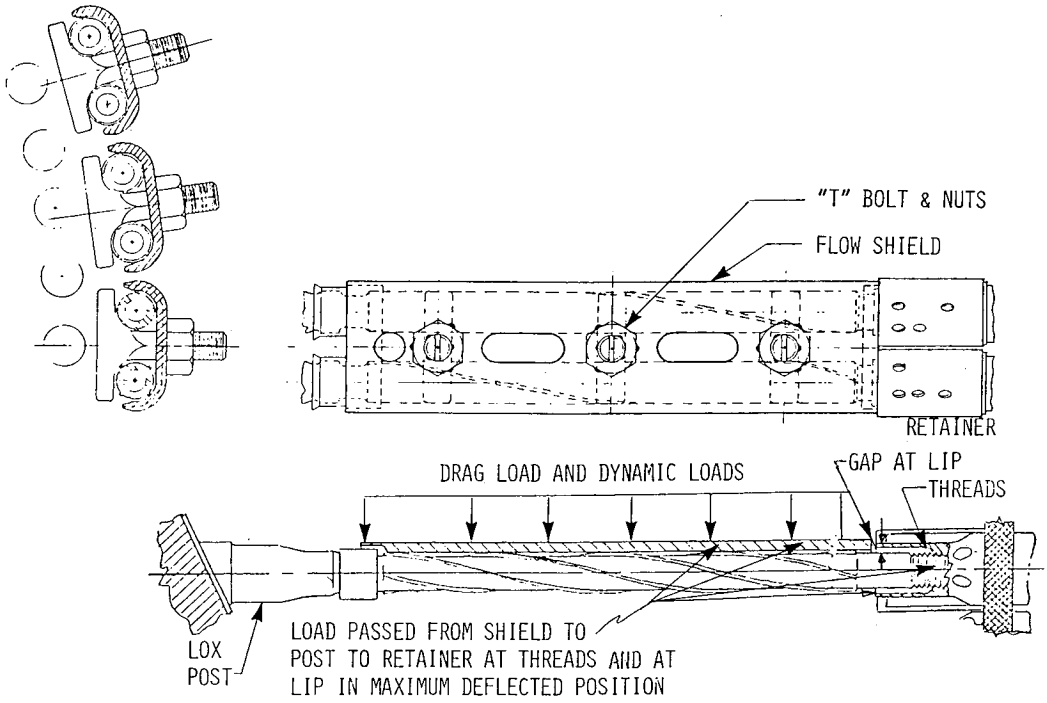


Figure 79. Lox post shield configuration.

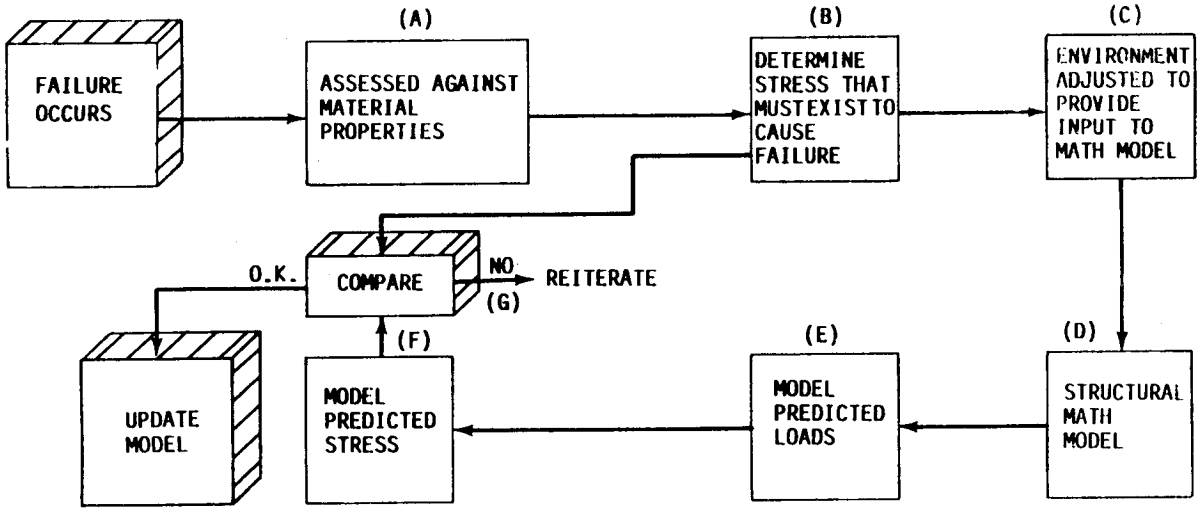


(1) EMPIRICALLY UPDATED MODEL CAN BE USED TO PREDICT REDESIGNED CONFIGURATION CAPABILITY.

(2) THE INPUT ENVIRONMENTS ARE NOT ACCURATELY CHARACTERIZED

(3) RESULTS ARE WELL ANCHORED BUT ARE ONLY RELATIVE IN TERMS OF ANY GIVEN ELEMENT DATA BASE.

(4) ANALYSES AND TEST ARE BEING USED TO UPDATE AND IMPROVE FIDELITY OF ENVIRONMENTS (C)

Figure 80. SSME lifetime verification analysis for special problem areas.

Certain aspects of the problem can be handled analytically with good success. For instance, the analysis has shown a mechanical and fluctuating pressure environment in the 1200 Hz regime, which couples with and drives the modes (natural frequencies) of the posts; these analytical modes have been verified experimentally and by instrumented lox posts in hot firings. Cold flow tests of the hot gas manifold, powerhead, and lox posts were used as a test bed for flow characteristics.

The lox post high cycle fatigue problem has been costly and time consuming; however, the effort has resulted in a much more efficient hot gas manifold design for application to the upgraded SSME planned in 3 or 4 years.

2) Turbine Blade. Turbine blade cracking has been a major refurbishment problem for SSME. In many aspects, it is of comparable nature to the lox posts. Only the fuel pump blades will be discussed.

The high pressure fuel turbopump (HPFTP) is a three-stage centrifugal pump that is directly driven by a two-stage hot-gas turbine. The turbine is powered by hydrogen rich steam generated by the fuel preburner. Hot gas enters the turbine and flows across the shielded support struts, through the first and second stage nozzles and blades, and is discharged into the hot gas manifold. Requirements for high performance within a restricted envelope have led to a complex, cyclic-load-producing configuration of 13 struts, 41 first stage turbine blades at the locations shown in Figure 81. Although none have precipitated an engine failure, turbine blade life improvement remains a major goal in the SSME program.

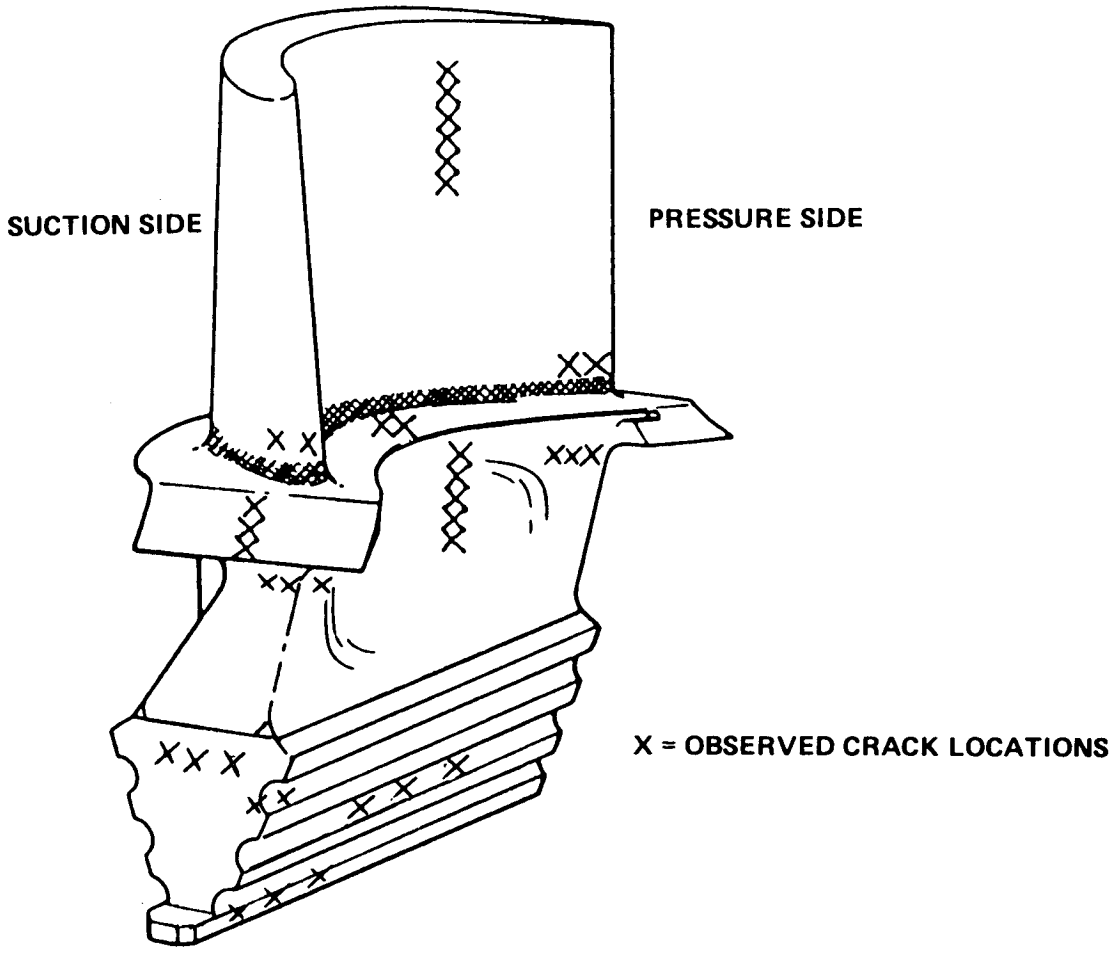


Figure 81. Areas of high stress and observed crack formation.

Loads analysis and lifetime prediction for the HPFTP turbine blades have presented problems similar to those encountered in the lox posts. Major problems have inlcuded environment definition, dynamic modeling, and static and alternating stress distribution. The environment definition is extremely complex for both the thermal and fluctuating pressure standpoints. The blades are near the preburner and use the hot preburner gas as the source of their power (flow forces). These environments are not uniform due to baffle posts, struts, etc., and the blade geometry. Fluctuating pressures present the same problem, plus the clear introduction of harmonics due to the struts and the multiblade passages. Dynamic modeling is complicated by the basic geometry, hot surface, boundary conditions at the wheel, and special dampers for reducing blade response. Stress is composed of static centrifugal force, power bending, steady-state thermal, cyclic thermal (start and shutdown transients), and fluctuating pressure components. Significant factors in the alternating stress are (1) tuning of strut wakes with blade lower modes, (2) multiblade relative motion of adjacent blades, (3) variable damping coefficients and lockup, (4) changes through engine operating range, and (5) startup and shutdown thermal and pressure cycles.

Each instance of blade cracking has been addressed using an analytical/empirical approach similar to that described for the lox posts; loads and stresses are calculated by analysis, and the models are adjusted as required to be compatible with observed phenomena. A detailed finite element model has been generated for the blades. Detailed definition of the forcing functions has been accomplished by accurate modeling of the strut/nozzle/blade configuration, and the output has been matched to results obtained from special air rig and "whirlygig" tests. Basic material strength and fatigue data have been obtained over a range of operating stresses and temperatures. Figure 82 shows the form of the engineering solution with all of the data taken into consideration, including the observed frequency of the particular blade cracking incident under investigation. Curve 1 is for rated engine power level (RPL) assuming 5,000 sec of life. Curve 2 is full or maximum engine power level (FPL) and 5,000 sec of life, while curve 3 is the same power level assuming 2,500 sec of life. The mean stress for RPL is 46 Ksi, and for FPL, it is 55 Ksi. The blade operating temperature is in the 1,600 to 1,700° range, resulting in a low allowable alternating stress.

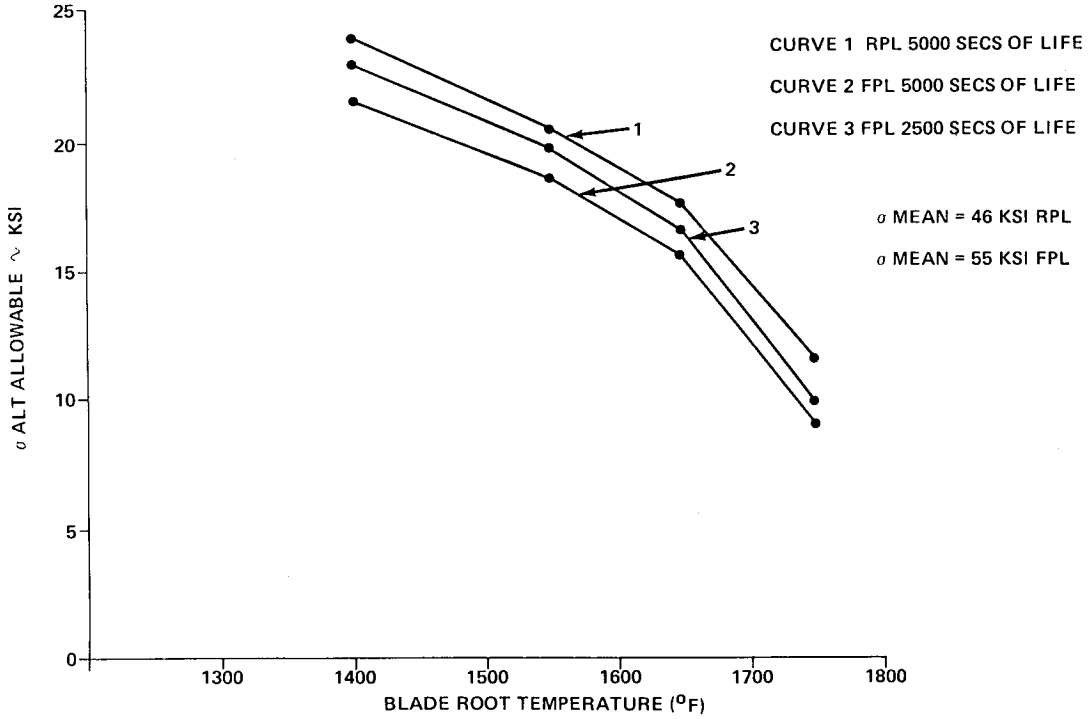


Figure 82. Alternating stress versus blade root temperature allowable.

At the present time, there are no serious blade cracking problems, although cracking still exists. Each instance of blade cracking has been solved by material-related improvements or environment modifications. Periodic inspections are required, however, and the average blade changeout interval of 3,000 to 5,000 sec is far short of the design goal of 27,000 sec. Studies for long-term improvement in blade life are in progress. Improved materials are being considered, including advanced superalloys in the single crystal form, and environment reduction techniques are under study, including different type dampers.

3) Nozzle and Steerhorn Engine Side Loads. The SSME nozzle has three engine downcomer coolant liners that take hydrogen from the main fuel valve to the aft nozzle manifold. The aft nozzle manifold feeds the coolant tubes which, in essence, is the engine nozzle. Two of these coolant lines have failed during hot engine firings due to high cycle fatigue. Figure 83 gives the basic configuration, showing the downcomer line (steerhorn). A history of cracking nozzle tubes has also plagued the engine.

The loads on the line nozzle system arise from firing of a high-expansion-ratio nozzle at sea level atmospheric conditions. The plume does not fill the nozzle until the internal pressure is greater than atmospheric pressure. As the nozzle plume flow velocity increases, it passes through a region where a Mach disc or cone exits the nozzle (Fig. 84). Two distinct phenomena occur during this thrust buildup phase. The first occurs around 600 to 700 psia chamber pressure. In this case, the plume is basically cylindrical in nature and is directionally unstable, moving around radially within the nozzle. The loads induced by this case drive the actuator design. The second occurs around 1,200 psia where the Mach cone leaves or enters the nozzle, creating high local shock loads. Figure 85 shows a typical thrust buildup and shutdown curve and stress response measured on the nozzle steerhorn. Response due to the side loads is clearly shown in this figure. The large strain amplitude occurs due to the excitation of the n = 0 (expansion mode) and the n = 6 (shell mode). Notice that the response is very sharp and around 250 Hz (the insert shows a blowup of the response) [2,48,59].

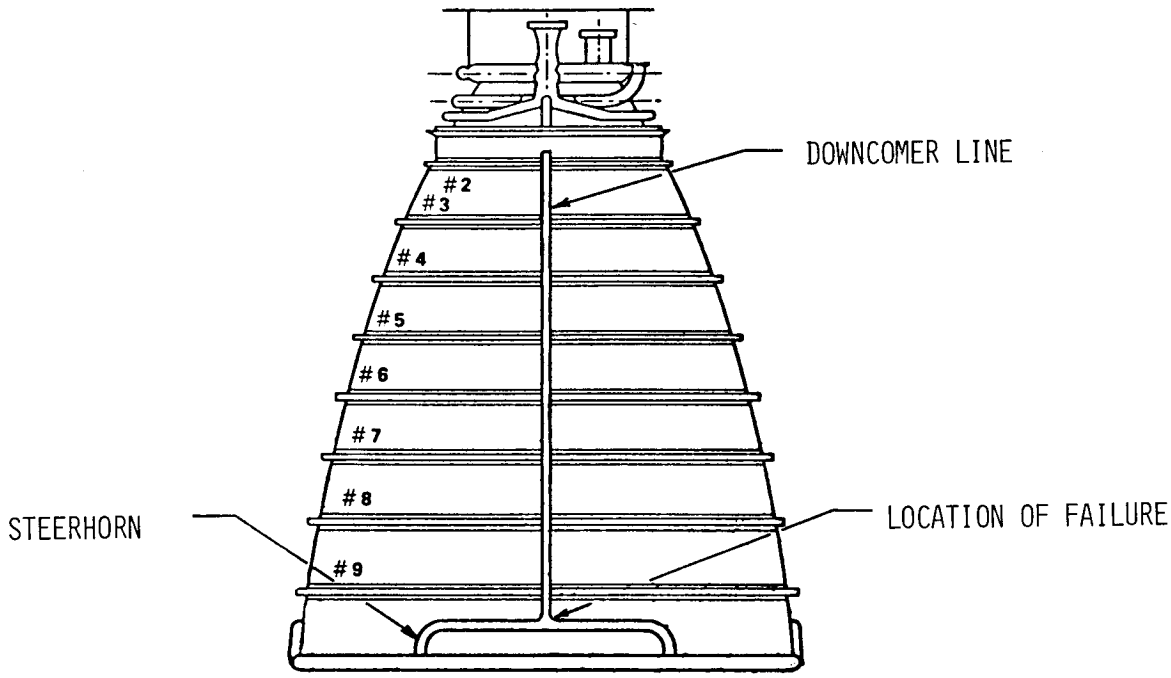


Figure 83. Description of nozzle system.

PHENOMENON: SHOCK WAVE OSCILLATIONS ASSOCIATED WITH TEEPEES/ MACH DISC

ANALYSIS + OBSERVATIONS: MOVIES INDICATE THAT THE SEPARATED FLOW TEEPEES ARE ABOVE THE SECOND RING FRAME AT FAILURE TIME WITH THE TEEPEES GROWING AND CHANGING SPATIALLY CONSERVATIVE ESTIMATE OF ENVIRONMENT SHOWED POTENTIAL.

MECHANISM

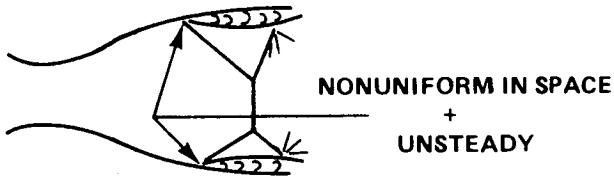


Figure 84. Shock wave oscillations.

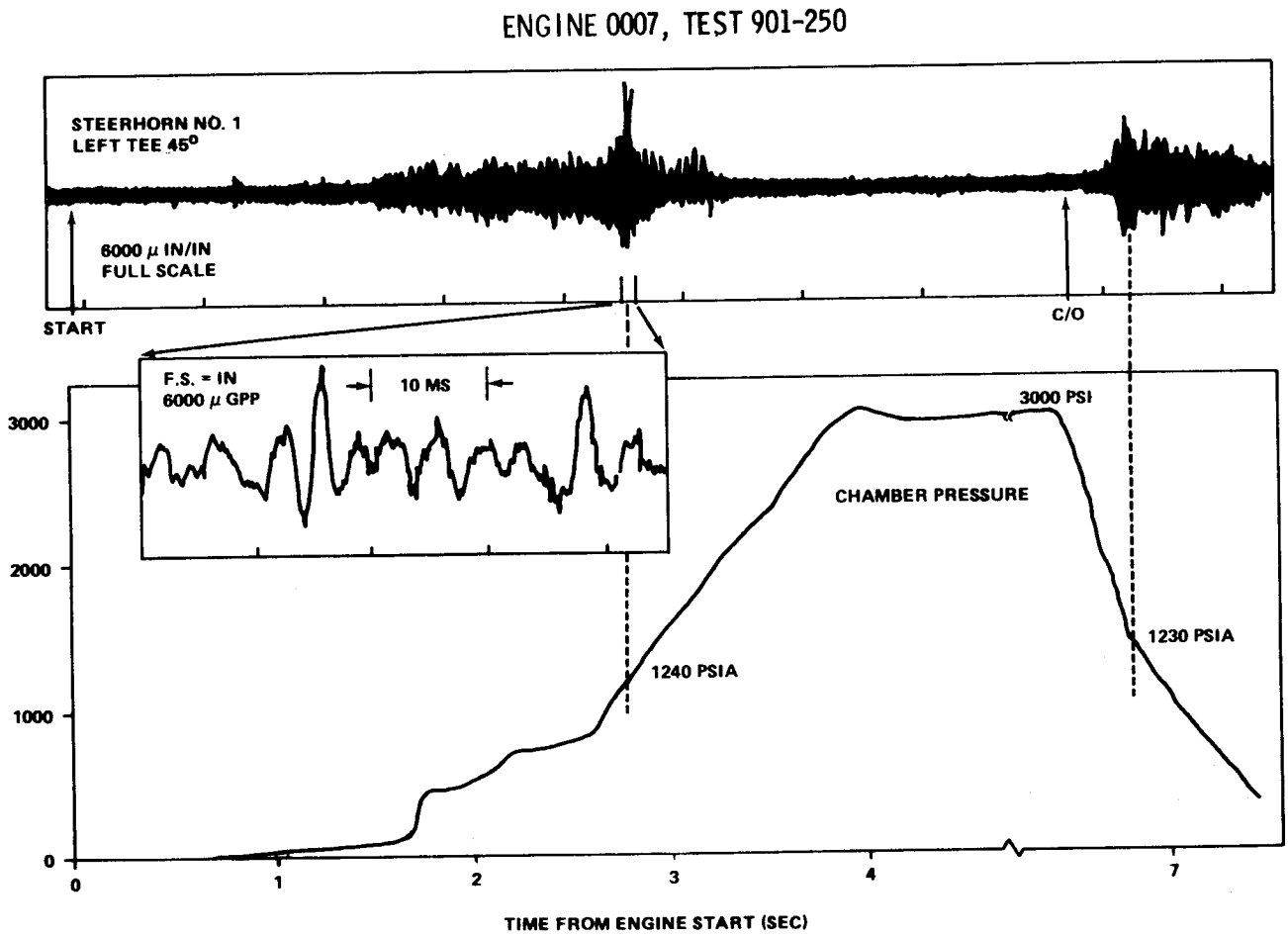


Figure 85. Steerhorn strains in transient operation.

Figure 86 depicts the n = 6 shell mode on the right-hand side. The left-hand side of the figure shows the shell mode frequencies as a function of n-number. At the bottom of the figure is a spectrum of the measured acceleration of the engine nozzle aft manifold showing presence of all n modes but by far the larger peak occurring for the n = 0 and n = 6 modes.

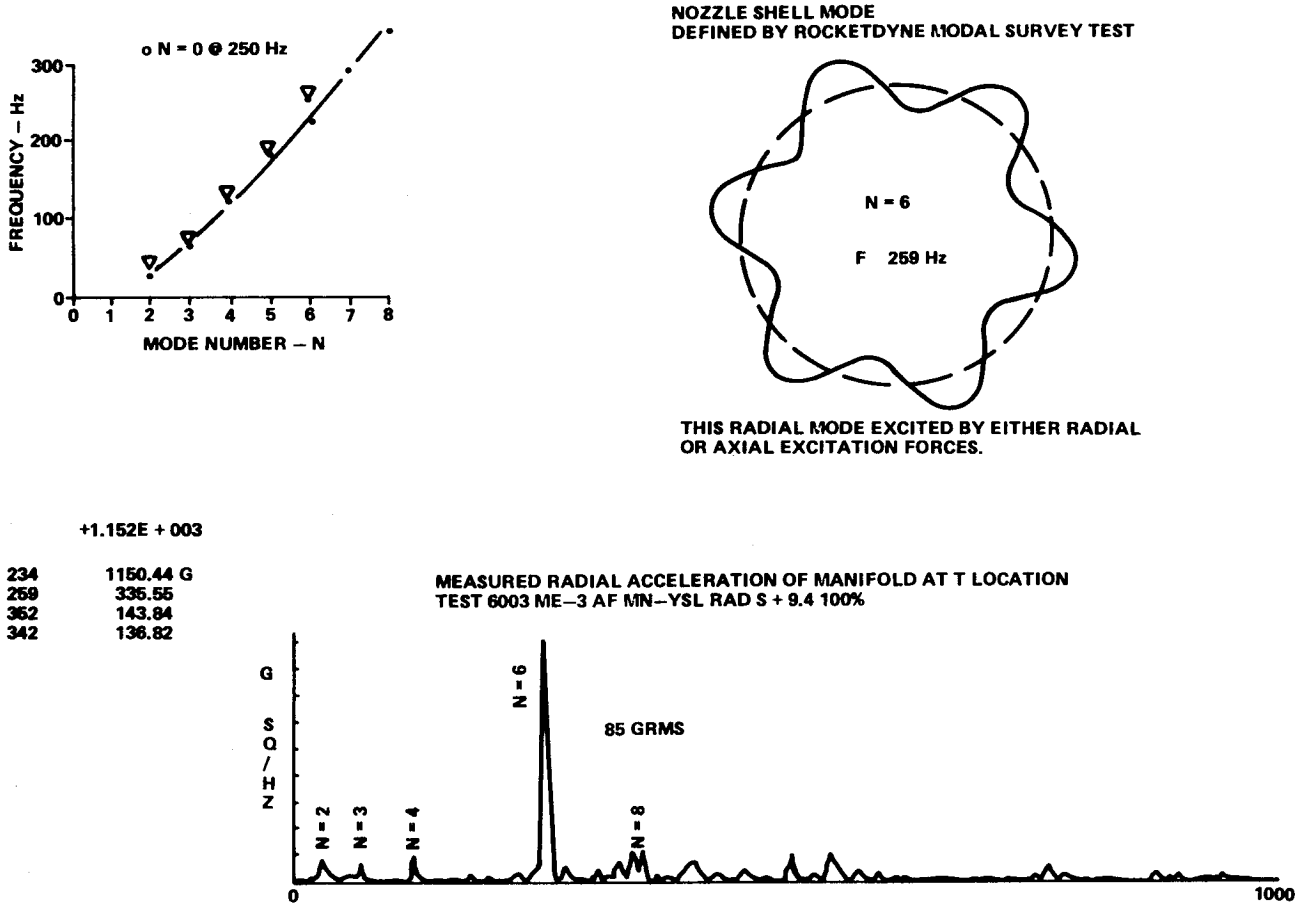


Figure 86. Nozzle shell mode defined by modal survey test.

The presence of this large load at the discrete frequency of 250 Hz (near resonance with nozzle modes) created many engine design and program problems, particularly during the developmental firing program. Two things had to be accomplished. The underdesigned steerhorn had to be fixed so that firings could continue, and the steerhorn had to be redesigned for operational flights. Since initially an internal pressure forcing function was not available, it was decided to take the hot-firing measured accelerations at the aft manifold and use these to base drive a dynamic model of the steerhorn. The first major result obtained was that just thickening the tube did not help the problem. The increased mass offsets the increased stiffness so the frequency stays the same. The nozzle-induced driving force is not changed; therefore, the increased mass increases the steerhorn loads proportionally to the mass increase. As a result, a sensitivity analysis and redesign matrix was pursued as a means of obtaining a solution.

The conclusion of this study was that this horizontal run of the steerhorn must be fixed to the nozzle stiffness ring to reduce loads. This meant that a steam loop had to be incorporated above the hatband to take out thermally induced expansion loads. The other major result was that for the T area (original design) a nickel-plating would provide adequate life for developmental engine firings and first Shuttle flights. The redesigned steerhorn was incorporated on the FPL engines.

Two test programs were instituted to finalize these loads and the redesign: Scale model engine cold-flow test and full-scale flight nozzle dynamic test (Fig. 87). The dynamic model used in this analysis was verified in a full-scale dynamic test. Analytical modes had good agreement with test modes. The cold-flow model test varied the flow rate, etc., and determined the forcing functions. A full set of pressure gauges was mounted so that the force distribution could be determined. These results were scaled to full scale.

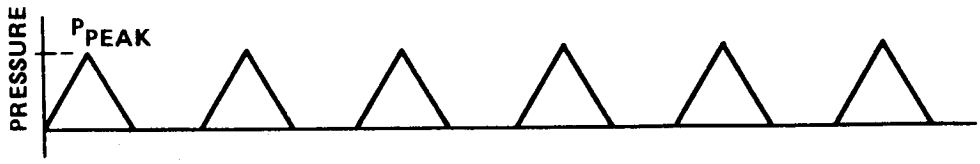


| LOCATION | $P_{PEAK}$ (PSI) |
|---|---|
| BETWEEN MANIFOLD AND 9TH HATBAND | 34 |
| BETWEEN 9TH AND 8TH HATBAND | 24 |
| BETWEEN 8TH AND 7TH HATBAND | 7 |

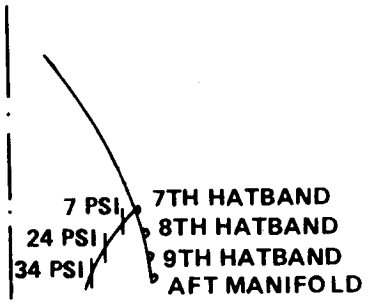


PRESSURE DISTRIBUTION IS UNIFORM CIRCUMFERENTIALLY

Figure 87. Nozzle model pressure pulses.

Using these test-derived forcing functions, a dynamic response analysis was made for both the original design and the redesigned steerhorn configurations (steam loop). Good agreement with hot-firing data was obtained. The reduction in loads is approximately 40 percent for the redesigned case, providing infinite life. Based on this analytical work and the statistics of the hot-firing data, a lifetime prediction of the redesigned steerhorn was accomplished verifying a redesign that would meet the 55-mission lifetime requirement.

4) Heat Exchanger (HEX). The heat exchanger is a multipath, single-pass, coil pack installed in the oxidizer side of the hot-gas manifold (HGM). It has an orificed bypass line directly outside. It converts liquid oxygen to gaseous oxygen pressurant for ET oxygen tank and pogo accumulator pressurization. The coil pack consists of a helically wound, small tube approximately 30.6 in. long, in series with two parallel, larger tubes each approximately 310 in. long. The coil pack is held in place by a support assembly that is attached to the HGM liner. The cross-flow of hot turbine exhaust gases from the high-pressure oxidizer turbopump (HPOTP) provides the heat energy needed to convert liquid oxygen to gas (Fig. 88). A failure occurred during main engine hot firing where a line fractured due to vibration at a point where the welder struck a bad arc. The prime cause was a defect from welding. In addition, tube wear has been a concern where the tubes pass through the supports. The wear has not led to a failure. In fact, under extensive vibration testing (7.5 hr in each axis) the wear did not cause failure. Wear cannot be predicted analytically. As a result, the special tests have been run (in addition to the 7.5 hr, 5 each axis) in order to verify that manufacturing tolerances would not lead to a problem. Great care must be expended to insure that no problem occurs since gaseous oxygen is present producing high potential for fires. The vibration of coils and lines are typical of the kind of dynamic problems engineers must be continually aware of.

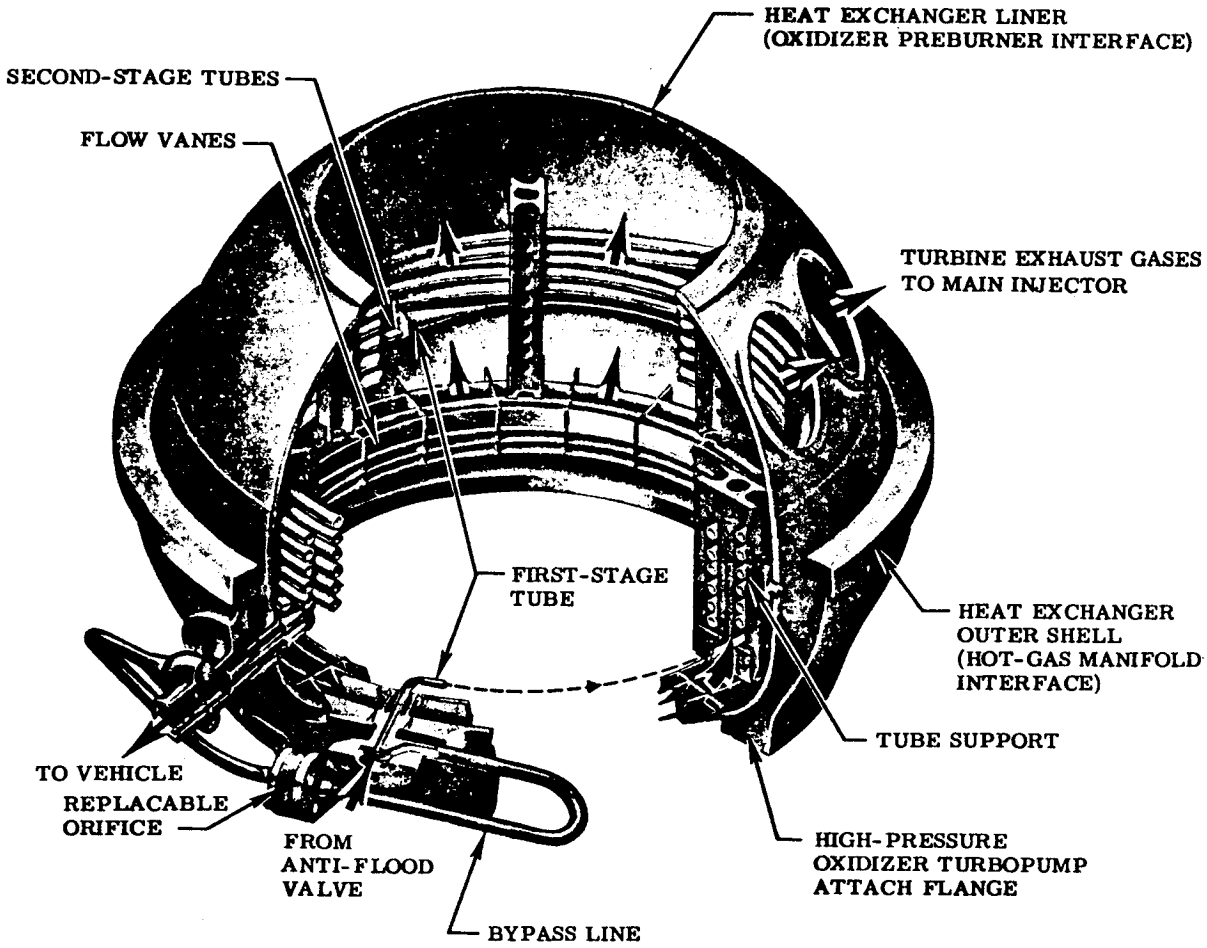


Figure 88. SSME heat exchanger.

5) Coolie Hat/Nut. The HPFTP is powered by hot-gas (hydrogen-rich steam) generated by the fuel preburner (FPB). The preburner hot gas flows directly on the coolie hat (flow diverter and protector) which is held in place with a large nut (Fig. 89). Early in the program, the nut kept loosening due to thermal cycles and vibration. No major problems resulted; however, it was deemed worthy of a redesign. The redesign allowed some leak paths, since the cavity behind the coolie hat was a lower pressure than the hot gas. In addition, the Augmented Spark Igniter (ASI) system created poor mixing and a direct impingement of oxidizer and fuel on the nut. As a result, the unit was burned in the coolie hat area, shutting down an engine. Figure 90 shows this impingement and hot gas flow path. Obviously, the problem had to be solved through a redesign eliminating the leak path. The problem illustrates how apparently small changes instituted to solve one problem and improper evaluation and design can lead to a more dramatic problem. It also illustrates the various problems encountered in high performance systems with stringent environments. Failures of this nature also have large program impacts, since a failure board was formed with indepth investigation and some schedule slip.

6) Imbalance and Rubbing in SSME Parts. Rotary dynamics is one of the more fascinating fields in dynamics. It is an area all are familiar with from one standpoint or another. Any automobile driver has experienced wheel imbalance, brake squeal, etc. Homemakers find it in the motor driven appliances, etc. For the Shuttle Main Engine, these problem areas are compounded several orders of magnitude in the high pressure fuel and lox pumps due to the high energy concentration (energy density) and speed ranges. For example, the high pressure fuel pump has a maximum 70,000 h.p. output contained within a volume of approximately 20 in. x 20 in. x 40 in. and spins up to 40,000 rpm. That

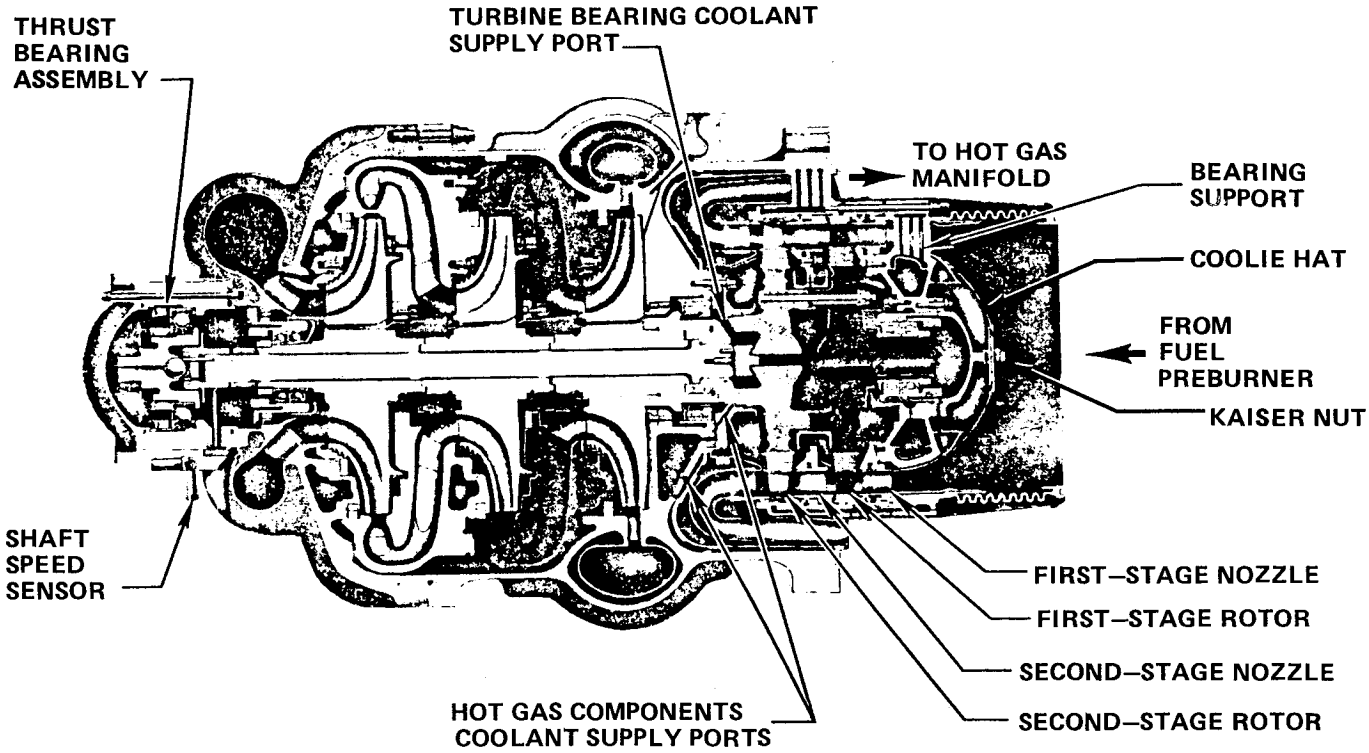


Figure 89. Fuel pump cut away showing coolie hat.

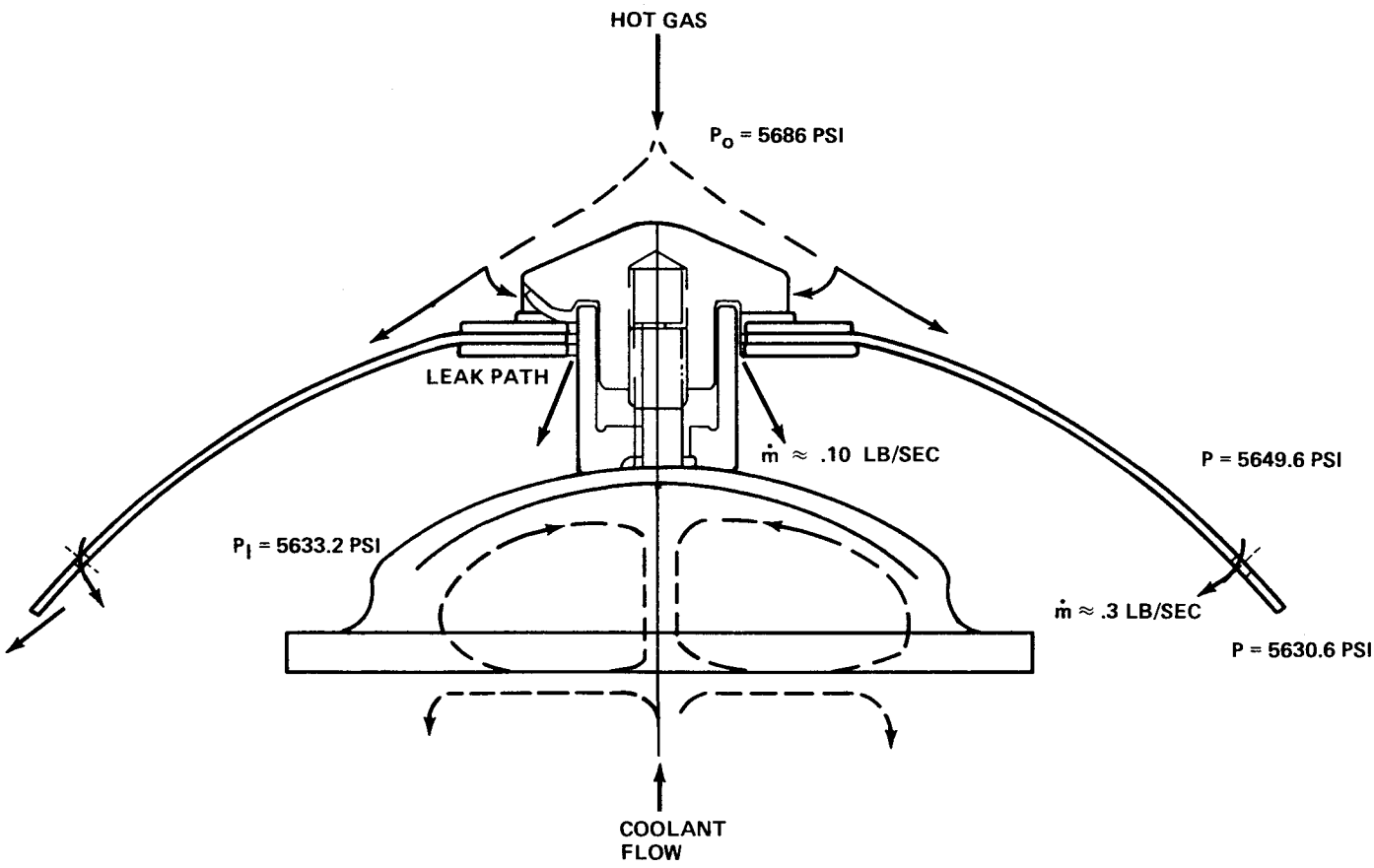


Figure 90. Hot gas flow from preburner on coolie hat.

is more horsepower than a large diesel locomotive. As a result, supposedly small changes (causes) are greatly magnified in the responses. Since bearing life of these pumps is limited and is to a large degree a function of the dynamic response, the health of the pumps is monitored using acceleration data. These data are obtained from a set of accelerometers mounted on various locations of the pump housing. Also, maintaining or designing and manufacturing in low responses has been a major problem. Very accurate tolerances must be met. In addition, due to imbalance problems (high synchronous vibration) early in the program, special analytical and mechanical balancing procedures had to be developed. In addition, other problems associated with deteriorating hardware can be detected from the vibration data. Defective ball bearings show up as accelerations in a frequency which is a fractional part of the rotational speed. Tables of these various frequencies are available for data evaluation. Rubbing of parts usually show up at two or three times the rotating speed. Instabilities (discussed previously), such as whirl, show up as a subsynchronous vibration. Two distinct areas of whirl frequencies have been found in SSME pumps around 50 percent and 90 percent of rotation speed.

The importance of this information to the SSME and the inability to analytically determine many effects in this machinery have led to the development of a very comprehensive set of data reduction, data evaluation tools, and an automated data bank of these data for all hot firings. Over 1,000 engine firing results are available in this data bank. Problems have been characterized and normal pump characteristics have been statistically formatted. Through the use of this data base system and accelerometer data from each engine firing and Shuttle flights, pump status is determined and refurbishment scheduled averting major problems.

Problems that have been experienced cover the entire range possible. These include imbalance, whirl, bearing deterioration, rubbing, impeller cracking, turbine blade, etc. The following paragraphs will illustrate some typical experiences and the corresponding data.

First, so that the reader has some reference point, the response statistics for three accelerometer measurements on the lox pump for all 109 percent power level firing (percent of original engine design thrust level) are shown on Table 5. Two tables are given, one for the composite level (0 to 1,000 Hz RMS levels) and the other for synchronous (levels taken from spectrum at rotating speed). Information comparable to this for all measurements and power levels are available. Also, data can be compiled by pumps, engines, builds, etc., as desired.

As mentioned previously, the pump response is very sensitive to small changes. Figure 91 is the average response of one pump for each of its eight builds (each build is a changeout of bearings, seals, or turbine blades, etc.; however, all major parts are the same). Notice the large variation in response even though each met all specifications including rebalancing. Responses range from 1.5 to 9 g's synchronous.

A typical pump response (isoplot) is shown on Figure 92. The predominant response is synchronous with a small 2 N response. Isoplots are a series of spectrum plots every 0.4 sec giving a pictorial of frequencies versus time. Amplitude is shown but is hard to read due to the overlapping of spectrums. Individual spectrums are used to get correct amplitudes. Anomalous behavior would show up as additional frequencies on the isoplot.

Figure 93 is an isoplot for a pump with rubbing. Notice the distinct 3N and 4N frequencies. Also, notice that distinct frequencies exist slightly above 3N and 4N. These are indicated on the individual spectrum placed above the isoplot. Many times, these frequencies are not constant with power level but move around indicating something like brake squeal going on (Fig. 94).

## TABLE 5. STATISTICAL SUMMARY OF SSME VIBRATION DATA

COMPOSITE @ 109% POWER LEVEL

| TEST STAND | FUEL PUMP RAD 0 # TESTS | $\bar{G}$ RMS | SIG | MAX G RMS | FUEL PUMP RAD 90 # TESTS | $\bar{G}$ RMS | SIG | MAX G RMS | FUEL PUMP RAD 174 # TESTS | $\bar{G}$ RMS | SIG | MAX RMS |
|---|---|---|---|---|---|---|---|---|---|---|---|---|
| A1 | 52 | 6.3 | 2.8 | 15.5 | 49 | 7.7 | 3.3 | 21.0 | 4 | 10.6 | 2.8 | 13.8 |
| A2 | 49 | 5.8 | 2.8 | 17.0 | 48 | 6.1 | 3.2 | 17.0 | 1 | 6.0 | 0 | 6.0 |
| A3 | 58 | 7.3 | 4.0 | 20.0 | 59 | 8.2 | 3.2 | 21.0 | 11 | 6.4 | 1.0 | 8.2 |
| COMBINED | 159 | 6.5 | 3.3 | 20.0 | 156 | 7.4 | 3.3 | 21.0 | 16 | 7.4 | 2.4 | 13.0 |

SYNCHRONOUS @ 109% POWER LEVEL

| | FUEL PUMP RAD 0 # TESTS | $\bar{G}$ RMS | SIG | MAX G RMS | FUEL PUMP RAD 90 # TESTS | $\bar{G}$ RMS | SIG | MAX G RMS | FUEL PUMP RAD 174 # TESTS | $\bar{G}$ RMS | SIG | MAX G RMS |
|---|---|---|---|---|---|---|---|---|---|---|---|---|
| A1 | 52 | 4.9 | 2.8 | 14.0 | 46 | 3.6 | 1.7 | 8.0 | 4 | 6.9 | 3.4 | 11.4 |
| A2 | 48 | 4.2 | 2.5 | 9.5 | 45 | 3.0 | 1.7 | 7.6 | 0 | 0.0 | 0.0 | 0.0 |
| A3 | 56 | 6.1 | 3.8 | 18.0 | 58 | 4.3 | 2.1 | 11.0 | 11 | 3.7 | 1.3 | 5.3 |
| COMBINED | 156 | 5.1 | 3.2 | 1.8 | 149 | 3.7 | 1.9 | 11.0 | 15 | 4.6 | 2.4 | 11.4 |

TEST # 'S A1291–436, A2195–331, A3047–232

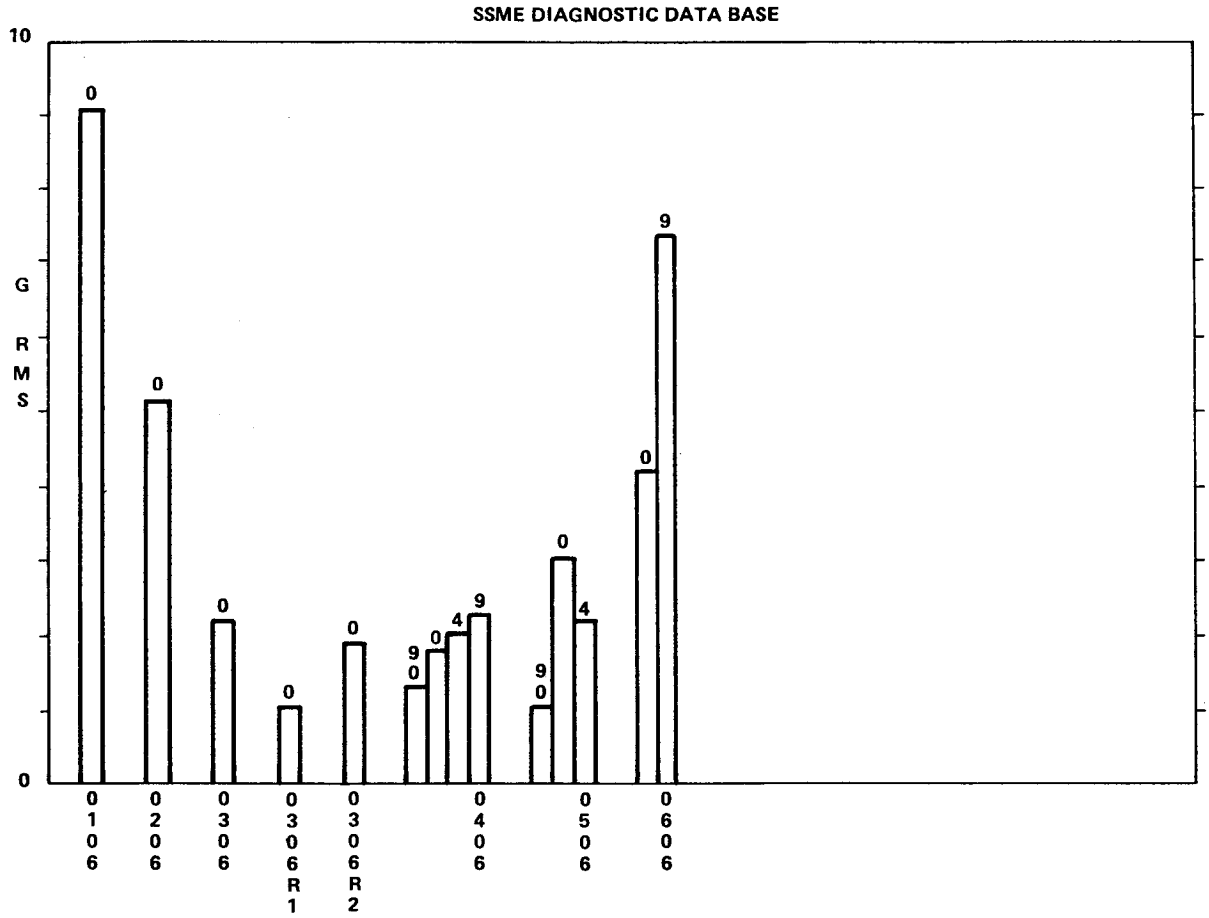


Figure 91. Pump response variation as function of builds (refurbishment).

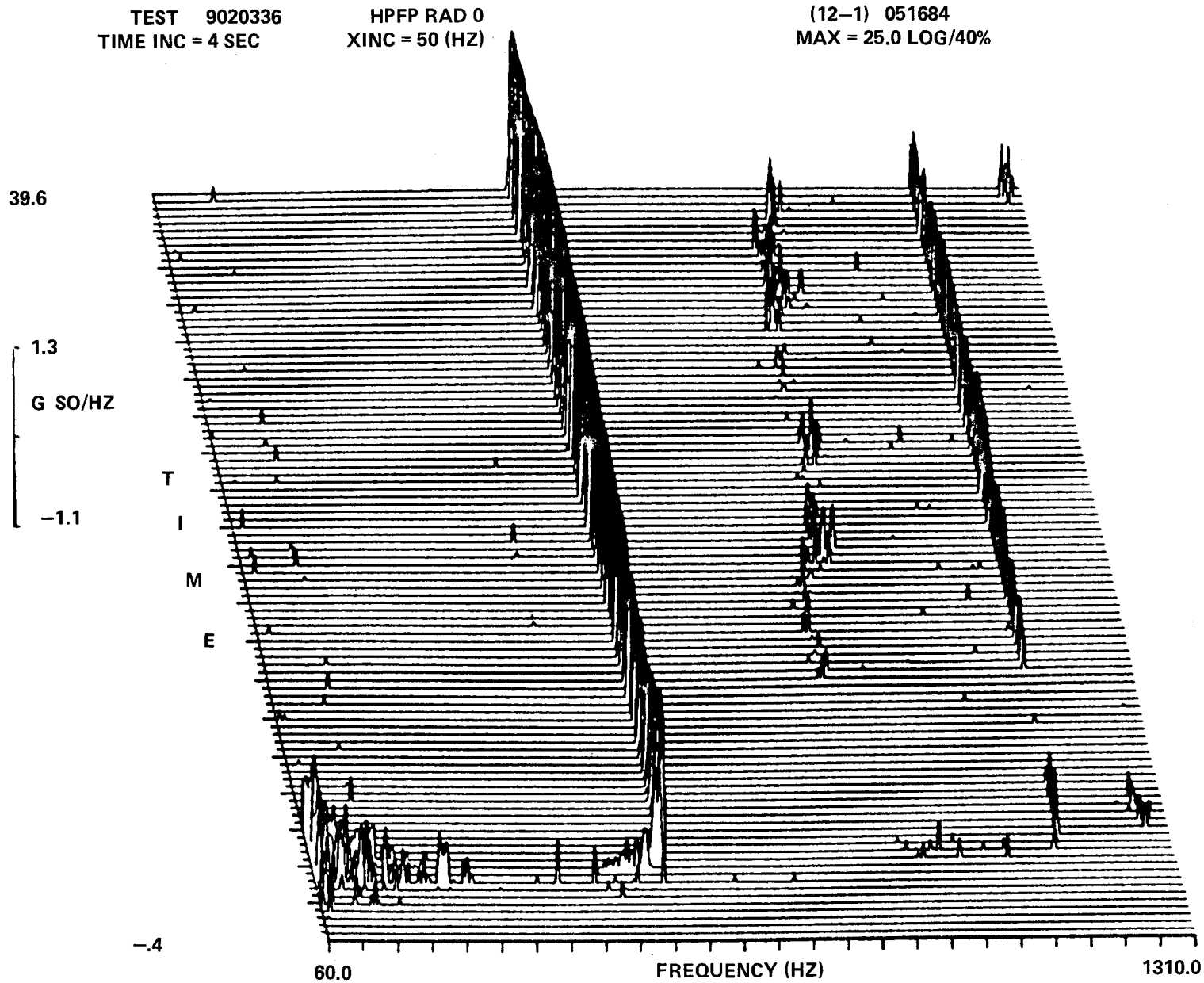


Figure 92. Typical isoplot of a pump accelerometer response.

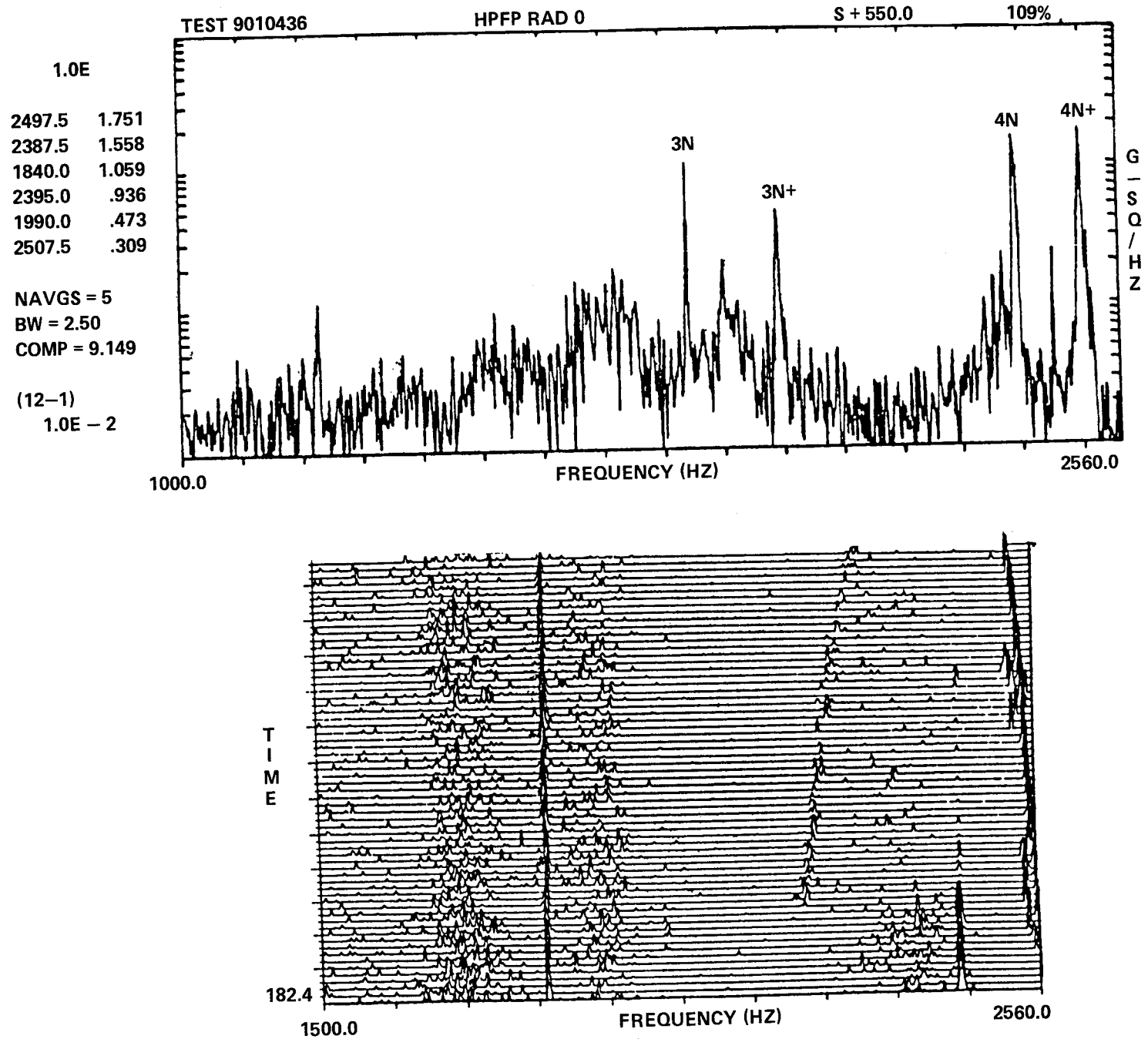


Figure 93. Isoplot showing frequencies indicating rubbing.

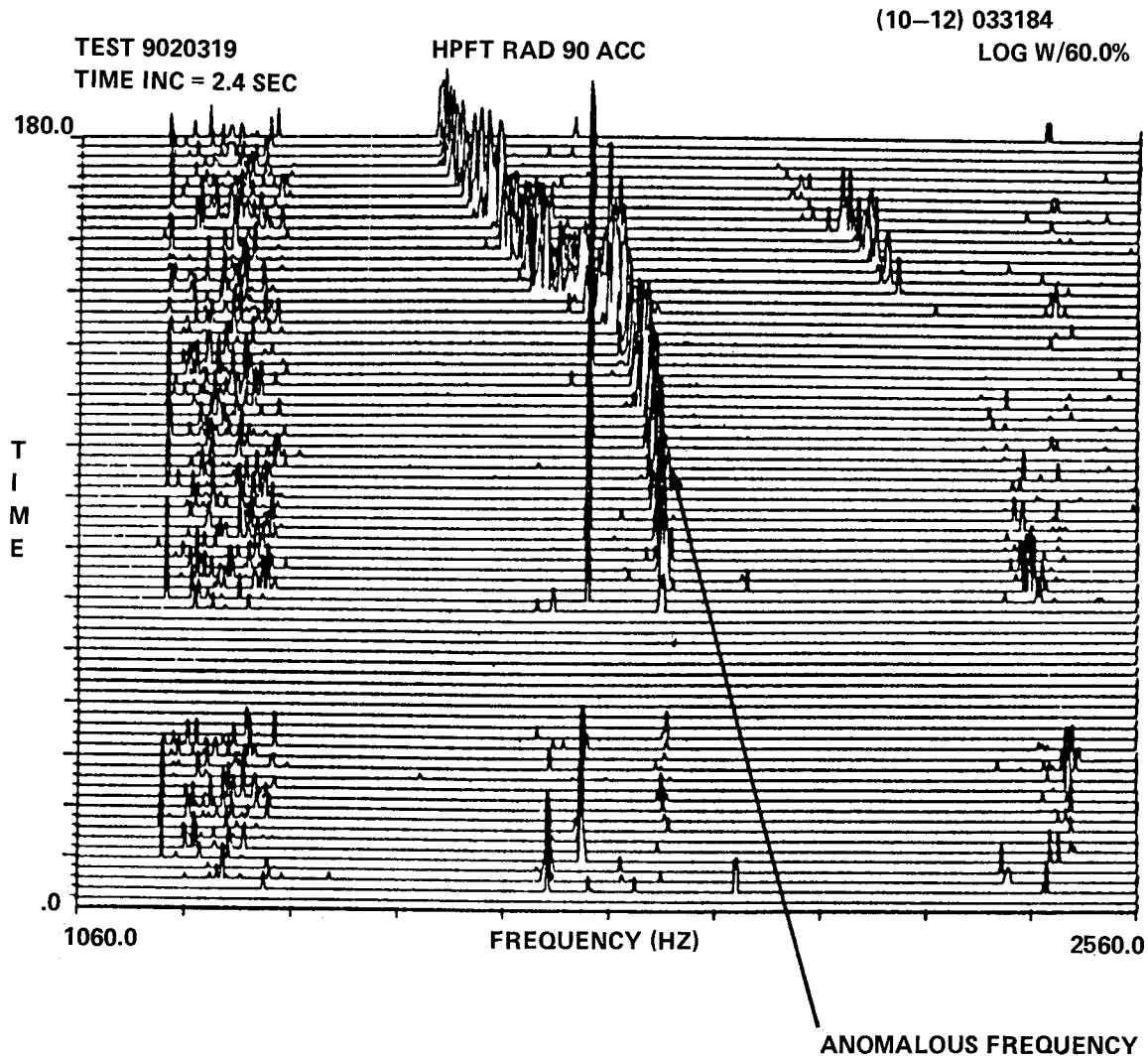


Figure 94. Anomalous frequencies in response data.

On one occasion, the frequencies indicating rubbing (2, 3, and 4N) came in at the start of the firing very high, then after approximately 100 sec it went away (Fig. 95). This indicates that either the rubbing went away or the rubbing became continuous around the shaft.

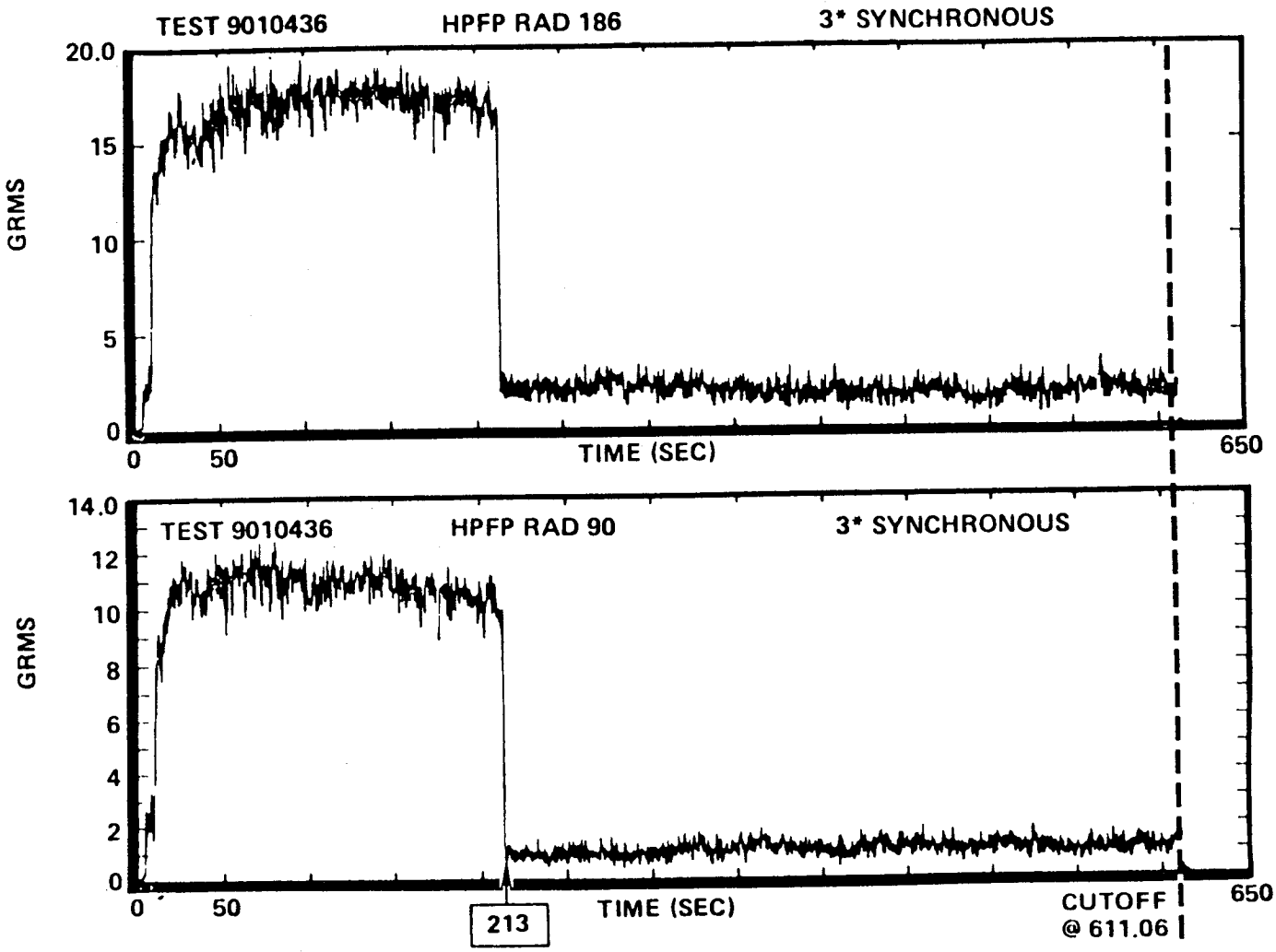


Figure 95. three times synchronous response anomaly.

Interpretation of the data sometimes is clouded by the structural response of the pump housing. In one case, a small level 3N response (typical, on all pumps) drove a case resonance, indicating very large amplitudes and confusing the issue. In another case, the small change in pump speed (synchronous) excited a case mode. The tuning was very narrow band, going away with a very small speed shift (20 rpm) and coming back in briefly during throttle ramp. Pump speeds vary from build to build due to engine balance changes from one engine to another, putting some housing in resonance while the others are quiet.

Whirl will show up on the isoplots and in the spectrums in the same manner as the other frequencies. Because of the concerns over whirl, the data bank was interrogated for all pumps with whirl. The results in terms of whirl rpm, initiation, and levels are shown on Figure 28 (section of instability), showing the magnitude of the problem and the value of a data bank for assessing the problems.

Other indicator frequencies, such as a bearing ball pass, are hard to find in the data due to the inability to get instrumentation at the bearings but must depend on accelerometers mounted on the pump housing. Shell mode response of the housing also clouds these data. In a few cases, ball pass frequencies have been observed in the data then chipped bearings found at teardown inspections.

One additional problem area in rotary dynamics which continues to surprise dynamicists is the disk modes. These modes can be stationary with respect to the structure or move forward or backward. Many times these modes can tune with either the inlet wakes or outlet wakes of impellers or turbines. If these pulses generate forcing functions with patterns and frequencies coinciding with the mode shapes, large amplitude responses and fatigue failure can occur. Also, blade disks tuning occurs for turbines in such a manner as to increase blade response leading to cracking. In either case, very high frequency, high modal numbered modes can get involved and are very difficult to determine analytically. This results in major dynamic test programs of impellers, turbines, etc. Since it is hard to accurately and sufficiently instrument these type of systems, remote sensing, such as laser holography, is used to produce very good descriptions of both the modes and frequencies. Two problems have occurred in the main engine in this category, the high pressure fuel pump impeller cracking (high cycle fatigue) and high pressure pump lox blade cracking. In the case of the fuel pump impeller, it is a high N number mode which also has harmonics of other modes that tune with the wakes of the outlet vanes. In this case, it is not the basic mode but the impurities due to unsymmetry, which is actually driven by the wakes. Blade disk tuning leads to numerous modes with the gains (modal response increase), particularly at the blades being determined by the differences in the individual blade frequencies. This type of blade disk coupling has lead the aircraft industry to accurately characterize each blade, eliminating potentially bad couplers from usage. At the time this paper was written, both these problems were still being worked. The modal characteristics of very high ordered N modes have been determined in test using laser holography and the final verification has been accomplished.

This short treatment of dynamic problems in rotating machinery does not begin to give the full flavor of this area. It is hoped that the reader grasps some idea of the potential problem.

7) General (SSME). The other problems listed in the matrix for SSME, controller isolation, flowmeter, ASI, and capacitor probe, are typical of response and fatigue problems discussed in other project areas. The SSME controller was responding to a high level of mechanical engine noise and required isolation. The lox flowmeter responded to the fluctuating pressures from the lox pump failing in fatigue. Through a better use of other system data, such as fuel flowmeter output, the lox flowmeter could be eliminated, solving this problem. The capacitor probe was an attempt at measuring bearing deflections in a lox pump. Vibration caused rubbing, starting a fire. A different approach has been developed for getting bearing loads in a few development pumps. The ASI was a structural failure due to shock that occurred during shutdown when hydrogen was sucked back into the ASI and burned (small explosion). A change in shutdown flow solved this problem.

## 6. Space Telescope, HEAO, IPS

### a. Space Telescope

Space Telescope, to fly in 1986, has had some minor problems in the dynamics area. Loads variability, creak, and jitter were discussed in a previous section. The other main problem areas have been associated with the Scientific Instrument (SI) latches. These are latches installed so that the SI can be removed on-orbit for maintenance, film retrieval, etc. The SI's and their latches are both axial and radial (Figs. 96 and 97). The latches and their response characteristics were very important to the individual instrument pointing accuracy (line-of-sight) and to the overall dynamic response for loads. Because of the criticality of these, an extensive qualification program on a vibration shake table was performed. Static and dynamic tests to determine the appropriate stiffnesses of the latches were also performed.

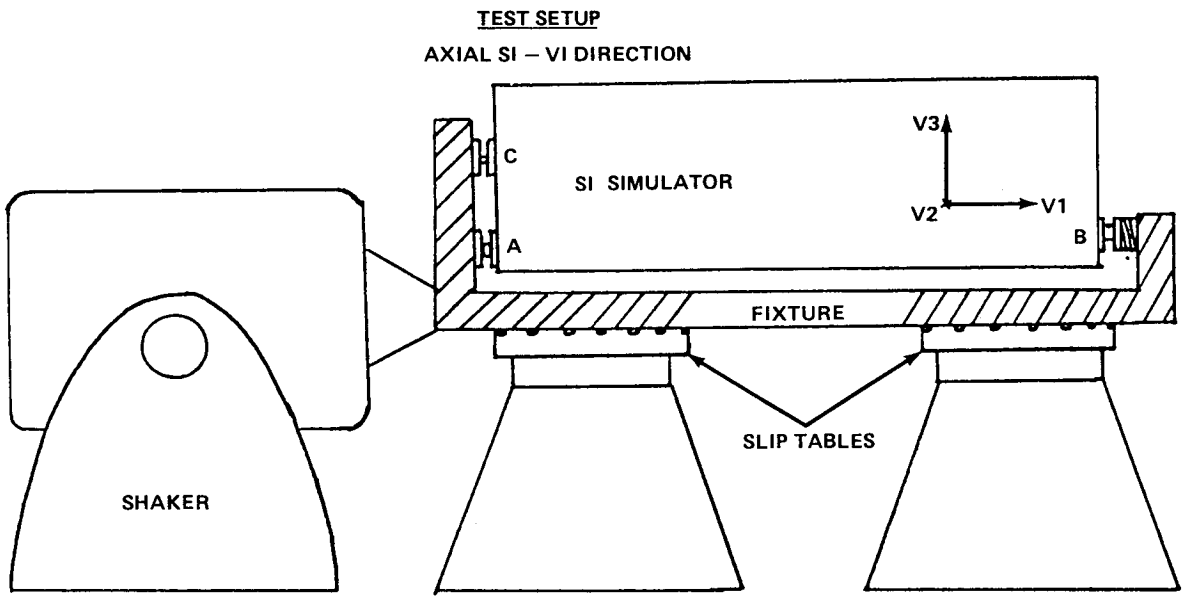


Figure 96. ST axial latch in test setup.

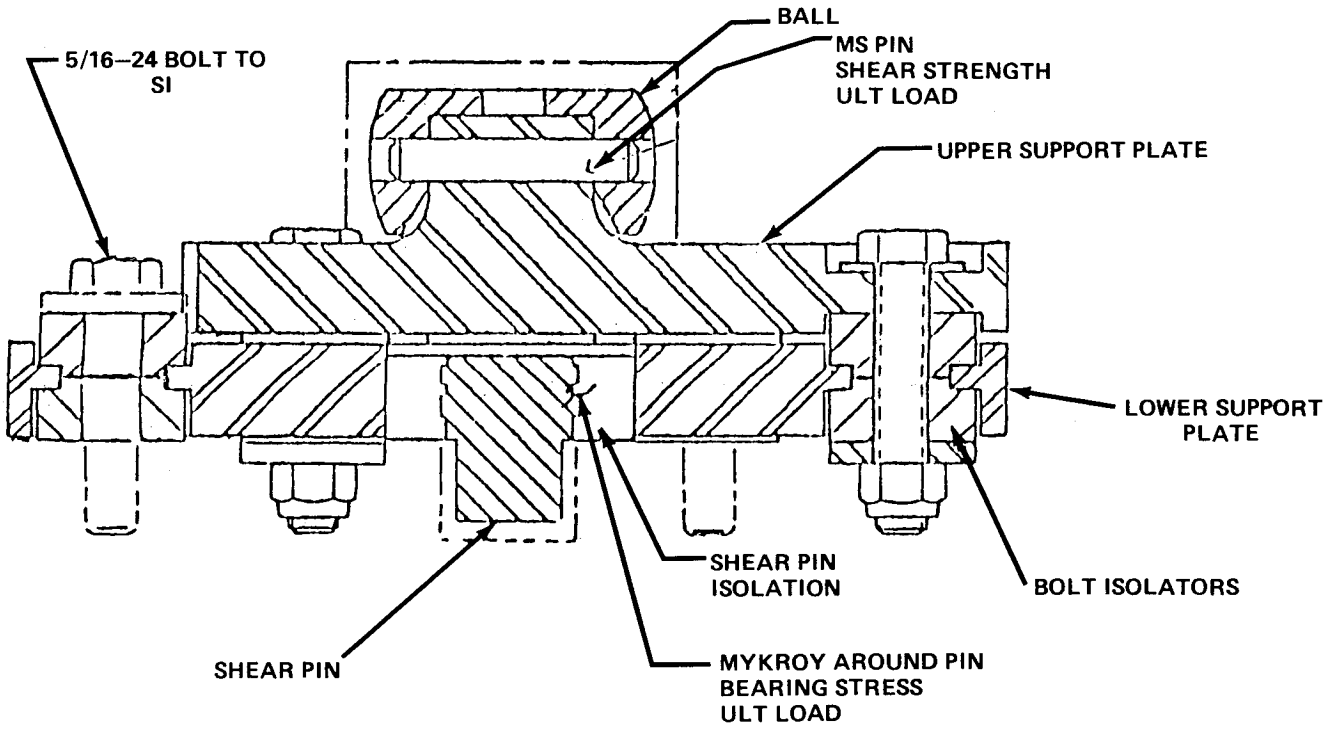


Figure 97. Typical axial latch.

The first attempt to vibration qualify the latches was not successful. Latches were damaged beyond use (cracking and surface wear). This was not an acceptable condition. Various coatings have been tried to solve the problem. Tungsten-carbide-cobalt coatings were added to the retainers of the axial SI latches A and C. Additionally, the aluminum oxide coating on the 440C ball of the A latch was eliminated. The modified hardware successfully completed vibration qualification testing without degradation. Similar modifications were made to the radial SI latches. Subsequent vibration qualification testing of the modified radial latches generated particulates at the B and C latches. Although the wearing of the latch surfaces was not significant, the small particles presented a potential contamination problem for the ST optical elements. Brayco lubricant has been added to the latches to entrap the particulates. Figure 96 shows the test setup for the axial SI showing the latches A, B, and C. Figure 97 is a detail

of latch A. Tests and final verification have been completed. In complex, high performance systems, the design and verification of many apparently insignificant parts become key to the success of the mission.

b. HEAO

HEAO had a unique dynamic problem that was uncovered during development and verification vibration testing. Isolators had been installed to allow for thermal expansion and contraction during operations on-orbit in order to allow for pointing accuracies. The isolators chosen handled well the thermal cycles; however, they were highly nonlinear under dynamic situations such as liftoff, maximum dynamic pressures, stage separation, etc. This resulted in a major program to accurately define the isolator characteristics. In addition, stringent acceptance criteria were instituted in order to narrow this range and obtain compatible isolators.

This is a brief coverage of various problems experienced in the forced response area. More information can be obtained from references given throughout the report.

## C. Modeling

Problems in modeling the dynamics of systems have continued to plague engineers. In many cases, it is more of an "art" than it is a "science." With the advent of larger (storage) and faster computers in conjunction with finite element techniques, order of magnitude improvements are being made. Modeling can be thought of as existing at three levels, subsystems, elements, and systems. The models must account for all disciplines which interact in the system, such as fluids, structure, control, hydraulic, electrical, etc. Modeling correctly the interaction of these various disciplines constitutes a major challenge in many systems.

Several problems have been experienced in the modeling world. Some of them were of a classical nature; however, most were well within the state-of-the-art modeling techniques. The reason the problems were encountered was oversight, not modeling in enough detail, or not being aware of certain system requirements.

1. Apollo

Two modeling problems that were of the classical type occurred in the Apollo Program. One dealt with local deflection, the other with structural fluid interaction (hydroelastic).

a. Instrument Unit Local Deflection

The local effect problem occurred in the Instrument Unit (IU) stage at the rate gyro location. The rate gyro deflection was much larger than classical beam modes predicted. The effect was not found in scale model testing due to reduced fidelity in this area of the structure. Full scale dynamic testing uncovered the effect. The IU stage was located on top of the S-IVB stage. On the upper side were the SLA panels which were the interstage between the IU and the service module. Inside this area was the Lunar Excursion Module (LEM). Since the service module was a smaller diameter than the IU, the SLA panel loads were at an angle to the IU creating both a static and dynamic distortion (Fig. 98). Not anticipating this angular load path caused the modeling error. At the time this error was found, finite element modeling was less critical. As a result of the modeling error correction, the control system (filter) was redesigned and all flights experienced no problem in this area. The lesson is clear, know what is critical to the system, then model that area accurately.

b. Hydroelastic Coupling in Propellant Tanks

The hydroelastic effect was discussed briefly under the pogo section. Early dynamic models for pogo treated the bulkhead and tank wall as rigid in terms of the pressure pulse set up in the propulsion system. Basically, the whole tank was assumed to move dynamically, moving the fluids as a unit setting up the pressure wave in the tank (Fig. 99). In the case of S-IC pogo, this approach was adequate. The S-II pogo problem could not be adequately represented with this simplified model.

As shown previously, the S-II pogo problem was caused when the tank/fluid bulkhead mode was resonating with the longitudinal mode and engine thrust frame crossbeam mode. In this case, the pressure wave was greatly amplified due to the hydroelastic effect (Fig. 100). Initially, an experimental program was run to obtain data for analysis. In the final phases of this program, an analytical hydroelastic model was developed and verified.

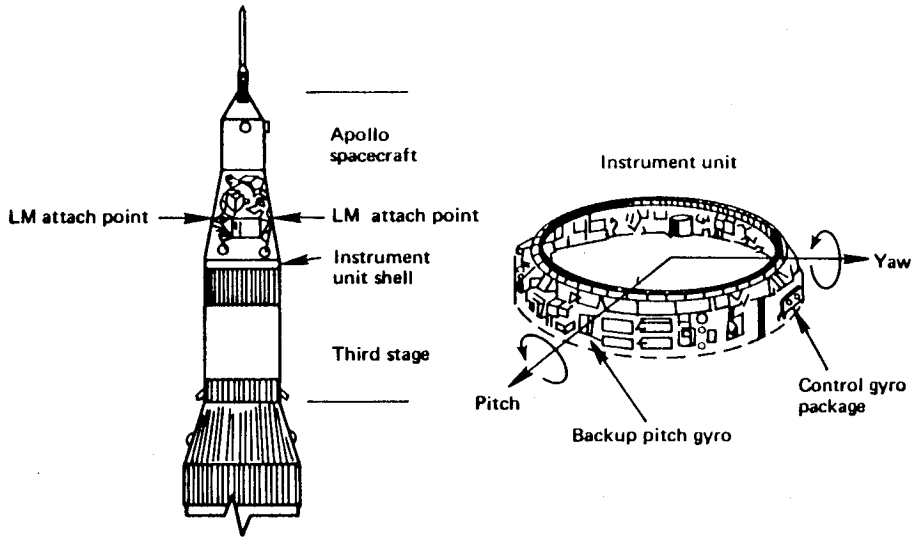


(a) Saturn V instrument unit.

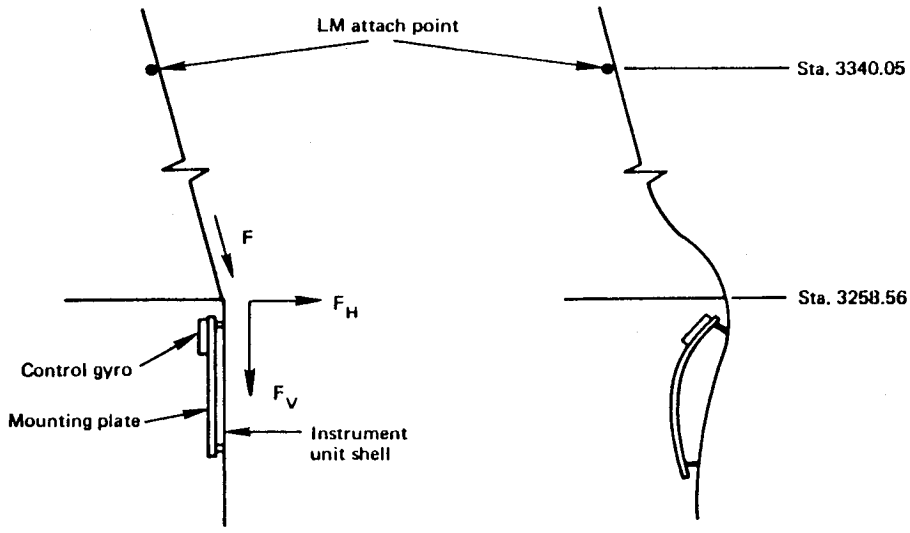


(b) Schematic of Saturn V control gyro mounting and local deformations.

Figure 98. Saturn V local deformation.

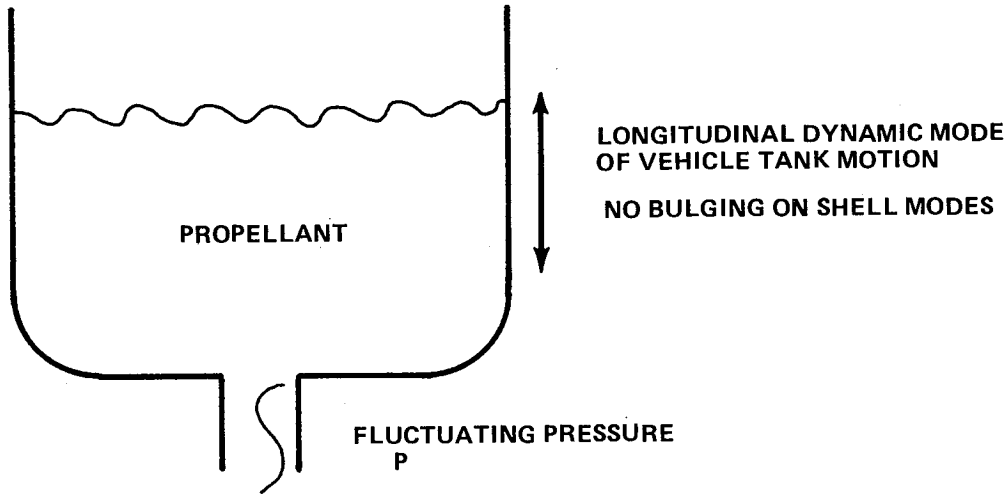


Figure 99. Early tank bottom pressure model.

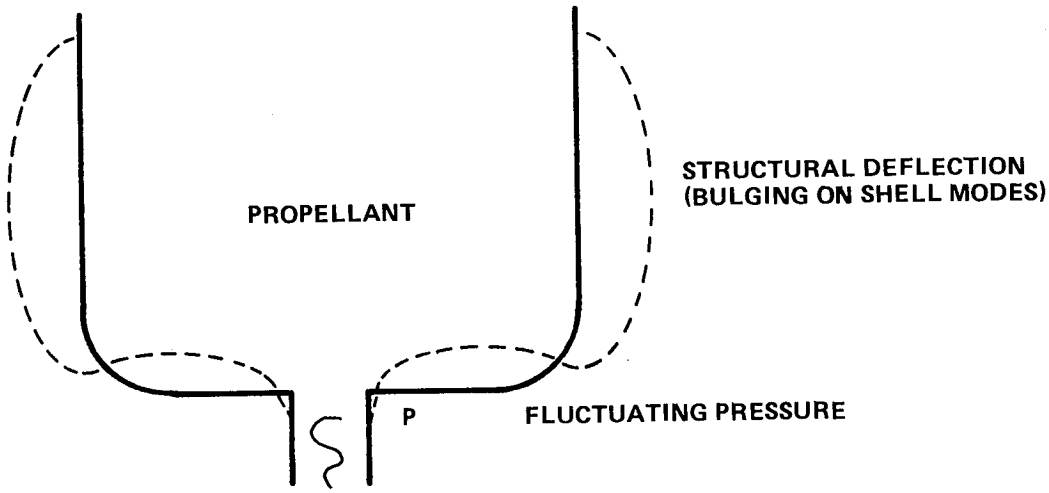


Figure 100. Hydroelastic effect.

At this time in the program technology was not ready to meet the needs of the program and had to be developed. Many times, these needs cannot be envisioned. Hydroelastic problems had been anticipated and were under development at the time of the S-II pogo problem but not to a state of art condition. The lesson: Phases A and B of a program or project must uncover critical technologies and develop approaches and capabilities for their solution.

c. S-IVB Slosh Model/Structural Model

The behavior of liquid propellants in conjunction with structural dynamics and/or control has led to some surprises. One occurred in the modeling of the S-IVB structural modes. Modelers had generally assumed that liquids behave as mass loading on equivalent beam type models. This simplification did not hold up for the S-IVB stage of the Saturn which had an elliptical shaped lox tank. In this case, the liquid mass did not act as a rigid mass but performed rotary motion during bending oscillations (somewhat like the rotating egg experiment). Analytical models did not correlate with full scale dynamic testing until corrections were made in the assumed rigid body liquid propellant rotary inertia term. Correcting the term to account for liquid rotation gave good correlation of analysis and test. Equivalent mass-spring slosh models had to have corrections made to include rotation terms.

d. S-IV Slosh Baffle Damping

Early in the Apollo Program, it was thought that slosh baffles should be perpendicular to the tank wall under the assumption that the fluid velocity during sloshing would be along the tank wall. This assumption was wrong since in reality the propellant oscillates about the thrust vector centerline as the vehicle is essentially in a controlled or propelled free fall, hence the basic fluid flow energy is in this direction and not along the tank wall. These facts were made very clear when verification slosh baffle tests were performed with the baffles located perpendicular to the tank wall. The surprise was that no damping was apparent from baffles installed in this orientation. When the baffle was oriented perpendicular to tank centerline, damping was good and as expected. Obviously, the total physics of the problem must be understood and test programs are the way to get this understanding.

2. Space Shuttle

a. Systems

Structural dynamic modeling from an overall systems viewpoint missed a couple of significant characteristics of the Space Shuttle. One of these, the SRB roll made against the interfaces of the External Tank, was very interesting. The other was a local deflection of the rate gyro mount.

1) SRB Roll Mode. Because of cryogenic effects of the propellant, there is a 7-in. stacking allowance between the SRB and External Tank. When the cryos (propellants) are loaded, the tank shrinks to take up this gap. During full scale mated ground test, water was used for propellants so no shrinkage occurred. This meant that the aft SRB to tank struts were at a small angle and not perpendicular, thus the load into the aft tank ring had an axial force creating a torque on the tank I-beam. As a result, the effective stiffness on the tank side was changed leading to an error in prediction of the SRB gear train mode. Watching the test, one could see the tank skin oil canning as the I-beam rolled when this mode was excited (Fig. 101).

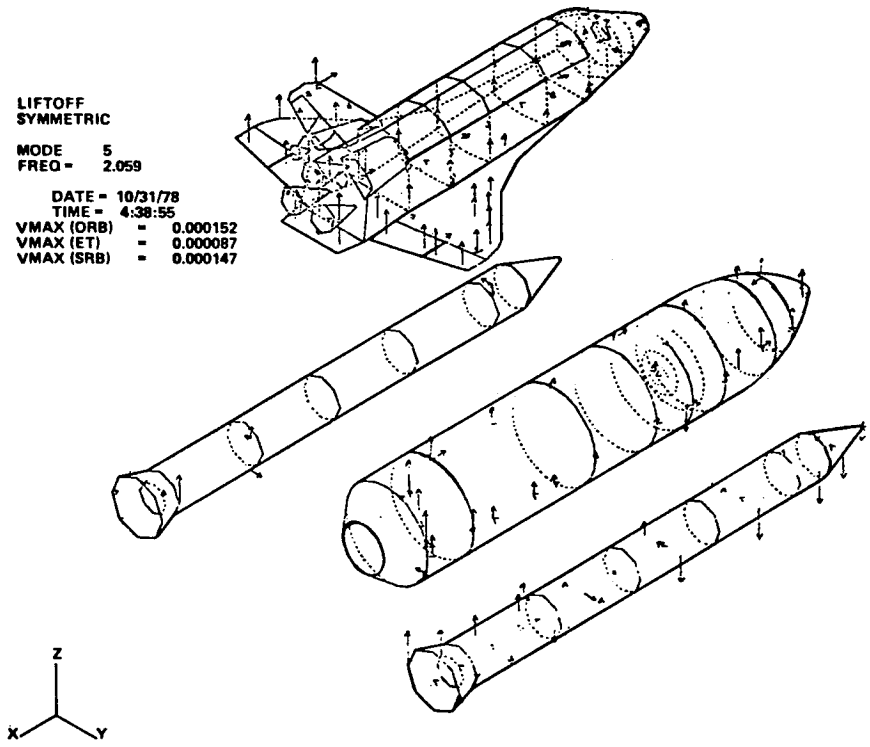


Figure 101. Liftoff symmetrical mode shape.

Essentially, the SRB's acted as rigid bodies with the flexibility being in the struts and tank. The accuracy of this mode was very important to liftoff loads predictions, since the SSME ignition and buildup prior to SRB ignition stored energy into this mode. This energy was released at liftoff ringing out this mode due to the stored energy. As a result of the MVGVT findings, both axial and radial stiffnesses of the tank strut attach had to be put in the tank model used for system modes.

2) Local Deflection of Rate Gyro Mount. Local deflection of rate gyro mountings was the second problem uncovered on the full scale ground vibration test. This distortion was caused by the local modes of the instrument ring frame in the front of the SRB forward segment. The ring was not modeled as a flexible element under the assumption that its frequency would be too high to respond elastically to the first fundamental bending modes. The assumption turned out to be erroneous and had to be corrected. Two things had to be accomplished. The finite element model was corrected giving a good match to test data. This was a simple task, merely putting in the extra elastic elements associated with the gain or change the control system shaping networks (bending mode filters). It was decided to stiffen the ring with brackets (Figs. 102 and 103) and test verify. This was accomplished first using the forward SRB interstage while the liftoff (full SRB) configuration was being unstacked and the SRB burnout (empty SRB) configuration was restacked for dynamic testing of the condition. The fix was preliminarily verified using this element test, then finally verified from the system standpoint during the SRB burnout dynamic test.

In the final analysis, the second problem was not a real modeling problem. It occurred because of the need to make models as simple as possible to reduce size for system analysis, thus making a simplifying assumption without adequately checking it out analytically. In this case, a very simple shell model of the forward section would have shown the error in the assumption.

The last system modeling was not an error in modeling, but the effect on elastic body characteristics in conjunction with external forces. The effect of the fast rise of the internal pressure at SRB ignition (0 to 920 psi in 400 msec) stretches the system, adding greatly to liftoff dynamics (refer to Section B on forced response systems). The lesson is clear. All interacting effects must be properly modeled. This obviously means the modeler must understand all system aspects and sensitivities in order to provide adequate models.

b. External Tank (Hydroelastic Coupling of Unsymmetrical Tank)

Basically, the overall model of the External Tank was very straightforward. The lox tank hydroelastic model was an exception. The lox tank, in order to save weight, does not have uniform thicknesses around the tank bulkhead and tank wall. Since the tank is tilted during flight, one side of the tank can be thinner than the other; therefore, a quarter symmetric model could not be used. Both sides of the tank had to be modeled independently including a tilted propellant surface. Using finite element hydroelastic modeling techniques in conjunction with quarter-scale and full-scale, lox tank dynamic testing produced a very good analytical model. Martin-Marietta Corporation did this modeling.

c. Solid Rocket Booster (SRB)

Three basic modeling or dynamic problems have occurred for the SRB, viscoelastic propellant effects on system dynamics, internal pressure effects on Shuttle system dynamics, and filament wound case (FWC) (composite case) dynamic modeling.

1) Viscoelastic Modeling Problems. Viscoelastic effects of solid propellants are very complex. The elastic properties of the propellant are highly nonlinear, being a strong function of strain rate, temperature, pressure, and age. Elasticity of the propellant was so sensitive that the mean bulk propellant

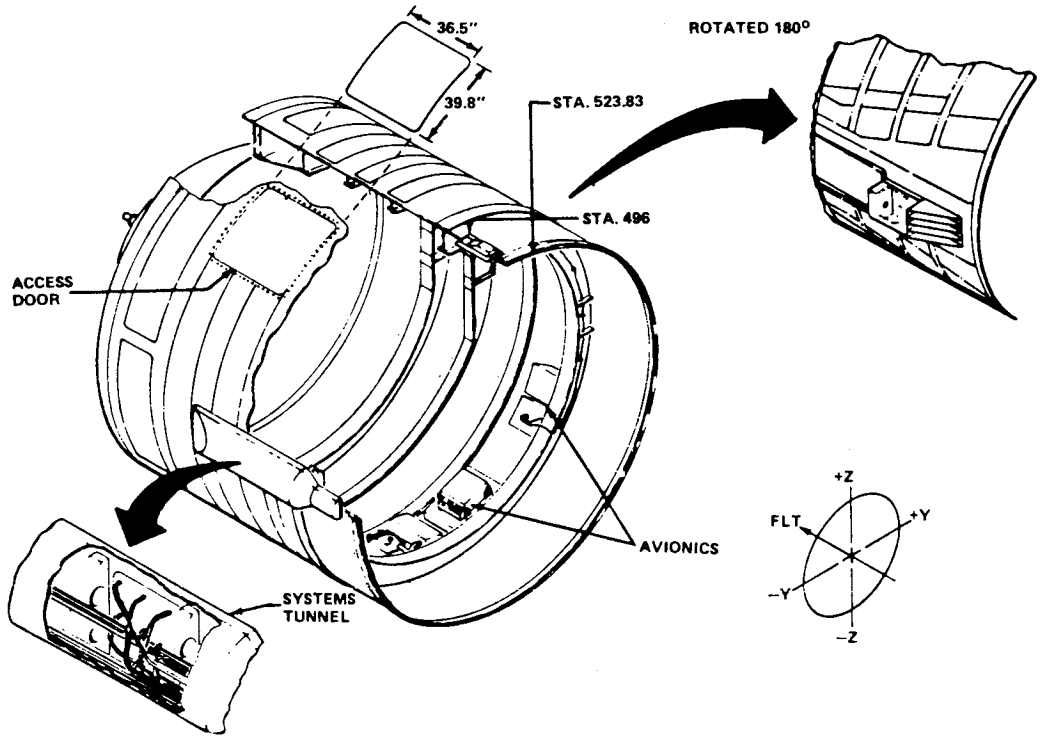


Figure 102. SRB forward interstage section.

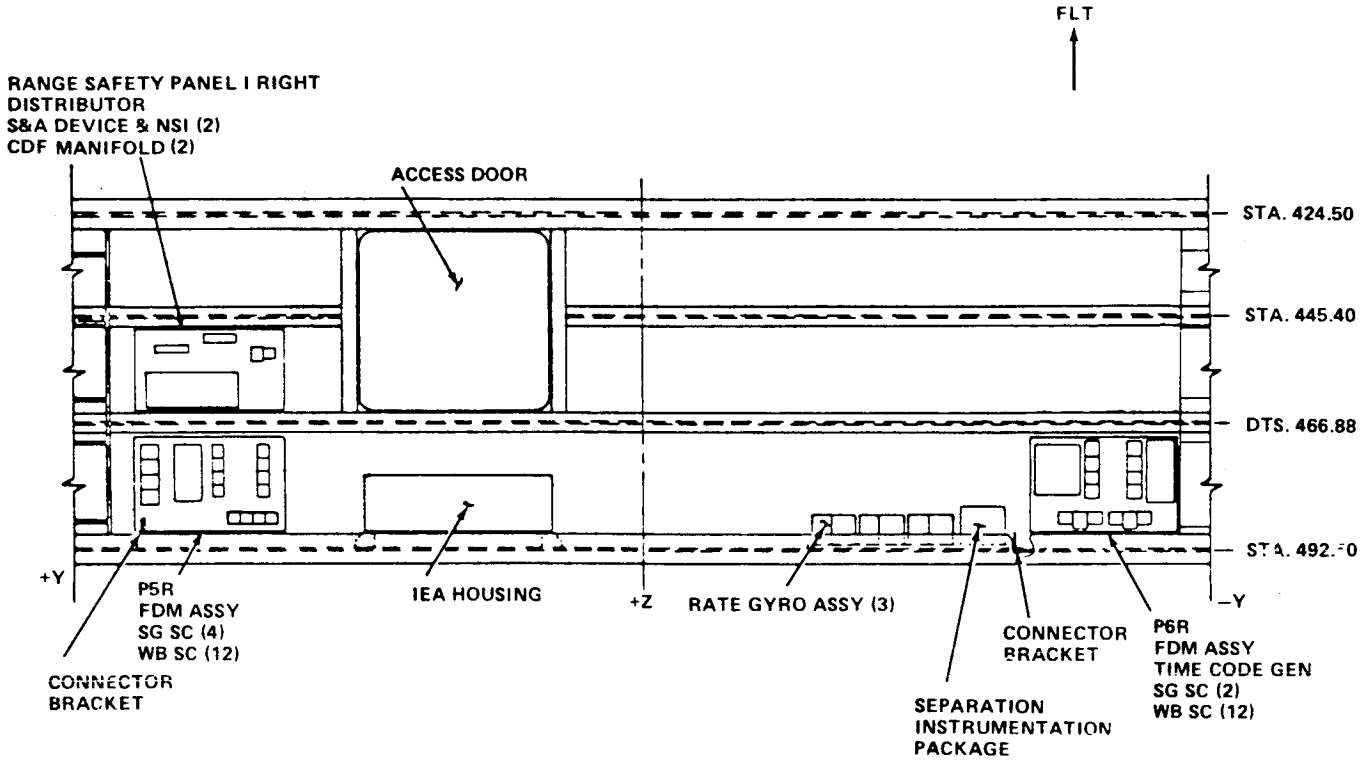


Figure 103. SRB forward interstage section.

temperature between a winter launch and a summer launch led to the requirement for two different dynamic models of the SRB's. The propellant elasticity affected two basic vehicle modes, the longitudinal mode of the propellant moving dynamically relative to the SRB skin and the SRB gear train mode of the solids rolling in a rigid body sense against the rear SRB to External Tank interface, discussed under system response. Analytically, it was very hard if not impossible to model the viscoelastic effects. In order to achieve an adequate model, extensive dynamic test programs in addition to the full scale and allup quarter scale test programs were carried out. The first was a coupon test which determined the material properties of the propellant as a function of temperature, pressure, frequency, age, and amplitude [60]. Using properties derived in this manner, the pre-liftoff model was determined. Figure 104 shows how the gear train mode frequency varies as a function of propellant shear modulus, with the SRB/ET struts fixed to ground. Running the quarter scale model without internal SRB pressure showed the model to be good in terms of propellant shear modulus, with the SRB/ET struts fixed to ground. Running the quarter scale model without internal SRB pressure showed the model to be good in terms of elasticity and shell stiffness. In this case, however, special modulus tests had to be run on the inert propellant used in the dynamic test, since it had different characteristics than live propellant.

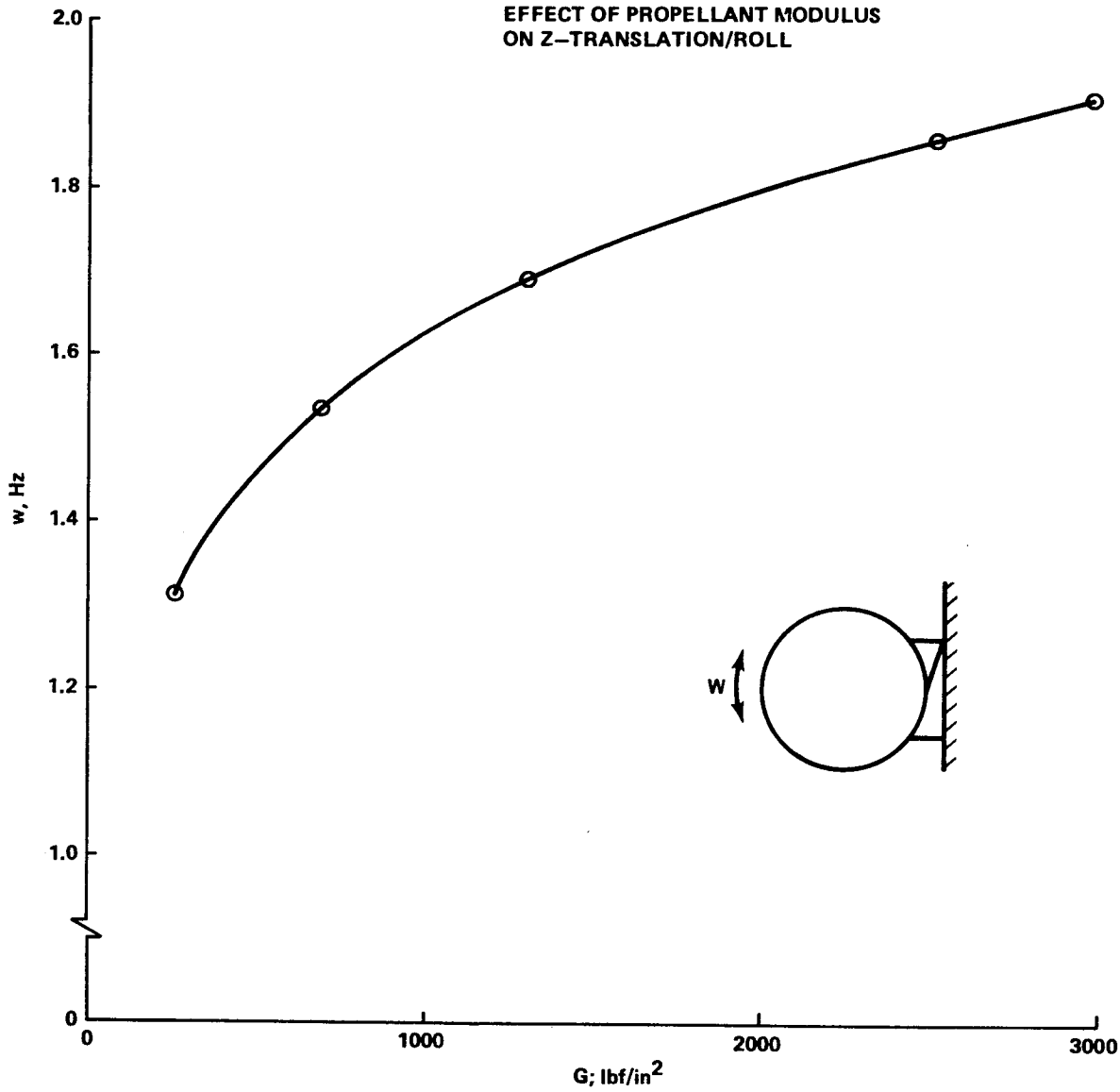


Figure 104. Gear train mode frequency as a function of propellant shear modules.

2) Dynamic Effects on Stiffness of Internal Pressure. The next problem occurred when internal pressure was included. Differential stiffness analytical techniques grossly overpredicted the stiffening effect of pressure in a dynamic situation. The same technique predicts accurately static effects for a radial punch load. No reason has been determined for this overprediction. As a result, the stiffening effect of pressure was determined experimentally using the quarter scale SRB element model fixed to ground. Figure 105 shows the frequency of the translation/roll mode as a function of internal pressure for an SRB with no propellant and one with the propellant fully loaded. Notice that the mass and viscoelastic effects of the propellant reduced greatly the pressure effect [60].

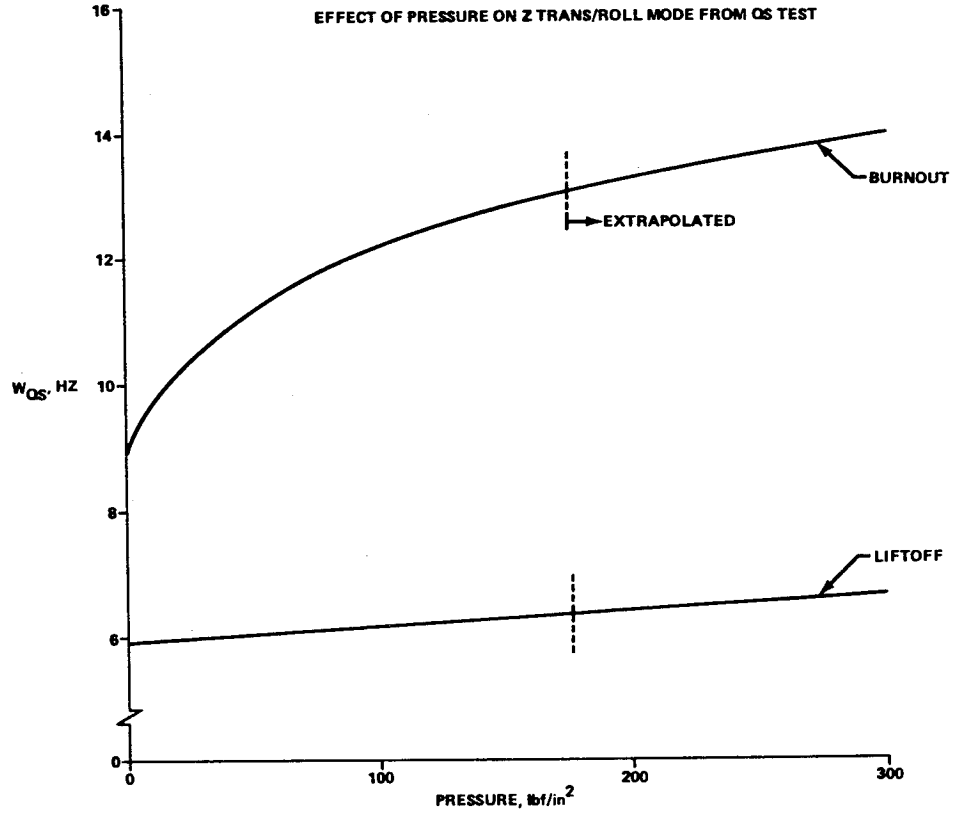


Figure 5. Gear train mode frequency as a function of internal pressure.

Finally, the Shuttle's response during liftoff has verified the models derived in this manner. As a result of these problems and the various effects predominant in the Shuttle mission, specialized models had to be generated for the following events and sequences.

I. Pre-Liftoff Models (Unpressurized)
   A. Winter Months
   B. Summer Months
II. Liftoff (Pressurized)
   A. Winter Months
   B. Summer Months
III. Max "q" (Pressurized)
   A. Winter Months
   B. Summer Months
IV. Pre-SRB Separation (Unpressurized, No Propellants)

The message is the same as stated previously relative to sensitivities, environments, etc. Generate models for the specific uses if there is a change in the system characteristics, the models must be updated to account for the changes.

3) Modeling Concerns and Problems of Composite Solid Rocket Propellant Cases. The final modeling surprise came when the Filament Wound Case (FWC) SRB was baselined as a performance enhancement approach (weight savings). Due to the liftoff loads sensitivity (discussed previously), the longitudinal stiffness (elongation) and the hoop stiffness were specified (design specification) to be the same as the steel case SRB. Meeting these criteria and verifying these characteristics has been a major problem. The first sacle model FWC section when tested dynamically did not produce a good match when compared to values from the steel case or to predictions. As a result, an extensive program was conducted on proper fiber wrap angles to achieve correct characteristics and to develop techniques for determining the total set of material properties for use in dynamic modeling and dynamic analysis. This work has been completed. In addition, the quarter scale element test approach used for the steel case has been expanded and used for the FWC (pressure and viscoelastic effects). An adequate model resulted.

Analytical models can be no better than the experimental input data, such as material properties. These data base definition programs cannot be emphasized enough in any program.

d. Modeling Verification Summary

Modeling of structures and the verification through dynamic test has been full of surprises and interesting. Many of the preceding discussions have covered key areas. Dynamic testing, in general, has been the mechanism through which these problems have been uncovered. In the Saturn I dynamic test program, the suspension system (cables) dynamically coupled with the vehicle clouding the test data. A very simple fix was used. Two by fours were tied between the cable and the test stand uncoupling the cable mode from the vehicle. Suspension system can directly influence test results and must be correctly designed.

Verification testing is very important in dynamic analysis and ideally should follow a building block approach, e.g.:

- Generic Structures
  - Phenomenon Characterization
  - Element
  - Subsystem
  - System
- Scale Model Prototype
  - Element
  - Subsystem
  - System
- Full Scale
  - Element
  - Subsystem
  - System
- Program scope is determined by subsystem and system requirements on model accuracy and control system complexity risk trade.

– Program should make maximum use of other test programs to obtain subsystem dynamic characteristics.

– Shuttle dynamic test program is an example of basic approach although some desired tests were eliminated.

All space programs of the past have used dynamic test programs. A summary of this history is given in Table 6 and should serve as a handy reference of the experiences discussed in this report. Table 7 gives general guidelines for selecting a test approach. Table 8 lists concerns of dynamic testing with particular emphasis on orbit space systems such as space station. The Apollo and Space Shuttle program modeling problems, a few of which have been discussed, delineate the major problem areas structural dynamic modelers face. The areas which must receive special attention in both modeling and test if adequate models are achieved are (1) joints, (2) load paths, (3) point loads, (4) nonlinear material characteristics, and (5) special environment effects such as pressure.

## D. Acoustical Tuning

One of the most interesting and awe inspiring dynamic problems occurs when local acoustical modes tune with local structural dynamic modes. The energy extracted from the flow field is transferred to the acoustical and then into structural response to a degree that cannot be imaged. The experiences have been few in the history of the space program but were very dramatic in nature. Only one of any significance was experienced in the Apollo Program. Several have occurred in the Shuttle Program, mainly due to the higher performance requirements thus greater sensitivity.

### 1. Apollo

The main acoustical tuning problem in Apollo was in the F-1 engine main combustion chamber. This was a circumferential mode which created many problems. The problem was solved with baffles called the kitchen sink approach.

### 2. Space Shuttle

The Space Shuttle, due to its high performance requirements leading to more optimized design, less margins, and higher environments, experienced several acoustical tuning problems. The first occurred in the main propulsion system test program in the External Tank which was discussed in the forced response section. The others have occurred in the SRB and SSME.

#### a. SRB Reentry and Internal Motor Cavity Acoustics

Scale model testing of the SRB to determine acoustical environments produced a major surprise. The levels were greater than 175 dB, which were a major design problem for components mounted in the near the aft skirt, in particular the APU actuator propulsion unit, actuators, and rear IEA. Due to the high levels and lack of understanding of the cause of the high levels, several activities were carried out to understand the problem. As mentioned previously, the SRB reenters the atmosphere tail first and basically broad side. This creates a flow across the skirt and nozzle. Due to reentry dynamics, the angle can vary significantly from flight to flight and flight time to flight time. Initially, the SRB nozzle was intact with a charge installed to sever it at the skirt end station before water impact to reduce flex seal loads. Later, in order to reduce acoustics, the aft nozzle section was severed prior to

TABLE 6. DYNAMIC TESTING EXPERIENCE IN PAST PROGRAMS

| TEST PROGRAM | PROBLEMS DISCOVERED | HARDWARE IMPACTED | CONSEQUENCES IF NOT DISCOVERED |
|---|---|---|---|
| SATURN V DTV | LOCAL ROTATION OF THE FLIGHT GYRO SUPPORT PLATE. VEHICLE DYNAMIC SHEARS AND MOMENTS DEFORMED SUPPORT PLATE. THE MATH MODEL UNDER PREDICTED THIS DEFORMATION BY 135 PERCENT. | THE GYROS WERE RELOCATED TO THE BOTTOM OF THE SUPPORT PLACE WHERE THE LOCAL ROTATION WAS MUCH LESS. THIS REQUIRED WIRE HARNESSES OF NEW LENGTH. THE FLIGHT CONTROL FILTER NETWORK WAS REDESIGNED | FLIGHT CONTROL INSTABILITY RESULTING IN LOSS OF VEHICLE. |
| MARL | DESIGN DEFICIENCY IN THE IU STABLE PLATFORM. COUPLING BETWEEN THE STABLE PLATFORM AND THE RING MODES OF THE IU PROVIDED A MECHANISM FOR ACOUSTICALLY DRIVING THE PLATFORM ACCELEROMETER AGAINST THE STOPS. | SHORT CHANNEL STIFFENERS WERE ADDED TO AS 501 ON THE PAD. DAMPING MATERIAL AND A SOFTWARE "REASONABLENESS" TEST WERE ADDED LATER IN THE PROGRAM. | LARGE GUIDANCE ERRORS THAT COULD CAUSE LOSS OF LUNAR MISSION. |
| SATURN V DTV | DESIGN DEFICIENCY IN THE CSM INTERFACE. THE SINGLE TORSIONAL SWAY BRACE PRODUCED UNPREDICTED HIGH COUPLING BETWEEN COMMAND MODULE TORSIONAL MOTION AND S-1C ENGINE DEFLECTION. | ADDITIONAL TORSIONAL SWAY BRACES WERE INSTALLED ON AS 501 ON THE PAD. SUBSEQUENTLY, THE F 1 ENGINES WERE REORIFICED TO REDUCE LOADS AT ENGINE CUTOFF. AN ENGINE PRECANT PROGRAM WAS IMPLEMENTED TO MAINTAIN STRUCTURAL INTEGRITY IN CASE OF ENGINE OUT. | STRUCTURAL FAILURE OF THE CSM INTERFACE WITH LOSS OF VEHICLE AND POSSIBLE CREW LOSS. |
| SATURN V DTV | DESIGN DEFICIENCY IN THE SPS TANK SUPPORTS. UNEXPECTEDLY HIGH LOCAL RESONANT COUPLING WAS DETECTED BETWEEN SPS TANK AND BULKHEAD SUPPORT. | THE UPPER SUPPORT BRACKET FOR THE SPS TANKS WAS REDESIGNED TO ELIMINATE A STRONG TANK CANTILEVER MODE. | HARDWARE FAILURE RESULTING IN LOSS OF MISSION AND POSSIBLE CREW LOSS. |
| SATURN V DTV | HIGH LOX AND FUEL DYNAMIC TANK BOTTOM PRESSURES. THESE PRESSURES WERE UNDER PREDICTED BY A FACTOR OF 2. THE SIGNIFICANCE OF THESE PRESSURES WAS NOT UNDERSTOOD UNTIL AFTER POGO OCCURRED ON AS 502. | THE HIGHER TANK PRESSURES CONTRIBUTED TO THE S 1C POGO. | POTENTIAL LOSS OF VEHICLE AND CREW DUE TO POGO. |

TABLE 6. (Continued)

| TEST PROGRAM | PROBLEMS DISCOVERED | HARDWARE IMPACTED | CONSEQUENCES IF NOT DISCOVERED |
|---|---|---|---|
| SATURN V DTV | HIGH 18 HZ S–1C CROSSBEAM MODE GAINS. DTV DATA SHOWED THAT AN ACCUMULATOR SHOULD NOT BE USED ON THE INBOARD ENGINE. | ELIMINATION OF A PLANNED INBOARD ENGINE ACCUMULATOR. | POTENTIAL LOSS OF VEHICLE AND CREW DUE TO POGO BETWEEN AN 18 HZ ACCUMULATOR MODE AND THE 18 HZ CROSSBEAM MODE. |
| SATURN V SHORT STACK | STRONG PITCH/LONGITUDINAL COUPLING CAUSED BY THE LUNAR MODULE INCREASED THE S–1C POGO GAIN FACTOR BY 30 PERCENT. THIS EFFECT COUPLED WITH THE TANK PRESSURE UNDERPREDICTION WAS THE REASON AS–502 POGO WAS NOT PREDICTED. | DEVELOPMENT AND INSTALLATION OF THE OUTBOARD LOX ACCUMULATORS. | POGO INSTABILITY WITH POTENTIAL LOSS OF VEHICLE AND CREW. |
| SATURN V MINI A/C | THE MECHANISM TRIGGERING S–II POGO WAS DEFINED. COUPLING BETWEEN THE FIRST FOUR LOX TANK HYDROELASTIC MODES WHEN THEY COALESCED WITH THE 16 HZ CENTER ENGINE CROSSBEAM MODE PRODUCED THE POGO INSTABILITIES. | AN ACCUMULATOR WAS DEVELOPED FOR THE CENTER ENGINE. A BACK–UP CUTOFF SYSTEM WAS ALSO DEVELOPED. THE ACCURATE MATH MODEL DEVELOPED DURING THIS TEST SUPPORTED EXTENSIVE THRUST STRUCTURE DESIGN MODS ON SUBSEQUENT VEHICLES WITHOUT FURTHER TESTING. | POGO INSTABILITY WITH POTENTIAL LOSS OF VEHICLE AND CREW. |
| SKYLAB ATM TEST | STRONG CROSS COUPLING BETWEEN LONGITUDINAL AND LATERAL MOTIONS INDICATED A POSSIBLE STRUCTURAL FAILURE AT S–1C CUTOFF. | A 1–2–2 ENGINE CUTOFF HARDWARE AND SOFTWARE MOD WAS DEVELOPED TO REDUCE THE LONGITUDINAL INPUT TO THE ATM. HARDWARE REDESIGNS WERE LAID OUT IN EASE THEY WERE PROVEN NECESSARY BY FURTHER STUDY. | HARDWARE FAILURE WITH POTENTIAL LOSS OF MISSION. |
| SKYLAB MODAL SURVEY | THE STRONG CROSS COUPLING IN THE ATM PROVED TO BE ATTENUATED RATHER THAN AMPLIFIED BY THE WAY ATM CROSS COUPLING REACTED THRU VEHICLE INTERFACE. | TEST OF THE TOTAL SKYLAB LAUNCH CONFIGURATION PROVED THE 1–2–2 FIX WAS ADEQUATE AND THAT NO HARDWARE CHANGES WERE REQUIRED. | THIS TEST SAVED A POSSIBLE REDESIGN OF THE ATM BY VERIFYING STRUCTURAL INTEGRITY UNDER THE 1–2–2 CUTOFF. |

TABLE 6. (Concluded)

| TEST PROGRAM | PROBLEMS DISCOVERED | HARDWARE IMPACTED | CONSEQUENCES IF NOT DISCOVERED |
|---|---|---|---|
| SHUTTLE MVGVT | SRB MOUNTED RATE GYROS EXHIBITED ABNORMALLY HIGH TRANSFER FUNCTIONS. THE RATE GYROS MOUNTED ON THE FORWARD SRB RING FRAMES RESONATED AT LOCAL FREQUENCIES AND HIGH GAINS, WHICH WERE CRITICAL TO FLIGHT CONTROLS. | STRUCTURAL REDESIGN WAS REQUIRED TO STIFFEN SRB RING FRAME, WHICH REVISED THE LOCAL RESONANT FREQUENCIES AND REDUCED THE GAIN. | FLIGHT CONTROL INABILITY AND POSSIBLE LOSS OF VEHICLE. |
| SHUTTLE MVGVT | AXIAL SSME FREQUENCIES AND MODE SHAPES DID NOT CORRELATE WITH PRETEST ANALYSIS. A HALF SHELL DYNAMIC MATH MODEL USING SYMMETRY WAS USED IN THE PRETEST ANALYSIS. | A NEW THREE DIMENSIONAL ASYMMETRIC MATH MODEL OF THE SSME ENGINES AND THRUST STRUCTURE WAS REQUIRED. NO HARDWARE CHANGES WERE NECESSARY. | POGO STABILITY ANALYSES WOULD HAVE BEEN SUSPECT. |
| SHUTTLE MVGVT | TEST RATE GYRO VALUES SHOWED GREATER RESPONSE VARIATIONS THAN ANALYSIS. RESPONSE VARIATIONS BETWEEN RGA'S WERE MUCH LARGER THAN THOSE USED IN THE ANALYTICAL STUDIES IN DETERMINING THE REDUNDANCY MANAGEMENT (RM) TRIP LEVELS. | RM SOFTWARE TRIP LEVELS AND CYCLE COUNTER LEVELS WERE INCREASED. THE FAULT ISOLATION ROUTINE WAS MODIFIED TO INHIBIT KICKING OUT RGA'S AND ACC'S AFTER FIRST SENSOR FAILURE. (FOR STS-1 FLIGHT ONLY; OTHER FLIGHTS WILL BE EVALUATED.) | FLIGHT CONTROL INSTABILITY AND POSSIBLE LOSS OF VEHICLE. |
| SHUTTLE QUARTER SCALE | INTERNAL SRB PRESSURE EFFECTS ON STIFFNESS OVER PREDICTED. | LOAD IMPACTS WITH MINOR REDESIGN OF INTERFACE BACKUP STRUCTURE. | POTENTIAL FAILURE OF INTERFACE AND LOSS OF VEHICLE. |

TABLE 7. GUIDELINES TO SELECTING ANALYSIS AND TEST APPROACHES (GENERAL)

- MISSION REQUIREMENTS
  - LIFETIME
  - RELIABILITY AND SAFETY (MANNED VERSUS UNMANNED, ETC.)
  - VARIABILITY (PAYLOADS, MISSION PHASES, GROWTHS, ETC.)
  - ACCURACY REQUIREMENTS (FLIGHT MECHANICS, POINTING, ETC.)
  - MANEUVERS, ETC.
  - COSTS AND SCHEDULES
  - COMPLEXITY
- CONFIGURATION CHARACTERISTICS
  - JOINTS AND INTERFACES
  - TYPE OF MATERIALS
  - STATIC AND DYNAMIC COUPLING
  - ENVIRONMENTS
    - THERMAL
    - ACOUSTIC
    - PROPULSION
    - INERTIAL
    - AERODYNAMIC
    - PRESSURES
  - DISCIPLINE INTERACTION
    - STRUCTURAL/PROPULSION
    - STRUCTURAL/CONTROL
    - AEROELASTIC
    - HYDROELASTIC
    - STRUCTURAL/FLIGHT MECHANICS/CONTROL/THERMAL
  - SENSITIVITY OF DYNAMIC CHARACTERISTICS TO ELEMENT AND SUBSYSTEM CHANGES
- TOOLS AVAILABILITY
  - ANALYSIS
  - TESTING
    - MODAL
    - ELEMENT
    - FULL SCALE
- DESIGN REQUIREMENTS
  - DATA SCHEDULE
  - HARDWARE AVAILABILITY
  - ACCURACIES
- ORGANIZATION COMPLEXITY
  - NUMBER OF INDEPENDENT ORGANIZATIONS DESIGNING VARIOUS ELEMENTS
  - ORGANIZATION LOCATION
  - ORGANIZATION PHILOSOPHY

TABLE 8. CONCERNS

- LIMITED TO SELECTED MODES ONLY (SMALL NUMBER, NOT ALL MODES).
- SIZE AND COST OF FULL SCALE TEST PROGRAMS ARE NEARING THE PROHIBITIVE STAGE, PARTICULARLY ZERO G EFFECTS IN 1 G ENVIRONMENT.
- ABILITY TO SIMULATE ENVIRONMENT IS WEAK OR NONEXISTENT. TESTING IS VALID WHERE THE ENVIRONMENT IS NOT INFLUENTIAL TO MODAL CHARACTERIZATION.
- SELECTION OF MODES IN HIGH MODAL DENSITY DURING TESTING.
- QUANTIFYING OF CONSTRAINTS AND BOUNDARY CONDITIONS.
- SCALE MODEL MANUFACTURING TOLERANCE REQUIREMENTS. ZERO G SIMULATION.
- ACCURATE CRITERIA FOR MODAL GOODNESS, PARTICULARLY NONLINEAR SYSTEMS.
- SCALING LAWS BETWEEN DIFFERENT SYSTEMS NOT THE SAME; ELIMINATING COUPLING EFFECTS IN SCALE MODELING.
- CONTROL OF HARDWARE CONFIGURATION TO INSURE ADEQUACY.
- MEANS OF INSURING UNKNOWNS ARE FOUND.
- DEFINITION OF EXCITATION AND OTHER FORCES REQUIRED.

SRB reentry. The first step towards resolving this problem was to analytically predict results in conjunction with scale model wind tunnel tests and 2-D water flow tests. Table 9 lists the problem solution tasks pursued. Figure 106 shows the effects of the large angles of attack produced in the water flow test.

These angles of attack expected during reentry introduce large cross flows which create a hydraulic jump (shock) and a shear layer. Carrying this information to the three-dimensional SRB during reentry and conducting analytical analysis, it was found that there existed an oscillating shear layer off the nozzle lip coupling with the basic acoustical cavity mode of the internal motor cavity. At certain Mach numbers, these modes are in resonance. Figure 107 depicts the basic phenomenon.

A plot of the longitudinal SRB cavity acoustical modes are plotted as solid lines on Figure 108. The nozzle shear layer excitation modes (sharp edge created) are illustrated as dotted lines. Notice the resonance for K = 3 and the M = 1 modes at a local Mach number of approximately 0.6.

These modes were verified in MSFC's 14-in. wind tunnel, the AEDC tunnel, and Ames using a larger model. At the same time, many means for reducing the environments were investigated. Figure 109 shows the environment as a function of angle of attack with and without the nozzle thermal curtain, showing that the curtain reduced the environments. This led to the preliminary requirement that the thermal curtain must survive reentry. Later studies have eliminated this requirement.

TABLE 9. SRB REENTRY ACOUSTICS-FLUCTUATING PRESSURES

- ANALYTICAL PREDICTIONS BASED ON LOCALIZED FLOW CONDITIONS
- DEVISED & CONDUCTED SCALE MODEL TESTS AT MSFC'S 14 x 14 INCH WIND TUNNEL WITH OLD BASELINE CONFIGURATION
  - PROMPTED REMOVAL OF EXTENDED NOZZLE SECTION
  - PROVIDED INPUTS FOR ACOUSTIC RESPONSE DESIGN/TEST CRITERIA
- VERIFIED TRENDS VIA LARGER MODEL & EXPANDED TEST CONDITIONS AT AEDC
- NOTED SEVERE ACOUSTIC DISCRETES ASSOCIATED WITH MOTOR CAVITY RESPONSE* USE WATER TABLE TO INVESTIGATE*
- CONSIDERED TRAJECTORY STATISTICS & ENVIRONMENTAL ZONING FOR RESPONSE CRITERIA UPDATE
- DESIGNED & TESTED VARIOUS AERO–FIX CONFIGURATIONS
  - VERIFIED ACOUSTICAL NEED FOR A FLEXIBLE HEAT SHIELD
  - ESTABLISHED BLAST SHIELD EFFECT
- PREPARING FOR FLIGHT ENVIRONMENTAL VERIFICATION TEST AT AMES WITH REVISED BASELINE & A FIX CANDIDATE

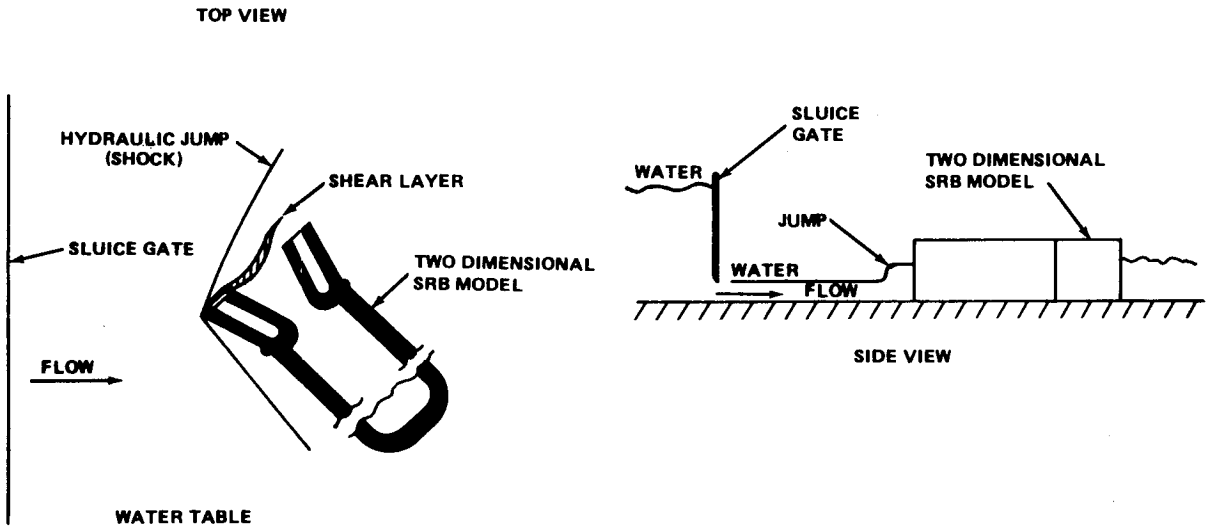


Figure 106. Water table test setup and results.

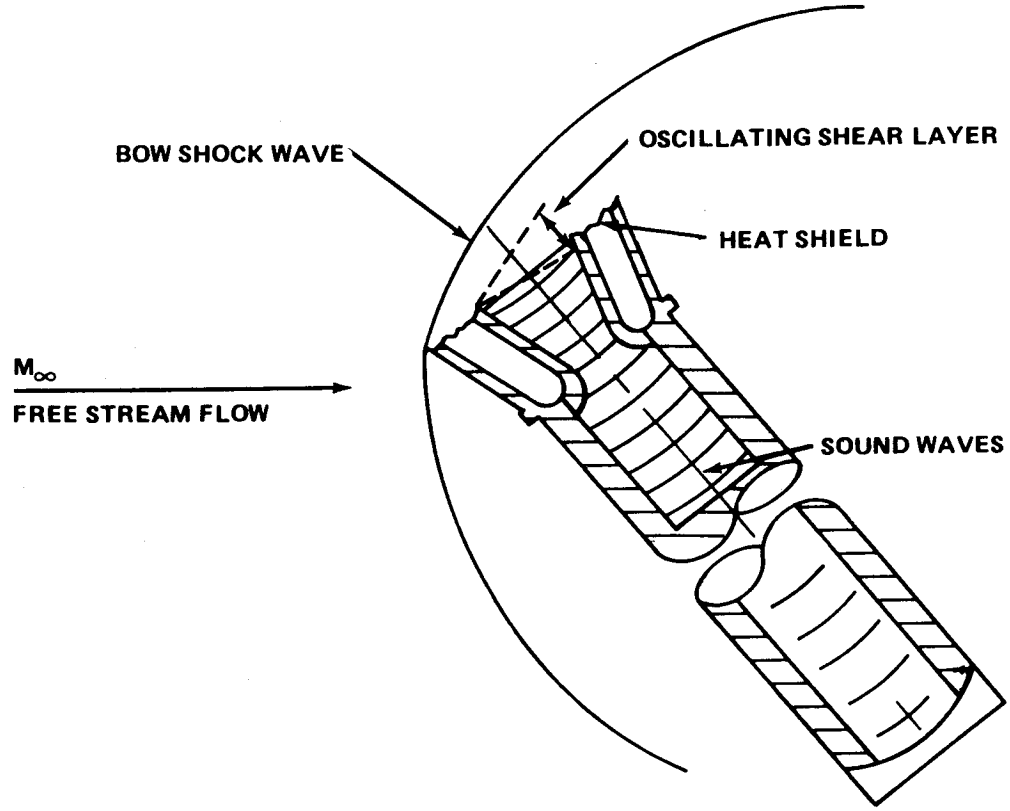


Figure 107. Resonance modes.

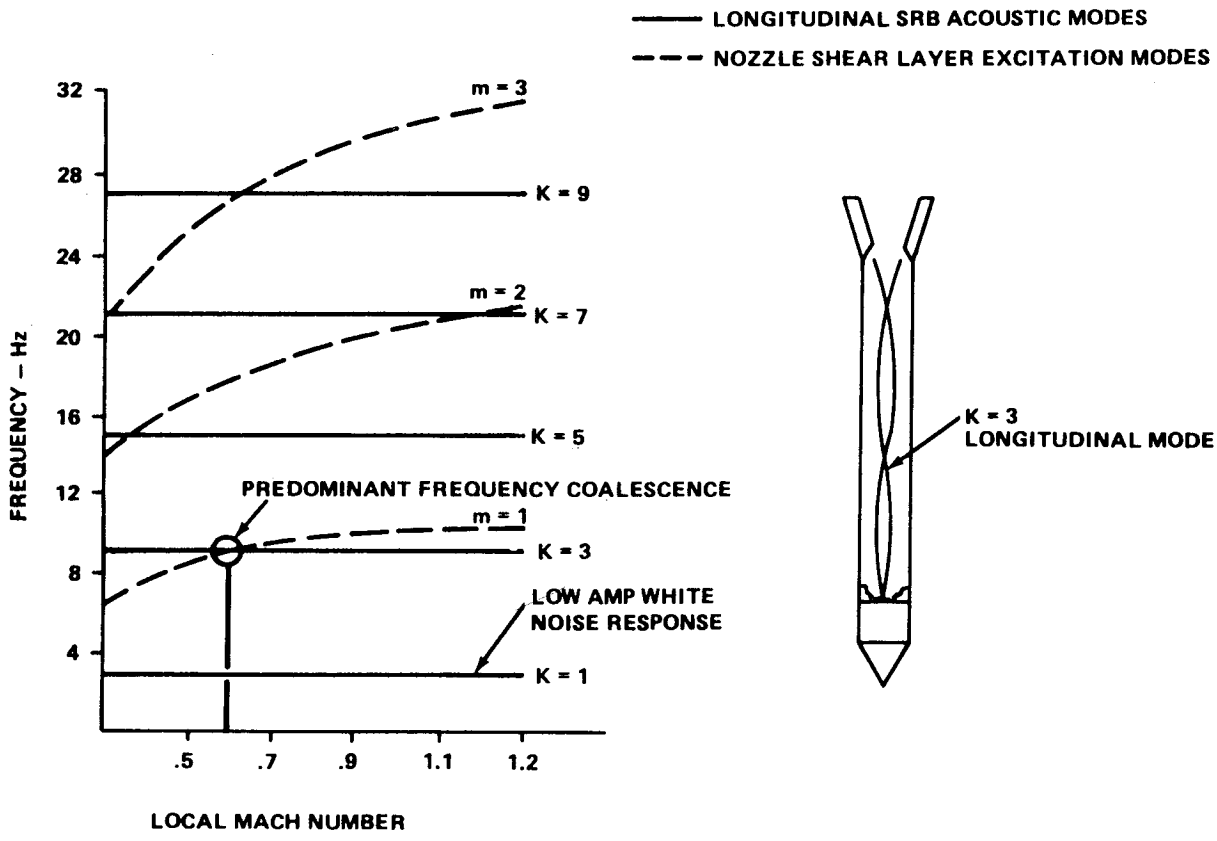


Figure 108. SRB motor frequency prediction model.

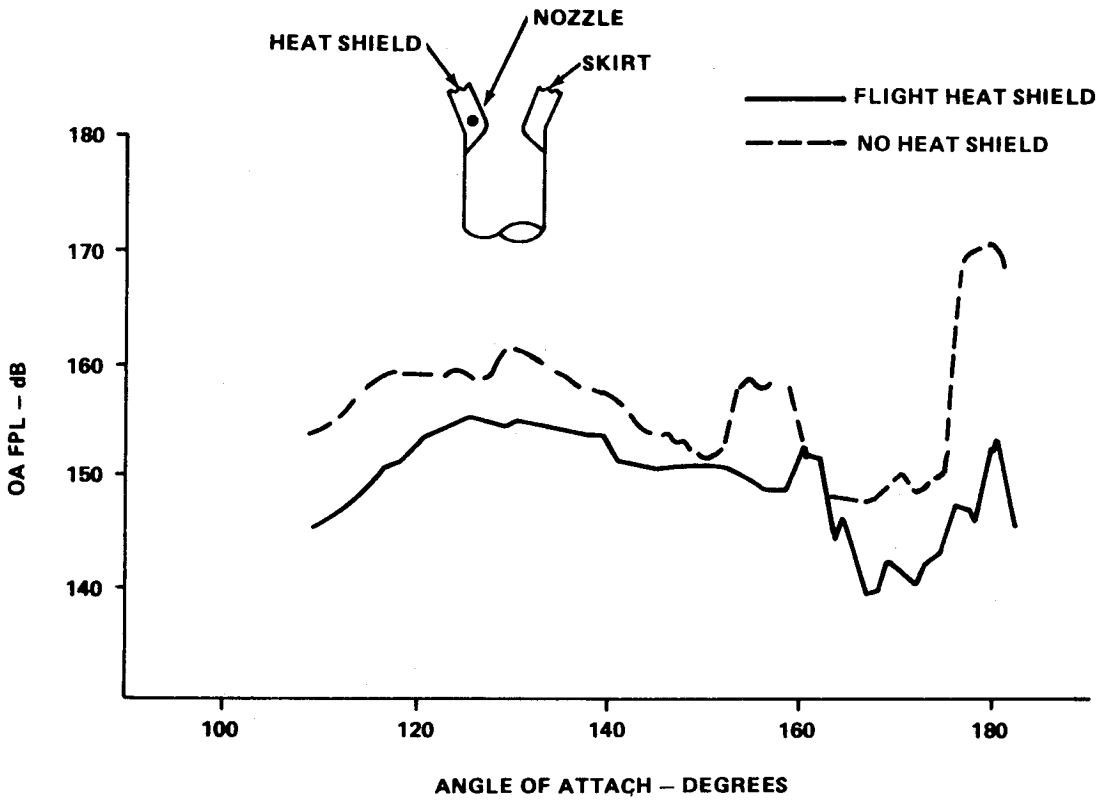


Figure 109. Environment as a function of angle of attack.

In addition to this requirement, it was decided to develop envelopes as a function of probability of the reentry conditions (angle of attack and q) as a function of Mach number using a Monte Carlo analysis. Key parameters which varied were the aerodynamic characteristics, SRB separation-induced initial conditions, and vehicle center of gravity.

Special wind tunnel tests were run for these various orientations of SRB roll angle conditions to define the aerodynamic data base. The simulation developed for the trajectory response was quite detailed giving SRB response in pitch, yaw, and roll. Through this systems approach, it was possible to verify the SRB aft components design without redesign and impacts. This problem illustrates the need for the results obtained when key disciplines have good communication and work together on a problem. This same type analysis and working relations were key in developing the parachute (recovery system) and predicting water impact loads. It also clearly shows the high response levels that can occur from modal tuning.

Acoustical tuning also occurs internally in the SRB main cavity. This second SRB acoustical mode tuning has occurred during the later portions of SRB burn (80 to 120 sec). In this case, the normal longitudinal internal cavity acoustical mode was excited and driven by a gap mode associated with the gap and thermal protectors between each segment joint (Fig. 110).

The phenomenon varies from flight to flight due to the small changes in the gap. Resulting vehicle accelerations have not been dangerous but are felt on the total structure including Orbiter. A large statistic. base of response from static firings have been used to quantify the phenomenon. Figure 111 shows analytically how gap size and flow conditions. Although it is probably impossible to predict

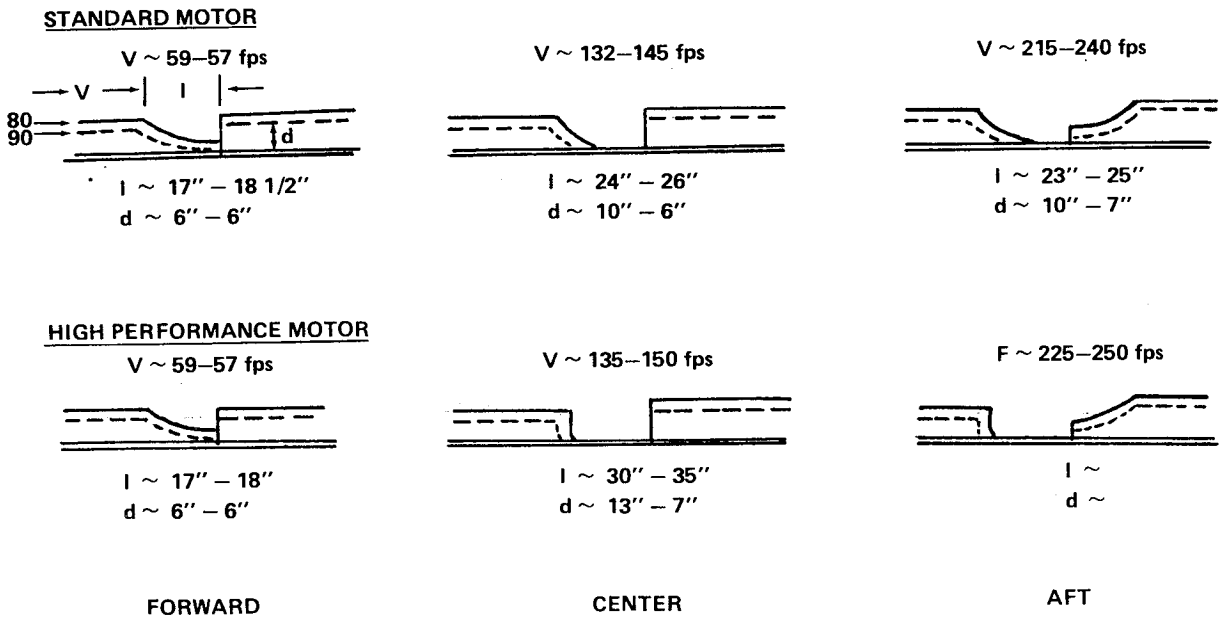


Figure 110. SRM motor segment and cavities.

all possible acoustical tuning conditions, design must be constantly aware of the potential and search out ones that can lead to problems. The next section gives added emphasis to this conclusion discussing two cases that happened to the SSME.

b. SSME Acoustical Cavity Tuning

The SSME has experienced acoustical modes tuning with structural modes. One major engine failure has occurred as a result of this type tuning. This involved the main oxidizer valve (MOV) which caught fire due to the high acoustical energy inducing high thermal loads on the valve seal. At the time of the initial failure, acoustical tuning was not considered as a probable cause. Flutter created by valve position was the generally accepted cause. Much analysis and extensive ground flow testing of the valve were required to isolate the cause. This was achieved by systematically closing off each internal cavity with putty. The fix was simply to "close" the gap with a filler washer. Figure 112 shows the (MOV) location on the engine and where it fits in the flow from the lox pump. Figure 113 shows the basic geometry and two different sleeve configurations showing the gap at the valve to line fitting flange that was the acoustical cavity which caused the problem.

Figure 114 shows how the dynamic pressure at various locations in the lox system responds during hot firing test. Notice the large amplification of the 16N pump induced pressure due to tuning the MOV and downstream at the main combustion chamber inlet. The resulting acceleration of the valve was very large as shown on Figure 115. The phenomenon that occurs is illustrated on Figure 116, which shows how the gap mode tunes with the longitudinal standing wave in the valve sleeve areas.

Much analytical work was accomplished to define these modes and their variations due to manufacturing tolerances. Figure 117 shows these two modes with the potential tuning areas. Shown on the same graph are the results obtained with a blowdown ground test program verifying the cause. The fix was simply a washer put in to the seal cavity (Fig. 118). This fix solved the problem as shown in Figure 119, which is a comparison of the response before and after the fix. No further evidence of MOV tuning has occurred [46,47].

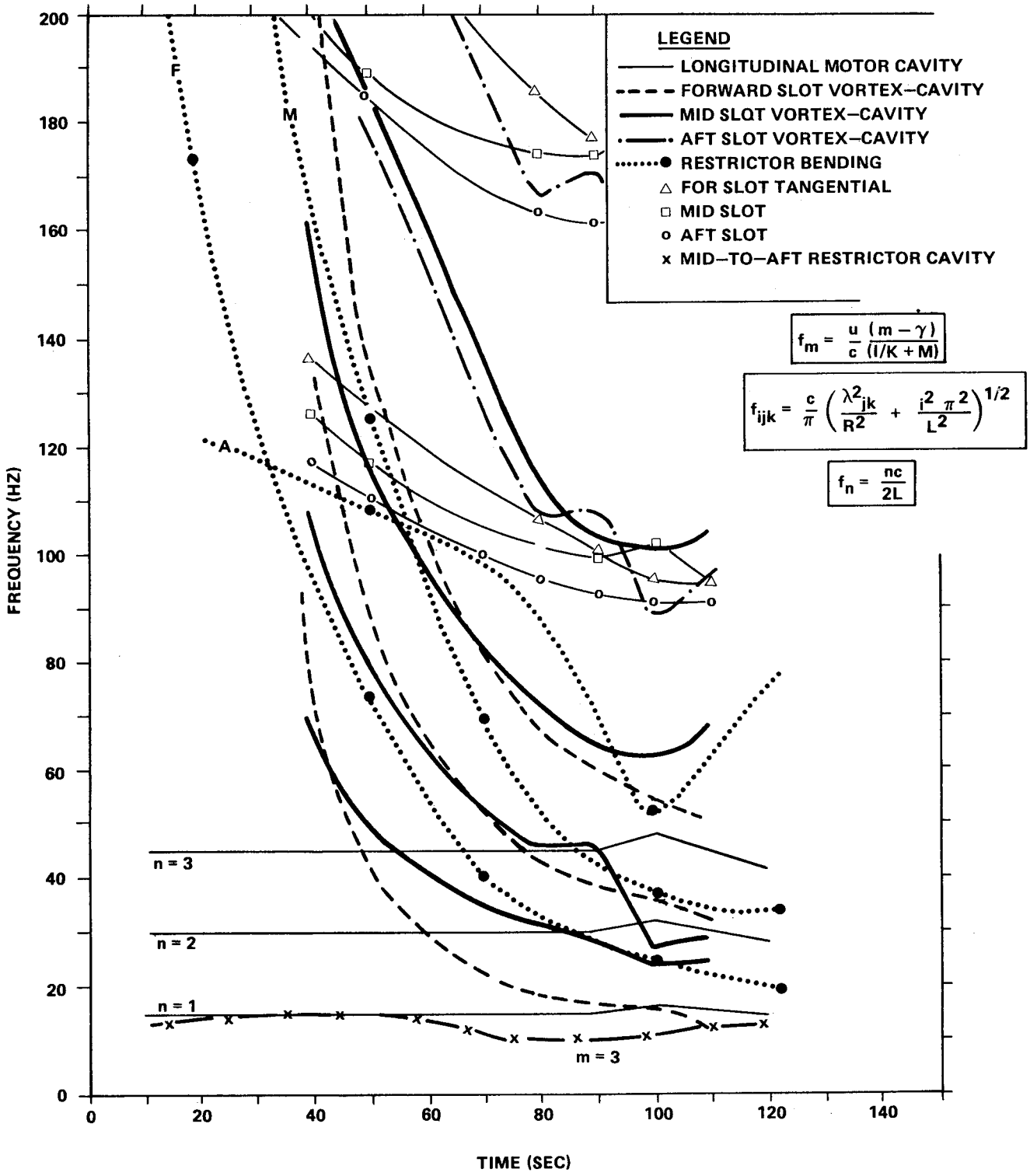


Figure 111. Segment gap longitudinal motor cavity tuning.

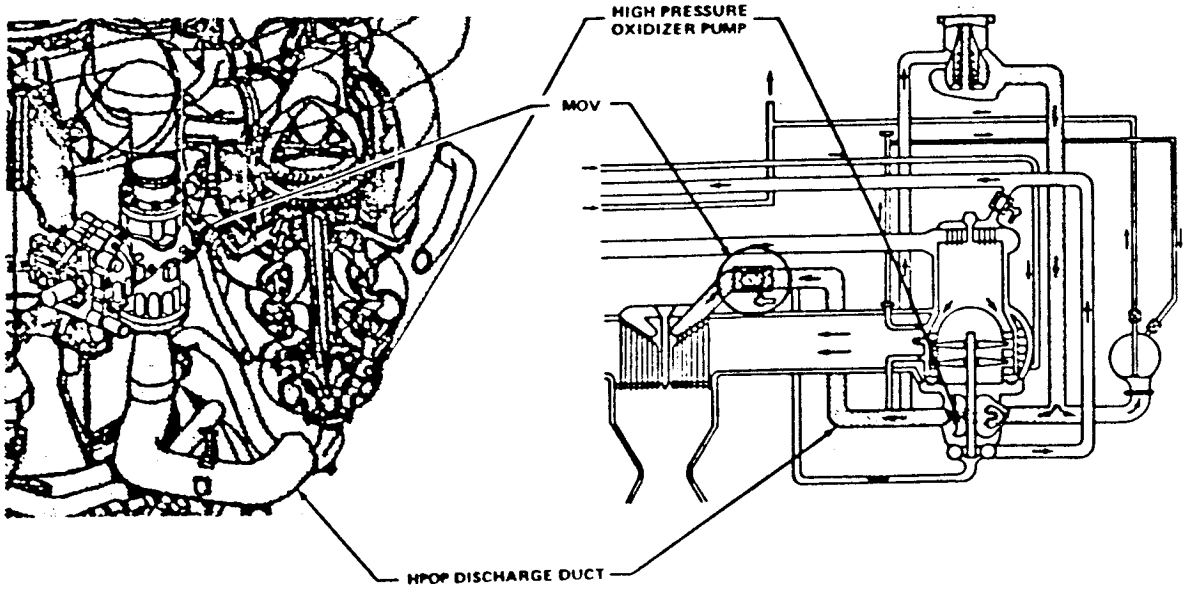


Figure 112. Location and function of main oxidizer valve.

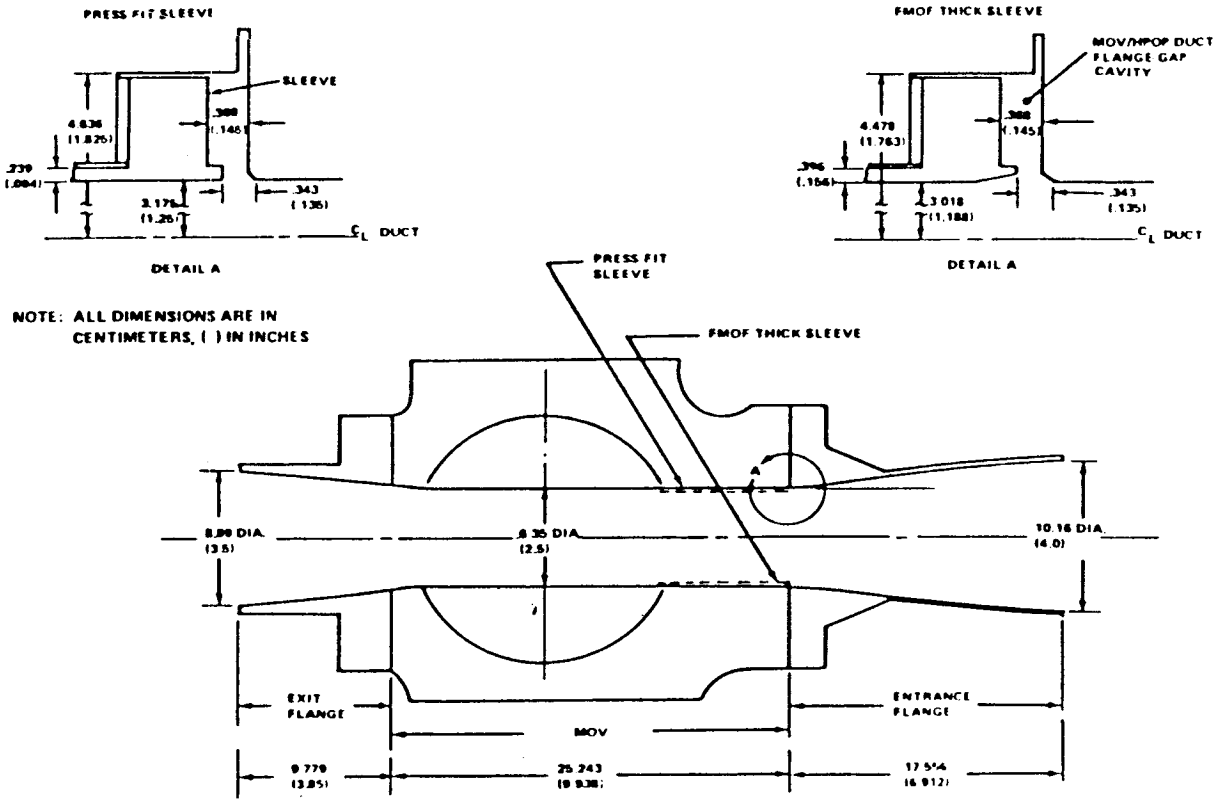


Figure 113. Nominal dimensions associated with main oxidizer valve.

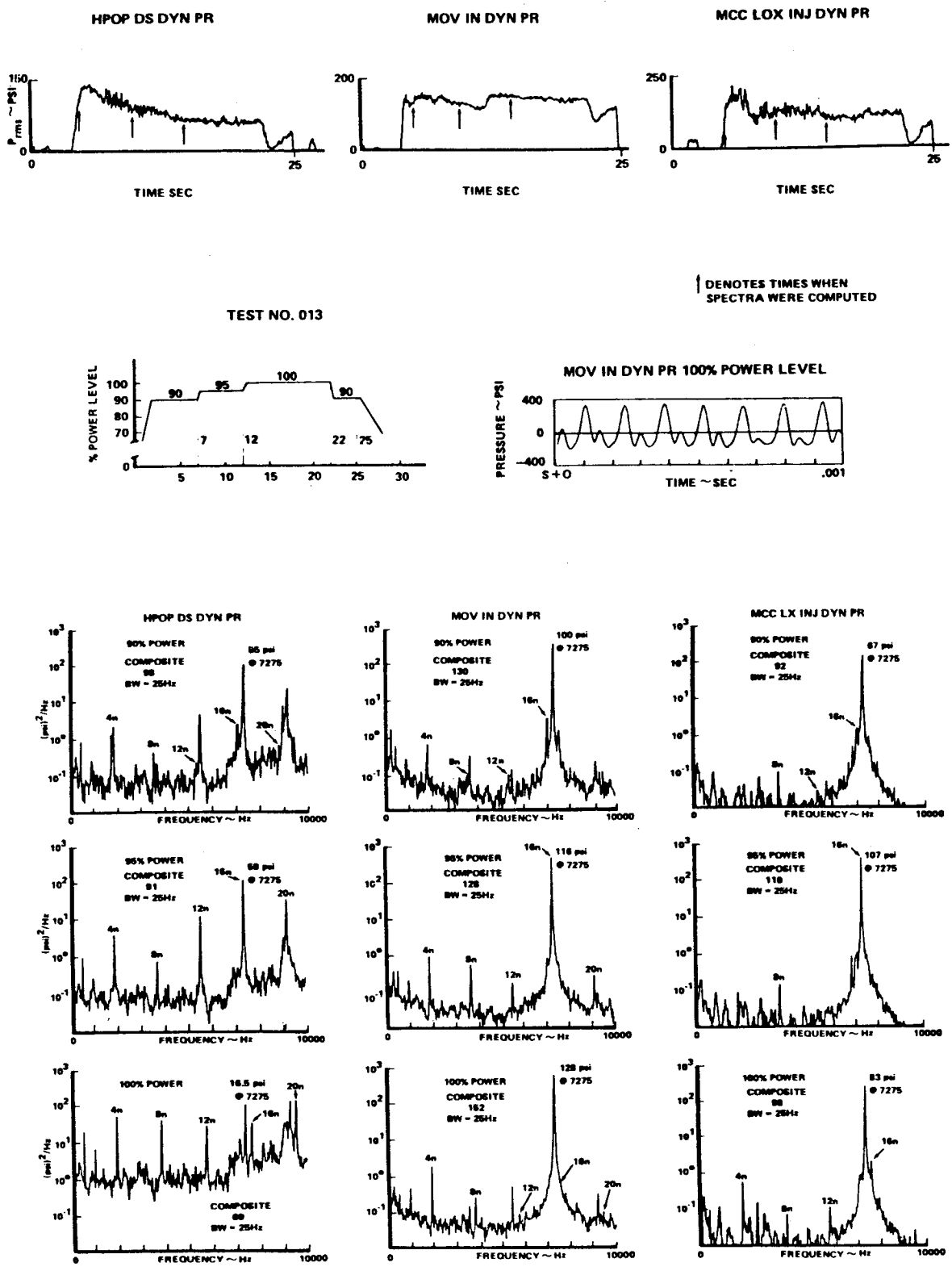


Figure 114. Typical fluctuating pressure spectral distribution (Test 013).

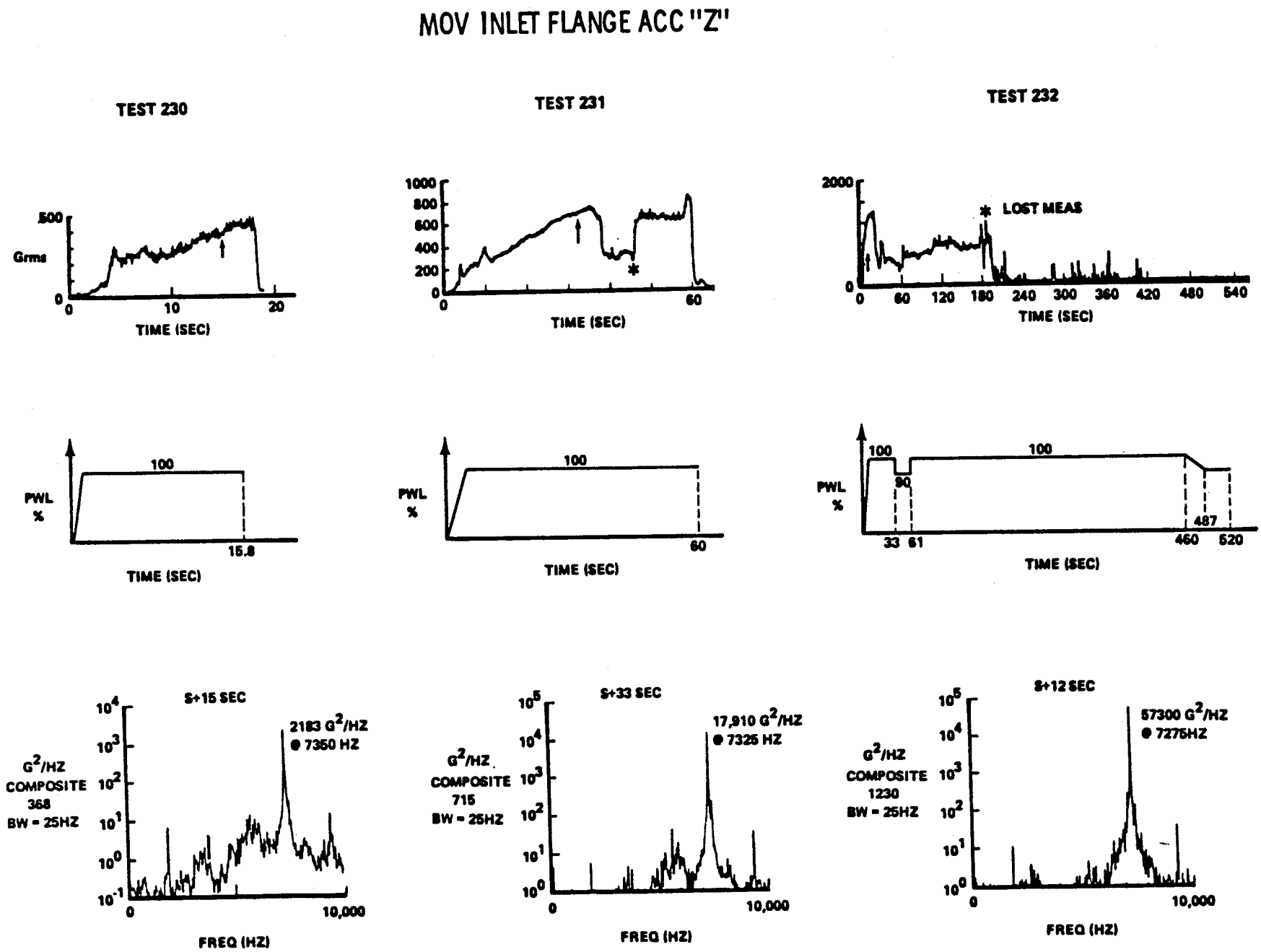


Figure 115. Variation in g-level from test to test.

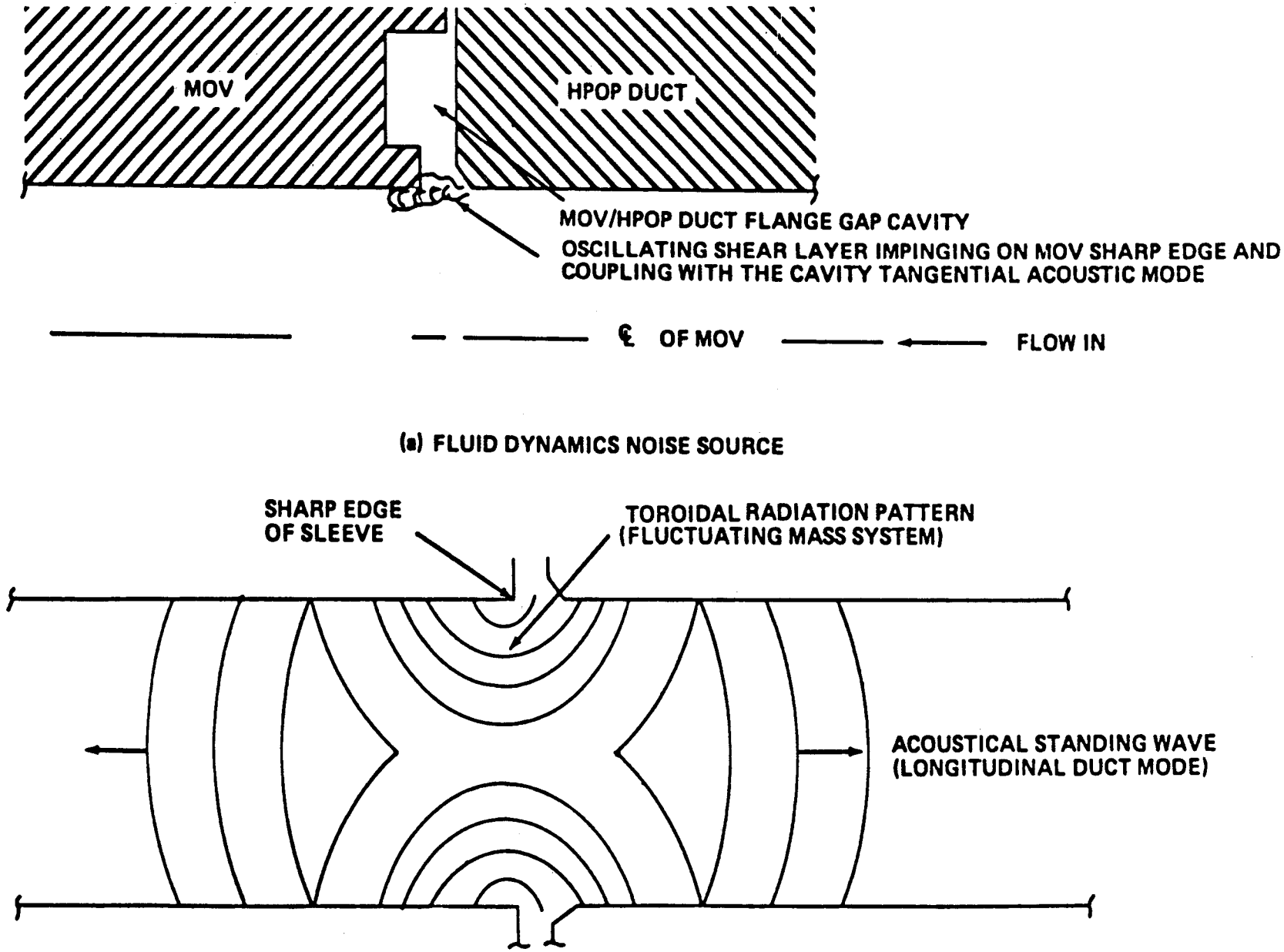


Figure 116. Mechanism relating to anomalous discrete frequency.

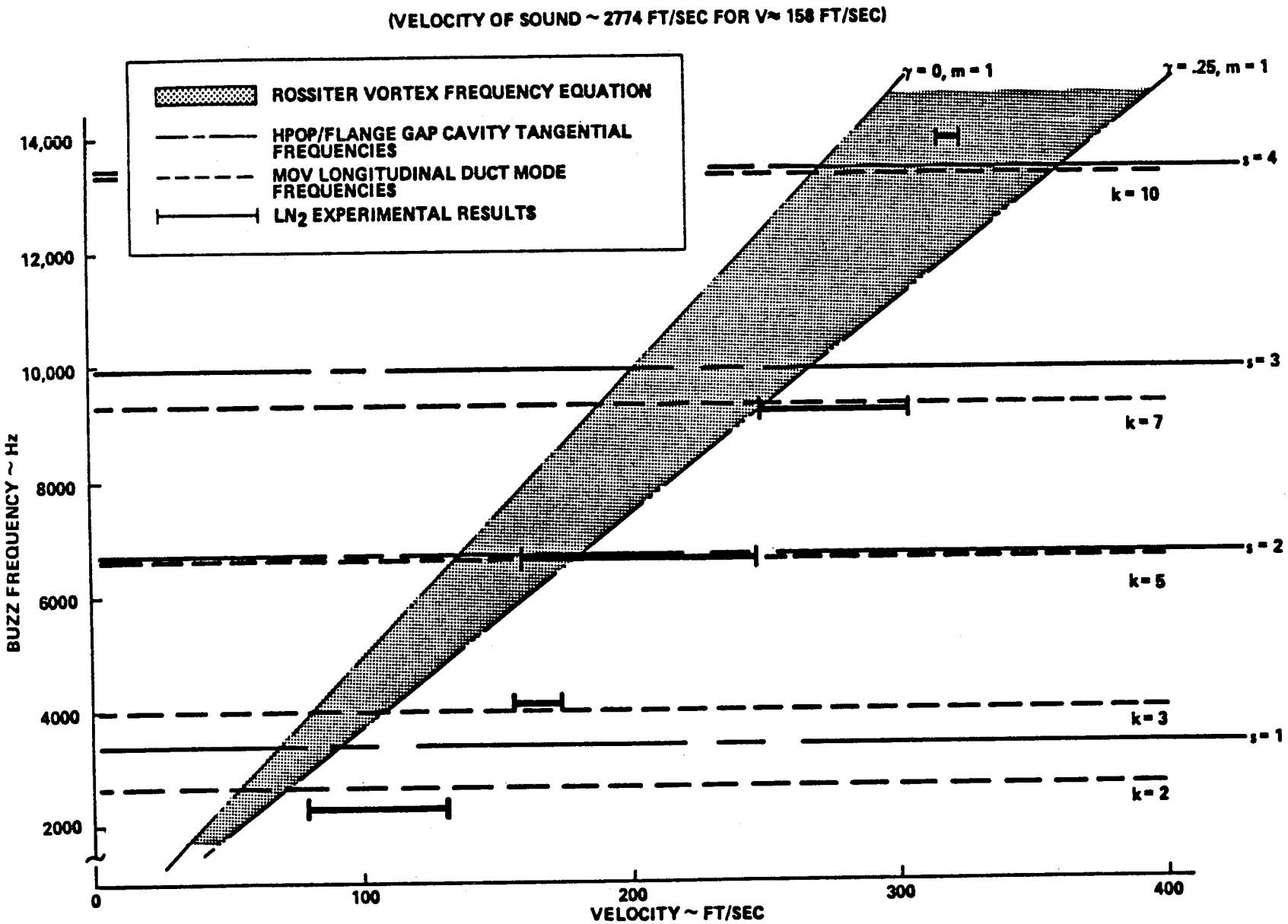


Figure 117. Anomalous discrete frequency mechanism.

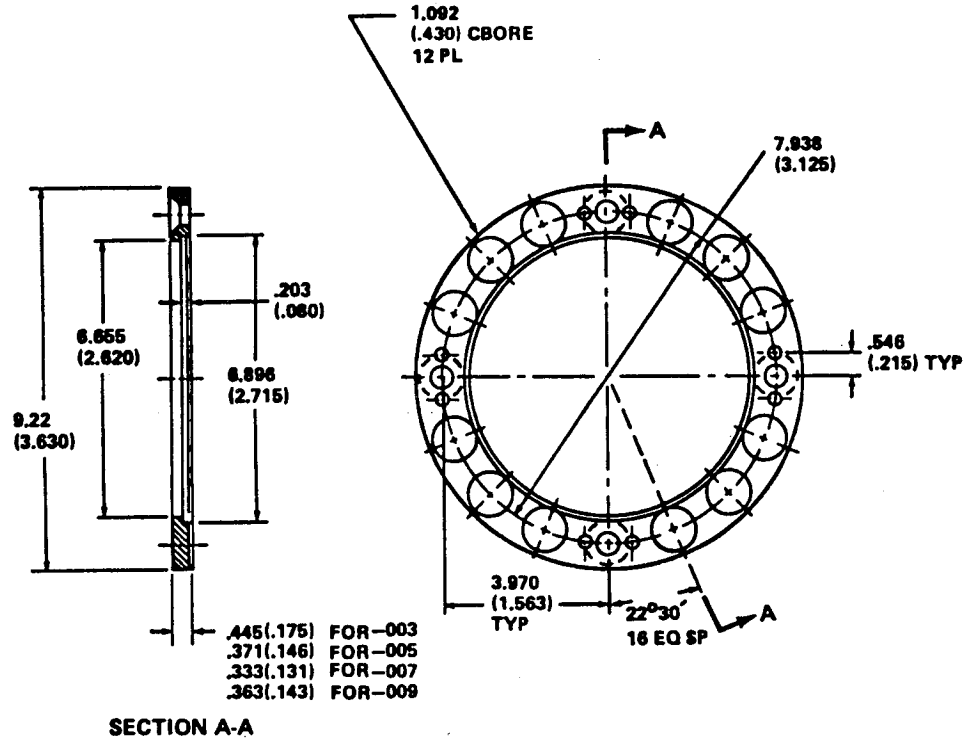


Figure 118. Main oxidizer valve shim fix configurations.

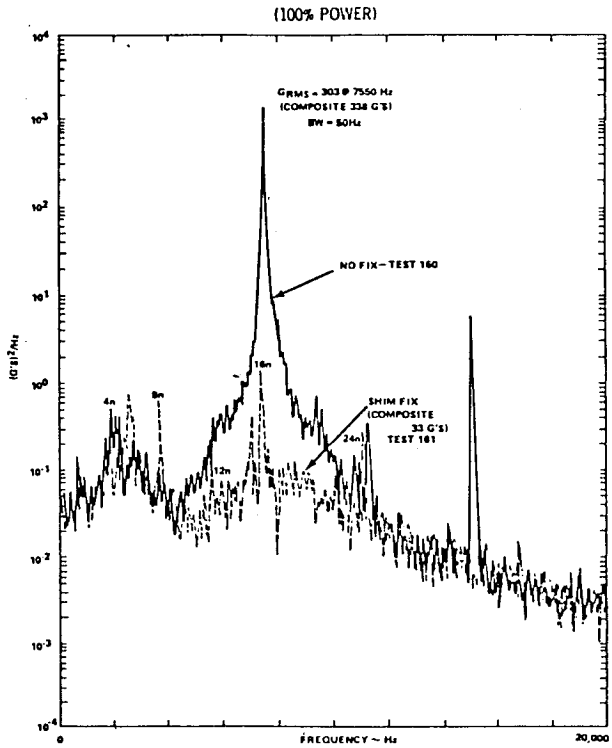


Figure 119. Comparison of hot firing axial accelerometer with and without fix.

The second failure involving dynamic tuning did not involve the total engine, but only the fuel preburner oxidizer system ASI line and orifice which failed. Figure 120 shows the flow and where the failure occurred.

The problem occurs at shutdown when the engine is chugging, sucking hot gas and hydrogen into the ASI line just above the igniter. This gas explosion creates a pressure wave. This pressure wave is doubled at the orifice, failing the part and in one case the liner. The pressure wave varies substantially from one shutdown to the other depending on the amount and mixture of the gas sucked up into the line.

The fix was very simple: Change the shutdown purge to eliminate the gas backflow. As an added precaution until ground hot firing test verified the changed purge, the ASI line was also wrapped with a fiber and epoxied. No further incident has occurred in ground testing or on Shuttle flights.

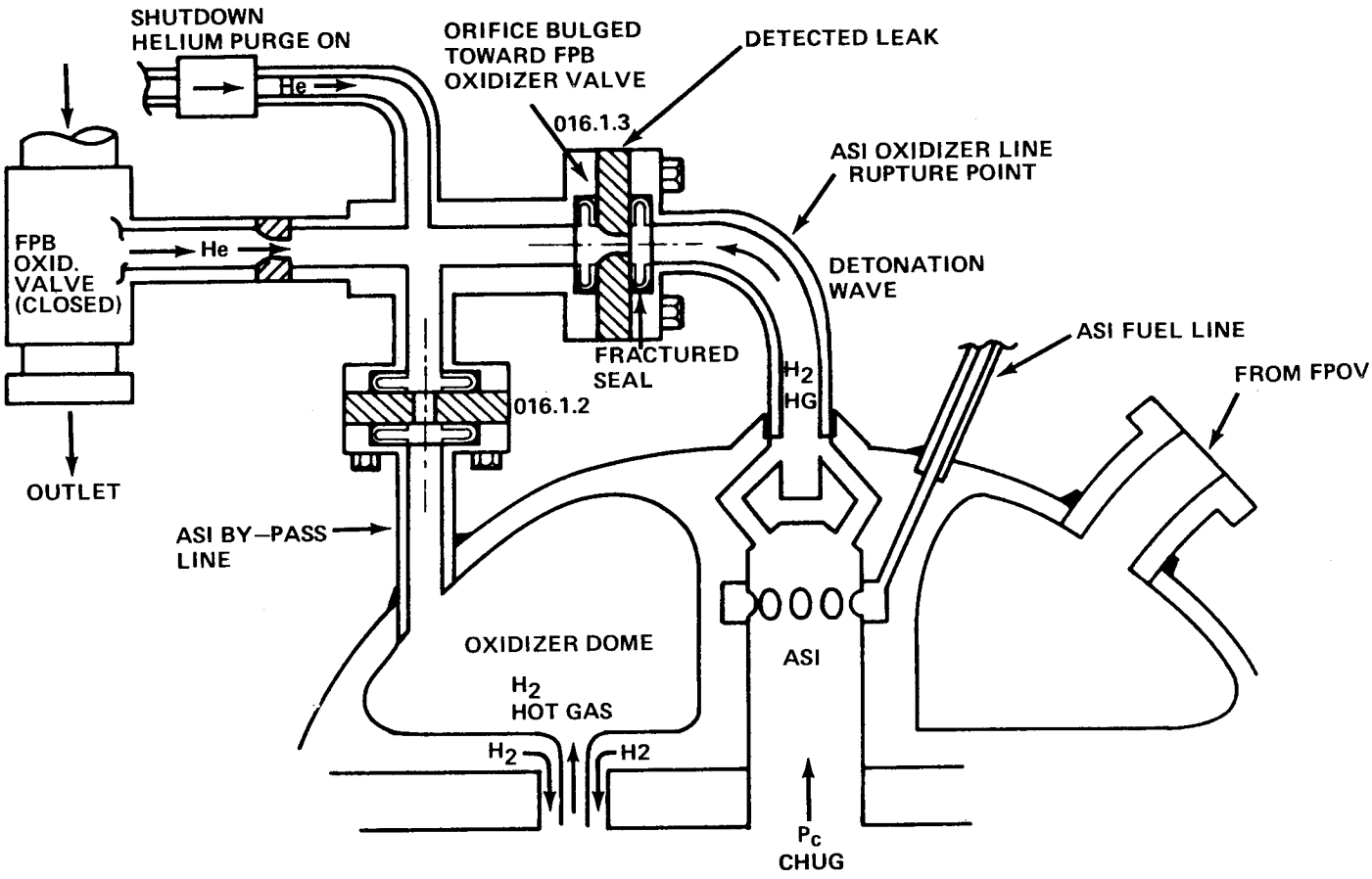


Figure 120. Fuel preburner oxidizer system.

### E. Modal Tuning

Modal tuning changes drastically the system response when lightly damped element modes tune or detune. Previous sections discussed how these tunings change payload and systems loads by several factors. The same was true for the G-switch early signal on the SRB parachute system and the Viking payload simulator discussed earlier.

## 1. ET Lox Tank Tuning

One very interesting problem of this type occurred during the lox tank hydroelastic dynamic testing of the ET. The damping of the second $LO_2$ tank bulge mode varied up to an order of magnitude depending on the fill level and tank tilt angle (Fig. 121). The complete explanation of modes which tuned has not been formulated; however, the results were very clear. Many special tests were run to determine if something in the test setup was the culprit. Nothing was found. It was finally decided that the full scale Shuttle system test would be used as a final verification of this effect and determine the damping to be used for system analysis. The full scale system test verified the full scale lox tank test values showing the effect was real. Since the Shuttle has an excellent pogo suppression system, the low damping values were of no consequence. The lesson: One must be ready at all times for surprises and problems in verification testing that takes time and effort to verify and understand [61].

## 2. Saturn I Tank Coupling

The Saturn I and Saturn IB were clustered configurations of Redstone and Jupiter sized tanks, eight tanks surrounding one. The thrust frame coupled them at the rear and a spider beam coupled the tanks at the tip. This type configuration presented the structural dynamic modeler and the control analysts many new problems. The clustered tank with the spider beam at the top was a nightmare for basic beam analysis. Also, basic unsymmetrical pitch modes between the clustered tanks coupled into roll. Also, the sloshing in the outer tanks coupled into the vehicle roll control. Modeling of the structure required innovative ideas such as calculating pin fixed outer ring tank bending modes, spider beam modes, and modes of the center tank and upper stages and coupling them together. The technique used was what is known today as modal coupling. In order to calculate the spider beam modes, a crude type of finite element analysis was used. Many modes had to be calculated and used in loads and control analysis due to the many dynamic possibilities between the nine tank elements, thrust frame, and spider beam, greatly increasing the computational effort, analysis complexity, and analysis time. Dynamic tuning between similar elements are very complex and has led to most of the modeling problems encountered.

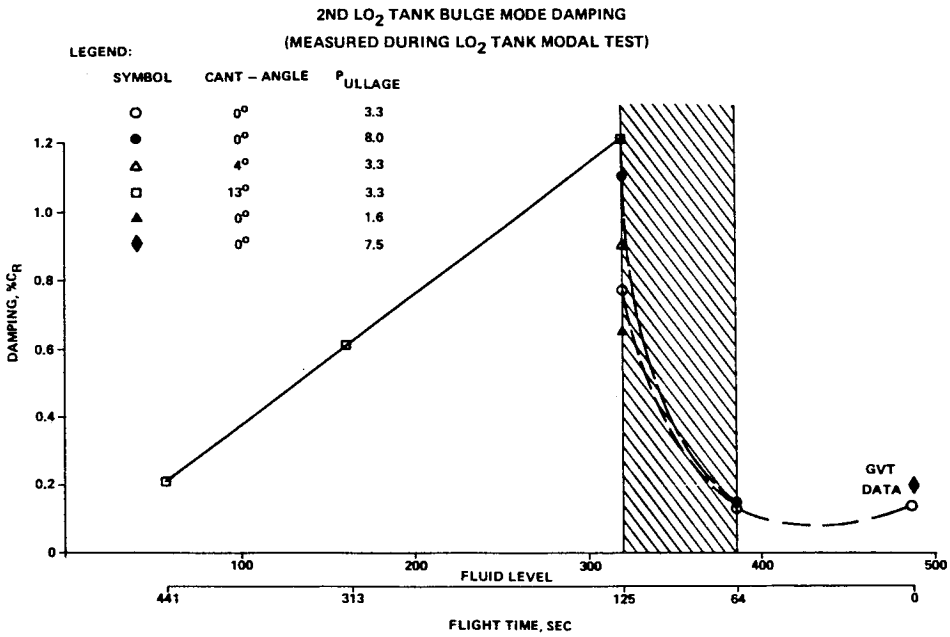


Figure 121. ET hydroelastic mode damping.

## F. Manufacturing and Quality

Manufacturing procedures and quality control are fundamental to good design and acceptable hardware. Several problems discussed previously have their sensitivity rooted in manufacturing tolerances; namely, high pressure engine pump whirl and imbalance, the MOV seal failure and the SRB nozzle erosion. Two other engine problems have occurred in this area, one leading to an engine failure and the other a continuous area of engineering assessment. The first was a mixup of weld wire that resulted in a steerhorn failure, gutting an engine. The other is weld offsets that occur when welding two line segments.

The weld wire mixup occurred at the vendor, where a small number of a much softer wire out of a specific lot was mixed in with the specified harder wire. Random sampling of the delivered wire was not large enough to catch the error. The result was a fatigue failure of the weld joint on the steerhorn. Rocketdyne had kept a detailed log of each wire used, where used, etc., which allowed assessment and verification of each weld that potentially could have been made with wrong weld rods. No additional damage was experienced; however, laborious activity was required to clear the engines that were affected.

The weld offset problem has resulted in an intensive effort to establish the magnitude of each weld offset and the degradation in capability of each weld. Figure 122 shows a typical line while Figure 123 shows the type of weld offset experienced. Much effort has been required to analytically and experimentally determine actual capabilities of all welded lines on the SSME.

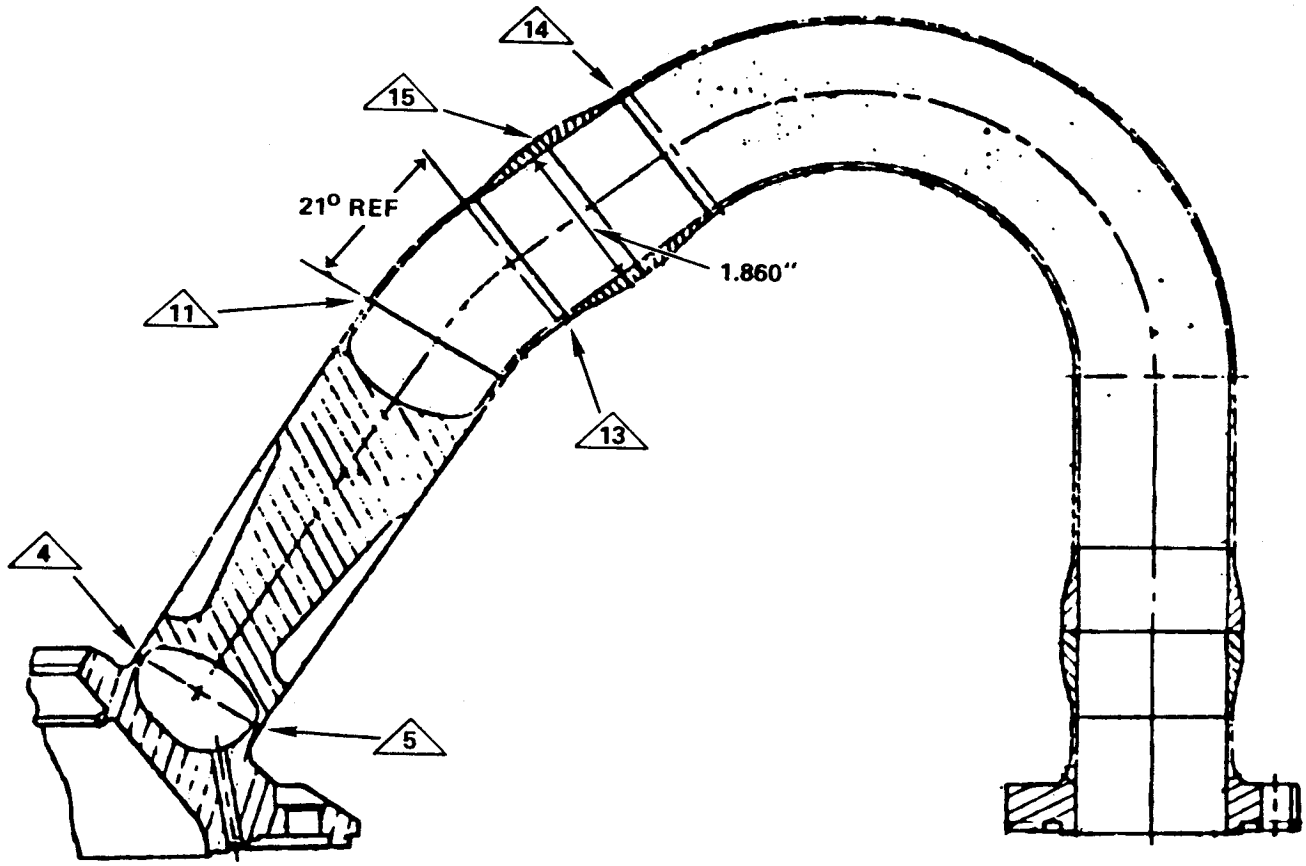


Figure 122. Main combustion chamber inlet weld offset.

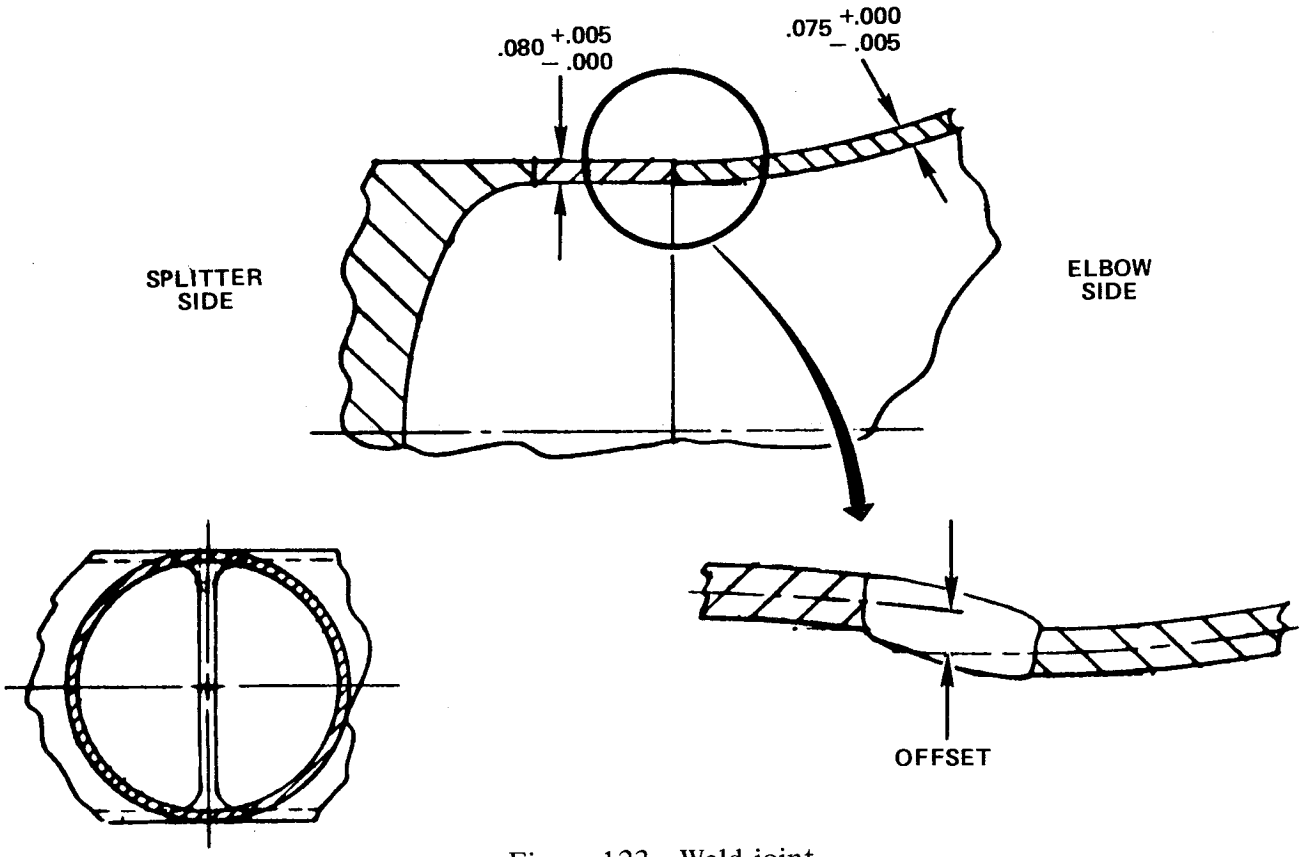


Figure 123. Weld joint.

In summary, the final goodness of the hardware is determined by the manufacturing and quality procedures.

## IV. DYNAMIC PROBLEMS ENVISIONED

Future launch vehicles, payloads, and satellites are expected to have the same type of problems discussed in this report. Engineering attention must be given to each of these potential problems as the system is designed and analyzed.

Orbiting space stations will have many new problems; however, they will still fall into the same categories discussed. In particular, the large size coupled with lighter structure and unique control requirements drive toward a more difficult situation [4, 62-67].

The active control of large flexible structures, such as the Space Station, requires the development and verification of a new technology. At least a major extension of the present separate technologies of structural dynamics and controls is required. The technology arises from the unique requirements of the station that leads to a unique structural configuration, which is unsymmetrical, multi-body, connected through joints with many, very flexible elements, such as solar arrays, that must be oriented in space with certain elements requiring fine pointing and/or shape control. The control system is composed of a myriad of control sensors and actuators located throughout the structure with each, or each subset, having their own specialized design and operational requirements.

This is essentially a unique situation relative to standard control system design practices where, in general, the basic control system could be designed treating the spacecraft as a rigid body, then compensating through filtering to eliminate elastic body feedback. The assumption of rigidity is not a reasonable one for Space Station concepts; therefore, the control system must take on a different form and include elastic body effects, the degree determined by the configuration and operational requirements.

The result of this unique situation is that both the control engineer and the structural dynamicist become a team and, in essence, create a new discipline, "structural control interaction." The new field can be split into the following discipline areas:

1) Analytic modeling and model reduction.

2) System identification.

3) Control-law design methodology.

4) Integrated structure/control design methodology.

5) Sensor and actuator development.

6) Ground testing.

7) On-orbit testing.

The selection of technology drivers and the resulting technology that will determine problems of the future depends on several design philosophies and structural dynamic assumptions. Three design philosophies are generally accepted, which could strongly drive control/structure interaction technology.

1) Design structure in conventional approach using strength as drivers and then design the control system to control it. This approach can lead to a very complex control system, heavier structure, and in some cases, performance compromises. In general, space systems have been designed in this manner.

2) Design system optimally using the control system to augment the structure providing delta damping and stiffness over what is afforded by the structure alone. This approach gives the lightest structure with the highest performance (approach used in certain high performance aircraft design). The major problem is the additional failure modes that are introduced coupled with a more complex control system and design and verification activities.

3) Conventional structural design with minor mods of passive devices and active control to solve problems. Control system is designed to control this basic structural system. This is the least risky approach for current systems which meets basic performance goals without pushing or extending technology limits too far. Planning, discussed later, will use this least risky approach, even though the optimized design philosophy is very appealing to most in the technical fields of control and structures.

The next consideration has to do with the assumption one makes in terms of how well structural dynamic characteristics can be predicted. Figure 124 shows these three assumptions and the advantages and disadvantages in terms of technology. Exact knowledge of the structural dynamic characteristics (Case 1) is obviously desirable since it will lead to a simple control approach and a highly reliable system requiring limited simulation and analysis activities; however, obtaining accurate knowledge of the

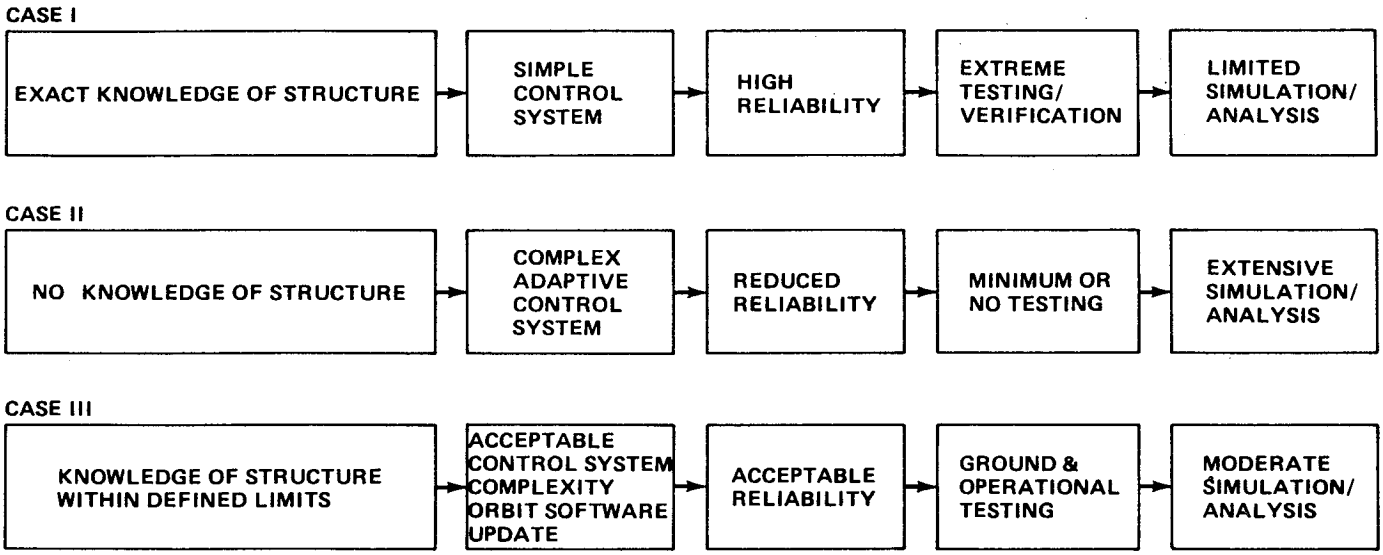


Figure 124. Structural control interaction design approaches.

structure would require extreme testing and verification. Dynamic testing technology would have to be extended in instrumentation, excitation, zero-g simulation test fixtures, and facilities. Even with this technology extension, it is very doubtful that for a Space Station the dynamic characteristics accuracy could ever meet this assumption. The opposite side is to assume that it is not possible to have any knowledge of the structure. In this case (Case II), a learning adaptive control system would be required leading to reduced flexibility, extensive simulation, and analysis task plus extending extensively the control system technology world which may be beyond the realm of possible achievement. These two extremes drive toward the only acceptable approach that appears feasible, which is to define and verify the structural dynamic characteristics within a defined set of limits (Case III). These limits define additional parameters that must be considered in the design and verification process of the system. It would result in a control system with acceptable complexity. The system would have adequate performance with achievable ground and operational testing and moderate simulation/analysis tasks. Taking this approach automatically requires that design and verification analysis techniques be extended to handle large sets of parameter variations. Some extension of control technology and testing technology, including operational testing, on-orbit control software update appears achievable. It should be pointed out that the two extreme assumptions require some analysis to set limits and define evaluation criteria for the chosen set, Case III.

Having chosen assumption 3 as the approach to take raises one additional question which becomes technology selection's driver. Here, the question deals with the form of the structural dynamic model. Figure 125 shows three options. The first option uses a very detailed finite element structural dynamic model which identifies the structural dynamic characteristics using all the resulting modes for control system design activities. This would require development of new control system analysis tools and large amounts of computer time. The question is obviously open as to whether the present tool technology could be extended this far. The next option utilizes a truncated (reduced) large finite element

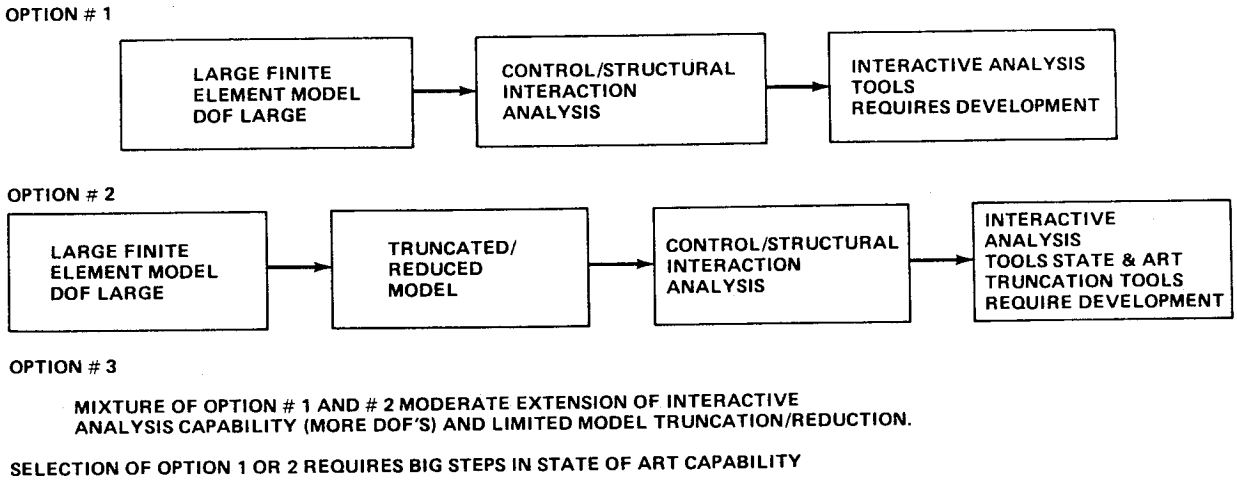


Figure 125. Options for control interactive analysis.

model for the interaction analysis. The truncated model allows use of generally available interaction analysis tools; however, adequate truncation tools require development. Truncation here is defined in a very broad sense. Equivalent models of very limited degrees-of-freedom fit in this category as do the normal modal selection and modal reduction techniques. Option 3 is really a combination of 1 and 2, where a moderate extension is made of the interaction analysis capability and the truncation tools and is the preferable way to go. In any case, as discussed previously, a major problem exists, how to vary modal data inaccuracies (modal parameters) and combine individual modes and other system parameters.

Other questions which influence technology tasks are not as clearly defined as the ones previously discussed. It is not known, for example, whether the Space Station concepts coupled with various performance requirements will drive dynamic characterization and interaction analysis into the nonlinear range or not. It is the current belief that it will not; however, if it does, many technology issues and new problems arise. Figure 126 shows some modeling options that are open for handling this situation. Other approaches and options can probably be developed. It is clear that using a total nonlinear analysis approach is not feasible for most situations. The particular performance situation would dictate whether one would have to drive towards model options 2 or 3. Questions other than nonlinearity will arise as more analysis and concepts are developed.

Several characteristics must be inherent in a ground test program designed to understand and validate this new or expanded area. First and foremost, the program must start with a very simple system and proceed to more complex structural sets with cross coupling and finally evolve to the complex system with overall control, pointing control, and shape control. Figure 127 shows these three general categories of configuration complexity with bubbles indicating the various dynamic and control characteristics that can be investigated. Secondly, the structural and control system models at each level of testing must have considerable flexibility. The structural model must have the ability to vary the modal characteristics; to demonstrate frequency and mode shape uncertainties; and to validate the ability of the control system to handle these variations. Time-varying modal characteristics are also important characteristics to simulate. Third, inclusion of various disturbances and environments, such as man motion, docking, aerodynamics, operation of onboard equipment, etc., is a requirement and can be simulated. The induced response should be characteristic of what is expected on orbit. Fourth, modal coupling, unsymmetrical systems, and modal density are key characteristics to simulate. The actual frequencies and/or bandwidth are not necessary to simulate. Fifth, the individual test articles and the

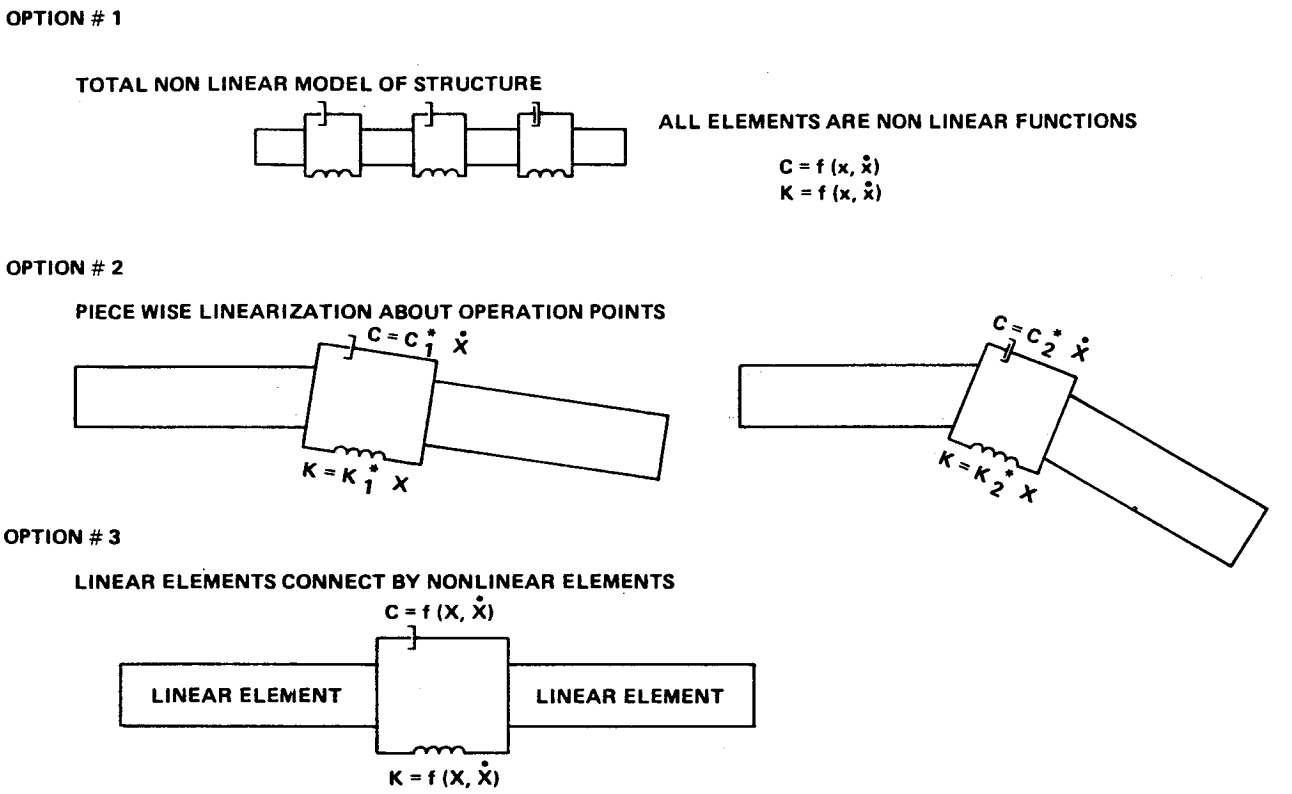


Figure 126. Non-linear/localized damping.

test plan must be constructed such that the article is tested first without control to validate the structural dynamic model before environmental excitation and control feedback tests are run. Validation of basic control loops before closing on the elastic body system is also needed.

The kind of interaction requirements that drive these flexibilities arise from basic operational and performance specifications. Some general ones are (1) orientation and control of the overall Space Station, (2) general pointing of elements, such as solar arrays, (3) fine pointing of elements such as telescopes and antennas, (4) shape control, such as antennas, (5) control and stability overall during reboost and maneuvering, (6) response and load relief control during docking, (7) control of disturbances, such as man motion, (8) configuration growth and assembly. Others probably exist; however, these appear to be the drivers.

The generic validation plan should be evolutionary and phased, starting with simple configurations (Phase I) and building up to the more complex (Phases II and III). Figure 128 is a flow of a Phase I test plan which includes definition of the structural complexity and where available structures could be used. Where no available structure is listed, the hardware would have to be designed and built. The flow starts with a symmetrical constant parameter structure and proceeds through a three-staged tuned structure to a time-varying system. The same sequence is followed for the asymmetric model and test. Phase II has increasing complexity over Phase I and rings out more of the problem areas as well as giving more indepth validation of technology covered in Phase I (Fig. 128). The various characteristics of this article are listed on the chart and include crew motion, larger scale, many symmetrical and antisymmetrical modes, variable frequency, variable damping, etc. Phase III would follow from Phase II adding elements with pointing control requirements. Obviously, in each of these phases, structural model verification would proceed closed loop verification as discussed earlier.

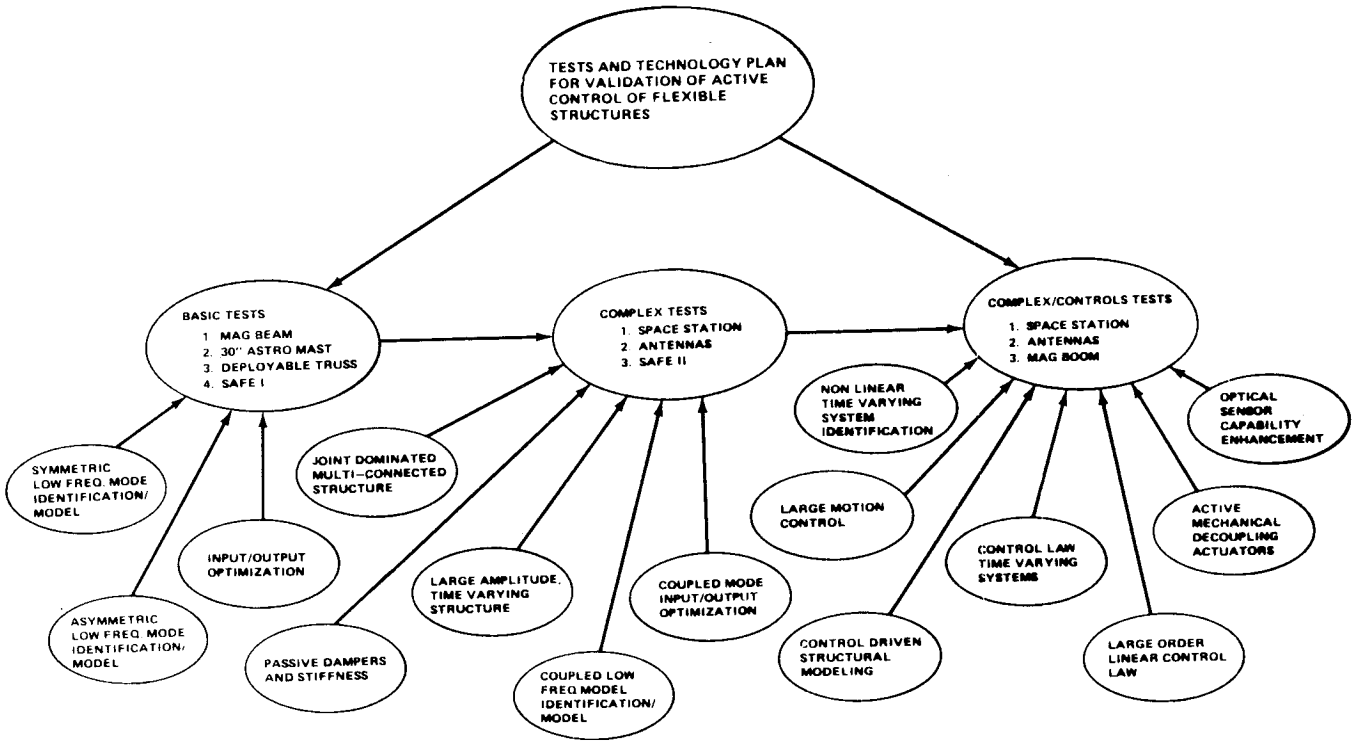


Figure 127. Space Station structural/control interaction ground test plan.

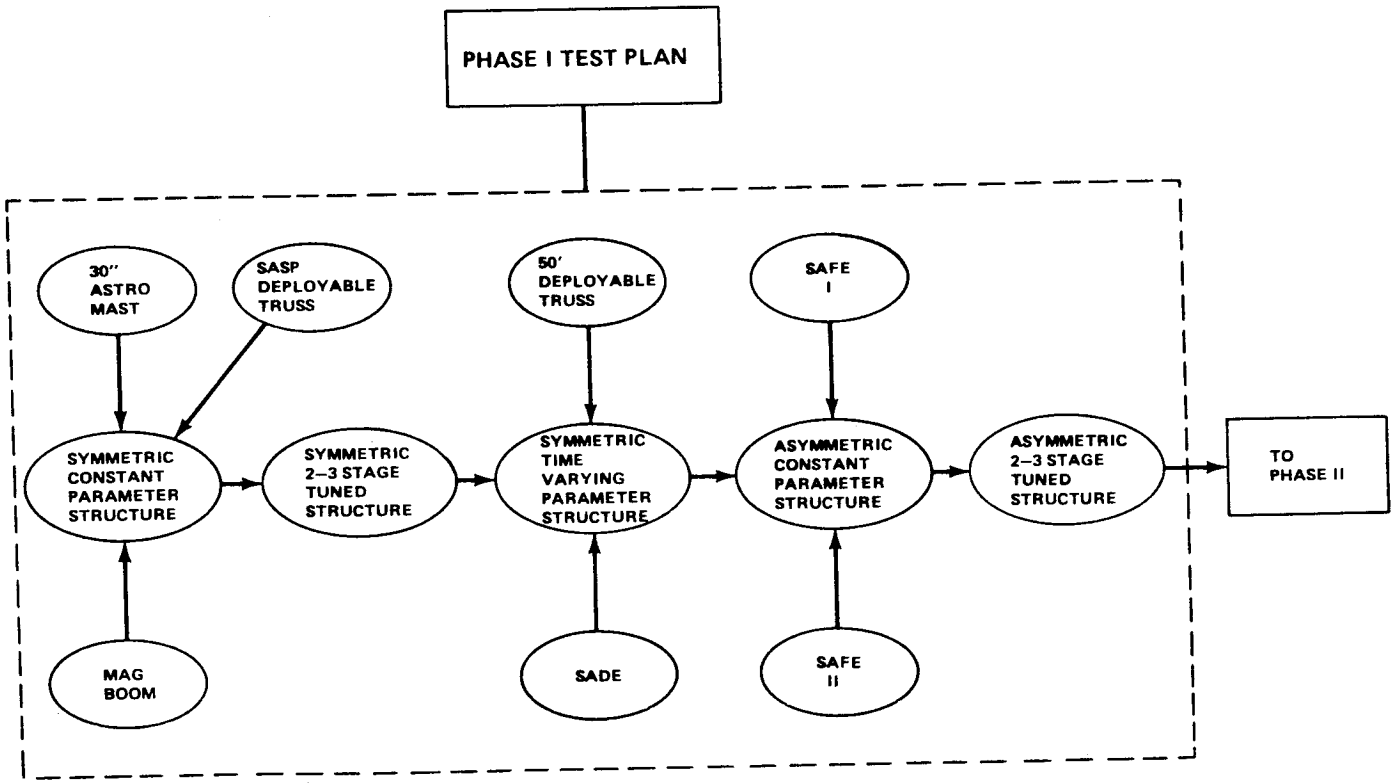


Figure 128. Space Station structural/control interaction ground test plan Phase I.

In summary, the same problem areas are envisioned for future systems; however, they take new forms. In particular, the area of structural control interaction will bring out a different look to these old friends. Thermal effects in this coupling can be large. References 2 and 68 list the technology implications of the Shuttle and other experiences. This list is still valid.

## V. SUMMARY AND LESSONS LEARNED

### Summary

The analysis and the experiencing of dynamic problems are exciting and inspiring work. The frustration of failures not expected are par for the course. Murphy's law seems to reach its pinnacle when dynamics are present. Even though one must learn to live with the unexpected, careful attention to problems of the past allows the purchase of good insurance against problems in the future. This report is a very brief survey of dynamic problems experienced on various space programs carried out by NASA and in particular at MSFC. The references provide additional information; however, much of the data are in the minds of engineers and in their files. Preservation of the information is a major problem. The matrix summarizing the problems by project and discipline provides a quick reference. It is the desire of the authors that somehow this report will eliminate some problems in the future. As a final attempt to accomplish this goal, the summary concludes with a list of lessons learned.

### Lessons Learned

1. Problems anticipated and worked on usually do not happen in operations.

2. Problems anticipated and worked without adequate technology tools cause false security and lead to major operational problems (example, S-IC and S-II pogo).

3. Always do a complete systems analysis, or a change that fixes one problem can lead to another which has greater consequences.

4. Design with as much margin as feasible using the best technical solution in order to reduce the sensitivity to small environmental changes and manufacturing and quality slips.

5. Understand all the system sensitivities, system interactions, and sequences for a sound modeling foundation; otherwise, key problems will be missed leading to major failures or operational problems.

6. Analytical models are only as good as the experimental input data, such as material properties.

7. The goodness of the hardware is determined by the manufacturing and quality procedures. Tolerance criteria should be based on sensitivity analysis.

8. Marginally stable systems are very sensitive to parameter variations and can easily move into unstable regimes.

9. Marginally stable systems near the instability point act like a response limited forced response system.

10. Very accurate definition of all forces, manufacturing, control, and system models are required if the system must operate near the stability boundary.

11. Adequate instrumentation on development flights is mandatory for understanding problems that develop. This instrumentation must be engineered early in the design phases and cover all disciplines.

12. Know what is critical to the system, then model and analyze that area accurately.

13. Check out all assumptions to see if they are valid for the case being analyzed.

14. Simple models can and should be derived from complex models for use in system analysis once the critical characteristics have been determined.

15. Analytical models can be no better than the assumption made and the accuracy of the experimental input data, such as material properties.

16. When a potential problem exists that has energy source levels high enough to cause large responses (loads), analysis and testing must totally ring out the problem, identifying all key parameters and sensitivities.

17. When a technical dissenter exists during design and verification, hear him out. He probably has good insight and just might have the answer.

18. Specially instrumented and increasingly complex development flights are mandatory for any space system which is pushing state-of-the-art technology.

19. Multi-body systems with low damping have many dynamic modes, which can tune, drastically affecting responses, many times causing failures.

20. Phases A and B of a program must uncover critical technologies and develop approaches and capabilities for their solutions.

## REFERENCES


1. Compton, W. David and Benson, Charles D.: Living and Working in Space, A History of Skylab. NASA SP-4208, National Aeronautics and Space Administration, Washington, D.C.

2. Ryan, R. S., et al.: System Analysis Approach to Deriving Design Criteria (Loads) for Shuttle and Its Payloads. NASA TP 1949 and 1950, December 1981.

3. Garrick, I. E. and Reed, III, Wilmer H.: Historical Development of Flutter. AIAA-81-0591-CP, Atlanta, GA, April 6-8, 1981.

4. Ryan, R. S.: Keynote Address, 54th Shock and Vibration Symposium, Pasadena, CA, October 1983.

5. Sterett, J. B. and Riley, G. F.: Saturn V/Apollo Vehicle Pogo Stability Problems and Solutions. AIAA 7th Annual Meeting and Technical Display, Paper No. 70-12346, Houston, TX, October 19-22, 1970.

6. Ryan, R. S., et al.: A Study of AS-502 Coupling Longitudinal Structural Vibration and Lateral Bending Response During Boost. AIAA 7th Aerospace Science Meeting, New York, January 20-23, 1969.

7. Ryan, R. S. and Kiefling, L. A.: Simulation of Saturn V S-II Stage Propellant Feedline Dynamics. AIAA 6th Propulsion Joint Specialist Conference, San Diego, CA, June 15-19, 1970.

8. Garrick, I. E.: Aeroelasticity – Frontiers and Beyond. 13th Von Karman Lecture, AIAA Journal of Aircraft, Vol. 13, No. 9, September 1976, pp. 641-657.

9. Ryan, R. S.: Control Feedback Flutter Analysis of Jupiter. Army Report AM-13, DA-TM-91-58, Redstone Arsenal, AL, December 18, 1958.

10. Ryan, R. S.: Response Locus Curves of the Control Systems for Jupiter. Army Report AM112, AIN 3200, and 207, Redstone Arsenal, AL, 1958.

11. Ryan, R. S.: Control Stability Characteristics for Jupiter 10C Missile. Army Report MPT-AERO-60 -18, Redstone Arsenal, AL, December 16, 1960.

12. Ryan, R. S., Nurre, G. S., Scofield, H. N., and Sims, J. L.: Dynamics and Control of Large Space Structures. Journal of Guidance, Control, and Dynamics, Vol. 7, No. 5, September-October 1984.

13. Ehrich, F. and Childs, D.: Self-Excited Vibration in High-Performance Turbomachinery. Mechanical Engineering, May 1984, pp. 66-79.

14. Marmol, R. A., Smalley, A. J., Tecza, J. A.: Spline Coupling Induced Nonsynchronous Rotor Vibrations. ASME Paper No. 79-DET-60, Design Engineering Technical Conference, St. Louis, MO, 1979.

15. Childs, D. W.: The Space Shuttle Main Engine High Pressure Fuel Turbopump Rotordynamic Instability Problem. Transactions of the ASME, Vol. 100, January 1978, pp. 48-57.

16. Ek, M. C.: Solving Subsynchronous Whirl in the High-Pressure Hydrogen Turbomachinery of the SSME. AIAA Journal of Spacecraft, Vol. 17, No. 3, May-June 1983, pp. 208-218.

17. Abramson, N.: The Dynamic Behavior of Liquid in Moving Containers. NASA SP-106, 1966.

18. Buchanan, H. and Bugg, F.: Orbital Investigation of Propellant Dynamics in a Large Rocket Booster. NASA TN D-3968, May 1967.

19. Ryan, R. S.: Vehicle Response to Atmospheric Disturbance. Chapter 7 ADARDograph 115, Wind Effects on Launch Vehicles, E. D. Geissler, Editor, The Advisory Group for Aerospace Research and Development, NATO, February 1970.

20. Smith, O. E.: Vector Wind and Vector Wind Shear Models 0-27 Km Altitude for Cape Kennedy, FL, and Vandenberg AFB, CA. NASA TMX-73319, July 1976.

21. Ryan, R. S.: Space Vehicle Response to Atmospheric Disturbances. Space Shuttle Symposium, Cleveland, OH, June 1970.

22. Ryan, R. S.: Wind Induced Loads on a Launch Vehicle and Operational Procedures for Determination of Space Vehicle Response to In-flight Wind Turbulence. Fourth National Conference on Aerospace Meteorology, Las Vegas, NV, May 1970.

23. Ryan, R. S.: Dynamic Loads of a Launch Vehicle Due to Inflight Winds. New Orleans Joint AIAA Meeting, May 6, 1968.

24. Ryan, R. S.: Use of Wind Shears in the Design of Aerospace Vehicle. Journal of Spacecraft and Rockets, November 1967.

25. Ryan, R. S.: A Technique for Analyzing Control Gains Using Frequency Response Methods. Journal of Spacecraft and Rockets, March 1967.

26. Ryan, R. S.: The Influential Aspects of Atmospheric Disturbances on Space Vehicle Design Using Statistical Approaches for Analysis. NASA TMX-53565, January 13, 1967, and NASA TN-D-4963, January 1969.

27. Ryan, R. S.: Influence of Wind Shears on Space Vehicle Design. Structures and Materials Panel Meeting, NATO, Paris, France, October 4, 1966.

28. Ryan, R. S.: A Technique for Analyzing Control Gains Using Frequency Response Methods. AIAA Meeting, Los Angeles, CA, June 28, 1966.

29. Ryan, R. S.: A Practical Approach to the Optimization of the Saturn V Space Vehicle Control System Under Aerodynamic Loads. NASA TNX-53298, July 21, 1965.

30. Aero-Astrodynamics Research Review No. 3. NASA TMX-53389, October 15, 1965, pp. 90-100.

31. Aero-Astrodynamics Research Review No. 4. NASA TMX-53462, April 1, 1966, pp. 28-36, 96-100.

32. Ernsberger, G.: Wind Biasing Techniques for Use in Obtaining Load Relief. NASA TMX-64604, June 14, 1971.

33. Ryan, R. S., Jones, J., Verderaime, V., and Guest, S.: Propulsion System Ignition Overpressure for the Space Shuttle. NASA TM 82458, December 1981.

34. Guest, S., Nesman, T., and Dougherty, S.: Shuttle SRB Ignition Overpressure Model Suppression Test Program and Flight Results.

35. Jones, J. H.: Scaling of Ignition Startup Pressure Transients in Rocket Systems as Applied to the Space Shuttle Overpressure Phenomenon.

36. Christian, D.: Space Shuttle Liftoff Dynamic Model. NASA TMX-64993, March 1976.

37. Kross, D. A., Murphy, N. C., Rawls, E. A.: Water Impact Laboratory and Flight Test Results for the Space Shuttle Solid Rocket Booster Aft Skirt. 54th Shock and Vibration Symposium, October 18, 1983.

38. Bacchus, D. L., Kross, D. A., Moog, R. D.: The Aerodynamic Challenge of SRB Recovery. Space Shuttle Technology Conference, JSC, Houston, TX, June 20-23, 1983.

39. Kross, D. A., Kiefling, L., Murphy, N. C., Rawls, E. A.: Space Shuttle Solid Rocket Booster Initial Water Impact Loads and Dynamics Analysis, Tests, and Flight Experience. AIAA/ASME/ASCE/AHS Structures, Structural Dynamics, and Materials Conference, Lake Tahoe, NV, May2-4, 1983.

40. Kross, D. A., and Moog, R.: Space Shuttle Solid Rocket Booster Reentry and Decelerator System Loads and Dynamics. 52nd Shock and Vibration Symposium, Bulletin 52, October 27-29, 1981.

41. Kross, D. A., and Webb, R. W.: Space Shuttle Solid Rocket Booster Decelerator Subsystem Rocket Sled Test Program. AIAA 6th Decelerator Balloon Technology Conference, Houston, TX, March 5-7, 1979.

42. Kross, D. A., Moog, R. D., and Sheppard, J. D.: Space Shuttle Solid Rocket Bosoter Decelerator Subsystem Drop Test Results. AIAA 6th Aerodynamic Decelerator and Balloon Technology Conference, Houston, TX, March 5-7, 1979.

43. Kross, D. A., and Rawls, E. A.: A Study fo the Space Shuttle Solid Rocket Booster Nozzle Water Impact Recovery Loads. 46th Shock and Vibration Symposium, Houston, TX, October 21-23, 1975.

44. Kross, D. A.: A Scale Model Water Impact Study of the Space Shuttle Solid Rocket Booster. AIAA Aerospace Technology Conference, Huntsville, AL, June 13-14, 1975.

45. Kross, D. A., Madden, R., and Wright, H. A.: Scaling of Water Impact Data for Space Shuttle Solid Rocket Booster. 44th Shock and Vibration Symposium, August 1974.

46. Ryan, R., Schutzenhofer, L., Jones, J., and Jewell, R.: Mechanism Associated with the Space Shuttle Main Engine Oxidizer Valve Duct System, Anomalous High Amplitude Discrete Acoustical Excitation. AIAA/ASME/ASEE/ATTS Structural Dynamics and Materials Conference, Seattle, WA, May 1980.

47. Ryan, R., Schutzenhofer, L., Jones, J., and Jewell, R.: Elimination of Discrete Frequency Acoustical Phenomenon Associated with the Space Shuttle Main Engine Oxidizer Valve-Duct System. 50th Shock and Vibration Symposium, Colorado Springs, CO, October 1979.

48. Kiefling, L.: Space Shuttle Main Engine Nozzle Steerhorn Dynamics. AIAA/ASME/ASCE/AHS 22nd Structures, Structural Dynamics, and Materials Conference, Paper No. 81-0505-CP, Atlanta, GA, April 6-8, 1981.

49. Ryan, R. S., Salter, L., Munafo, P., and Young, G.: SSME Lifetime Predictions and Verification, Integrating Environments, Structures, Materials, The Challenge. Shuttle Symposium Challenge to Achievement, Houston, TX, June 1983.

50. Thompson, J. R.: Space Shuttle Main Engine. In the 14th Space Congress, April 27-29, 1977.

51. Colbo, H. I.: Space Shuttle Main Engine – The Liquid Rocket Engine Technology Leader. AIAA Student Journal, Vol. 17, 1979-1980, pp. 22-26.

52. Bankoff, Walter, Herr, Paul, and Mailwain, Melvin: Space Shuttle Main Engine (SSME) – The "Maturing" Process. Aeronautics and Astronautics. January 1983.

53. Rocketdyne Report RSS-8559-1-1-1 E4100: Space Shuttle Technical Manual, SSME Description and Operations. January 15, 1981.

54. Sanchini, D. J. and Colbo, H. I.: Space Shuttle Main Engine Development. AIAA Paper No. 80-1129, 1980.

55. Colbo, H. I.: Development of Space Shuttle Main Engine. AIAA Paper No. 79-1141, 1979.

56. Thompson, J. R., Jr.: Space Shuttle Main Engine. In 17th Space Congress, April 30-May 2, 1980.

57. Edgar, R.: Prime Power for the Shuttle. Spaceflight, Vol. 17, February 1975, pp. 70-73, 80.

58. Johnson, J. R. and Colbo, H. I.: Space Shuttle Main Engine Progress Through the First Flight. In AIAA, SAE, and ASME 17th Joint Propulsion Conference, July 27-29, 1981.

59. Larson, E. W.: Investigation of the Fuel Feedline Failures on the Space Shuttle Main Engine. In AIAA/SAE/ASME 16th Joint Propulsion Conference, June 30-July 2, 1980.

60. Bugg, F.: Viscoelastic Propellant Effects on Space Dynamics. NASA TM-82403, March 1981.

61. Ryan, R. S., Jewell, R., Bugg, F., Ivey, McComas, R., Kiefling, L., and Jones, J.: Dynamic Testing of Large Space Systems. NASA TM-78307, September 1980.

62. Card, Michael F.: Trends in Aerospace Structures. Astronautics and Aeronautics, July/August 1978, pp. 82-89.

63. Morosow, G., Dublin, M., and Kordes, E. E.: Needs and Trends in Structural Dynamics. Aeronautics and Astronautics, July/August 1978, pp. 90-94.

64. Amos, A. K. and Goetz, R. C.: Research Needs in Aerospace Structural Dynamics. 20th Structures, Structural Dynamics, and Materials Conference, Paper 79-0826, St. Louis, MO, April 4-6, 1979.

65. Bernstein, E. L.: Natural Frequencies of an Orbiting Space Station. AIAA Journal of Spacecraft, September 1971.

66. Riley, G. F.: Advancements in Structural Dynamic Technology Resulting from Saturn V Programs. The Boeing Company, Aerospace Group, Southwest Division, D5-17015, January 1, 1970.

67. Worley, E., Brady, W. L., and McDonough, G.: Preliminary Analysis of a Cable Retrieval Technique for the Tethered ATM Workshop. NASA TMX-53583, 1967.

68. Ryan, R. S., Nurre, G. S., Scofield, H. N., and Sims, J. L.: Dynamics and Control of Large Space Structures. Journal of Guidance, Control, and Dynamics, Vol. 7, No. 5, September-October 1984.

69. Buchanan, H. and Bugg, F.: An Orbital Facility for Low Gravity Fluid Mechanics Experiments. NASA TMX-53561, 1966.

70. Ferebee, R.: Application of a Computerized Vibroacoustic Data Bank for Random Vibration Criteria Development. NASA TP 1998, March 1982.

71. Harcrow, H. and Demehak, E.: Analysis of Structural Dynamic Data from Skylab. NASA CR-2727, August 1976.

72. Jewell, R. E., Jones, J., and Fenwich, J.: Diagnostic Analysis of Vibration Signals Using Adaptive Digital Filtering Techniques. In 52th Shock and Vibration Symposium, October 1981.

73. Kiefling, L.: Multiple Beam Vibration Analysis of Saturn I and IB Vehicles. NASA TM-53072, 1964.

74. Kiefling, L.: Structural Deformations in the Saturn Instrument Unit. NASA TMX-53673, 1967.

75. Lewis, J. R.: Materials and Process for Space Shuttle's Engines. Metal Progress, Vol. 107, March 1975, pp. 41-43.

76. McBride, J. E. and Harrison, P. M.: Spacelab-1 Vibroacoustics. Payload Conference, JPL, Pasadena, CA, January 1984.

77. Muller, G. R.: Finite Element Models of the Space Shuttle Main Engine. NASA TM-78260, January 1980.

78. Nave, L. H. and Coffey, G. A.: Sea Level Sideloads in High-Area-Ratio Rocket Engine. AIAA Paper No. 73-1284, 1973.

79. Pinson, Larry D. and Leonard, H. Wayne: Longitudinal Vibration Characteristics of 1/10-Scale Apollo/ Saturn V Replica Model. NASA TN-D5159, April 1969.

80. Riley, G.: Saturn V Dynamic Test Vehicle Test-Analysis Correlation. Boeing Report D5-15722, The Boeing Company, Huntsville, AL, November 1967.

81. Ryan, R. S.: Stability Considerations of a Space Vehicle in Bending Oscillations for Various Control Sensors. MTP-AERO-62-64, August 20, 1962.

82. Ryan, R. S., Bacchus, D. L., Hall, C. E., and Mowery, D. K.: Space Shuttle Engine Gimbal Requirements. IN-AERO-71-1.

83. Ryan, R. S.: A Look at Control Law Influence on the Rigid Body Bending Moments for Boost Vehicles with Various Degrees of Aerodynamic Stability. AIAA Guidance Control and Flight Mechanics Conference, Hofstra University, Hempstead, NY, AIAA Paper 71-918, August 16-18, 1971.

84. Schwinghamer, R. J.: Materials and Processes for Shuttle Engine, External Tank, and Solid Rocket Booster. NASA TN-D-8511, 1977.

85. Ryan, R. S., Mowery, D. K., Winder, S. W., and Worley, H. E.: Structural Control Interaction. NASA TMX-64732, 1973.

86. Ryan, R. S. (Editor): Payload Loads Survey, Government/Industry Workshop on Payload Modeling and Dynamic Testing Technology. NASA, Marshall Space Flight Center, AL, November 1978.

87. Schwinghamer, R. J.: Materials and Processes for Shuttle Engine, External Tank, and Solid Rocket Booster. In Internal Aeronautics Federation, INF Paper 76-202, October 10-16, 1976.

88. Schwinghamer, R. J.: Materials and Processes for Shuttle Engine, External Tank, and Solid Rocket Booster, NASA TN-D-8511, 1973.

89. Aero-Astrodynamics Research Review No. 1. NASA TMX-53189, October 1967, pp. 54-69.

90. Aero-Astrodynamics Research Review No. 6. NASA TMX-53647, October 1967, pp. 56-66.

TECHNICAL REPORT STANDARD TITLE PAGE

| 1. REPORT NO. | 2. GOVERNMENT ACCESSION NO. | 3. RECIPIENT'S CATALOG NO. |
|---|---|---|
| NASA TP-2508 | | |

| 4. TITLE AND SUBTITLE | 5. REPORT DATE |
|---|---|
| Problems Experienced and Envisioned for Dynamical Physical Systems | August 1985 |
| | 6. PERFORMING ORGANIZATION CODE |
| 7. AUTHOR(S) | 8. PERFORMING ORGANIZATION REPORT # |
| Robert S. Ryan | |
| 9. PERFORMING ORGANIZATION NAME AND ADDRESS | 10. WORK UNIT NO. |
| George C. Marshall Space Flight Center<br>Marshall Space Flight Center, Alabama 35812 | M-494 |
| | 11. CONTRACT OR GRANT NO. |
| | 13. TYPE OF REPORT & PERIOD COVERED |
| 12. SPONSORING AGENCY NAME AND ADDRESS | Technical Paper |
| National Aeronautics and Space Administration<br>Washington, D.C. 20546 | 14. SPONSORING AGENCY CODE |

15. SUPPLEMENTARY NOTES

Prepared by Systems Dynamics Laboratory, Science and Engineering Directorate.

16. ABSTRACT

The use of high performance systems, which is the trend of future space systems, naturally leads to lower margins and a higher sensitivity to parameter variations and, therefore, more problems of dynamical physical systems. To circumvent dynamic problems of these systems, appropriate design, verification analysis, and tests must be planned and conducted. The basic design goal is to define the problem before it occurs. The primary approach for meeting this goal is a good understanding and reviewing of the problems experienced in the past in terms of the system under design.

This paper reviews many of the dynamic problems experienced in space systems design and operation, categorizes them as to causes, and envisions future program implications, developing recommendations for analysis and test approaches.

| 17. KEY WORDS | 18. DISTRIBUTION STATEMENT |
|---|---|
| Dynamics<br>Instability<br>Structures<br>Control | Unclassified - Unlimited<br><br>Subject Category 15 |

| 19. SECURITY CLASSIF. (of this report) | 20. SECURITY CLASSIF. (of this page) | 21. NO. OF PAGES | 22. PRICE |
|---|---|---|---|
| Unclassified | Unclassified | 146 | A07 |

MSFC - Form 3292 (May 1969)

For sale by National Technical Information Service, Springfield, Virginia 22161

NASA-Langley, 1985